

Design, synthesis and biological evaluation of novel multi-receptor ligands with potential application in schizophrenia therapeutics

by

Donna MacMillan



A thesis presented to WestCHEM, Department of Pure and Applied Chemistry, University of Strathclyde in fulfilment of the requirements for the degree of Doctor of Philosophy.

2012

Declaration of Copyright

This thesis is the result of the author's original research. It has been composed by the author and has not been previously submitted for examination which has led to the award of a degree.

The copyright of this thesis belongs to the author under the terms of the United Kingdom Copyright Acts as qualified by University of Strathclyde Regulation 3.50. Due acknowledgement must always be made of the use of any material contained in, or derived from, this thesis.

Signed:

Date:

Acknowledgements

I would like to thank Professor Colin J. Suckling and Dr. Colin L. Gibson, firstly, for the opportunity to do a PhD within the group and most importantly for all their help (and patience!) throughout the past three years. I would also like to extend my gratitude to Professor Judy A. Pratt and Professor Brian J. Morris, and the rest of PsyRING, for their invaluable assistance with the biological assay work. My thanks also go to Dr John Mitcheson for supplying my hERG cells free of charge and to Dr Ben Pickard for his help with culturing of the cells. This multi-disciplinary PhD would not have been possible without the joint input from all of the above.

I'd also like to thank all the technical and stores staff at Strathclyde, especially Pat Keating and Craig Irving for their assistance with all mass spec and NMR woes, respectively. I would also like to thank Dr Alan Kennedy for carrying out all the X-ray crystallography work.

It is a great pleasure to have worked with everyone who passed through the Suckling/Gibson group during my time there. I'd especially like to thank Abed, Dave and Craig, particularly for their help in the early days. I would also like to thank Dave, Craig and Fraser for all the philosophical/hypothetical 'discussions' (arguments) about every topic imaginable, it certainly kept the lab lively. Finally, during my time in TG416 it was brought to my attention that everyone loathes my music taste, and on that note, where's my bloody Morrissey CD Craig?

My thanks also go to Dr Craig Jamieson, not only for his considerable knowledge of hERG but also for his willingness to act as a sounding board during my writing up phase. I'd also like to thank Nicola Caldwell for carrying out Gaussian calculations on my behalf and the Jamieson/Watson group for putting up with my constant thesis chat.

Finally, I'd like to thank my family for all their support throughout my entire time at Strathclyde, especially my mum, who listened to my all my complaints and worries without a word of criticism. I couldn't have done it without you guys.

Abbreviations

5-CT	5-carboximidotryptamine
5-HT _x	5-hydroxytryptamine (serotonin) receptor subtype x
AChEI	acetylcholinesterase inhibitor
CBS	Corey-Bakshi-Shibata
CCR5	C-C chemokine receptor type 5
CDI	1,1'-carbonyldiimidazole
CHO	Chinese hamster ovary
clogP	calculated logarithm of partition coefficient
CNS	central nervous system
D _x	dopamine receptor subtype x
DCE	dichloroethane
DCM	dichloromethane
DIPEA	<i>N,N</i> -diisopropylethylamine
DISC1	disrupted in schizophrenia 1
DMAP	4-dimethylaminopyridine
DMF	<i>N,N</i> -dimethylformamide
DSM-IV-TR	Diagnostic and Statistical Manual of Mental Disorders
ECG	electrocardiogram
ED ₅₀	half maximal effective dose
EPS	extra-pyramidal side-effects
e.r	enantiomeric ratio
ESI	electrospray ionisation
equiv.	equivalents
EWG	electron-withdrawing group
FDA	Food and Drug Administration
FT-IR	fourier transform infra red
GDP	guanosine diphosphate
GPCR	G-protein coupled receptors
GTP	guanosine triphosphate
H _x	histamine receptor subtype

HBA	hydrogen bond acceptor
hERG	human ether-à-go-go related gene
HPLC	high performance liquid chromatography
HRMS	high resolution mass spectrometry
HTS	high-throughput screening
i.p.	intraperitoneal
IC ₅₀	half maximal inhibitory concentration
K_D	dissociation constant
K_i	inhibition constant
K_v	voltage-gated potassium ion channel
LHS	left hand side
LQTS	long QT syndrome
LRMS	low resolution mass spectrometry
LSD	lysergic acid diethylamide
M_x	muscarine receptor subtype x
mAChR	muscarinic acetylcholine receptor
mGluR2	metabotropic glutamate receptor 2
mGluR3	metabotropic glutamate receptor 3
min.	minutes
MW	microwave irradiation
n	number of independent experiments
nAChR	nicotinic acetylcholine receptor
Na_v	voltage-gated sodium ion channel
NNRTI	non-nucleoside reverse transcriptase inhibitor
NMDA	<i>N</i> -methyl- <i>D</i> -aspartate
NMR	nuclear magnetic spectroscopy
NMS	<i>N</i> -methylnscopolamine
NOE	nuclear Overhauser effect
NOESY	nuclear Overhauser effect spectroscopy
NR2B	<i>N</i> -methyl <i>D</i> -aspartate receptor subtype 2B
NRG1	neuregulin 1
PCP	phenylcyclidine

PDB	protein data bank
PET	positron emission tomography
pK_a	acid dissociation constant
pK_i	inhibition constant
RHS	right hand side
SAR	structure-activity relationship
sat.	saturated
SIDR	Strathclyde Innovations in Drug Research
SPECT	single-photon emission computed tomography
SSRI	selective serotonin re-uptake inhibitor
TD	tardive dyskinesia
TEA	triethylamine
TdP	torsades de pointes
TFA	trifluoroacetic acid
THF	tetrahydrofuran
TLC	thin layer chromatography
VEGFR-2	vascular endothelial growth factor receptor 2

Contents

Chapter 1 – Introduction	1
1.1 The nature of schizophrenia	2
1.1.1 History of schizophrenia	2
1.1.2 Symptoms.....	3
1.1.3 Epidemiology and aetiology	3
1.2 First generation antipsychotics and the dopamine hypothesis	5
1.2.1 First generation antipsychotics.....	5
1.2.2 The dopamine hypothesis.....	8
1.3 Second generation antipsychotics	10
1.4 Other neurotransmitters in the pathophysiology of schizophrenia	13
1.4.1 Glutamate	13
1.4.2 Serotonin (5-HT).....	15
1.4.3 Muscarine	18
1.5 Multiple-target compounds	20
1.6 The <i>serominic</i> concept	23
1.7 Human ether-à-go-go gene (hERG) activity	29
1.7.1 Structure and function of hERG.....	29
1.7.2 Drug-induced hERG blockade	32
1.7.3 Mitigating undesirable hERG activity	35
1.8 Research programme.....	39
Chapter 2 - Results and discussion	45
2.1 Amidine-linked compounds	46
2.1.1 Resynthesis of amidine units.....	46
2.1.2 Enantio-enriched amidines.....	52
2.1.3 Summary of amidine-linked compounds	59
2.2 Linker modifications – Nitroalkenes.....	60

2.2.1	New route to nitroalkene-linked compounds	64
2.2.2	Alternative approaches to nitroalkene-linked compounds.....	67
2.2.3	Geometry of nitroalkene double bond.....	72
2.2.4	Summary of <i>N,N'</i> -disubstituted nitroalkene compounds	74
2.3	Linker modifications – Cyanoguanidines	76
2.3.1	Summary of <i>N,N'</i> -disubstituted cyanoguanidines.....	81
2.4	Linker modifications - Trifluoroethanimidamides.....	82
2.4.1	Summary of <i>N,N'</i> -disubstituted trifluoromethyl compounds	85
2.5	Linker modifications – Hydrazides and ureas.....	86
2.5.1	Summary of synthesis of <i>N,N'</i> -disubstituted hydrazide and urea compounds	91
2.6	Linker modifications – Triazenes	92
2.7	Haloperidol analogues with potentially reduced hERG liability	100
2.7.1	Summary of haloperidol analogues.....	102
2.8	Summary of synthetic phase of research programme	103
Chapter 3 - Biological results – 5-HT₇ and M₄		104
3.1	Biological results – 5-HT ₇ and M ₄	105
3.1.1	Series 1 assay results.....	106
3.1.2	Series 2 assay results.....	112
Chapter 4 - Biological results – hERG		120
4.1	Biological results – hERG.....	121
4.1.1	Effects of linker modification on hERG activity	121
4.1.2	Effects of discrete structural modification on hERG activity.....	124
4.1.3	Effects of clogP on hERG activity	128
4.1.4	Conformational analysis and potential implications for hERG activity .	131
4.1.5	Haloperidol analogues with reduced hERG liability	136
4.1.6	Summary of biological assay results.....	137
Chapter 5 - Conclusions and further work		139
5.1	Conclusions and further work	140

5.1.1 Synthesis	140
5.1.2 Biological assays	142
Chapter 6 - Experimental	150
6.1 Experimental	151
6.1.1 General	151
6.1.2 Synthesis	153
6.1.3 Materials and methods for bioassays	212
Chapter 7 – References	216
Chapter 8 - Appendix	226
8.1 Crystal data.....	226
8.2 ¹ H NMR spectra	264
8.3 NOESY spectra	279
8.4 IC ₅₀ example graphs	282
8.4.1 5-HT ₇ IC ₅₀ example graphs	282
8.4.2 M ₄ IC ₅₀ example graphs	285

Chapter 1 – Introduction

1.1 The nature of schizophrenia

1.1.1 History of schizophrenia

Psychiatrist Emil Kraepelin significantly assisted progress in the understanding of mental illnesses in the late 18th century. He observed that mental illness could be classified according to symptoms, pathology and aetiology in much the same way as other diseases.¹ He recognised that identical symptoms were present in a range of psychotic disorders and classified these symptoms into two broad but distinct forms, *manic-depressive* and *dementia praecox* (senility of the young). *Dementia praecox* was then used as an umbrella term for early onset idiopathic psychoses ending in complete functional deterioration. In 1911, after observing that *dementia praecox* did not always occur in the young and did not always end in deterioration, psychiatrist Eugene Bleuler re-named these psychoses as *schizophrenia*.²

In the 19th century, asylums and prisons for the mentally insane were slowly being replaced by hospital care but treatment was primitive. The first treatments for schizophrenia were employed in the 20th century and included prolonged narcosis using barbiturates, insulin coma, electro-convulsive therapy, and frontal lobotomy. These treatments were mostly ineffective but frontal lobotomies gained popularity in the 1940s and were widely used.³ Fortunately, psychosurgery was short-lived due to the discovery of the first antipsychotic drug in 1952, chlorpromazine (**1**), and the subsequent emergence of the field of psychopharmacology.⁴

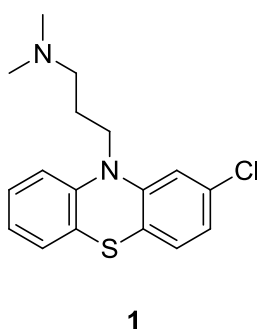


Figure 4: Chlorpromazine (**1**), the first antipsychotic drug, discovered in 1952.

1.1.2 Symptoms

The American Psychiatric Association (Diagnostic and Statistical Manual of Mental Disorders (DSM-IV-TR)) defines schizophrenia as ‘a disorder that lasts for at least 6 months and includes at least one month of active-phase symptoms (i.e. two or more of the following: delusions, hallucinations, disorganised speech, grossly disorganised or catatonic behaviour and negative symptoms)’.⁵

The clinical features of schizophrenia are divided into three domains: positive symptoms, negative symptoms, and cognitive deficits (Table 1).⁶ Positive symptoms are often thought of as an exaggeration of normal functions and are characterised by hallucinations (visual or auditory), delusions, thought disorder and disorganised speech and/or behaviour. Negative symptoms involve a blunting or loss of normal function, typically manifested as alogia (poverty of speech), anhedonia (inability to experience pleasure), avolition (lack of initiative), apathy, social withdrawal and emotional blunting.⁷⁻¹¹ Impairments in cognition include lack of working memory and problems with attention (Table 1).^{8, 12}

Positive Symptoms	Negative Symptoms	Cognitive Effects
Hallucinations	Blunted affect	Memory
Delusions	Anhedonia	Attention
Thought disorder	Avolition	Executive function
Disorganised speech	Apathy	Language

Table 1: Summary of schizophrenia symptomology.⁶

1.1.3 Epidemiology and aetiology

Schizophrenia is reported to affect approximately 1 % of the population worldwide and is currently a considerable societal burden.¹³ Schizophrenia was estimated to cost \$62.7 billion annually in the US in 2002 including direct medical costs such as drug treatment and long term care, and indirect costs such as unemployment and premature mortality.¹⁴ The age of onset (where onset is defined as first incidence of psychosis) is usually earlier for men than that of women, but can vary between mid adolescence and later adult life.¹⁵

A genetic component to schizophrenia has been well established and lifetime risk of developing schizophrenia is associated with increased genetic affinity to a person suffering from schizophrenia.^{16, 17} This increased risk is not solely attributed to the heritability of schizophrenia as certain environmental factors are usually shared by close relatives, however a higher risk is also observed in studies where offspring of schizophrenics are raised in foster homes.¹⁸ Additionally, if schizophrenia was solely genetic, it would be expected that monozygotic twins of schizophrenics, sharing 100 % genetic material, would have 100 % risk of developing schizophrenia but the actual risk is approximately 48 %, therefore environmental factors must play a considerable role.¹⁶

Relationship	% shared genes	% risk
General population	-	1
Spouse of patient	-	2
3 rd degree relative	12.5	
First cousins		2
2 nd degree relatives	25	
Uncles/aunts		2
Nieces/nephews		4
Grandchildren		5
Half-siblings		6
1 st degree relatives	50	
Parents		6
Children		9
Siblings		13
Siblings with one schizophrenic parent		17
Dizygotic twin		17
Monozygotic twin	100	48
Children with two schizophrenic parents	100	46

Table 2: Risk of schizophrenia for relatives of schizophrenic patients.¹⁶

More recently, work has focused on specific genes such as DISC1 (disrupted in schizophrenia 1) and NRG1 (neuregulin 1) after genome studies implicated mutations of these as susceptibility markers in schizophrenia.¹⁹ However, numerous environmental factors such as season of birth,²⁰ pre-natal maternal infection,²¹ and cannabis use²² have been heavily implicated as risk factors of schizophrenia and it is now generally accepted that there is a genetic predisposition to schizophrenia which,

when exposed to certain environmental risk factors, triggers the onset of the disease.¹⁶

1.2 First generation antipsychotics and the dopamine hypothesis

1.2.1 First generation antipsychotics

In the context of disease management, the serendipitous discovery in the 1950s of chlorpromazine (**1**), the first antipsychotic drug, revolutionised treatment of psychosis. Studies on chlorpromazine, (originally developed as an antihistaminic agent) revealed that chlorpromazine was a potent hypnotic in human trials on psychotic patients, an enormous breakthrough in psychiatry.⁴ The subsequent launch of another antipsychotic, indole alkaloid reserpine (**2**), a few years later was another landmark and the field of psychopharmacology was born (Figure 5).²³

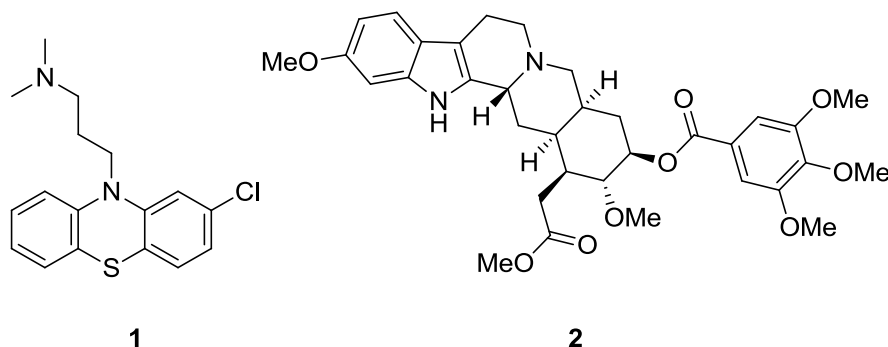


Figure 5: First drugs discovered with antipsychotic activity, chlorpromazine (**1**) and reserpine (**2**).

The first generation of antipsychotics are known as typical antipsychotics and refer to compounds that exert their effect through dopamine D₂ antagonism. A number of other chlorpromazine analogues based around the phenothiazine core were also found to display antipsychotic activity, piperidine thioridazine (**3**) and piperazine fluphenazine (**4**) (Figure 6).

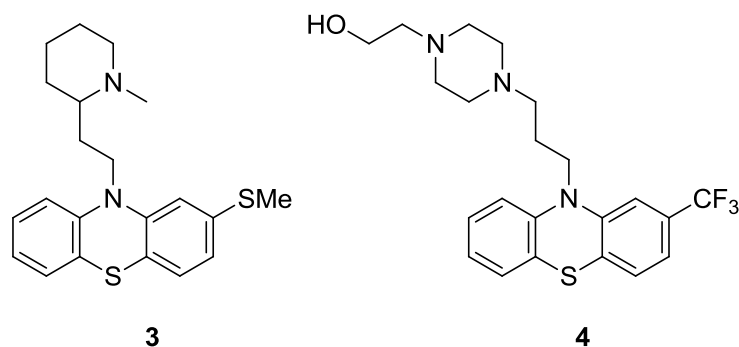


Figure 6: Phenothiazines class of typical antipsychotics – thioridazine (3), and fluphenazine (4).

In general, phenothiazines have affinity for a range of receptors including dopamine D₁ and D₂, histamine H₁, serotonin 5-HT₂ and mAChR (muscarinic acetylcholine receptors), which leads to a number of undesirable side-effects. In particular, extrapyramidal side-effects (EPS) and tardive dyskinesia (TD)^{24, 25} are commonly observed and are thought to result from dopaminergic receptor blockade.²⁶

EPS usually occur in the first few weeks of treatment, occasionally declining with time and are usually reversible on stopping drug treatment. There are three components of EPS, one, acute dystonia, is characterised by involuntary movements such as protruding tongue, muscle spasms and a fixed upwards gaze. Parkinsonian symptoms are also present such as tremors, rigidity and bradykinesia (slowing of executed movement). Akathisia is the final main side-effect, and is characterised by restlessness, such as rocking back and forth. EPS have also been suggested as the main cause of schizophrenic patients discontinuing drug use, but EPS can normally be controlled by anti-EPS medication (such as procyclidine or benztropine).²⁷

Tardive dyskinesia (TD) is a more serious side-effect and usually develops after long term use of typical antipsychotics. It is often irreversible, even after discontinuation of drug treatment and is characterised by involuntary repetitive movements of the face such as lip smacking, pursing and puckering of the mouth, and protrusion of the tongue.²⁷

However, the discovery of the very potent haloperidol (5), quickly overtook the low potency, high EPS-inducing chlorpromazine (1). In 1958, whilst searching for novel potent opioid analgesics, Paul Janssen of Janssen Pharmaceutica noted that butyrophenone compounds induced catalepsy in animal trials, much like the recently

introduced clinical compound chlorpromazine (**1**). It was reasoned that these butyrophenones could potentially be used as antipsychotics and this led to synthesis of similar derivatives until the discovery of haloperidol (**5**, Figure 7).²⁸

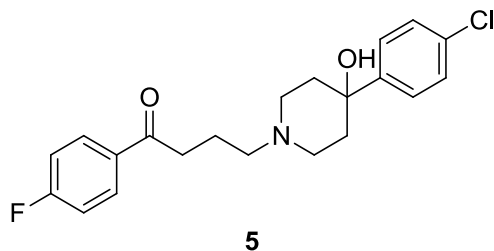


Figure 7: Typical antipsychotic haloperidol (**5**).

Haloperidol is a very potent selective dopamine D₂ antagonist, which alleviates the positive symptoms of schizophrenia substantially but has little effect on negative symptoms and cognitive deficits.^{29, 30} This D₂ selectivity and relatively low affinity for other receptors eliminated a number of side-effects caused by phenothiazine compounds like chlorpromazine. However, haloperidol itself induces a number of undesirable side-effects. Certain dopamine pathways play an important role in secretion of prolactin, a hormone synthesised by the pituitary gland responsible for lactation, regulation of ovarian and testicular function and reproductive behaviour. The potent D₂ antagonism caused by haloperidol results in hyperprolactinaemia which can then induce a number of other side-effects such as sexual dysfunction and decreased bone density.³¹

Haloperidol also carries a high risk of EPS³² and TD.³³ Furthermore, it has also been associated with undesirable cardiovascular side-effects³⁴ (discussed further in Section 1.7.2) but is still commonly used as a first line treatment for schizophrenia owing to its high potency.

The identification of first generation antipsychotics, capable of substantially alleviating the positive symptoms of schizophrenia, was a groundbreaking discovery that paved the way to increased knowledge of the disease and led to the eventual dopamine hypothesis of schizophrenia.

1.2.2 The dopamine hypothesis

The dopamine hypothesis of schizophrenia postulates that dopaminergic dysfunction is key to the pathophysiology of schizophrenia, supported by the discovery that typical antipsychotics chlorpromazine (**1**) and haloperidol (**5**) exert their effects through dopamine D₂ antagonism.³⁵

Dopamine receptors are a class of G-protein coupled receptors (GPCR). The neurotransmitter dopamine (**6**) is the primary endogenous ligand for these receptors (Figure 8).

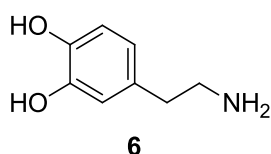


Figure 8: Neurotransmitter dopamine (**6**).

A ligand, such as dopamine (**6**), binds to the receptor, causing a change in conformation and the formation of a new binding site. A G-protein (with guanosine diphosphate (GDP) bound) binds to the newly exposed binding site then releases the bound GDP to allow guanosine triphosphate (GTP) to bind in its place. This results in another conformational change and the release of the α -subunit and the $\beta\gamma$ -dimer. The receptor-ligand complex can activate several G-proteins in this manner, leading to signal amplification. The α -subunit and $\beta\gamma$ -dimer, dependant on type, can activate/inhibit multiple targets including adenylate cyclase and can be the first step in a cell signalling cascade (Figure 9).³⁶

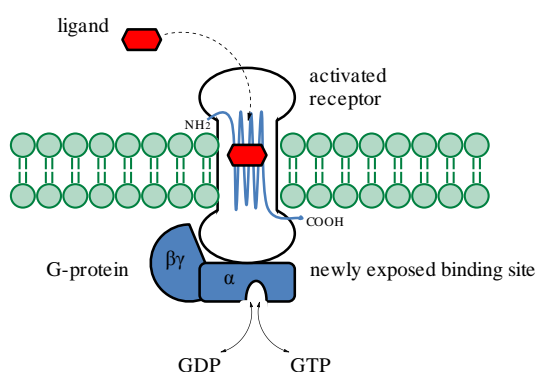


Figure 9: Schematic of GPCR.

The origin of this hypothesis is attributed to Carlsson and Lindqvist who in 1963 experimented by administering chlorpromazine (**1**) or haloperidol (**5**) to mice. They observed increased concentrations of dopamine and norepinephrine metabolites in the brain and postulated that this was caused by blockade of dopamine receptors.³⁵ Carlsson later received a share of the Nobel Prize in Physiology or Medicine for "*for discoveries concerning signal transduction in the nervous system*" for his work related to dopamine and other neurotransmitters.³⁷ Other lines of evidence supporting the dopamine hypothesis includes the discovery that *in vitro* binding affinity of antipsychotics to dopamine D₂ directly correlates to their pharmacological potency.^{38, 39}

Another cornerstone of the dopamine hypothesis is the observation of psychotomimetic behaviour induced by dopamine agonists such as amphetamine (**7**) or cocaine⁴⁰ (**8**, Figure 10) in non-schizophrenic subjects which can be alleviated by haloperidol (**5**).⁴¹ Amphetamine (**7**) has also been shown to exacerbate psychotic symptoms of schizophrenic patients.⁴² As a result of these findings, amphetamine is commonly used to model schizophrenia in animal studies.^{43, 44}

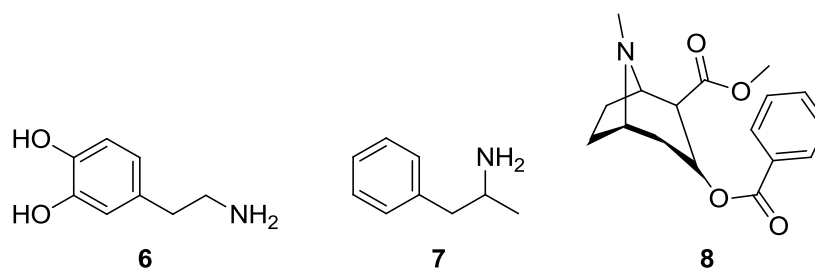


Figure 10: Dopamine agonists dopamine (**6**), amphetamine (**7**) and cocaine (**8**).

Results from 3-D nuclear medicine imaging techniques using radioisotope tracers also support the dopamine hypothesis. PET (positron emission tomography) and SPECT (single-photon emission computed tomography) studies have shown that administration of amphetamine releases more dopamine in drug-naïve schizophrenics than healthy volunteers and this increase in dopamine correlates with a worsening of positive symptoms.^{42, 45, 46}

Although there is compelling evidence for a role for dopamine in the pathophysiology of schizophrenia, it has been challenged in recent years. For

example, dopamine hypofunction cannot explain all symptom domains as typical antipsychotics such as haloperidol (**5**) alleviate only the positive symptoms of schizophrenia and have little to no effect on negative symptoms and cognitive deficits.^{29, 30} Furthermore, the advent of second generation (atypical) antipsychotics, typified by their low affinity for dopamine D₂ and multi-receptor profiles indicated a key role for other neurotransmitters in the pathophysiology of schizophrenia.

1.3 Second generation antipsychotics

Second generation antipsychotics (atypical antipsychotics) refer to more recently developed drugs, of which clozapine (**9**, Figure 11) is the most well known. Their atypicality is defined by their low affinity for dopamine D₂ receptors, contrary to the mechanism of action of typical antipsychotics, and their resultant low propensity to cause EPS and elevated prolactin levels.

Clozapine (**9**) belongs to the dibenzodiazepine class of compounds and is mainly effective against positive symptoms of schizophrenia, with minor improvements in negative symptoms reported.⁴⁷ Compared to typical antipsychotics, it improves cognitive deficits⁴⁸ and has a slightly decreased risk of EPS.⁴⁹ Clozapine has also been shown to be particularly effective for treatment-refractory schizophrenia.⁵⁰ The mechanism of the improved therapeutic efficacy of clozapine (**9**) is unknown but it has been proposed that the high D₂/5-HT_{2A} ratio (characteristic of a number of atypical antipsychotics) is the main reason these drugs have a low incidence of EPS and increased effectiveness against negative symptoms and cognitive deficits compared to typical antipsychotics.⁵¹

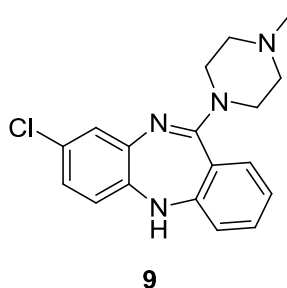


Figure 11: Clozapine (**9**), a member of the dibenzodiazepine class of atypical antipsychotics.

Unfortunately, clozapine is not without side-effects: drowsiness, hypotension, tachycardia and weight gain are all associated with its use and can lead to non-compliance of patients.⁵² The most serious side-effect is agranulocytosis,⁵³ a dangerous blood abnormality, which ultimately led to its withdrawal in 1984. However, clozapine was later re-introduced due to its unparalleled success in treatment-resistant patients but is restricted and requires weekly blood cell count monitoring.⁵⁰

A number of other atypical antipsychotics have been identified that have improved pharmacological profiles. Eli Lilly's blockbuster drug olanzapine (Zyprexa™, off-patent in 2011) (**10**, Figure 12) is structurally related to clozapine but without the associated agranulocytosis risk.⁵⁴ It has a greater effect on the positive and negative symptoms of schizophrenia compared to haloperidol and less frequent incidence of EPS^{29, 55, 56} and TD.⁵⁷ Additionally, it has little to no effect on prolactin levels.^{55, 58} Janssen's risperidone (Risperdal™) (**11**), although significantly different structurally from clozapine (**9**) and olanzapine (**10**), is also an atypical antipsychotic with reduced risk of agranulocytosis⁵⁴ and has been reported to improve positive and negative symptoms of schizophrenia with low incidence of EPS.^{56, 59} However, risperidone (**11**) has been associated with significantly high prolactin levels, comparable to typical antipsychotic haloperidol (**5**), which may be due, in part, to their increased structural similarity in comparison to dibenzodiazepine atypical antipsychotics.⁵⁸

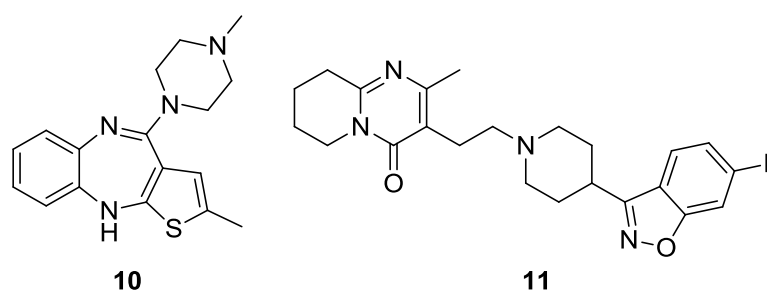


Figure 12: Atypical antipsychotics olanzapine (**10**) and risperidone (**11**).

Quetiapine (Seroquel™), AstraZeneca's blockbuster atypical antipsychotic medication was launched in 1997 (**12**, Figure 13). It displayed superior efficacy compared to chlorpromazine (**1**), was shown to be effective against some positive and negative symptoms and had low risk of EPS.^{54, 60, 61} Furthermore, no increase in prolactin levels was reported with administration of this compound.⁶² Finally, one of the more recent treatments for schizophrenia, asenapine (**13**), was marketed by Schering-Plough in 2007. It is a very potent, well-tolerated drug that does not elevate prolactin levels significantly and has been reported to be very effective against positive and negative symptoms of schizophrenia in clinical trials.⁶³

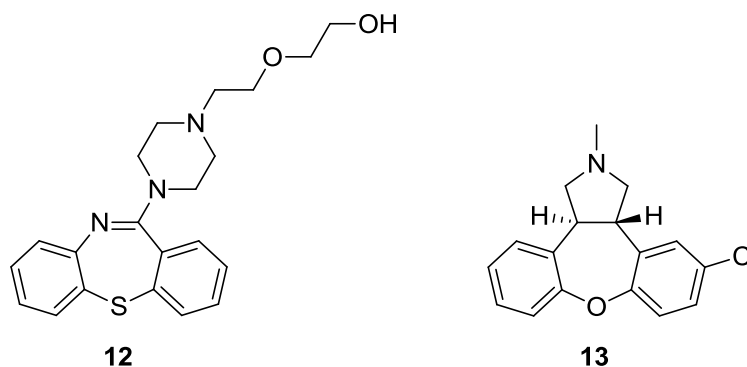


Figure 13: Atypical antipsychotics quetiapine (**12**) and asenapine (**13**).

The improved therapeutic profile of clozapine (**9**) and other atypical antipsychotics with decreased D₂ receptor affinity successfully challenged the dopamine hypothesis of schizophrenia although their precise mechanism of action is still unclear. These compounds have promiscuous pharmacological profiles⁵⁴ with high affinity for a range of other receptors. This suggests that other excitatory neurotransmitters are involved in the antipsychotic effect, but unfortunately this promiscuity can invoke a number of undesirable side-effects. Recent research has focused on glutamate,

serotonin, and muscarinic receptors in the pathophysiology of schizophrenia, providing additional receptor targets to focus on within drug discovery programmes.

1.4 Other neurotransmitters in the pathophysiology of schizophrenia

1.4.1 Glutamate

In recent years, interest has shifted to the role of other neurotransmitters in schizophrenia and in particular, glutamate (**14**, Figure 14), the major excitatory neurotransmitter in the brain. A number of receptors for glutamate exist including both ionotropic glutamate receptors such as the *N*-methyl-D-aspartate (NMDA) receptor and metabotropic glutamate receptors such as mGluR2/3.

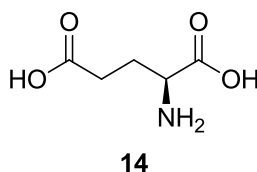


Figure 14: L-Glutamic acid (**14**) (glutamate).

Metabotropic glutamate receptors are GPCRs and function much in the same way as previously discussed for dopamine, whereas the NMDA receptor is a ligand-gated ion channel that is activated (opened) in response to binding of a chemical messenger such as glutamate. The NMDA receptor requires co-activation by another ligand (such as glycine) and allows the voltage-dependent flow of Na⁺, Mg²⁺ and Ca²⁺ ions into the cell and K⁺ out of the cell (Figure 15).

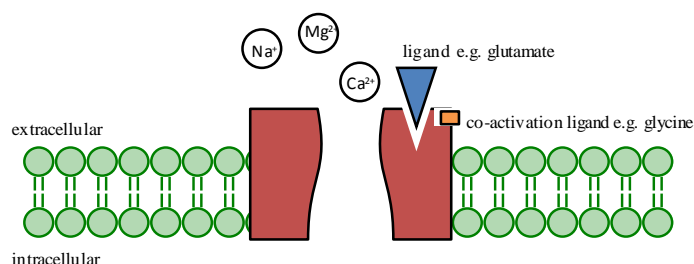


Figure 15: Schematic of an NMDA receptor showing glutamate binding and co-activation by glycine.

The glutamate theory of schizophrenia was first hypothesised by Kim *et al.* who, in 1980, found that the level of glutamate in the cerebrospinal fluid of schizophrenia patients was approximately half the level found in normal subjects.⁶⁴ This observation was confirmed by a number of studies, including a study showing that cerebrospinal fluid glutamate concentration correlated inversely with the severity of positive symptoms in unmedicated patients with schizophrenia.⁶⁵ However, the most compelling evidence for the glutamate hypothesis hinges on non-competitive NMDA receptor antagonists phencyclidine (**15**) (PCP) and ketamine (**16**) (Figure 16).

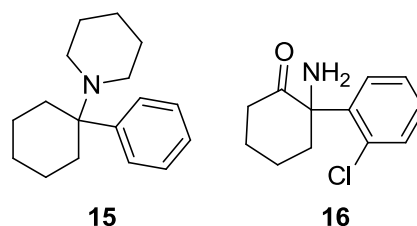


Figure 16: PCP (**15**) and ketamine (**16**).

PCP (**15**) and ketamine (**16**) were originally developed as anaesthetic drugs due to their dissociative effect but reports from patients of side-effects such as psychosis, hallucinations and disordered speech rendered clinical use not possible.⁶⁶

Evidence showed that PCP induced a schizophrenia-like psychosis in non-schizophrenic patients⁶⁷ and exacerbates these symptoms in schizophrenic patients.⁶⁸ Similarly, when ketamine was administered to drug-naïve schizophrenic patients positive symptoms, negative symptoms and cognitive deficits were exacerbated.^{69, 70} However, the positive symptoms were alleviated by clozapine (**9**), suggesting a role for glutamate in the therapeutic efficacy of clozapine.⁷¹

Based on the above evidence, PCP (**15**) and ketamine (**16**) are frequently used in animal models of schizophrenia due to the analogous positive symptoms, negative symptoms and cognitive defects induced upon administration.^{72, 73}

Glutamate itself cannot be used as a potential drug to modulate the NMDA receptor as high levels of glutamate may be neurotoxic. However, targeting the co-factor glycine has been explored as a therapeutic approach to the glutamergic dysfunction observed in schizophrenia.⁷⁴ Javitt *et al.* administered supplementary high doses of

glycine to patients receiving typical antipsychotics in a double-blind placebo controlled clinical trial and observed a significant decrease in negative symptoms in patients receiving adjunctive glycine therapy.⁷⁵ These findings have also been replicated by Heresco-Levy *et al.* using supplementary glycine with atypical antipsychotics olanzapine (**10**) and risperidone (**11**) to observe a marked improvement in negative symptoms and cognitive deficits.⁷⁶

More recently, interest has shifted to metabotropic glutamate receptors mGluR2 and mGluR3 as targets for schizophrenia therapeutics. Eli Lilly disclosed that a mixed mGluR2/mGluR3 agonist, LY354740, (**17**) attenuated schizophrenia-type symptoms in rats treated with PCP.⁷⁷ This was further supported by another Eli Lilly agonist, LY2140023 (**18**) (administered as a pro-drug), which significantly improved positive and negative symptoms of schizophrenia compared to placebo and olanzapine (**10**) in Phase II clinical trials (Figure 17).⁷⁸ However, some controversy exists around this initial chemical data as a second Phase II trial reported very high placebo effect, indistinguishable from therapeutic effects from olanzapine (**10**) and LY404039 (**18**).⁷⁹ This recent result called into question the therapeutic efficacy of the mGluR2/3 approach.

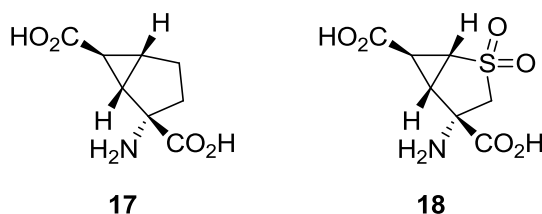


Figure 17: Lilly agonist LY354740 (**17**) and LY404039 (**18**).

1.4.2 Serotonin (5-HT)

A number of serotonin (5-HT, 5-hydroxytryptamine) receptor subtypes have been discovered to date: 5-HT_{1A-F}, 5-HT_{2A-C}, 5-HT₃, 5-HT₄, 5-HT₅, 5-HT₆ and 5-HT₇. Each of these receptors is a GPCR, except 5-HT₃, which is an ion channel, and all are activated by the endogenous neurotransmitter serotonin (**19**, Figure 18).^{80, 81}

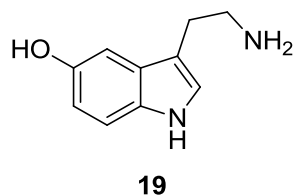


Figure 18: Serotonin (**19**).

Serotonin receptor function has been shown to be involved in mood, learning and memory, and cognition^{82, 83} and certain subtypes have been implicated in the pathophysiology of schizophrenia. The first line of evidence pointing toward serotonergic dysfunction as a facet of schizophrenia came from groundbreaking work from Glennon *et al.* They reported that hallucinogenic compounds such as lysergic acid diethylamide (LSD) (**20**), tryptamine (**21**) and phenylalkylamines such as phenylethylamine (**22**) (Figure 19) had great affinity for 5-HT₂ in *in vitro* binding assays and postulated a role for 5-HT₂ in their mechanism of action.⁸⁴

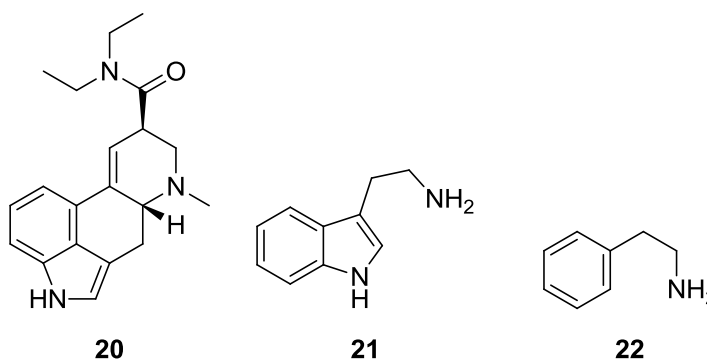


Figure 19: Psychoactive compounds, LSD (**20**), tryptamine (**21**) and phenylethylamine (**22**).

Further studies on more than 70 psychoactive tryptamine and phenylalkylamine compounds showed a positive correlation between psychotomimetic effect and 5-HT₂ binding affinities.⁸⁵⁻⁸⁷ However, additional work has indicated that selectivity between 5-HT_{1C} and 5-HT₂ is poor and drugs may be acting at both sites.⁸⁸

However, the 5-HT_{2A} receptor subtype in particular has been implicated in the mechanism of action of atypical antipsychotics by Meltzer *et al.*⁸⁹ They determined the D₁, D₂ and 5-HT_{2A} pK_i values for thirteen typical and seven atypical antipsychotic drugs and observed that most compounds displaying atypical antipsychotic activity had a D₂/5-HT_{2A} pK_i ratio of at least 1.12. When this ratio was applied to other antipsychotics, such as clozapine and risperidone, the compounds

were classified correctly with 92 % accuracy. Consequently, the atypicality of many antipsychotics is often attributed to high $D_2/5\text{-HT}_{2A}$ ratios, and these compounds are known as serotonin-dopamine antagonists. However, exemplar compounds of this type, such as clozapine and risperidone, still fall short of treating schizophrenia adequately.⁵¹

Other 5-HT receptor subtypes have gained increased interest in recent years, such as 5-HT₇, which was identified in 1993.⁹⁰ Through the synthesis of selective antagonists,⁹¹ 5-HT₇ has been suggested to play an important role in learning and memory, and has thus been implicated in schizophrenia.⁹²

Evidence that 5-HT₇ antagonism had potential as a schizophrenia therapy originally came from the findings that antagonists SB258741 (**23**) and SB269970 (**24**) could reverse the effects of PCP-induced reversal learning deficit in the rat (Figure 20).^{93, 94}

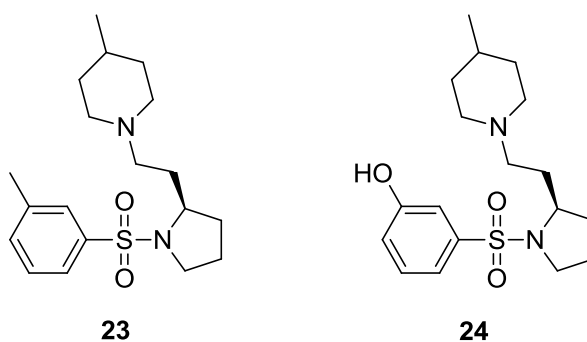


Figure 20: 5-HT₇ selective ligands: SB258741 (**23**) and SB269970 (**24**).

Additionally, a number of atypical antipsychotics display significant activity for 5-HT₇ such as risperidone (**11**) (Zyprexa) which has 20 fold selectivity for 5-HT_{2A} compared with D₂.⁹⁵

Furthermore, recent data from Meltzer *et al.* suggests that improvement of cognitive impairment by atypical antipsychotics in schizophrenia may be due to 5-HT₇ antagonism. They examined the effect of 5-HT₇ antagonism alone and with co-administration of an antipsychotic drug on a PCP-induced schizophrenia model in rats. Results showed that the selective 5-HT₇ antagonist, SB269970 (**24**), dose-dependently reversed the PCP-induced deficit and a sub-effective dose of SB269970 (**24**) in combination with sub-effective doses of atypical antipsychotics lurasidone

(**25**), amisulpride (**26**), or sulpiride (**27**) also reversed the PCP-induced deficit. Additionally, the improvement in PCP-induced deficits exhibited by amisulpride and lurasidone were reversed upon treatment with selective 5-HT₇ agonist AS19 (**28**) (Figure 21).⁹⁶

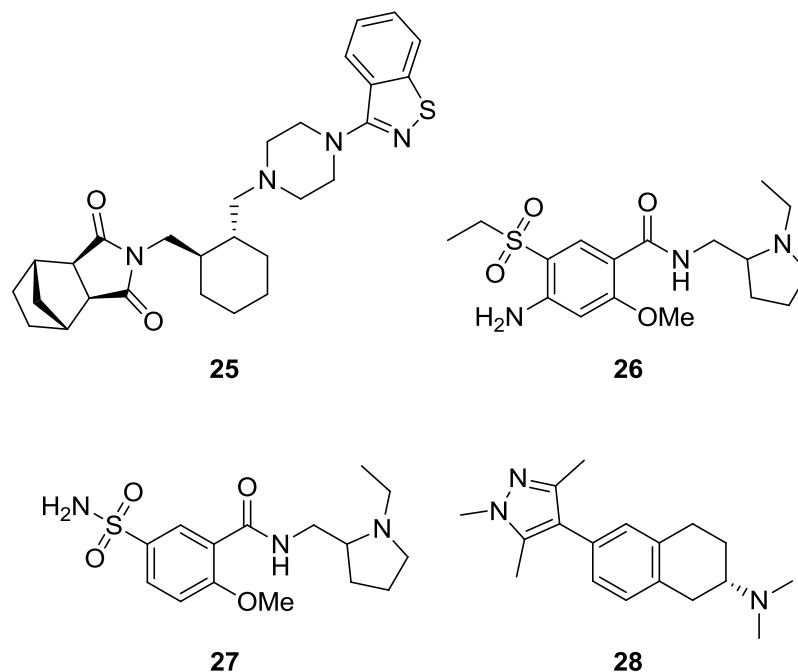


Figure 21: Atypical antipsychotics lurasidone (**25**), amisulpride (**26**), sulpiride (**27**) and 5-HT₇ selective agonist AS19 (**28**).

1.4.3 Muscarine

Acetylcholinergic dysfunction has been implicated in schizophrenia and there are two main types of cholinergic receptors, nicotinic and muscarinic, of which acetylcholine (**29**) is the natural ligand for both. Nicotinic acetylcholine receptors (nAChR) are ligand-gated ion channels and are particularly sensitive to nicotine (**30**) whereas muscarinic acetylcholine receptors (mAChR) are GPCRs and are particularly sensitive to muscarine (**31**) (Figure 22). Five muscarine subtypes, M₁, M₂, M₃, M₄ and M₅ have been cloned so far and are expressed throughout the CNS.⁹⁷

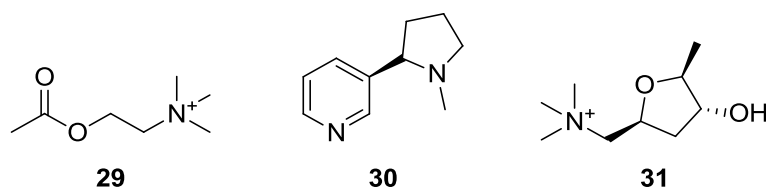


Figure 22: Endogenous ligands for acetylcholine receptors, acetylcholine (29), nicotine (30) and muscarine (31).

One of the first studies suggesting a role for acetylcholine (29) in management of psychiatric disorders was carried out in 1966. Neubauer *et al.* administered ditran (32, Figure 23) (a known psychotomimetic and anticholinergic drug) to a number of patients with psychiatric disorders including schizophrenia to induce a range of effects including neurological impairment, anxiety, thought disorder and hallucinations.⁹⁸

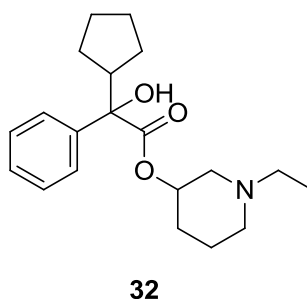


Figure 23: Ditran - 1-ethyl 3-piperidyl- α -phenylcyclopentylglycolate (32).

These results suggested that that reversal of acetylcholine blockade (agonism) could be therapeutically useful in schizophrenia and a more recent study found that galantamine (33, Figure 24), an acetylcholinesterase inhibitor (AChEI), increased cognition in schizophrenic patients stabilised on risperidone (11).⁹⁹ Furthermore, galantamine and a number of other AChEI compounds have been used extensively to improve cognitive deficits in Alzheimer's disease.¹⁰⁰

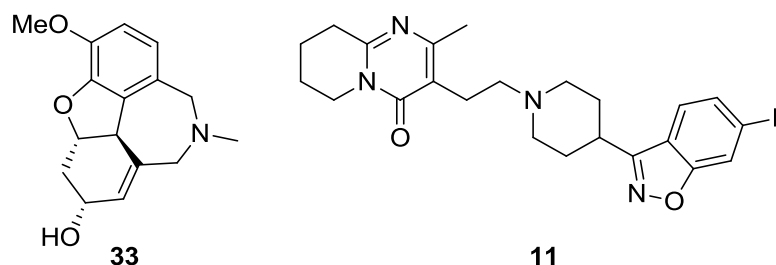


Figure 24: Acetylcholinesterase inhibitor galantamine (33) increases cognition in schizophrenic patients using risperidone (11).

Emerging evidence suggests that an M_4 receptor agonist in particular could be a rational target for the treatment of schizophrenia. Xanomeline (**34**, Figure 25), an M_1/M_4 selective agonist appears to be pharmacologically similar to atypical antipsychotics as observed in rats¹⁰¹ and inhibits amphetamine-induced schizophrenic behaviour in *Cebus apella* monkeys without inducing EPS, even with EPS-sensitised subjects.¹⁰²

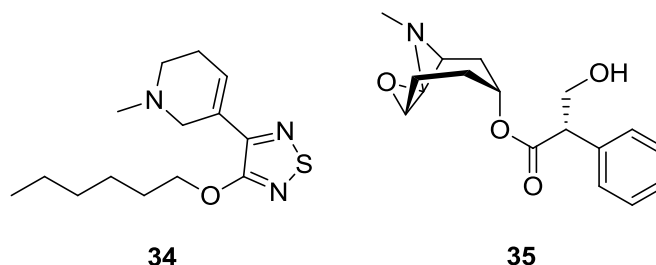


Figure 25: M_4 ligands, xanomeline (**34**) and *N*-methyl scopolamine (**35**).

Additionally, amphetamine-induced schizophrenic behaviour is alleviated by xanomeline (**34**) in wild type mice but importantly, this effect is absent in M_4 knockout mice.¹⁰³ Moreover, atypical antipsychotics such as clozapine (**9**) and olanzapine (**10**) are potent agonists at M_4 receptors with K_i values under 10 nM, therefore M_4 agonism could be key to the efficacy of these compounds.¹⁰⁴ Finally, *N*-methyl scopolamine (**35**, Figure 25), a muscarinic antagonist has been observed to impair working memory in healthy volunteers^{105, 106} providing further evidence for the role of M_4 agonism in improving cognition in schizophrenia.

The collective picture emerging is that it is unlikely that the pathophysiology of schizophrenia is caused by an abnormality in only one neurotransmitter system. The involvement of multiple receptors and signalling pathways is much more probable and supported by the fact that most atypical antipsychotics possess significant multi-receptor profiles in terms of their pharmacological activity. Consequently, more recent schizophrenia research has focused on multi-target compounds.

1.5 Multiple-target compounds

Rationally designed drugs that target more than one receptor simultaneously have gained increased attention in recent years and are generally designed in one of two ways: knowledge-based approaches or screening-led campaigns. Knowledge-based

approaches use existing biological data from known drugs to make new compounds, whereas screening approaches utilise high-throughput screening (HTS) of compound libraries to find compounds with the desired activity at each receptor.^{107, 108}

A number of drugs currently on the market have significant activity at more than one receptor but generally, this has been through serendipitous discovery utilising empirical pharmacology and not a designed feature. This has been observed for many antipsychotics, in particular for the early second generation atypical drugs (Table 3).

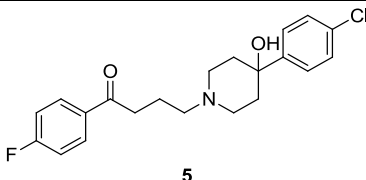
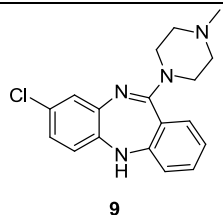
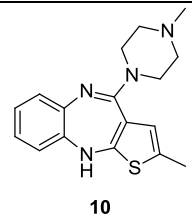
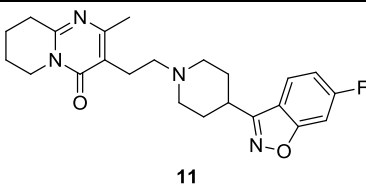
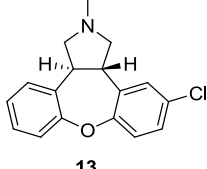
Name	Compound	K_i (nM)			
		D_2 (nM) ^a	5-HT _{2A} ^a	5-HT ₇ ^b	M ₄ ^a
Haloperidol	 5	1	78	263	N
Clozapine	 9	125	12	6.3	6
Olanzapine	 10	11	4	104	5
Risperidone	 11	3	0.6	1.4	N
Asenapine	 13	1.26 ^c	0.07 ^c	0.11 ^c	9120 ^c

Table 3: Selected receptor affinities adapted from ^aRoth *et al.*,¹⁰⁹ ^bBymaster *et al.*¹⁰⁴ and ^cShahid *et al.*¹¹⁰ N = inhibition of binding < 50 % at 10,000 nM.

With the exception of haloperidol (**5**), all these compounds were discovered to have a high $D_2/5\text{-HT}_{2A}$ ratio, thought to be the reason for the reduced EPS associated with these compounds.⁸⁹ A number of these compounds also display high affinity for 5-HT_7 (**9**, **11**, **13**) and M_4 (**9** and **10**), discussed previously as potential targets for schizophrenia. Clozapine (**9**), the most well-known atypical antipsychotic, was found to have a $D_2/5\text{-HT}_{2A}$ ratio of 10.4 but a high propensity to cause agranulocytosis.⁵³ Therefore, a number of compounds with a similar binding profile have been synthesised since to exploit this efficacy but induce fewer side-effects. Ziprasidone (**39**), developed by Pfizer, was one such drug and is composed of a number of pharmacophores (Figure 26).

Ziprasidone was identified through a combination of a dopamine-like fragment (**36**) with a 1-naphthylpiperazine fragment (**37**) to afford a compound with considerable activity at the desired receptors (**38**). However, incorporation of a 1,2-benzisothiazole unit (**39**) increased potency significantly whilst retaining a desirable $D_2/5\text{-HT}_{2A}$ ratio of 11, comparable to clozapine ($D_2/5\text{-HT}_{2A}$ ratio = 10.4). Ziprasidone (**39**) represents a novel efficacious atypical antipsychotic with low incidence of EPS and was launched in 2001 for the treatment of schizophrenia.^{111, 112}

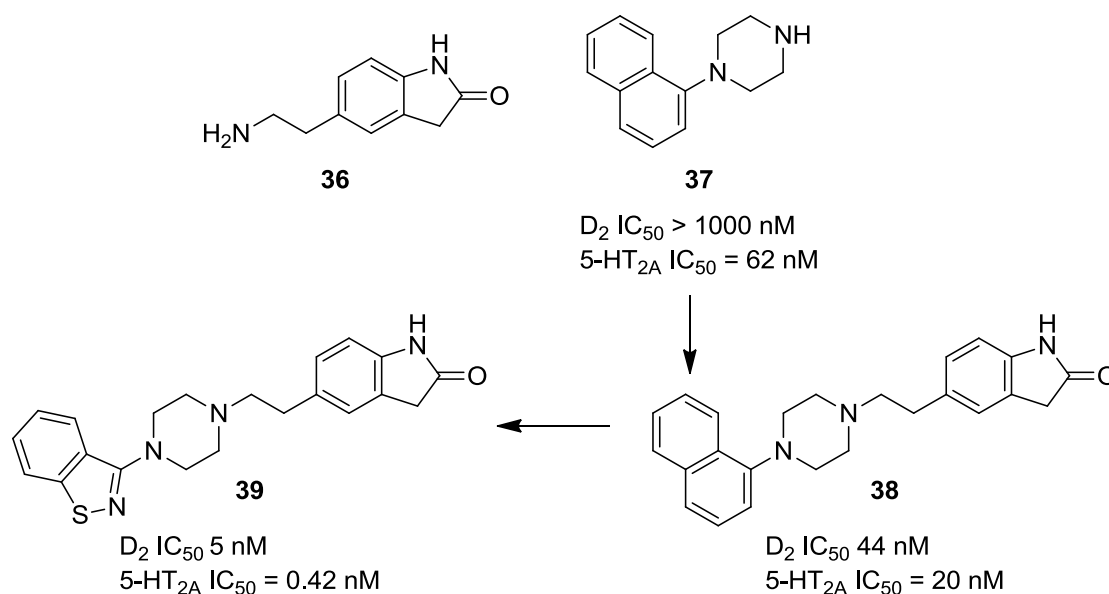


Figure 26: Rational design of ziprasidone (**39**).¹¹³

Although interest in rationally designed multiple target compounds is increasing, the field is still in its infancy and it is still a significant challenge to balance optimal

physicochemical and biological properties with reduced off-target hits. Additionally, the logistics of screening a large number of compounds is time and financially prohibitive for organisations other than large pharmaceutical companies. However, as more examples of serendipitous and rationally designed compounds are discovered, increased knowledge of the intricacies of designing multiple target compounds can be elucidated.

To summarise, none of the current therapies available for schizophrenia is able to effectively manage both positive and negative symptoms, at the same time as improving cognitive deficits and minimising side-effects. Many atypical antipsychotics have a broad pharmacological profile⁵⁴ due to their high affinity for a range of receptors, suggestive that a number of other receptors may be involved in the therapeutic effect.^{104, 109, 110} Therefore, compounds exploring other receptor subtypes could be beneficial to current knowledge of the pathophysiology of schizophrenia and could ultimately lead to novel therapies. In particular, there has been increased interest in 5-HT₇ and M₄ in the pathophysiology of schizophrenia, supported by the fact that a number of atypical antipsychotic compounds have significant affinity for these receptor subtypes (Table 3).

1.6 The *serominic* concept

As intimated above, typical antipsychotics such as haloperidol (**5**) (Figure 27) primarily treat the positive symptoms of schizophrenia and are often associated with extra-pyramidal symptoms (EPS)³² and tardive dyskinesia (TD).³³ Although the advent of atypical antipsychotics with reduced EPS represented a breakthrough in psychiatry, especially in treatment-resistant patients,¹¹⁴ significant side-effects are common¹¹⁵ and often resulting in non-compliance of the patient. Therefore, it is of paramount importance that new drug therapies for the management of psychotic disorders such as schizophrenia are investigated.

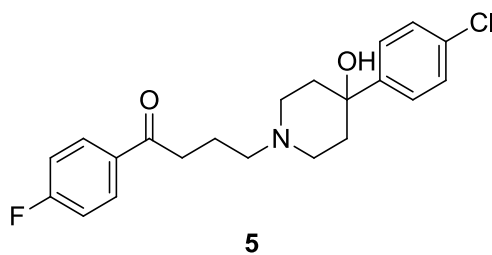


Figure 27: Typical antipsychotic, haloperidol (**5**).

As discussed previously, 5-HT₇ and M₄ receptors have been implicated in the pathogenesis of schizophrenia. 5-HT₇ antagonism has been associated with improvement of cognition especially in learning and memory⁸² and a number of typical and atypical antipsychotics, including clozapine and risperidone, have significant affinity for 5-HT₇.¹⁰⁹ M₄ agonists, such as xanomeline (**34**), induce antipsychotic-like effects in animal models^{101, 102, 116} and a number of atypical antipsychotics have M₄ agonist activity as part of their profile,¹¹⁷ most notably clozapine (**9**),¹¹⁸ and may have a role in their therapeutic efficacy. Furthermore, subsequent low D₂ antagonism may help alleviate positive symptoms without incidence of EPS.

Considering the above evidence, it was reasoned that a favourable multi-receptor profile for an antipsychotic drug could be a combined 5-HT₇ antagonist, M₄ agonist and low affinity D₂ antagonist. Such a profile is referred to herein as the *serominic* concept (**serotonin/muscarinic**).

As previously reported by co-workers,¹¹⁹ the Strathclyde Innovations in Drug Research (SIDR) natural products library at the University of Strathclyde was utilised to screen around 2000 plant extracts in radioligand 5-HT₇, M₄ and D₂ receptor binding assays.

Aporphine alkaloids such as liliotulipiferine (**40**) showed substantial ($K_i = 80$ nM) antagonism at the 5-HT₇ receptor but were inactive at the M₄ receptor ($K_i > 10$ μM). However, addition of an oxygen atom in ring C as demonstrated by liriodenine (**41**) increased M₄ agonism to sub-micromolar level (Table 4).

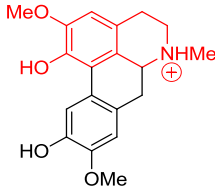
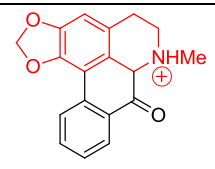
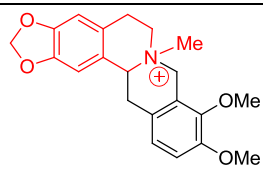
Compound	5-HT ₇ activity (K_i)	M ₄ activity (K_i)
 <p>40</p>	80 nM	inactive
 <p>41</p>	inactive	< 10 μM
 <p>42</p>	5 μM	2 μM

Table 4: Properties of aporphine alkaloids liliotulipiferine (**40**), liriodenine (**41**) and berberine (**42**). The 1,2,3,4-tetrahydroisoquinoline framework present in each is coloured red.

It was proposed that a multi-receptor *serominic* compound could be designed by hybridising features of liliotulipiferine (**40**) and liriodenine (**41**), namely the 1,2,3,4-tetrahydroisoquinoline framework (coloured red) retaining the hydrogen bond acceptors at the right hand side of the molecule. This was confirmed by the structurally similar library natural product, berberine (**42**), displaying micromolar activity for both 5-HT₇ ($K_i = 5 \mu\text{M}$) and M₄ ($K_i = 2 \mu\text{M}$) receptors, a *serominic* compound.

The dual receptor activity of this compound (**42**) can be rationalised by comparison with the natural ligands for 5-HT₇, serotonin (**19**) and M₄, muscarine (**31**) (Figure 28) denoted in red and blue, respectively. It appears that serotonergic activity in compounds such as berberine (**42**) hinges on the presence of an aromatic group (with hydroxyl or alkoxy substituents) at a distance of three bond lengths from a nitrogen atom (red). Similarly, muscarinic activity can be achieved by a positively ionisable nitrogen five bond lengths from a hydrogen bond acceptor (blue). This is further exemplified by Eli Lilly's muscarinic agonist (**43**) which was then used as a template for a compound with *serominic* activity.

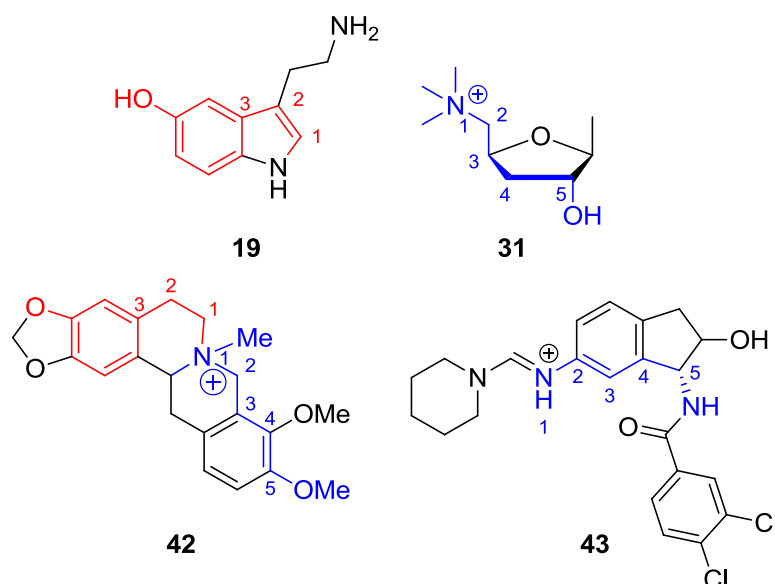


Figure 28: Structural similarities between berberine (**42**) and serotonin (**19**) (red) and Eli Lilly's M_4 agonist (**43**) and muscarine (**31**) (blue).

Pharmacologically, it is challenging to design a compound with two different receptors in mind. In order to strike the right balance, compounds must match the binding requirements for each receptor simultaneously. This can be achieved by designing a molecule where one side is 5-HT₇ responsive and one side is M_4 responsive, joined by an appropriate linker group. This strategy means that in principle each side of the molecule can be varied until the desired binding affinities for each receptor are reached.

After consideration of the above, essential pharmacophoric features likely to invoke *serominic* activity were identified (Figure 29):

- a framework containing a positive ionisable or quaternary nitrogen
- an aromatic system possibly with alkoxy substituents (5-HT₇ responsive group)
- a system with a hydrogen bond acceptor (M_4 responsive group)

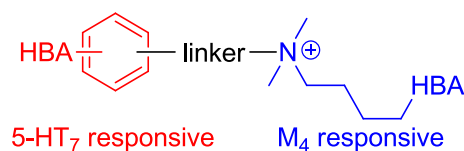


Figure 29: Pharmacophoric features potentially involved in *serominic* activity. Serotonergic features indicated in red, muscarinic features indicated in blue.

In the first instance, an exploratory series (*Series A*) was synthesised with a comparable molecular skeleton to the active natural products.¹¹⁹ Substituted 3,4-tetrahydro- β -carboline derivatives with side chain hydrogen bond acceptors were the focus of this series (Table 5). A number of compounds exhibited significant 5-HT₇ activity but were insufficiently M₄ active to be considered further (**48-50**). However, the D₂/5-HT₇ ratios observed were considered encouraging from a perspective of reducing EPS (**44-45**, **50**).

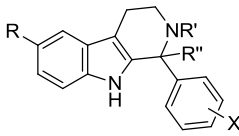
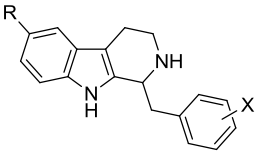
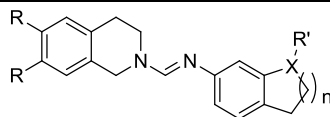
<i>Series A</i>							
 44-47				 48-50			
Compound	R	R'R''	X	5-HT ₇ K _i (μ M)	M ₄ K _i (μ M)	D ₂ K _i (μ M)	D ₂ /5-HT ₇ ratio
44	H	H H	3-OH	1.1	>30	88	80
45	H	H H	H	97	>300	>300	>300
46	H	=	3-OMe	0.8	42	31	39
47	H	H H	3-OMe	1.7	>300	-	-
48	H	-	3-OMe	0.026	35	1.6	62
49	OMe	-	3-OMe	0.045	18	1.5	33
50	H	-	3,4-OCH ₂ O	0.009	24	4.6	511

Table 5: Activity of selected compounds from *Series A*.

Series B was based on a 1,2,3,4-tetrahydroisoquinoline scaffold, observed in all the previously discussed natural products (**40-42**). This series was loosely based on Lilly's M₄ agonist (**43**): the general amidine-linked structure was retained and substituents varied on the tetrahydroisoquinoline and aliphatic benzofused ring, and the benzofused ring size modified (**51-57**, Table 6).

Series B



51-57

Compound	R	R'	n	X	5-HT ₇ K _i (μM)	M ₄ K _i (μM)	D ₂ K _i (μM)	D ₂ /5-HT ₇ ratio
51	OMe	OH	1	CH	0.4	0.3	>300	>750
52	H	OH	1	CH	2.7	2.8	>300	>111
53	OMe	OAc	1	CH	1.0	0.2	12.0	12
54	H	OAc	1	CH	0.1	1.6	1.7	17
55	OMe	OAc	2	CH	0.4	0.2	11.0	28
56	OMe	OAc	3	CH	0.5	0.2	14.0	28
57	OMe	CO ₂ Me	1	N	25.0	2.0	14.0	0.6

Table 6: Activity of selected compounds from *Series B*.

Several compounds in *Series B* showed significant binding to both 5-HT₇ and M₄ receptors and impressive D₂/5-HT₇ ratios (**51-52**), fulfilling the requirements for a *serominic* compound. M₄ functional assays were performed on two compounds with promising profiles, **51** and **55**, and the functional data indicated that both behaved as full agonists.¹¹⁹

In vivo antipsychotic activity of **51**, **53** and **55** was also assessed using the amphetamine-induced hyperactivity test in rats.⁴³ This assay was carried out at a dose of 10 mg/kg i.p. and despite the structural similarity and *in vitro* activity of the compounds, the corresponding *in vivo* activity was varied (Table 7). The most active compound, **51**, was found to suppress hyperactivity in a dose-dependent manner with an ED₅₀ of 8 mg/kg whereas **53** and **55** appeared to be inactive. This inactivity was attributed to differences in pharmacokinetics or CNS penetration of each compound.

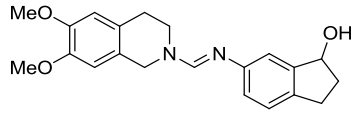
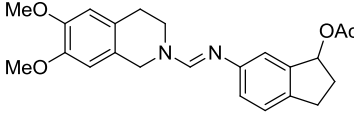
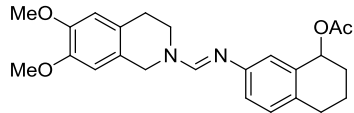
Compound	<i>In vitro</i> activity (K_i)			<i>In vivo</i> antipsychotic activity
	5-HT ₇	M ₄	D ₂	
 51	0.4	0.3	> 300	ED ₅₀ 8 mg/kg
 53	1.0	0.2	12.0	inactive
 55	0.4	0.2	11.0	inactive

Table 7: Assessment of *in vivo* antipsychotic activity of selected *serominic* compounds using the amphetamine-induced hyperactivity test in rats.¹¹⁹

Demonstrating antipsychotic activity without appreciable dopamine D₂ antagonism is a significant finding and these studies suggest the *serominic* concept is a promising area to investigate in the search for new antipsychotic drugs.¹¹⁹ Furthermore, formal design of a drug with a 5-HT₇ and M₄ multi-receptor profile allied with low D₂ antagonism is a novel approach to schizophrenia therapeutics.

The project collaborators, Mitsubishi Pharma Corporation, discovered that upon further profiling, the compounds displayed significant hERG (human ether à go go gene) activity and the series was temporised in favour of other assets. However, the project continued, but with a focus on reducing this undesirable off-target activity.

1.7 Human ether-à-go-go gene (hERG) activity

1.7.1 Structure and function of hERG

The human ether-à-go-go related gene (hERG) was discovered in 1994 having been identified as being closely related to the *Drosophila ether-à-go-go* gene family which encodes a voltage-gated K⁺ channel.¹²⁰ Information on structure and function of voltage-gated K⁺ ion channels (K_v) such as hERG has mainly been derived from mutagenesis studies by Mitcheson and Sanguinetti¹²¹ and X-ray crystal structures of

related bacterial and mammalian K^+ channels solved by the Mackinnon group.¹²²⁻¹²⁴ As a result, Professor Roderick Mackinnon was awarded the Nobel Prize in Chemistry for 2003 “*for structural and mechanistic studies of ion channels*”.¹²⁵

A single hERG subunit consists of 6 α -helical transmembrane domains (S1-6). The positively charged S4 domain senses membrane potential and S5-S6 make up the K^+ selectivity filter (Figure 30).

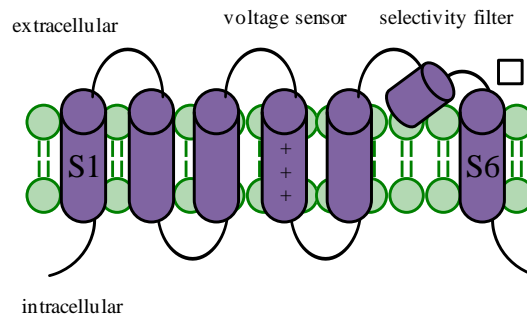


Figure 30: Schematic of a single hERG subunit comprising of transmembrane domains S1-S6.

Four identical subunits co-assemble to produce a functional tetrameric hERG channel, which allows passage of K^+ ions through a selectivity filter (Figure 31). This selectivity filter is highly conserved within voltage-gated potassium (K_v) channels which exhibit a signature amino acid sequence capable of coordinating potassium ions (Thr-Val-Gly-Tyr-Gly).¹²⁶

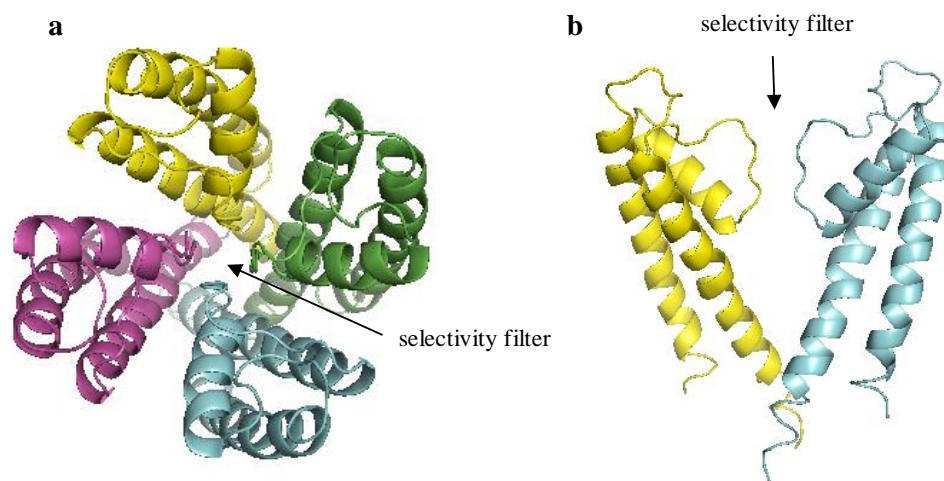


Figure 31: ^aCo-assembly of four bacterial KcsA ion channel subunits to form a tetrameric structure allowing passage of K^+ ions through the central selectivity pore.¹²² PDB ID 1BL8.¹²⁷ ^bStructure of a bacterial KcsA K^+ channel crystallized in the closed state. Only two of the four subunits are shown.¹²² PDB ID 1BL8.¹²⁷

Voltage-gated ion channels such as K_v are activated by changes in electrical potential difference near the channel, which induces a conformational change to either allow or disallow ions from passing through the cell membrane. At negative membrane potentials, the channel is closed, but depolarisation of the membrane induces the channel to open and allow passage of K^+ . As the membrane is depolarised further, the channel becomes inactivated (biophysically different from the closed state), and remains so until repolarisation (Figure 32).

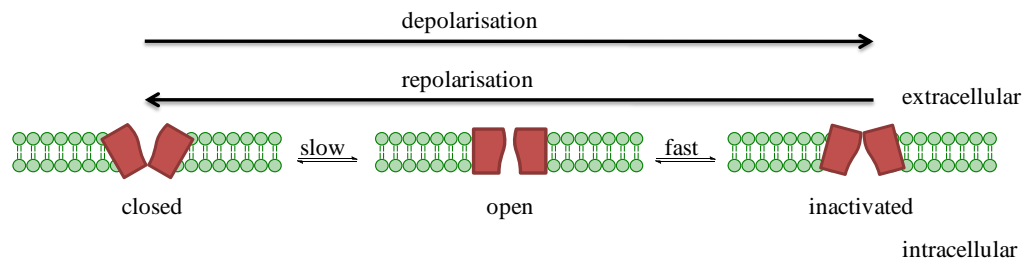


Figure 32: A hERG channel changes conformation depending on voltage. At negative voltages, channels are closed and membrane depolarisation slowly activates the channels, which then becomes inactivated rapidly, especially at higher potentials. Repolarisation of the membrane reverses the states.

The hERG channel is significantly expressed in the heart and plays a pivotal role in cardiac action potential as it conducts the rapid delayed rectifier K^+ current (I_{Kr}), discovered after mutations in hERG were found to cause long QT syndrome (LQTS).¹²⁸ The QT interval is measured by electrocardiogram (ECG) as the time taken for ventricular repolarisation during a single cardiac cycle and accordingly, LQTS is the prolongation of this interval (Figure 33). This leads to delayed cardiac muscle repolarisation that can induce torsades de pointes (TdP), a cardiac arrhythmia that can degenerate into ventricular fibrillation and cause sudden death.¹²⁹

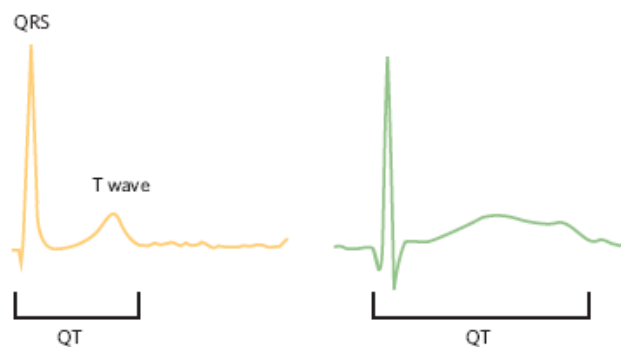


Figure 33: Normal ECG trace for a single cardiac cycle (left) and abnormal ECG trace with prolonged QT interval (right). The QRS complex represents depolarization, and the T wave indicates repolarisation of the ventricles.¹³⁰ Permission to reproduce figure was obtained from Nature through RightsLink® - license number - 2841910807255.

Although a number of ion channels are involved in cardiac repolarisation and congenital LQTS and subsequent TdP can be attributed to mutations in several of these,¹³¹ drug-induced LQTS has only been induced by hERG channel blockers clinically. Consequently, hERG has emerged as an important target for screening as a surrogate marker for cardiotoxicity.^{132, 133}

1.7.2 Drug-induced hERG blockade

Many drugs covering a wide range of therapeutic classes block hERG channels and cause QT liability. Compounds which significantly block hERG include antihistamines astemizole (**58**)¹³⁴ and terfenadine (**59**);^{34, 135} antiarrhythmics promethazine¹³⁶ and disopyramide;¹³⁷ a number of antipsychotics haloperidol (**5**),³⁴ sertindole (**60**),³⁴ thioridazine,³⁴ clozapine (**9**)¹³⁸ and risperidone (**11**);¹³⁹ as well as antimicrobial drugs such as grepafloxacin (**61**).¹⁴⁰ A number of blockbuster drugs within these important therapy areas have been withdrawn from the market due to instances of QT prolongation associated with hERG liability (Figure 34).

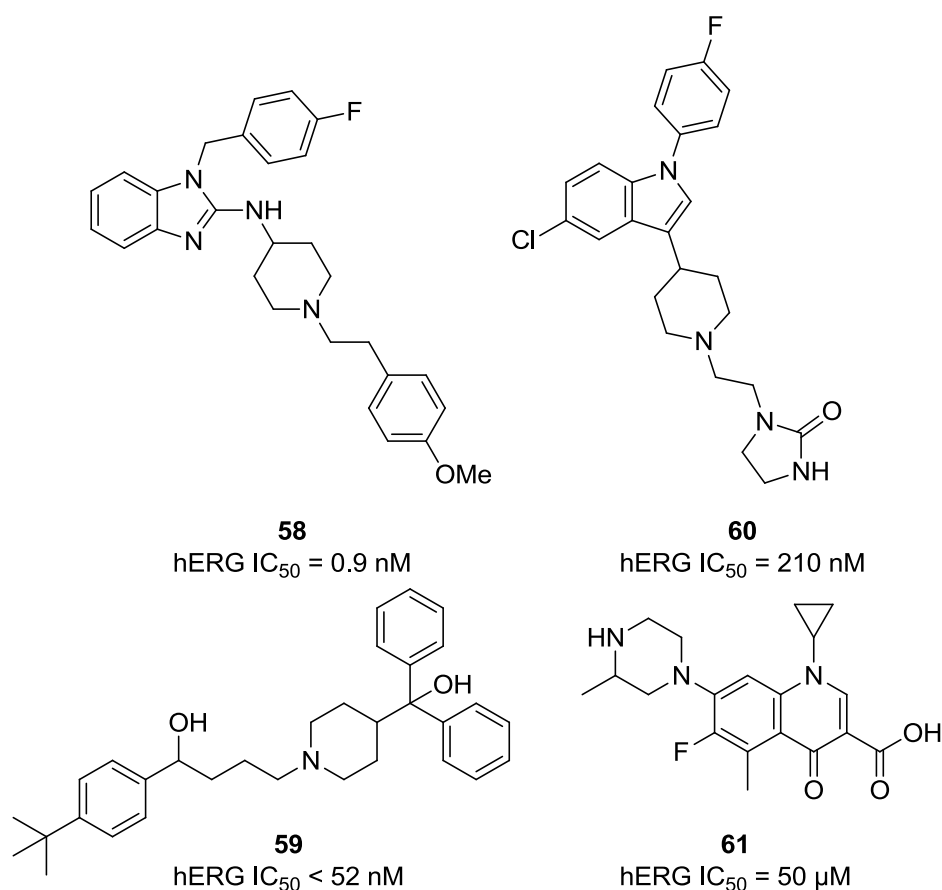


Figure 34: Blockbuster drugs withdrawn from the market due to hERG liability; antihistamines astemizole (**58**)¹³⁴ and terfenadine (**59**),^{12, 13} antipsychotic sertindole (**60**),³⁴ and antimicrobial grepafloxacin (**61**).¹⁴⁰

From consideration of homology models of hERG derived from bacterial channel KcsA it is apparent that the hERG channel has a large and promiscuous binding site to which many chemically diverse compounds bind.³⁴ Although LQTS could potentially be caused by drugs binding to a number of K⁺ channels involved in cardiac action potential, drug-induced LQTS has only been observed to be caused by blockade of hERG. This is attributed to a number of structural variations between hERG and other K_v channels. The pore helix is generally conserved between K_v channels but in the S6 region, hERG has Tyr and Phe residues whereas structural homologues generally have Ile and Val in these positions.¹⁴¹ These side chains face the inner cavity of the ion channel and alanine scanning mutagenesis has shown that aromatic residues Tyr652 and Phe656 on region S6 are required for potent block of hERG by MK-499 (**62**, Figure 35), a well-characterised hERG blocker.^{121, 142}

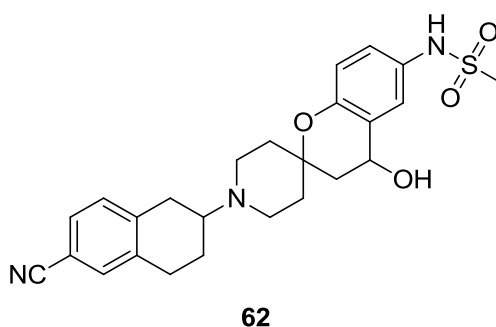


Figure 35: MK-499, a well-known hERG channel blocker (**62**).

The prevalence of drug binding for hERG over other K_v channels may be a result of these key Tyr652 and Phe656 residues. Moreover, other potassium channels generally contain Pro at one or both positions flanking Phe656 in hERG which is thought to introduce kinks in the inner cavity and an associated decrease in cavity size which may hinder drug binding.¹⁴³ Finally, polar interactions with polar residues Thr623 and Ser624 may be a key interaction of hERG blockers.¹⁴⁴

To summarise, mutagenesis studies allied with homology models have implicated a number of key interactions for hERG blockade: π -cation interaction with a basic nitrogen and Tyr652, π - π stacking with Phe656 or Tyr652, additional hydrophobic interactions with other Phe656 side chain and polar interactions with Thr623 and Ser624 at the bottom of the pore helix.^{121, 141, 145-147} A schematic of potential crucial interactions between a hERG blocker and hERG can thus be drawn (Figure 36). A typical hERG blocker will have hydrophobic interactions with Phe656, positive charge stabilisation by Tyr652 and either hydrophobic or hydrogen bond acceptor interactions with Thr623 and Ser624.¹⁴⁴

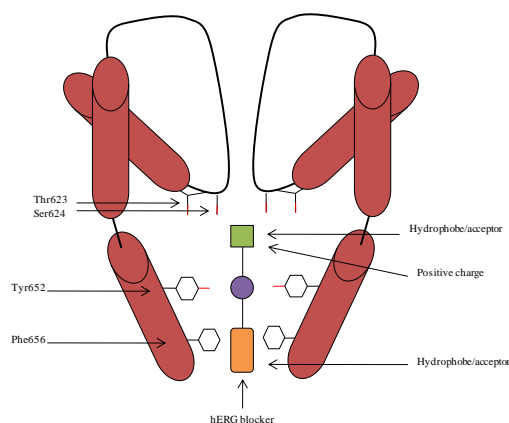


Figure 36: Schematic of hERG potassium channel with hERG blocker bound with a proposed hydrophobic interaction with Phe656, positive charge stabilisation by a cation– π interaction with Tyr652 and further hydrophobic and/or polar interactions with Thr623 and Ser624.¹⁴⁴ Adapted from reference.¹⁴⁴

1.7.3 Mitigating undesirable hERG activity

There are a number of *in silico* pharmacophoric models available to assess hERG activity¹⁴⁸⁻¹⁵¹ but a plethora of SAR data has been compiled in recent years leading to increased understanding of chemical characteristics likely to invoke undesirable hERG affinity. This has led to four known strategies used to mitigate hERG activity of a compound: manipulation of clogP, discrete structural modifications, use of zwitterions and lowering of pK_a .¹⁵²

1.7.3.1 Reducing clogP

Reducing lipophilicity is now a well-known strategy to mitigate hERG activity. In 2007, AstraZeneca screened over 7000 basic, neutral and acidic compounds in-house and proposed that reducing clogP below a threshold of 3 should reduce hERG activity.¹⁵³ Numerous examples appear in the literature supporting a correlation between hERG blockade and clogP (Table 8). For example, Vaz *et al.* from Aventis introduced a carboxamide substituent (**64**) to their series of human β -tryptase inhibitors (**63**) to reduce clogP by > 1 unit with a concomitant reduction in hERG.¹⁵⁴ Price *et al.* from Pfizer thoroughly explored SAR in their discovery of the CCR5 antagonist, maraviroc, and a number of compounds exhibited a hERG-clogP correlation such as **65** and **66**.¹⁵⁵ Irie *et al.* from Novartis reported a number of orally active and brain-penetrant cathepsin S selective inhibitors with low clogP, exemplified by the replacement of *N*-isopropyl (**67**) to the less basic *N*-acetyl (**68**) to

afford a 100-fold reduction in hERG activity although the effect of pK_a in this instance cannot be negated.¹⁵⁶

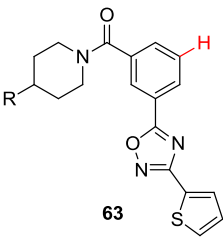
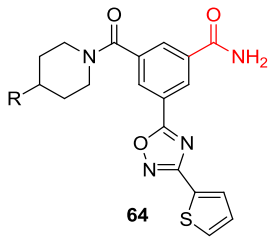
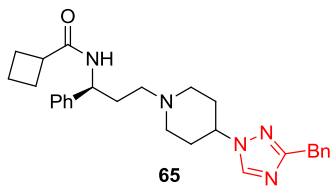
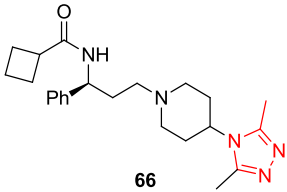
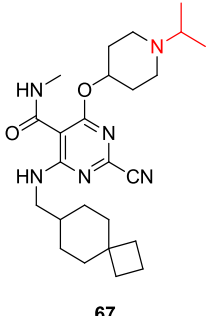
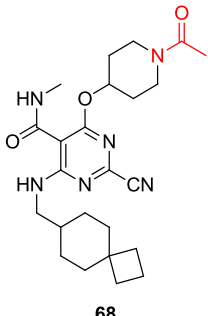
Compound	hERG activity	clogP	hERG optimised compound	hERG activity	clogP
 63	800 nM ¹⁵⁴	3.82	 64	17 μM	2.73
 65	44 % at 100 nM ¹⁵⁵	3.30	 66	5 % at 100 nM	1.52
 67	540 nM ¹⁵⁶	5.36	 68	> 30,000 nM	3.30

Table 8: Literature examples of series-dependant correlation between clogP and hERG activity.

1.7.3.2 Introduction of zwitterions

Use of zwitterions to detune hERG activity was first explored after the discovery that the therapeutic efficacy of terfenadine, (**69**, Table 9) (a second generation antihistamine, withdrawn from the market due to QT prolongation) was induced mainly by a carboxylate metabolite, which displayed no cardiotoxic effects. This carboxylate analogue was later marketed as blockbuster fexofenadine (**70**).¹⁵⁷ Zhang *et al.* observed a drop in hERG affinity between a methyl ester (**71**) and its carboxylic acid analogue (**72**) in their series of CCR2 antagonists.¹⁵⁸ Similarly, Zhu *et al.* found that the majority of their benzimidazole-containing factor Xa inhibitors displayed significant hERG activity (**73**) but incorporation of a carboxylate group at various locations resulted in hERG inactive compounds (**74**).¹⁵⁹

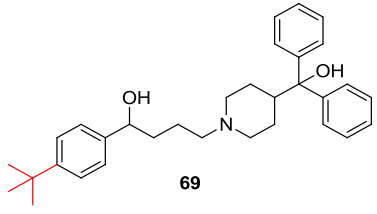
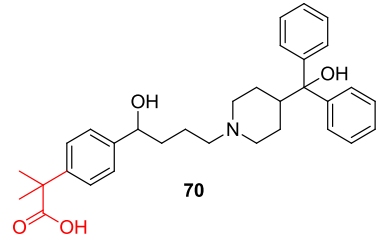
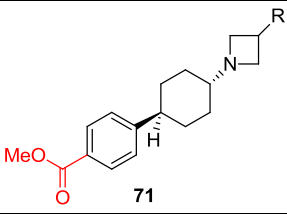
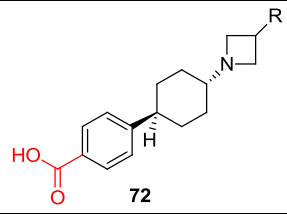
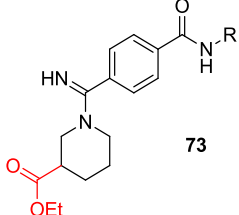
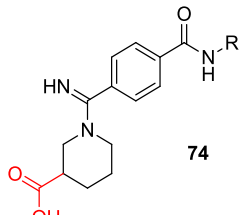
Compound	hERG activity	hERG optimised compound	hERG activity
 69	1 nM ¹⁵⁷	 70	15 nM
 71	1.3 μM ¹⁵⁸	 72	23.0 μM
 73	16 nM ¹⁵⁹	 74	> 10 μM

Table 9: Literature examples of series-dependant correlation between incorporation of zwitterion and hERG activity.

1.7.3.3 Discrete structural modifications

Discrete structural modifications encompass a wide range of more subtle modifications to a drug scaffold resulting in reduction of hERG activity, however, with no significant difference to other parameters known to affect hERG such as pK_a and $clogP$. This is demonstrated by Rao *et al.*¹⁶⁰ within their series of H₃ antagonists where switching from a 4-substituted (**75**, Table 10) to a 3-substituted pyridine (**76**) reduced hERG inhibition by over 40 % at 10 μM. Bregman *et al.* observed a similar effect in Na_v1.7 antagonists by changing from a pyrimidine (**77**) to a pyrazine (**78**) ring.¹⁶¹ Finally, in their series of VEGFR-2 inhibitors Sisko *et al.* simply removed a methyl group from a methyl-piperazine ring (**79**) to reduce hERG affinity significantly (**80**).¹⁶²

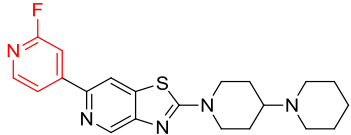
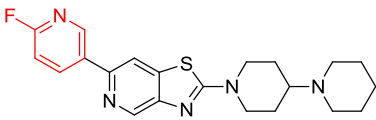
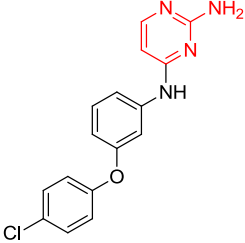
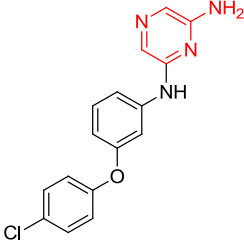
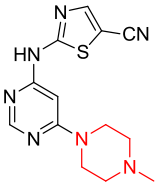
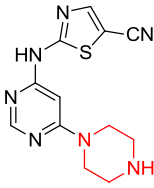
Compound	hERG activity	hERG optimised compound	hERG activity
	85 % at 10 μM ¹⁶⁰		51 % at 10 μM
75		76	
	0.3 μM ¹⁶¹		2.9 μM
77		78	
	0.9 μM ¹⁶²		21.5 μM
79		80	

Table 10: Literature examples of series-dependant correlation between introduction of discrete structural modifications and inhibition of hERG activity.

1.7.3.4 Reduction of pK_a

Reducing the pK_a of a basic nitrogen moiety can have a dramatic effect on hERG potency. An example of this is shown in Table 11 where Brown *et al.* found that replacing a basic secondary amine (**81**) with a non-basic amide analogue (**82**) reduced hERG activity 10-fold for their NR2B site NMDA antagonists.¹⁶³ Replacement of a piperazine ring (**83**) with a cyano-substituted piperidine (**84**) greatly decreased hERG affinity of a selective allosteric M_1 receptor modulator, as reported by Kuduk *et al.*¹⁶⁴ Interestingly, the starting compound is zwitterionic but still exhibits a degree of hERG activity. Furthermore, Nugiel *et al.* describe the first reported potent, non-basic functionally active antagonists of the 5-HT_{1B} receptor. These are based on a known 5-HT_{1B} antagonist template (**85**) but replacement of a piperazine with a substituted pyrazole and exchange of a morpholine group for an ether moiety (**86**) resulted in a 5-fold decrease in hERG affinity.

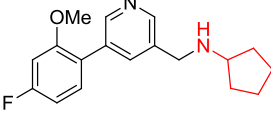
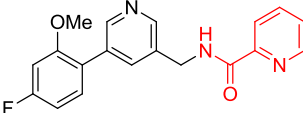
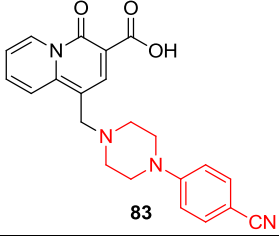
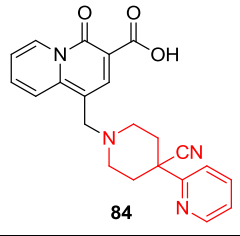
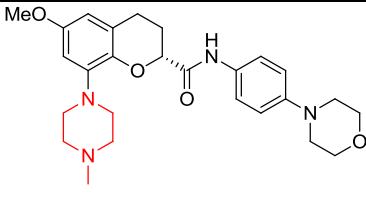
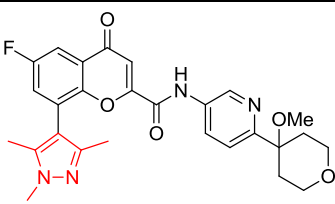
Compound	hERG activity	hERG optimised compound	hERG activity
 81	2 μM ¹⁶³	 82	27 μM
 83	7 μM ¹⁶⁴	 84	> 30 μM
 85	19 μM ¹⁶⁵	 86	95 μM

Table 11: Literature examples of series-dependant correlation between pK_a and hERG activity.

Additional examples have been reviewed more extensively in the literature¹⁵² but it is clear to see that lipophilic, hydrophobic drug compounds with basic nitrogen atoms are likely to exhibit hERG activity as well as wider off-target activity.^{166, 167} Having stated this it is possible, through a series of modifications, to reduce this undesirable activity. In the context of this programme of work and as previously discussed, the lead amidine compound (**53**),¹¹⁹ which displays hERG activity, will be modified in a number of ways, initially focusing on pK_a , however there will be significant interplay with the other strategies identified.

1.8 Research programme

The overall aim of the research programme is to synthesise novel compounds, active at both 5-HT₇ and M₄ receptors (*serominic*) with low hERG activity as potential pathfinder molecules towards novel treatment units in schizophrenia.

Firstly, the *serominic* lead from previously reported work will be synthesised for use as an internal control in *in vitro* assays (**53**, Figure 37).¹¹⁹

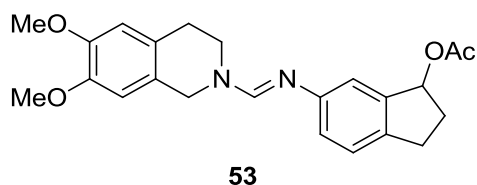


Figure 37: Previously prepared *serominic* compound (**53**) to be synthesised as a control compound.

Undesirable hERG activity was reported for the amidine compounds, and may be ascribed to their basicity. Amidines have a pK_a of 12, therefore a positive charge is present at physiological pH (Figure 38).¹⁶⁸

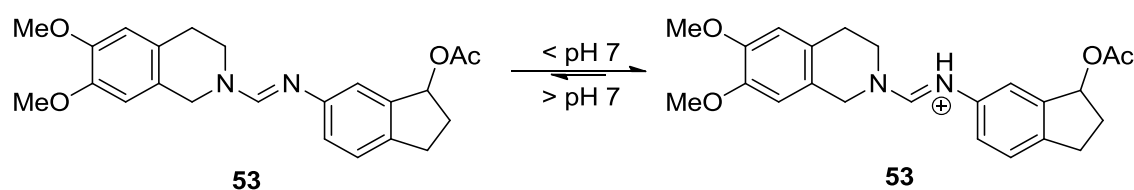


Figure 38: Charge of amidine compound **53** above and below pH 7.

In the context of hERG optimisation, and as discussed above, basic nitrogen atoms are known to engage in a key interaction within the hERG channel.¹⁴⁶ Aronov described this schematically by comparing the general conformation of a drug compound and placement of positively ionisable atom with hERG activity (Figure 39).¹⁴⁴

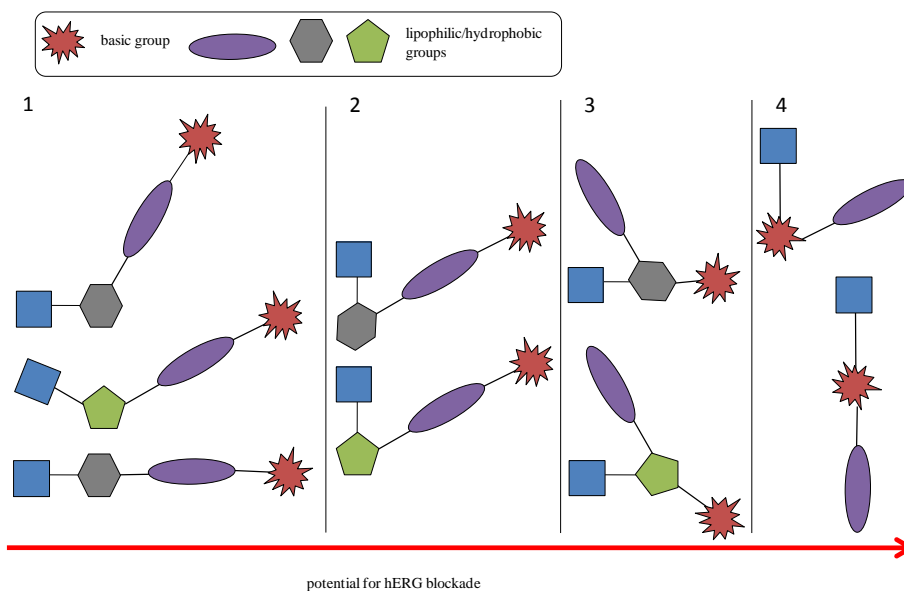


Figure 39: Potential for hERG blockade based on placement of basic group and conformation of molecule.¹⁴⁴ Adapted from reference.¹⁴⁴

The amidine-linked compounds obviously fall into the risky category (4) for undesirable hERG activity due to the basic nitrogen in the central part of the molecule. Consequently, reducing this basicity should destabilise this key interaction and potentially mitigate hERG activity of a given compound. Therefore, pK_a modulation is the main initial focus of this research programme, although variation of logP and the zwitterion approach will be explored.

This approach, of modulating pK_a whilst retaining a biologically active compound, is exemplified by the development of cimetidine, the world's first blockbuster drug.¹⁶⁹ Chemists at SmithKline and French were investigating anti-peptic ulcer drugs through ligand-based drug design, starting from the endogenous ligand, histamine (**87**, Figure 40). Upon the discovery that the structurally similar guanidine analogue (**88**) acted as an agonist at histamine receptor H_2 , it was thought that the positive charge may contribute to this undesirable activity ($pK_a = 14$)¹⁶⁸. Less basic analogues were investigated and a thiourea derivative, burimamide (**89**) ($pK_a -1.2$)¹⁶⁸ was found to have antagonistic properties alongside increased efficacy. Unfortunately, burimamide could not be given orally. However, a number of structural variations led to cimetidine (**90**), ($pK_a -0.4$)¹⁶⁸ a neutral, orally-available, high efficacy drug for peptic ulcers, the first of its kind.^{170, 171} Development of these anti-ulcer drugs is an important example of rational drug design from an endogenous ligand, histamine (**87**), for which Sir James Black received the Nobel Prize for Physiology or Medicine in 1988.¹⁷²

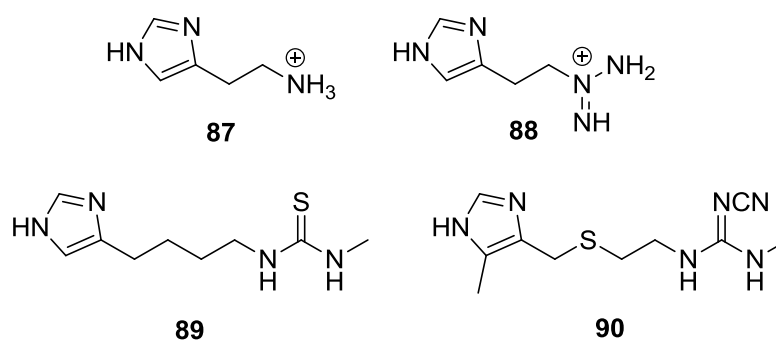


Figure 40: Cimetidine optimisation trajectory: histamine (**87**), a guanidine analogue (**88**), burimamide (**89**) and cimetidine (**90**).

Based on the above, a strategy mimicking this highly encouraging precedent was adopted. The simplest way to decrease basicity of the basic amidine nitrogen (**53**) in the current lead series is to introduce electron-withdrawing linker groups (EWG) in place of the amidine linker (**91-96**, Figure 41). These compounds will be significantly less basic, even neutral at physiological pH.

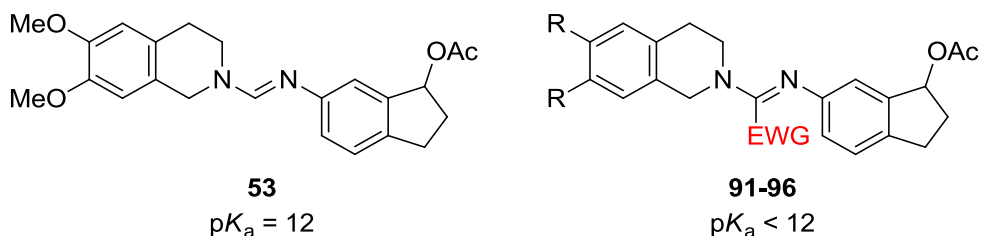


Figure 41: pK_a attenuation of amidine **53** upon insertion of EWG.

Accordingly, a range of alternative non-basic linkers were chosen, and the selection focused on encompassing a range of pK_a values, electronics and substituent bulk. Additionally, this will explore the role of conformation in hERG activity as some linkers allow free conformational flexibility and others are fixed.

The linkers selected were nitroalkene (**91**), cyanoguanidine (**92**), urea (**93**), hydrazide (**94**), triazene (**95**) and trifluoromethyl (**96**) substituents. These modifications were considered to be synthetically facile to implement and can be obtained, in principle, in an unprotracted manner using easily available starting materials.

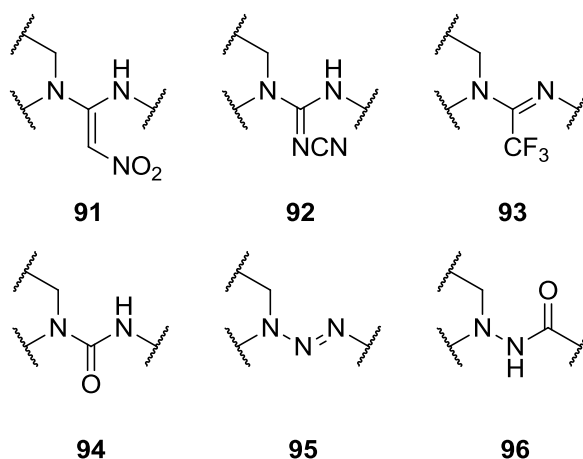


Figure 42: Alternative linkers to amidine (**91-96**) with reduced pK_a .

As discussed previously, the *serominic* amidine lead series can be divided into two fragments (Figure 43): a 5-HT₇ responsive fragment (red), and an M₄ responsive fragment (blue) joined by a 3-atom spacer (amidine).

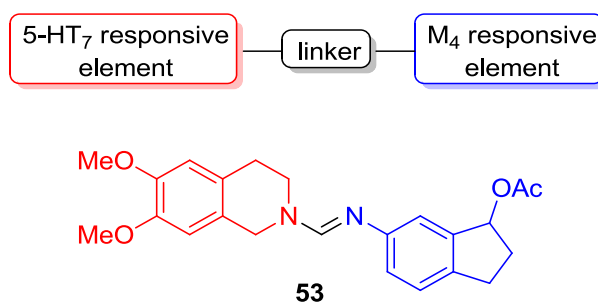


Figure 43: 5-HT₇ responsive fragment (red), and an M₄ responsive fragment (blue).

In addition to implementing electron-withdrawing linkers in place of the original amidine linker to mitigate hERG activity, a sub-goal of this programme will be to explore SAR around the *serominic* template. Structural changes to the M₄ responsive side, retaining the hydrogen-bond acceptor attached to the benzylic position, will be introduced using (*S*)-acetoxy (**98**), (*R*)-acetoxy (**99**), methyl ester (**100**), ethyl ester (**101**), carboxylate (**102**), phthalide (**103**), ketone (**104**), and hydroxyl (**105**) derivatives in place of the racemic acetoxy group (**97**) (Figure 44).

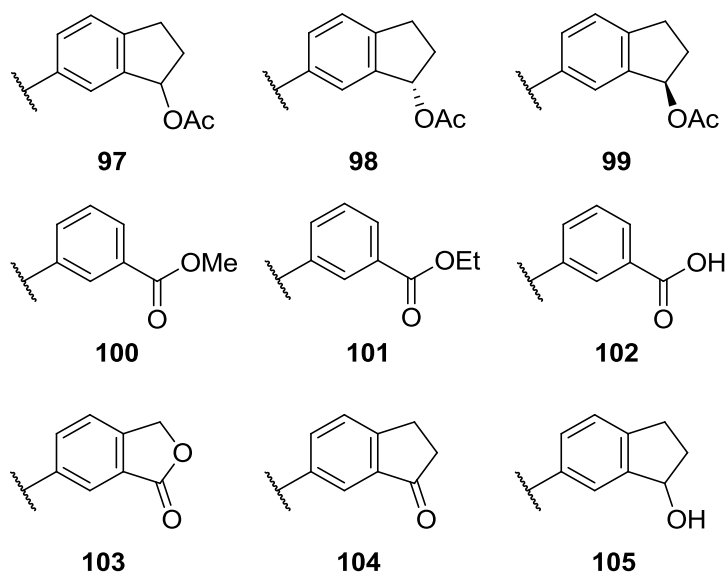


Figure 44: M₄ responsive SAR to be investigated.

Additionally, further investigation of the SAR between 6,7-dimethoxy substituted and unsubstituted 1,2,3,4-tetrahydroisoquinolines will also be investigated alongside other potentially 5-HT₇ responsive groups.

To summarise, the project was divided into two main areas, synthesis of new chemical entities and biological evaluation of these novel compounds. The main synthetic objective was to employ target-based synthesis to furnish a number of novel compounds encompassing a range of structural modifications: 5-HT₇ responsive, M₄ responsive, and linker modifications. The main biological objective was to develop radioligand binding bioassays using cell culturing and membrane preparatory techniques in Strathclyde Institute of Pharmacy and Biomedical Sciences. Biological evaluation would then ascertain which structural modifications are conducive to *serominic* activity and explore the effect of these changes on hERG activity.

Chapter 2 - Results and discussion

2.1 Amidine-linked compounds

2.1.1 Resynthesis of amidine units

As noted above in the case of the lead *seromycin* series, the amidine functional group is associated with significant biological activity and features in a number of naturally occurring and synthetic compounds of considerable importance. Natural products containing this functionality include the antiviral metabolite noformicin (**106**, Figure 45), isolated from *Nocardia formica*,¹⁷³ and the polypyrrole antibiotic distamycin A (**107**), isolated from *Streptomyces distallicus*.¹⁷⁴ Significant attention has been focused on analogues of distamycin A in particular and more potent and selective antibiotics have been discovered in recent years.¹⁷⁵

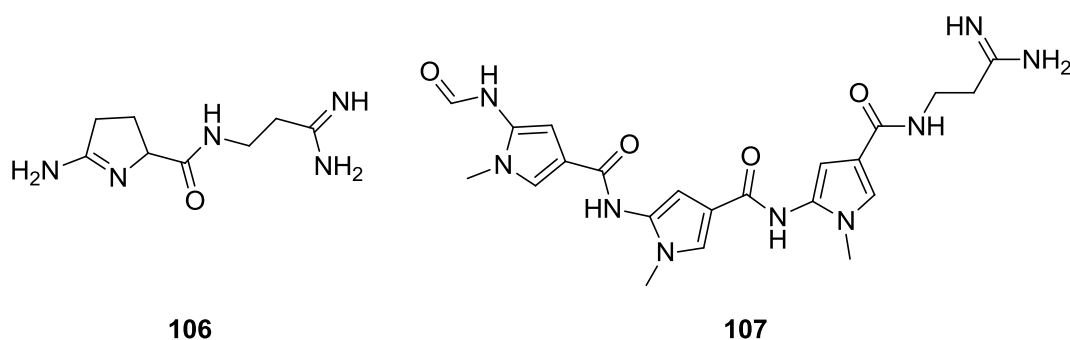


Figure 45: Noformicin (**106**) and distamycin A (**107**).

Amidines are also present in antiprotozoal drugs, many examples of which incorporate two benzimidazole units with an unsubstituted amidine functionality separated by a structural unit such as pentamidine (**108**, Figure 46).^{176, 177} Furthermore, cyclic amidines such as **109** have been used as chemotherapeutics.¹⁷⁸

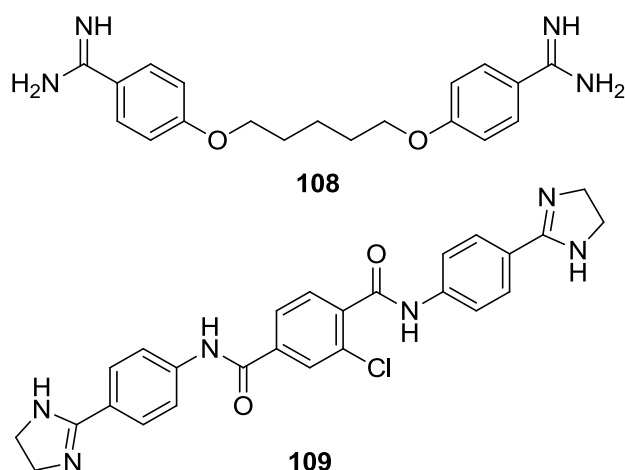
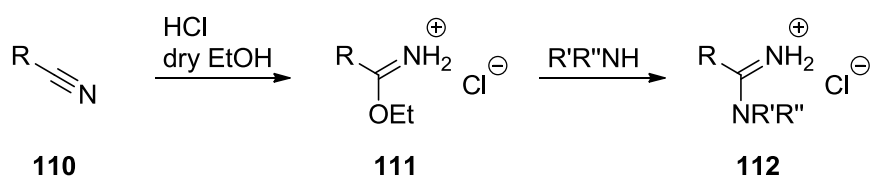


Figure 46: Amidine-containing antiprotozoal (**108**) and chemotherapeutic drugs (**109**).

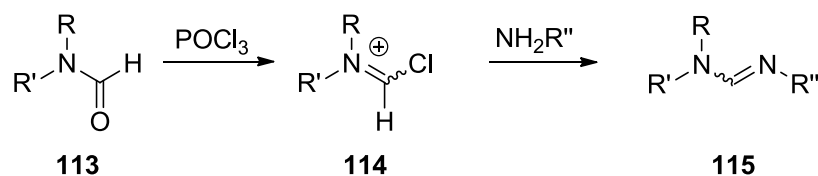
As substituted and unsubstituted amidine functional groups feature in many biologically active compounds, there is considerable interest in synthetic methods enabling their preparation.

Conventionally, amidine synthesis is achieved using the Pinner reaction (Scheme 1).¹⁷⁹ This involves reaction of a nitrile (**110**) and an alcohol in the presence of an acid catalyst, usually hydrochloric acid, to form an imidate salt (**111**). This imidate salt can be treated with ammonia or a secondary amine to furnish the desired amidines in high yield (**112**). Unfortunately there are limitations with the Pinner reaction: starting nitriles are often not readily available, and most importantly, *N,N'*-disubstituted amidines cannot be synthesised.



Scheme 1: Pinner reaction.

N,N'-disubstituted amidines (**115**, Scheme 2), however, can be easily prepared through imidoyl chloride intermediates (**114**) obtained by condensation of *N,N*-disubstituted formamides (**113**) with halogenating reagents such as phosphoryl chloride (POCl₃). Formamides are more suitable starting materials than substituted nitriles as they can be easily prepared from primary or secondary amines by formylation.



Scheme 2: Condensation of formamide (**113**) using POCl₃ for synthesis of *N,N'*-disubstituted amidines (**115**).

In the context of target synthesis of the amidines in the lead *serominic* series, *N*-formylation was achieved by aminolysis of the commercially available 6,7-dimethoxy-1,2,3,4-tetrahydroisoquinoline (**116**) and 1,2,3,4-tetrahydroisoquinoline (**117**) precursors under refluxing conditions using methyl formate in methanol to yield **118** and **119** in 60 % and 34 %, respectively (Table 12).

Additionally, *N*-formylation of 1,2,3,4-tetrahydroisoquinoline (**117**) was then repeated utilising microwave irradiation (MW) at 160 °C with the dual benefit of improving the yield to 77 % whilst concomitantly reducing reaction time from 18 h to 1 h.

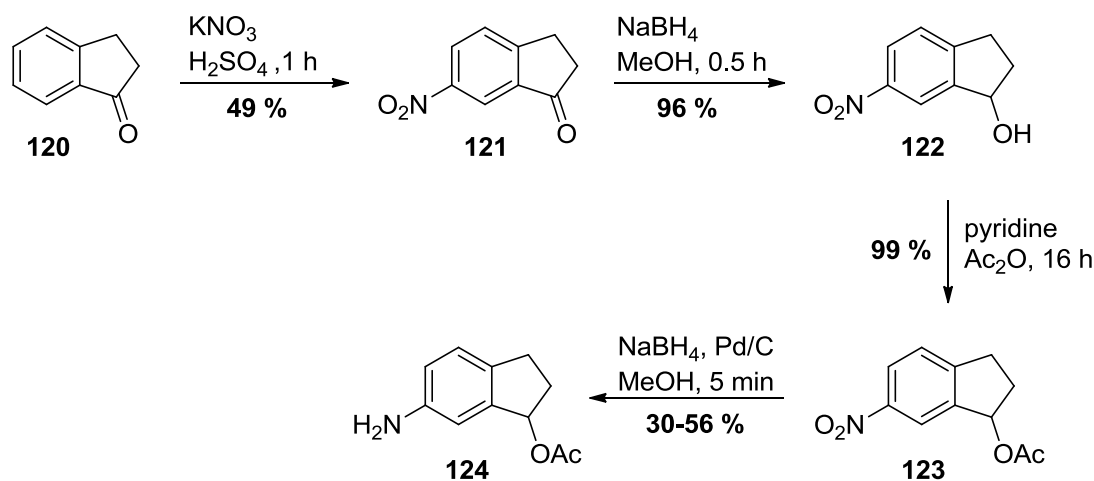
The reaction shows the N-formylation of 1,2,3,4-tetrahydroisoquinolines. The starting material is a tetrahydroisoquinoline ring with substituents R and MeO (for 116) or H (for 117). Reaction with methyl formate (O=CH-OMe) under thermal activation yields the N-formylated product (118 or 119).

Compound	R	Method of thermal activation	Solvent	Yield (%)
118	MeO	reflux (16 h)	MeOH	34
119	H	reflux (16 h)	MeOH	60
119	H	MW (1 h 160 °C)	MeOH	77

Table 12: *N*-Formylation of 1,2,3,4-tetrahydroisoquinolines **116** and **117**.

The requisite amine precursor (**124**, Scheme 3) was synthesised using precedent and robust chemistry. Nitration of 1-indanone (**120**) using potassium nitrate (KNO₃) and concentrated sulfuric acid (H₂SO₄) furnished the required 6-nitro-1-indanone isomer (**121**) in 49 % yield. Reduction of the ketone using sodium borohydride (NaBH₄) in methanol and subsequent acetylation using acetic anhydride in pyridine proceeded in almost quantitative yields (**122-123**). Reduction of the acetate protected intermediate (**123**) to the amine (**124**) was achieved using activated palladium on charcoal (Pd/C) with sodium borohydride in methanol.

Typically, this reduction proceeded in only low to moderate yields (30-56 %), due to competing side reactions. However, reducing reaction time from 40 min. to 5 min. increased yields to a maximum of 56 %.



Scheme 3: Synthesis of 6-amino-2,3-dihydro-1H-inden-1-yl acetate (**124**).

With significant quantities of each requisite precursor in hand (**118-119**, **124**), attention then focused on the union of each of the appropriate fragments to furnish the target amidine systems. Ethyl 3-aminobenzoate (**125**, Figure 47) was chosen as an additional fragment to replace amino indenyl acetate (**124**), the reasoning behind which was three-fold. This fragment was achiral, thus removing the potentially problematic stereocentre present. Additionally, the building block itself was cheap and commercially available, therefore reducing the number of synthetic steps to a final compound. Finally, hydrogen bond acceptor moieties (denoted in red) were retained in the same relative position as **124** (Figure 47).

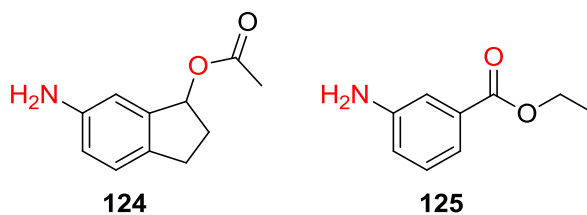


Figure 47: Fragments to be investigated within the research programme, 6-amino-2,3-dihydro-1H-inden-1-yl acetate (**124**) and ethyl 3-aminobenzoate (**125**).

Overall, three amidine compounds were synthesised using phosphoryl chloride in dry dichloromethane at room temperature (Table 13). The previously prepared racemic lead compound¹¹⁹ (**53**) was synthesised, primarily to be used as an internal control in

assays and two novel compounds incorporating ethyl 3-aminobenzoate (**126-127**) were also prepared.

Compound	R	Ar	Yield (%)
53	MeO		19
126	MeO		32
127	H		50

Table 13: Amidine compounds synthesised (**53**, **126-127**).

N-formamides **118** and **119** were found to exist as rotamers in a ratio of approximately 1.5:1 as determined by ^1H NMR. Configuration of *N,N'*-disubstituted amidine **53** was assigned using 2-D ^1H NMR studies. NOEs were observed between the iminium proton (δ_{H} 7.71 (2)), ortho aromatic protons (δ_{H} 6.96, 7.02 (3-4)) and isoquinoline methylene group (δ_{H} 3.68, 4.67 (1)). This was consistent with *E* configuration as indicated in red in Figure 48 and observed experimentally in Figure 49. Reduction of steric hindrance may be the driving force for this preference as no NOEs suggesting the presence of the *Z* isomers were observed (such as an NOE between 1 and 4). Additionally, only one sharp singlet peak was observed by ^1H NMR for the imino proton (δ_{H} 7.71) further supporting the presence of one isomer. .

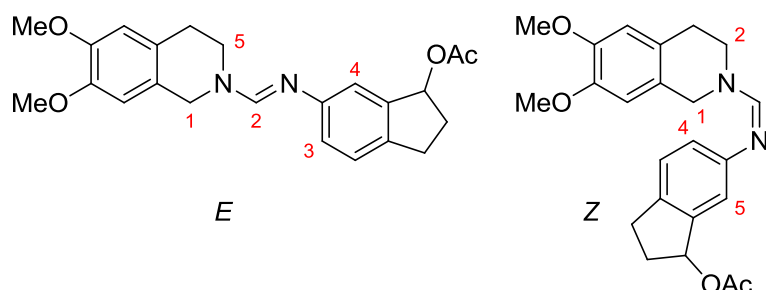


Figure 48: Potential NOEs expected for *E* (1 and 2, 1 and 5, 2 and 3-4) and *Z* (1 and 4-5, 2 and 3) configuration of amidine-linked compound **53**.

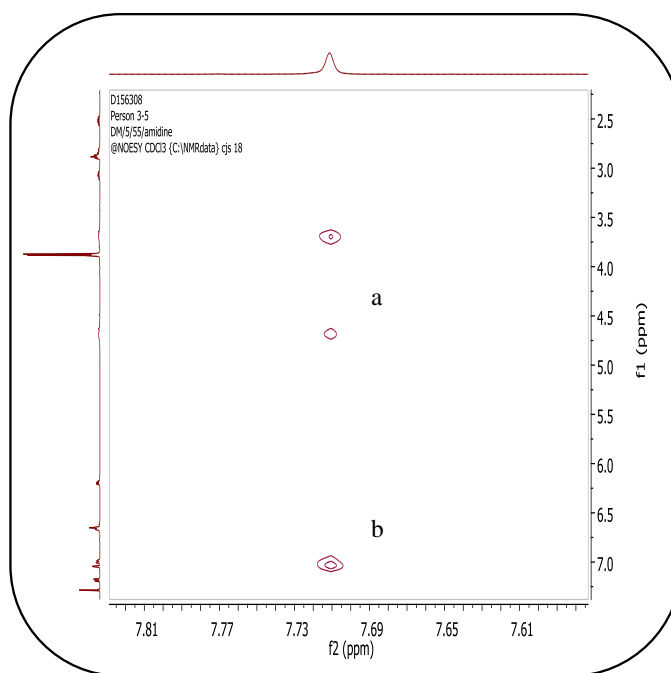
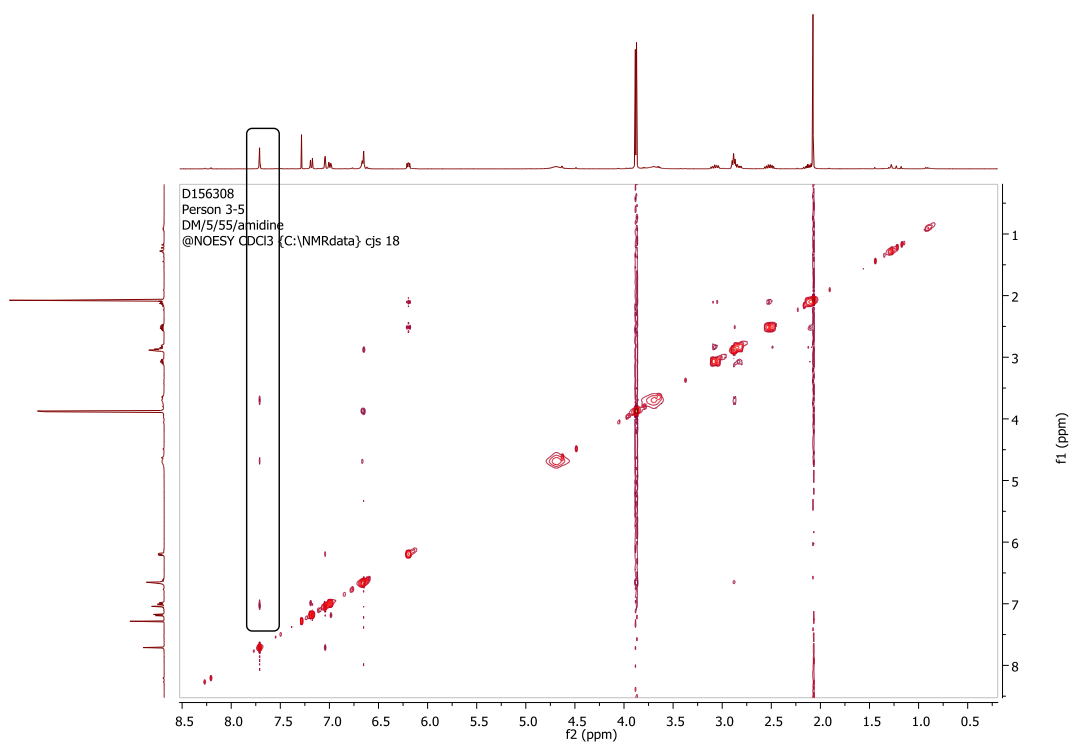


Figure 49: NOESY spectrum of amidine-linked compound **53** displaying NOEs between the iminium proton and methylene group (a) and the ortho aromatic protons (b) (black box). These NOEs suggest *E* configuration.

Conformational analysis was then carried out by N. Caldwell using Gaussian¹⁸⁰ (M06/6-311G(d,p)) and the energy minimised structure is depicted below (Table 14). This energy minimised compound is consistent with literature examples of a compound likely to have hERG liability, a fairly planar compound with a central basic nitrogen flanked by two aromatic/hydrophobic groups.¹⁴⁴

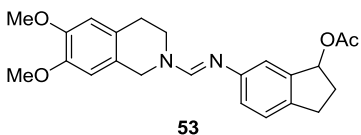
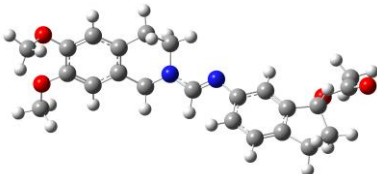
Compound	Energy minimised structure
 53	

Table 14: Conformational analysis of lead *serominic* amidine compound **53**.

2.1.2 Enantio-enriched amidines

Racemic drugs, such as lead amidine **53**, are generally not acceptable drug candidates for a number of reasons. The activity of one enantiomer may be undesirable (mutagenic, teratogenic) as exemplified by the well-known case of racemic morning sickness drug thalidomide which caused birth defects.¹⁸¹ If only one enantiomer is biologically active (and the other is inactive) within a racemic mixture then production of a drug that is 50 % inactive is financially prohibitive. Therefore, potentially expensive and time-consuming stereoselective synthesis must be implemented to synthesise a single enantiomer. Conversely, if both enantiomers are active, a racemic switch can be employed after patent expiry to further maximise profit.

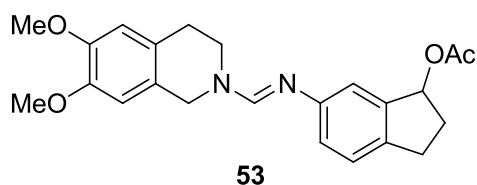
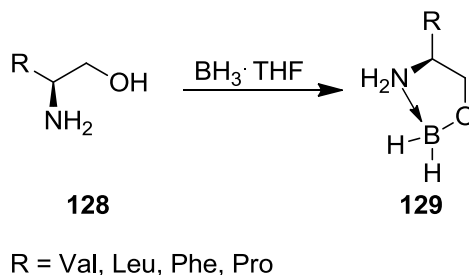


Figure 50: Racemic lead amidine **53**.

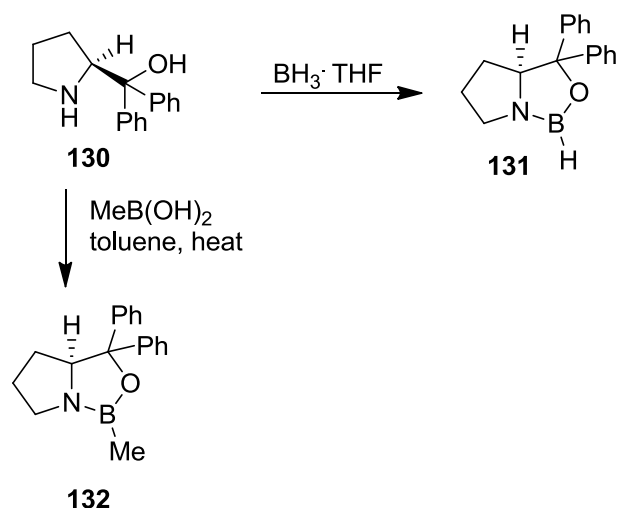
In recent years, a number of significant advances have made large-scale asymmetric synthesis economically viable, as evidenced by the fact that 50 % of the top 200 drugs by sales in the US in 2010 contained at least one stereogenic carbon.¹⁸²

Of particular relevance to this programme is the asymmetric reduction of ketones, which has been an area of considerable interest in chemistry for a number of years. In 1981, Itsuno and colleagues reported the use of alkoxy-amine-borane complexes which could facilitate enantioselective reduction of prochiral ketones.¹⁸³ Addition of borane complexes to amino acid derived β -amino alcohols (**128**, Scheme 4) formed 5-membered alkoxy-amine-borane ring complexes (**129**) which reduced a number of prochiral ketone to the corresponding secondary alcohol in yields in excess of 93 %, but only modest (up to 60 % e.e.) enantioselectivities, as determined by maximal optical rotation.



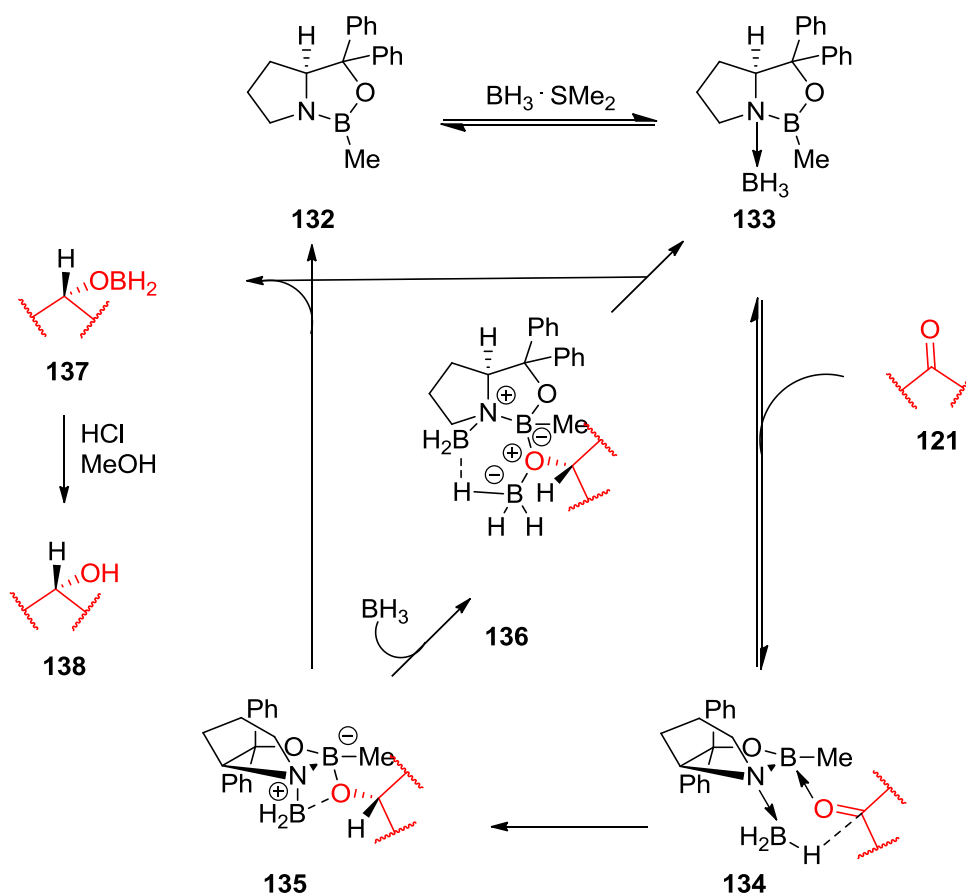
Scheme 4: Formation of 5-membered alkoxy-amine-borane ring complexes (**129**) from β -amino alcohols (**128**).

In 1987, pioneering work by Corey and co-workers demonstrated that the reaction of (*S*)-diphenyl prolinol (**130**) with borane liberated hydrogen and formed a fused oxazaborolidine (**131**, Scheme 5).¹⁸⁴ This was used catalytically with stoichiometric borane to reduce a range of ketones in near quantitative yields and high enantioselectivities. In addition, good recovery of the diphenyl prolinol ligand was possible. This catalyst was then surpassed by its boron-methylated analogue (**132**), which in contrast to **128** was stable to air and moisture, and exerted excellent stereocontrol. These oxazaborolidines, with a range of boron substituents, are known as CBS catalysts, in recognition of the work by Corey, Bakshi and Shibata. These are well-established tools in many types of enantioselective reduction with most enantiomeric excess values being observed in excess of 95 %.¹⁸⁵



Scheme 5: Fused oxazaborolidines known as CBS catalysts (**131-132**).

The mechanistic model outlined below explains the high enantioselectivities of the CBS oxazaborolidine catalysts (Scheme 6).¹⁸⁶ First, borane is activated by coordination of the Lewis basic nitrogen of the oxazaborolidine (**133**). This Lewis adduct binds to the ketone (**121**) at the less sterically-hindered electron lone pair, which serves to minimise steric interaction of the boron-methyl substituent and the larger ketone substituent (**133-134**). This aligns the coordinated borane and the ketone to favour a face-selective hydride transfer through a six-membered transition state (**136**). Acidic workup of the corresponding boron enolate (**137**) forms the desired chiral alcohol (**138**) and the catalyst is regenerated (**132**).



Scheme 6: Catalytic cycle and mechanistic rationale of stereoselectivity using (*S*)-CBS catalyst.

Enantioselectivity can also be predicted by using a simple mnemonic, which compares the relative bulk of each substituent on the ketone (**140**, Figure 51). Assuming the LHS substituent is larger than the RHS, (*S*)-CBS will reduce the ketone so the subsequent hydroxyl is pointing behind the plane (**141**), whereas the (*R*)-CBS complex will do the opposite and the hydroxyl will point upwards out of the plane (**139**).¹⁸⁶

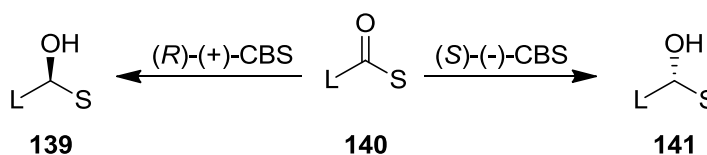
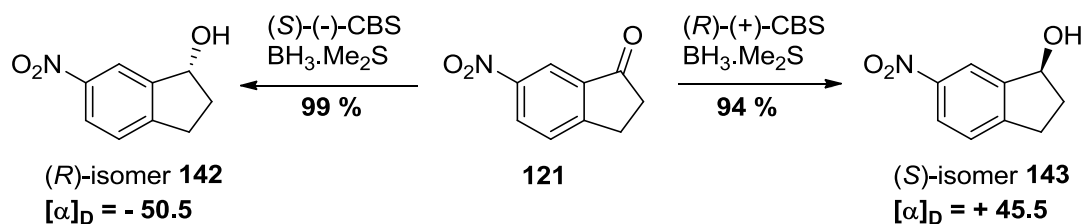


Figure 51: Sterically-controlled enantioselectivity.

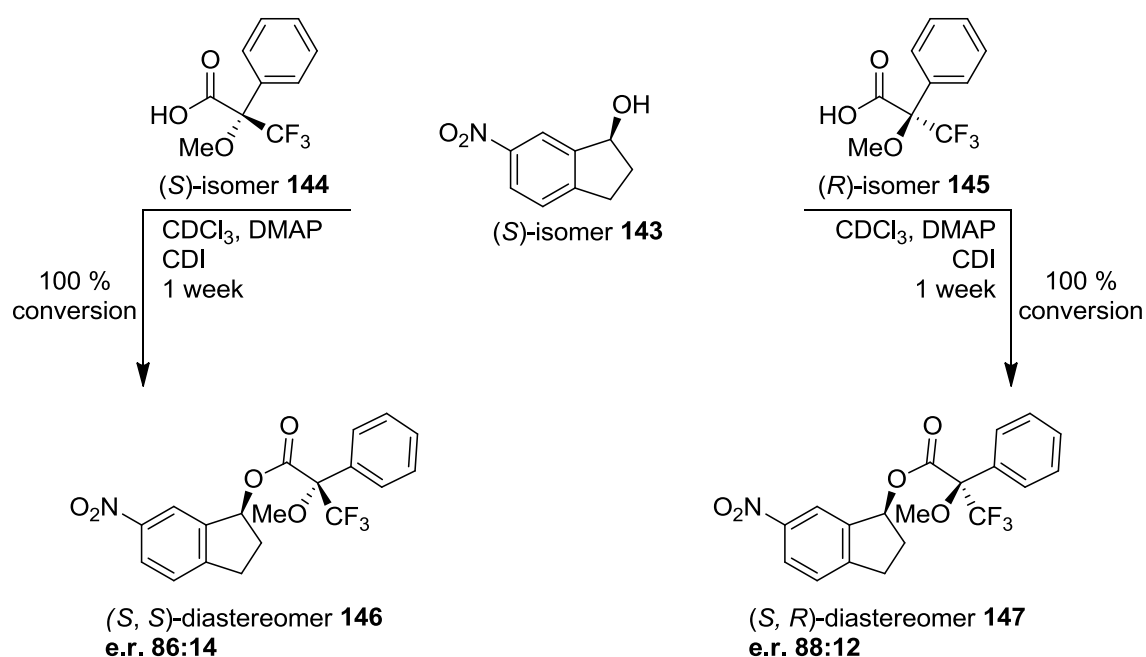
Given the impressive reactivity and selectivity profiles of the CBS system, it was decided to utilise these to prepare homochiral analogues of previously prepared racemate 6-amino-2,3-dihydro-1*H*-inden-1-yl acetate (**124**).

The boron-methylated, commercially available (*R*)- and (*S*)-CBS oxazaborolidines were treated separately with borane-methyl sulfide ($\text{BH}_3\cdot\text{Me}_2\text{S}$) to generate both Lewis adducts. Addition to 6-nitro-1-indanone (**121**) in dry dichloromethane under nitrogen with additional borane-methyl sulfide (10 equiv.) enantioselectively reduced the ketone to (*R*)- and (*S*)-6-nitro-1-indanol (**142**, **143**), respectively, (as evidenced by their almost equal and opposite optical rotation values) in near quantitative yields (Scheme 7).



Scheme 7: Enantioselective reduction of 6-nitro-1-indanone (**121**) using CBS catalysis.

Unfortunately, despite extensive experimentation, it was not possible to develop a chiral HPLC method to establish the exact enantiomeric ratio for each enantiomer. Instead, chiral derivatisation using Mosher's acid was carried out and followed by *in situ* ^{19}F NMR experiments (Scheme 8). The (*S*)-6-nitro-1-indanol (**143**) was added to a NMR tube containing catalytic 4-dimethylaminopyridine (DMAP), (*R*)- or (*S*)-Mosher's acid, 1,1'-carbonyldiimidazole (CDI) and CDCl_3 . The reactions were monitored at room temperature by the appearance of the diastereomeric trifluoromethyl groups by ^{19}F NMR until completion (Figure 52). The enantiomeric ratio was then determined by the relative areas of the diastereomeric trifluoromethyl peaks. The e.r. of (*S*)-6-nitro-1-indanol was calculated as 87:13 by averaging the enantiomeric ratio of each diastereomer. As the optical rotation for the (*R*)-6-nitro-1-indanol is approximately opposite and equal as to that of the (*S*)-6-nitro-1-indanol, it was presumed to have a similar enantiomeric ratio.



Scheme 8: Use of Mosher's acid to determine e.r. of CBS reduction as 87:13.

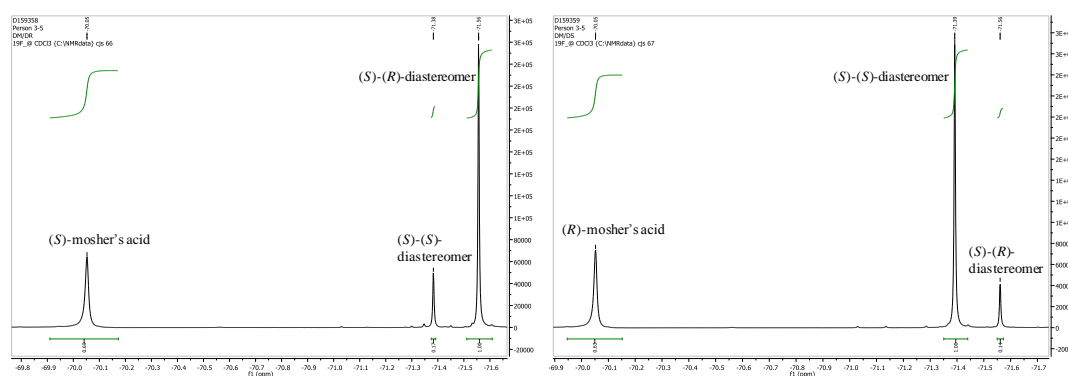
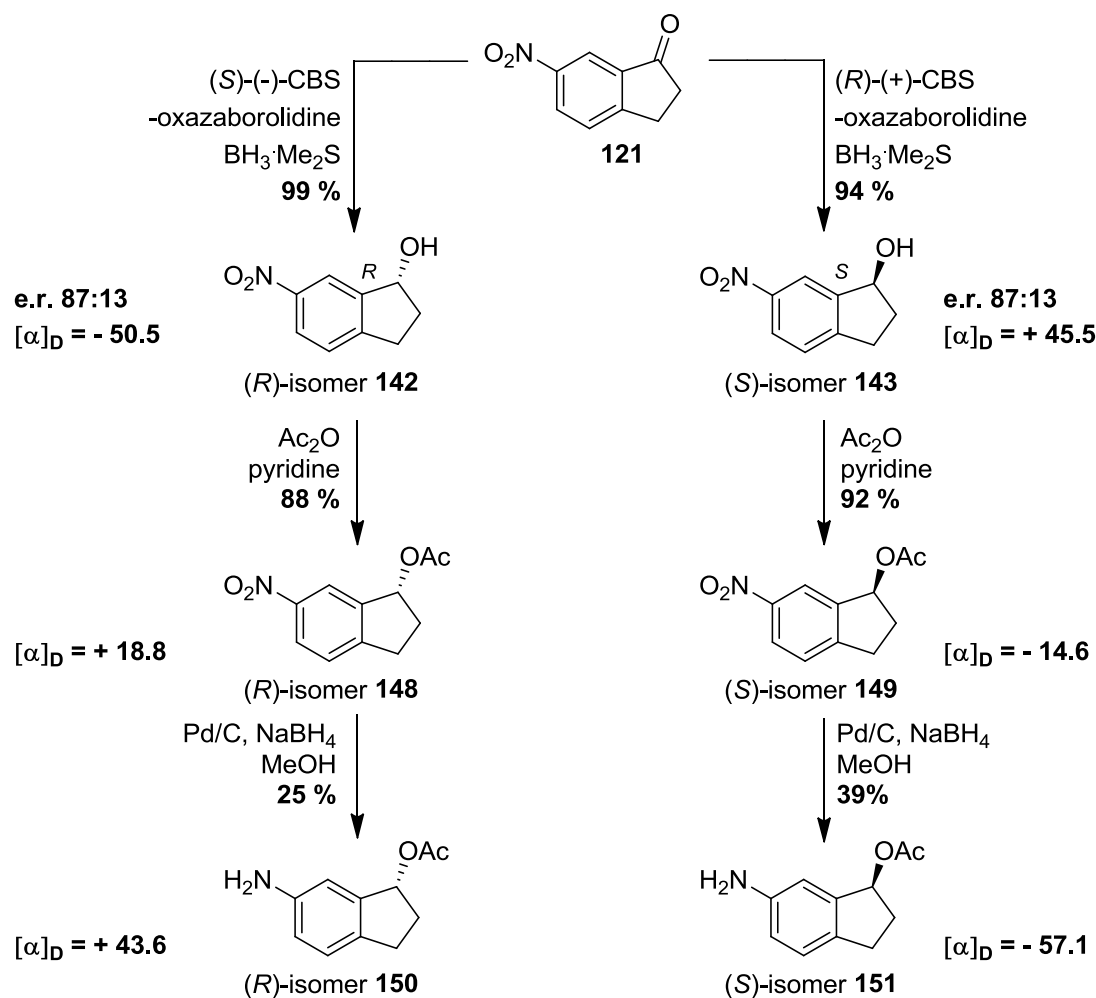


Figure 52: ^{19}F NMR spectra of **(S)**-6-nitro-1-indanol (**143**) coupled to **(S)**- and **(R)**-mosher's acid to give the **(S)-(R)**-diastereomeric $-\text{CF}_3$ group at -71.56 ppm (**146**) and the corresponding **(S)-(S)**-diastereomeric $-\text{CF}_3$ group at -71.39 ppm (**147**).

With an enantio-enriched route to both **(R)**- and **(S)**-6-nitro-1-indanols (**142-143**) established, functional group modification was initiated. Acetylation of the hydroxyl group and reduction of the nitro functionality was carried out as previously described for the racemate to afford both enantiomers of 6-amino-2,3-dihydro-1*H*-inden-1-yl acetate (**147-148**, Scheme 9) in moderate yield.



Scheme 9: Synthesis of 6-amino-2,3-dihydro-1*H*-inden-1-yl acetate enantiomers (**150-151**).

Optical rotation measurements at each stage ensured retention of chiral integrity as evidenced by the opposite signs of the optical rotation. Additionally, (*R*)- and (*S*)-6-amino-1-indanol (**152-153**, respectively) were obtained as by-products in the purification of (*R*)- and (*S*)-6-amino-2,3-dihydro-1*H*-inden-1-yl acetate (**150-151**). Crystallisation of **152** and subsequent X-ray analysis confirmed the presence of the (*R*)- enantio-enriched compound (Figure 53).

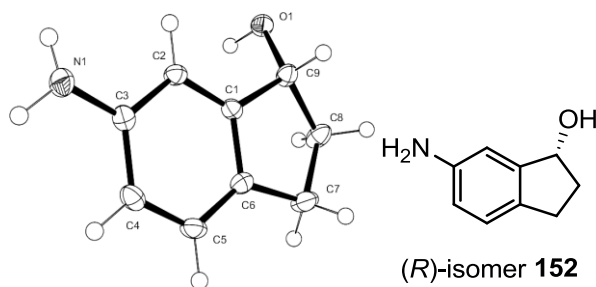
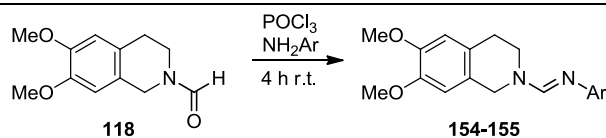


Figure 53: X-ray structure of (*R*)-6-amino-1-indanol (**152**).

With the two enantiomers in hand, (*R*)- and (*S*)- 6-amino-2,3-dihydro-1*H*-inden-1-yl acetate (**150-151**) were then coupled to 6,7-dimethoxy-3,4-dihydroisoquinoline-2(1*H*)-formamide (**118**) using phosphorus chloride to furnish both novel (*R*)- and (*S*)-enantiomeric amidines in 28 % and 33 % yield, respectively (**154-155**, Table 15).



Compound	Ar	$[\alpha]_D$	Yield (%)
(<i>R</i>)-isomer 154		+ 35.1	28
(<i>S</i>)-isomer 155		- 26.2	33

Table 15: Synthesis of enantio-enriched *seromimic* lead compounds (**154-155**).

2.1.3 Summary of amidine-linked compounds

Combining these enantio-enriched amidine compounds with those previously made furnished, in total, four novel amidines (**126-127**, **154-155**) and the previous lead compound (control, **53**) overall.

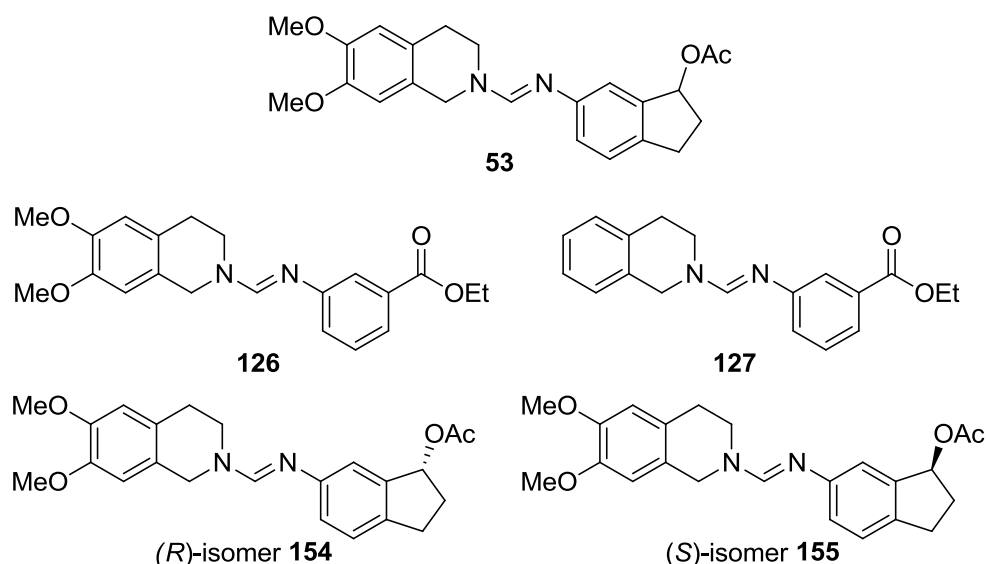


Figure 54: Four novel *N,N'*-disubstituted amidines synthesised including ethyl ester analogues (**126-127**), (*R*)- and (*S*)- enantiomers of the lead racemic amidine (**154-155**) and previously synthesised amidine (**53**).

2.2 Linker modifications – Nitroalkenes

As discussed previously in the outline of the Research Programme, amidine-linked *serominic* compounds were observed to exhibit hERG activity. As hERG affinity is frequently associated with highly basic compounds, introduction of an electron withdrawing linker in place of an amidine may decrease pK_a adequately to decrease hERG affinity.

Nitro groups are small, very powerful, dipolar electron-withdrawing groups capable of acting as hydrogen bond acceptors which makes them attractive functional groups for modifying electronics within a system. Introduction of a nitroalkene group will reduce the pK_a of the linker from that of the amidine ($pK_a = 12$)¹⁶⁸ significantly to approximately -1.¹⁸⁷ Additionally, the dipolar character of the linker may actually be advantageous (**87**). The positive charge on the nitro group may assist with any molecular recognition associated with the iminium positive charge (**156**) from the lead amidine but the negative charge also present (**87**) may destabilise key interactions within the hERG binding site and decrease hERG activity, as observed in the literature for carboxylic acids.¹⁵⁹

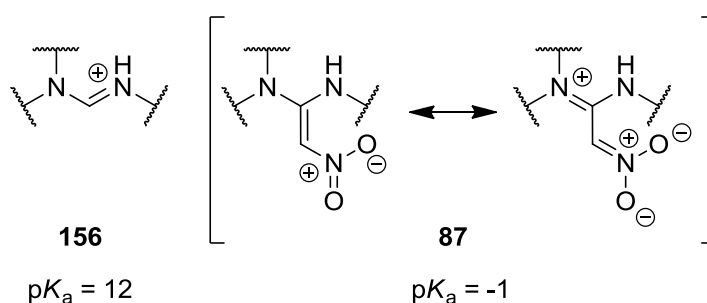


Figure 55: Modification of amidine pK_a (**156**) through insertion of nitroalkene linker (**87**).

The use of nitro groups is usually avoided in medicinal chemistry due to their reputation as mutagenic toxicophores¹⁸⁸ caused by *in vivo* metabolism by enzymes such as nitroreductases. These enzymes reduce (usually aromatic) nitro groups to toxic metabolites such as carcinogenic hydroxylamines and nitroso compounds.¹⁸⁹

However, there is strong precedent for drugs containing nitro functionalities, for example, Roche's potent hypnotic flunitrazepam (perhaps better known as Rohypnol™) has an aromatic nitro group (**157**, Figure 56). Of greater relevance to the current discussion, GlaxoSmithKline's blockbuster ranitidine, the worldwide best-selling prescription drug throughout the 1980s (**158**), and Eli Lilly's structurally similar nizatidine (**159**) both have nitroalkene functionalities and both act as histamine H₂ antagonists.

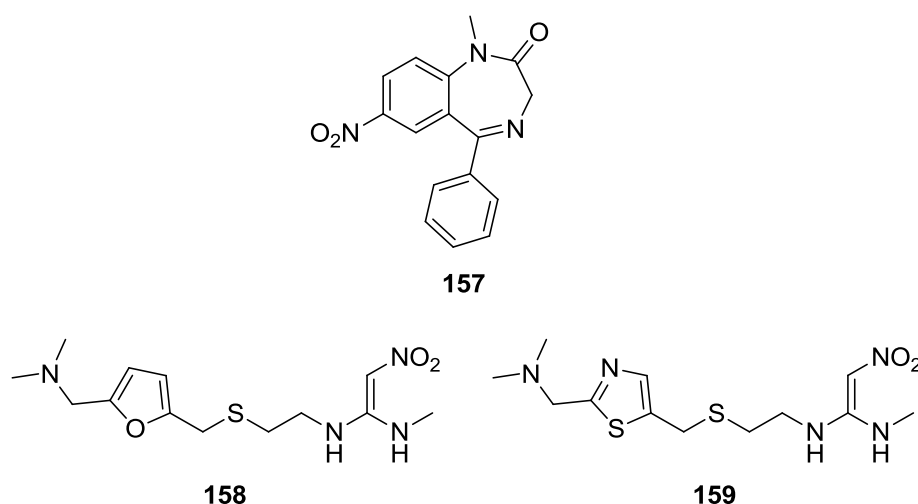


Figure 56: Well-known drugs containing nitro functionalities, flunitrazepam (**157**), ranitidine (**158**) and nizatidine (**159**).

The simplest way to introduce Michael acceptor-type linker groups such as nitroalkenes to molecules is to exploit straightforward addition-elimination

chemistry. Taking the desired functionality (in this case nitroalkene), with appropriate leaving groups X and Y (**160**, Figure 57) allows for conjugate addition of a nucleophile to take place with subsequent expulsion of one or both leaving groups.

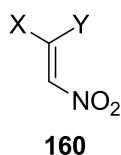


Figure 57: Nitroalkene functionality with appropriate leaving groups, X and Y (**160**).

Conjugate addition of a nucleophilic amine (**161**, Figure 58) to the commercially available 1,1-bis(methylsulfanyl)-2-nitroalkene (**162**) should result in elimination of the better leaving group. Given that leaving group potential correlates to the relative stability (lower pK_a) of the conjugate base ion, MeS^- rather than $\text{RR}'\text{N}^-$ will be expelled. The amine then donates electrons into the system which extends conjugation (**163**), and renders the quaternary carbon less reactive to nucleophilic attack by a second amine molecule, therefore in principle, only monosubstitution should be observed. From consideration of the contribution of this canonical form, it is likely that more forcing conditions would be needed to displace the second leaving group.

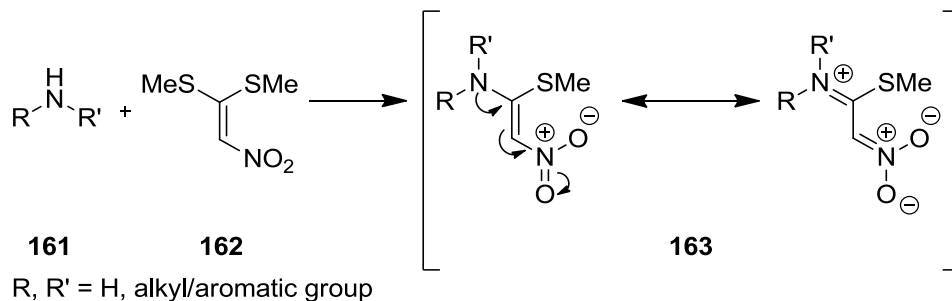


Figure 58: Electron donation from amino reduces electrophilicity of quaternary carbon (**163**).

However, leaving groups other than MeS^- , which are highly stabilised as anions (e.g. halides, triflates) may allow a second equivalent of amine to substitute on the same molecule.

Elimination reactions using 1,1-bis(methylsulfanyl)-2-nitroalkene (**162**) have been extensively reported in the literature using a range of aryl and aliphatic substituents, *para*-substituted benzylamines,¹⁹⁰ methylamine and 3-pyridinylmethylamine,¹⁹¹ aminoethylmorpholine¹⁹² and substituted piperazines¹⁹³ amongst others, using

ethanol as solvent with yields ranging from 31-75 %. Based on this encouraging precedent, the first proposed synthesis mirrored conditions reported within the literature.

The desired tetrahydroisoquinoline (**116-117**) was added to a stoichiometric amount of 1,1-bis(methylsulfanyl)-2-nitroalkene (**162**) in ethanol and a range of reaction times were evaluated (Table 16). Despite optimisation attempts, low isolated yields were obtained with a maximum of 28 % after heating for 0.33 h. A complex mixture was observed by thin layer chromatography (TLC), which apart from the product, contained components that could not be isolated. This suggests that ethanol may have been acting as a nucleophile, competing with the amine to give side-products.

$\text{MeO} = \mathbf{116}$
 $\text{H} = \mathbf{117}$

$\mathbf{162}$

$\text{MeO} = \mathbf{164}$
 $\text{H} = \mathbf{165}$

Compound	R	Solvent	Reflux time (h)	Yield (%)
164	MeO	EtOH	0.5	10
165	H	EtOH	0.33	28
165	H	EtOH	0.67	25
165	H	EtOH	1.5	13
165	H	Toluene	16	-
164	MeO	DCM	16	61
165	H	DCM	16	49

Table 16: Investigation on solvent effects on monosubstitution of tetrahydroisoquinolines.

Toluene, a non-nucleophilic solvent was next examined. A similar reaction profile was observed as for the previous reaction using ethanol. In this case, separation was very difficult and no product was isolated. The reaction was finally carried out in dichloromethane which increased the yield significantly, from 10 % to 61 % for **164** and from 28 % to 49 % for **165**, with no by-products observed by TLC. The reaction time, however, was increased from 0.2 h to 16 hours although this is unoptimised.

Continuing with the synthesis of the target compounds, *N*-substituted-1-(methylthio)-2-nitroalkene (**165**) was reacted with primary aromatic amines **124-125** to form *N,N'*-disubstituted nitroalkenes but coupling was unsuccessful under a range of solvent conditions (Table 17).

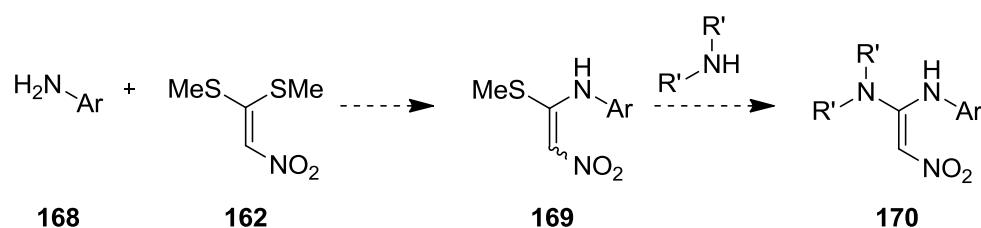
Compound	Ar	Solvent	Reflux time (h)	Yield (%)
166		EtOH	24	-
		DCM	96	-
167		Toluene	96	-
		MeOH	96	-
		DMF	96	-
		DCE	96	-
		THF	48	-

Table 17: Investigation of solvent effects on second substitution of *N*-substituted-1-(methylthio)-2-nitroalkene (**165**).

A complex by-product profile allied with difficult separation again rendered ethanol an unsuitable solvent for the preparation of a range of *N,N'*-disubstituted compounds. Following the discovery that dichloromethane increased yields substantially for the monosubstitution of 1,1-bis(methylsulfanyl)-2-nitroalkene (**162**) (Table 16), this solvent was employed but failed for the second substitution. Evaluation of a number of other solvents also proved unsuccessful even under forcing conditions, such as refluxing for 4 days (Table 17). This suggests either that the monosubstituted nitroalkene compound is intrinsically not reactive enough, or the aniline derivatives used are not nucleophilic enough, for nucleophilic attack and displacement of the methyl thiolate leaving group. As a result, an alternative approach for the preparation of *N,N'*-disubstituted nitroalkenes was sought.

2.2.1 New route to nitroalkene-linked compounds

The simplest and most obvious new synthetic route to the desired compounds is to reverse the order of addition reactants. Reacting the less nucleophilic aromatic amine (**168**) with 1,1-bis(methylsulfanyl)-2-nitroalkene (**162**) should allow the more nucleophilic aliphatic amine to overcome the ensuing decrease in reactivity encountered with the monosubstituted intermediate (**169**) and furnish *N,N*-disubstituted compounds (**170**).



Scheme 10: Proposed alternative route to *N,N'*-disubstituted nitroalkene compounds (**170**).

6-((1-(Methylthio)-2-nitrovinyl)amino)-2,3-dihydro-1*H*-inden-1-yl acetate (**171**) was synthesised by refluxing stoichiometric amounts of 6-amino-2,3-dihydro-1*H*-inden-1-yl acetate (**124**) with 1,1-bis(methylsulfanyl)-2-nitroalkene (**162**) for 16 hours in DCM. Subsequent flash chromatography furnished the product in 66 % yield (**171**, Table 18).

$\text{H}_2\text{N-Ar} + \text{MeS-C(SMe)=CH-NO}_2 \longrightarrow \text{MeS-C(SMe)=CH-NH-Ar}$				
$\text{124-125, 172} \quad \text{161} \quad \text{171, 173-174}$				
Compound	Ar	Solvent	Reflux time (h)	Yield (%)
171		DCM	16	66
173		DCM	16	73
174		DCM	16	-
		propan-2-ol EtOH	16 16	- -

Table 18: Synthesis of monosubstituted nitroalkenes (**171**, **173-174**).

6-Amino-1-indanol (**172**) was isolated as a by-product in the reduction of 6-nitro-2,3-dihydro-1*H*-inden-1-yl acetate (**123**) to the amine equivalent (**124**). Hydroxy substituted amidines demonstrated moderate *serominic* activity in *Series B*, as discussed earlier,¹¹⁹ therefore, **172** was taken forward to synthesise a nitroalkene example. Refluxing in dichloromethane for 16 hours provided the monosubstituted product in 73 % yield (**173**). However, an ethyl 3-amino benzoate (**174**) analogue was not successfully prepared even under a range of solvent conditions (Table 18), attributed to the reduced nucleophilicity compared to the corresponding indanyl acetate.

A crystal of 6-((1-(methylthio)-2-nitrovinyl)amino)-2,3-dihydro-1*H*-inden-1-yl acetate (**171**) was grown by slow evaporation in dichloromethane and X-ray diffraction showed the structure as being exclusively the *E* isomer (Figure 2.7). From consideration of the crystal structure data, an intramolecular H-bond between N2-H and O1 (1.88 Å) appears to be the driving force of the preferential formation of the *E* isomer.

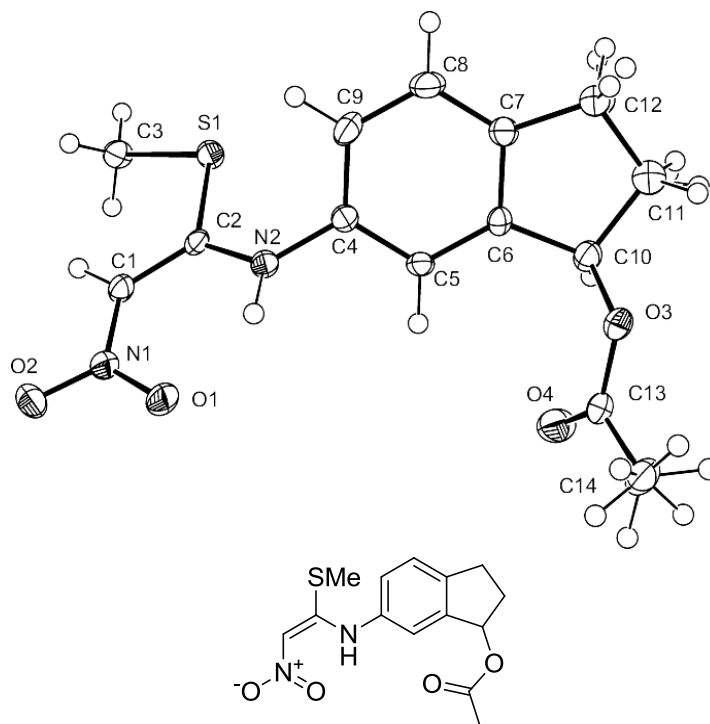


Figure 59: Crystal structure of *E*-((1-(methylthio)-2-nitrovinyl)amino)-2,3-dihydro-1*H*-inden-1-yl acetate (**171**).

With the desired *E* monosubstituted intermediates in hand, coupling to the relevant tetrahydroisoquinoline was carried out. Propan-2-ol was used as solvent, after observation of increased yields in the cyanocarboximidamide series, and three novel *N,N'*-disubstituted nitroalkene compounds (**175-177**) were synthesised in low to moderate yield after purification by flash chromatography and further HPLC purification as necessary (Table 19).

$\text{MeS}-\text{C}(=\text{O})-\text{NH}-\text{Ar} + \text{R-substituted piperazine} \xrightarrow[\text{reflux}]{\text{propan-2-ol, 16 h}}$

171, 173 **MeO = 116** **166, 175-176**
H = 117

Compound	Structure	Purification Method	Yield (%)
166		Flash chromatography and HPLC purification	14
175		Flash chromatography	38
176		Flash chromatography and HPLC purification	19

Table 19: Three novel *N,N'*-disubstituted nitroalkene compounds synthesised (**166, 175-176**).

The synthetic strategy for *N,N'*-disubstituted nitroalkenes initially appeared very simple but practical application proved challenging. Propan-2-ol and dichloromethane have been discovered to be appropriate solvents for the first substitution, but the second substitution reaction only succeeded in propan-2-ol.

Overall three *N,N'*-disubstituted nitroalkenes examples were synthesised (**166, 175-176**) utilising this methodology. Initial biological assay results (Chapter 3) suggested that the nitroalkene class of compounds could have *serominic* utility; therefore, further optimisation of the synthetic strategy was essential to enable thorough exploration of SAR.

2.2.2 Alternative approaches to nitroalkene-linked compounds

As described previously, synthesis of *N,N'*-disubstituted nitroalkenes was only achieved using propan-2-ol for the second substitution. Furthermore, ethyl 3-amino benzoate derivatives could not be synthesised despite examining a range of solvents (Table 18).

To explore SAR within the series more completely, a larger library of *N,N'*-disubstituted nitroalkenes was required; therefore, it would be advantageous to design a more efficient and general route to these compounds.

Initial assay results (Chapter 3) suggested the amino acetate fragment (**124**) was required for M₄ activity. The SAR exploration was directed at modifications to the 5-HT₇ responsive *N*-heterocycle and focused on piperidine (**177-178**, Figure 60), piperazine (**179**) and tetrahydro- β -carboline (**180**) scaffolds in place of the tetrahydroisoquinoline (**181**).

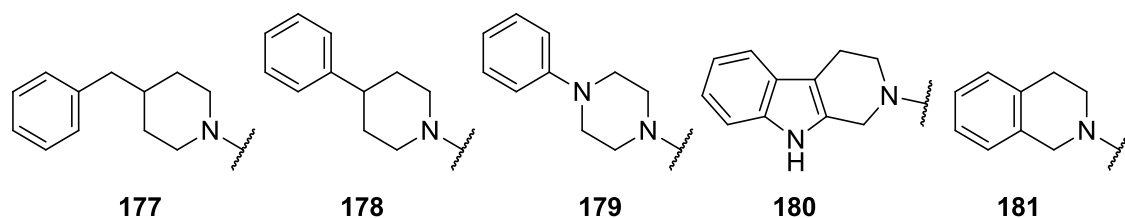


Figure 60: 5-HT₇ responsive groups to be introduced (**177-181**).

Piperidines and piperazines are ubiquitous in medicinal chemistry and are used heavily in the field of antipsychotics with haloperidol (**5**, Figure 61) and risperidone (**11**) both featuring a substituted piperidine ring, and clozapine (**9**) and olanzapine (**10**) containing substituted piperazine rings. Furthermore, clozapine (**9**) and risperidone (**11**) display significant affinity for 5-HT₇ and introduction of a piperidine or a piperazine ring to the nitroalkene series may exploit this.¹⁰⁹

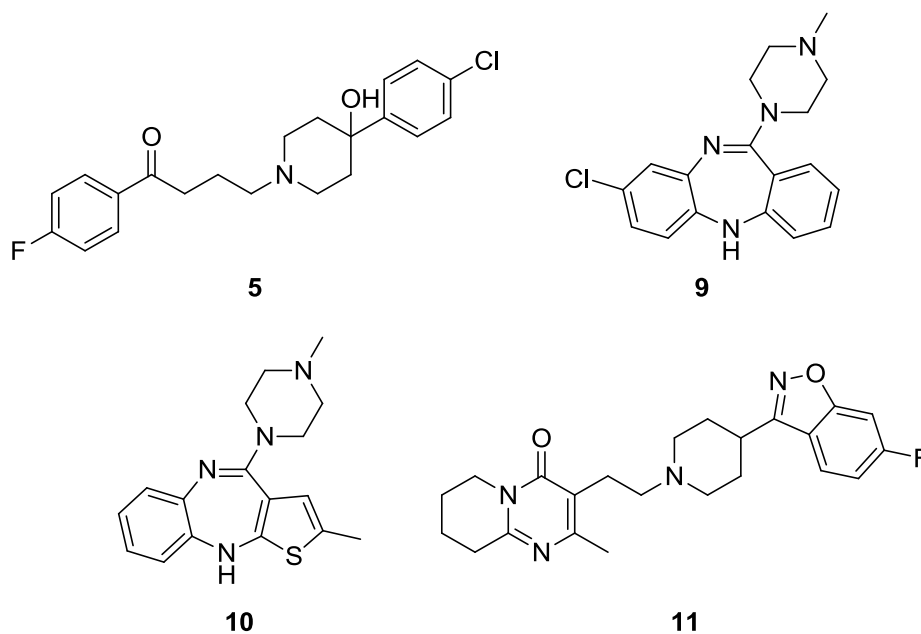


Figure 61: Selection of known antipsychotic drugs featuring piperidine and piperazine functionalities, haloperidol (**5**), clozapine (**9**), olanzapine (**10**) and risperidone (**11**).

The final *N*-heterocycle to be used to map out serotonergic space was tetrahydro- β -carboline (**180**, Figure 62), selected mainly for its structural similarity to serotonin (**19**) and subsequent high affinity of substituted tetrahydro- β -carbolines for 5-HT₇ as discovered previously in *Series A* (Section 1.6).¹¹⁹

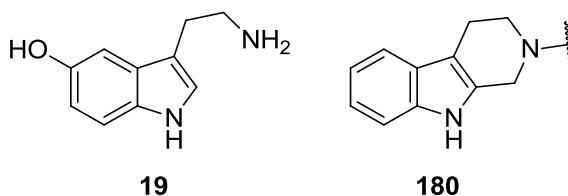


Figure 62: Serotonin (**19**) and tetrahydro- β -carboline (**180**).

Lastly, another non-chiral substrate, 6-amino-phthalide (**182**, Figure 63) was selected for use in SAR investigation. Again, this fragment has a hydrogen bond acceptor (denoted in red) in the same relative position as the chiral amino indanyl acetate (**124**) but is non-chiral.

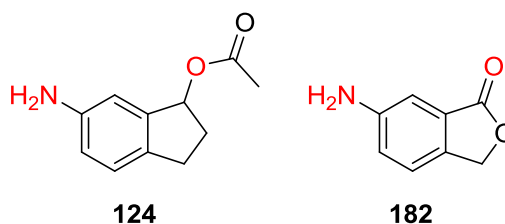


Figure 63: Potential M₄ responsive substrate, 6-amino phthalide (**182**).

Returning to the synthesis of novel nitroalkene compounds incorporating these structural changes, an alternative leaving group in the nitroalkene starting material was investigated. A precursor with a halide leaving group (**183**) was considered an attractive option as the 1-position of the vinyl system would be more electrophilic due to the inductive effect of the halide compared to the methyl thiolate analogue (**162**). In addition, this high electronegativity also makes halides better leaving groups as it stabilises the resultant anion.

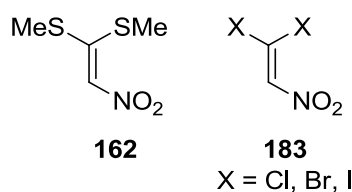
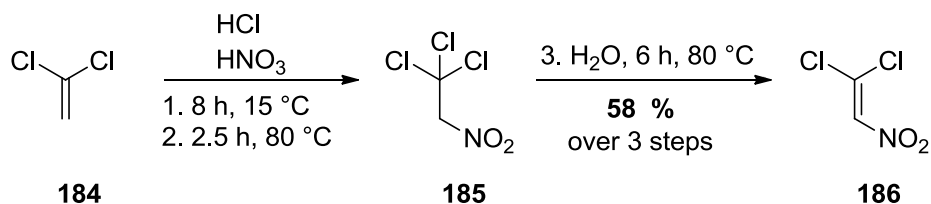


Figure 64: Alternative leaving groups for 1,1-bis(methylsulfanyl)-2-nitroalkene (**162**).

Accordingly, 1,1-dichloro-2-nitroalkene (**186**) was investigated as an improved precursor in the synthesis of *N,N'*-disubstituted nitroalkenes. 1,1-dichloro-2-nitroalkene has precedent in the literature and was synthesised following a modified method (Scheme 11).¹⁹⁴ 1,2-Dichloroethylene (**184**) was treated with concentrated hydrochloric and concentrated nitric acid to make 1,1,1-trichloro-2-nitroethane (**185**). Dehydrohalogenation under aqueous conditions afforded the desired 1,1-dichloro-2-nitroalkene (**186**) in a good yield of 58 % over 3 steps in a one-pot procedure.



Scheme 11: Synthesis of 1,1-dichloro-2-nitroalkene (**186**).

1,1-Dichloro-2-nitroalkene (**186**) was then used in a number of operationally simple one-pot reactions to synthesise *N,N'*-disubstituted nitroalkenes. Addition of the desired primary aromatic amine (**124-125** or **182**) to 1,1-dichloro-2-nitroalkene (**186**) at 4 °C for 40-90 min. and subsequent one-pot addition of the desired secondary amine (**177-181**) afforded a range of seven novel *N,N'*-disubstituted nitroalkenes in moderate yields (**187-193**, Table 20).

Compound	Ar	X	R	Yield (%)
187		CH	Ph	14
188		N	Ph	9
189		CH	Bn	21
190		CH	Ph	23

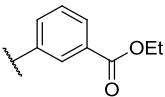
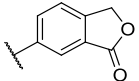
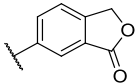
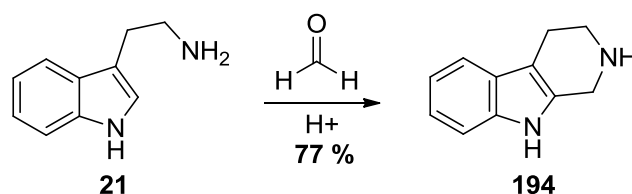
191		N	Ph	11
192		CH	Bn	27
193		CH	Ph	8

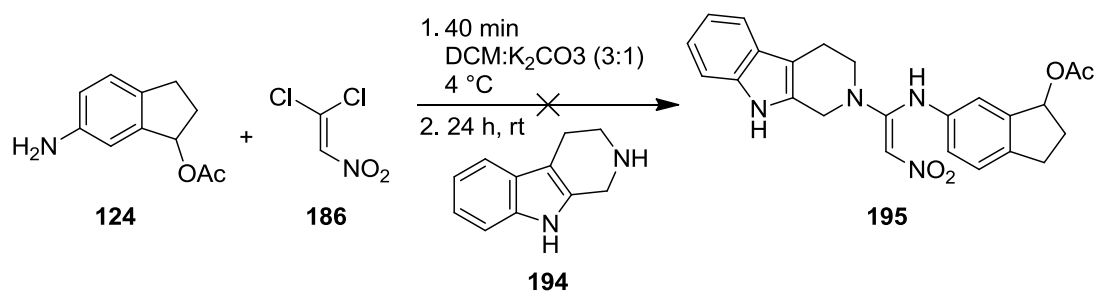
Table 20: Novel *N,N'*-disubstituted nitroalkenes synthesised using one-pot procedure (**187-193**) with 1,2-dichloro-2-nitroalkene.

As intimated above, there was also considerable interest in preparing the tetrahydro- β -carboline derivatives of the nitroalkene family. A Pictet-Spengler reaction utilising tryptamine (**21**, Scheme 12) and formaldehyde was carried out under acidic conditions to furnish the desired tetrahydro- β -carboline (**194**).^{195, 196}



Scheme 12: Pictet-Spengler reaction using tryptamine (**21**) and paraformaldehyde.

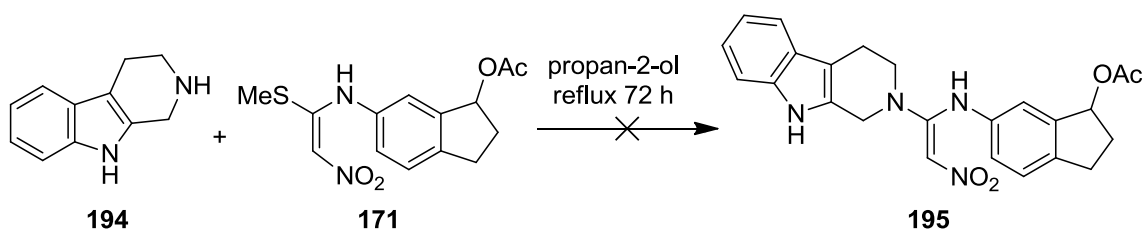
Unfortunately, although his reaction proceeded very well with 77 % yield, synthesis of a nitroalkene derivative was unsuccessful. Firstly, the 1,2-dichloro-2-nitroalkene route was attempted but the tetrahydro- β -carboline (**194**) was insoluble in dichloromethane therefore no reaction was observed (**Scheme 13**).



Scheme 13: Unsuccessful synthesis of nitroalkene derived tetrahydro- β -carboline compound (**195**).

In an alternative approach to the target compound, 6-((1-(methylthio)-2-nitrovinyl)amino)-2,3-dihydro-1*H*-inden-1-yl acetate (**171**) was refluxed with tetrahydro- β -carboline (**194**) in propan-2-ol, as was previously successful for the tetrahydroisoquinoline examples (Table 18), but this also failed (Scheme 14).

Against this background, the synthesis of the tetrahydro- β -carboline analogue (**195**) was discontinued.



Scheme 14: Unsuccessful synthesis of nitroalkene derived tetrahydro- β -carboline compound (**195**).

2.2.3 Geometry of nitroalkene double bond

Unfortunately, the double-bond geometry of N,N' -disubstituted nitroalkene compounds could not be assigned using X-ray analysis as crystal growth of the compounds proved challenging.

However, configuration was assigned using 2-D ^1H NMR studies. NOEs were observed between the vinylic proton (δ_{H} 6.68ppm (1)) and methylene groups on the piperidine ring (δ_{H} 2.81 and 3.58 (2)). This was consistent with E configuration as indicated in red in Figure 65 and observed experimentally in Figure 66. No NOEs were observed corresponding to the Z isomer and the driving force for this preference for E may be retention of the intramolecular hydrogen bond observed in the X-ray structure of a monosubstituted product. Additionally, only one sharp singlet peak was observed in the ^1H NMR spectra for the vinylic proton (between δ_{H} 6.63-6.80 ppm depending on substrate), further supporting the presence of just one isomer.

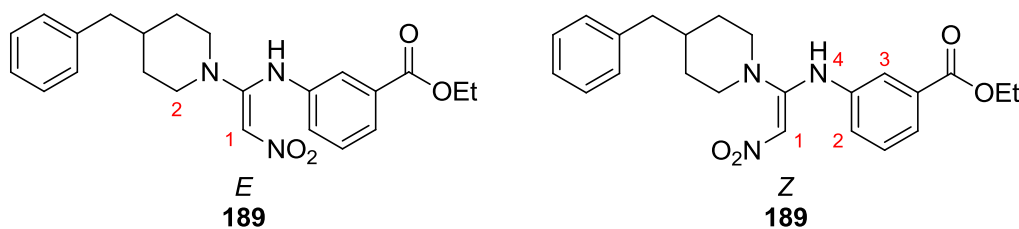


Figure 65: Potential NOEs (depicted in red) expected with E (1 and 2) and Z (1 and 2-3, 1 and 4) configuration of N,N -disubstituted nitroalkene **189**.

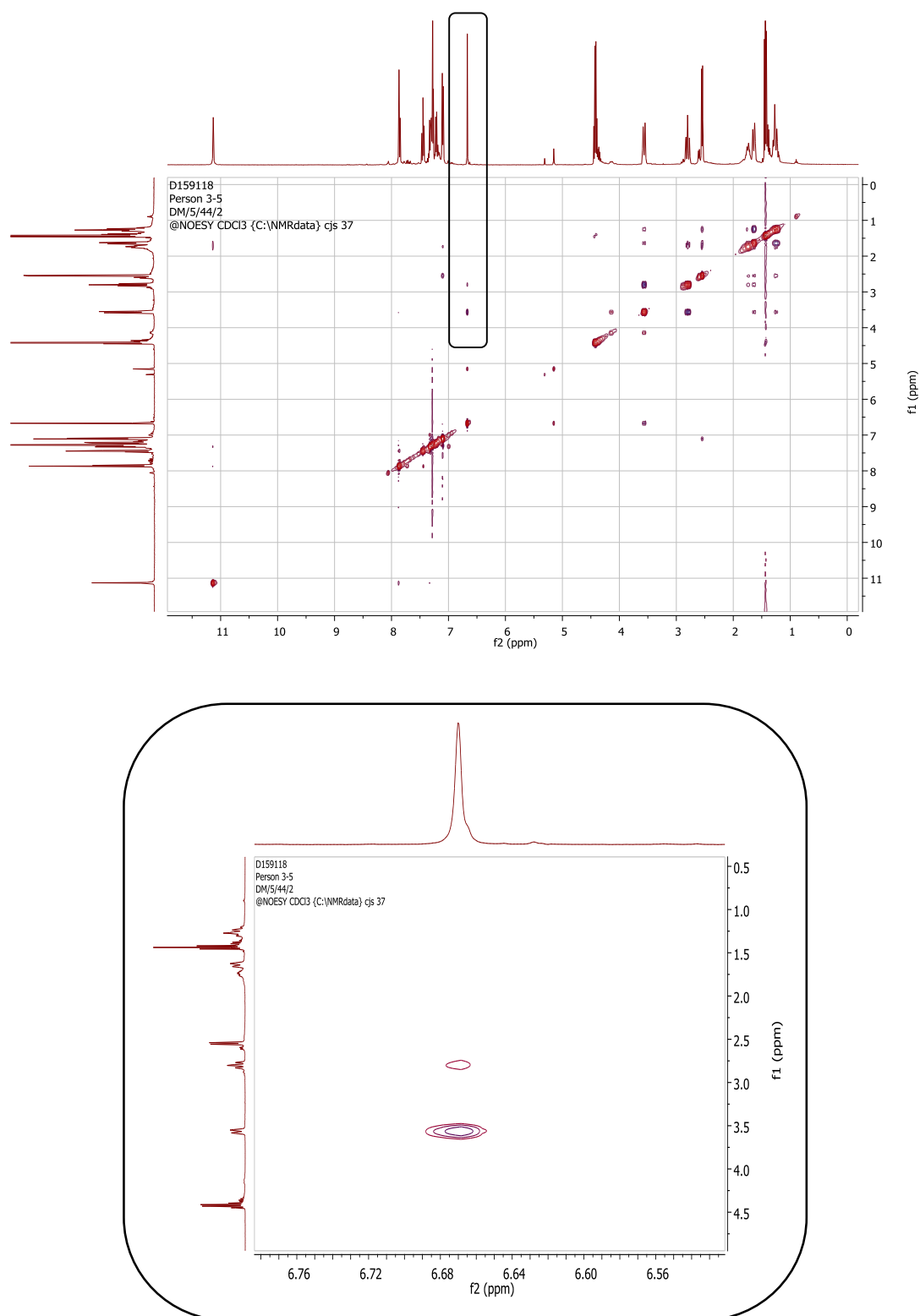


Figure 66: NOESY spectrum of nitroalkene-linked compound **189** displaying NOEs between the vinylic proton and two methylene groups (black box). These NOEs suggest *E* configuration.

Conformational analysis using Gaussian¹⁸⁰ was carried out on **191** and the energy minimised structure is depicted below (Table 21). This energy minimised compound adopts a bent conformation which may be risky for hERG activity¹⁴⁴ but the reduction in basicity by incorporation of the nitroalkene group may decrease hERG liability.

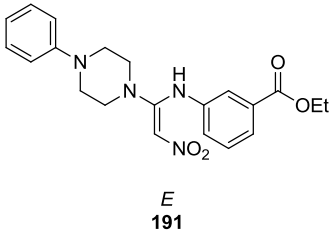
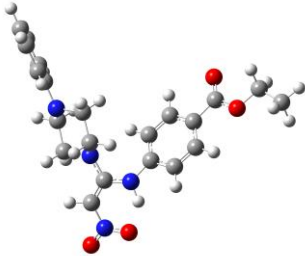
Compound	Energy minimised structure
 <i>E</i> 191	

Table 21: Conformational analysis of *N,N'*-disubstituted nitroalkene compound **191**.

2.2.4 Summary of *N,N'*-disubstituted nitroalkene compounds

Overall, ten novel *N,N'*-disubstituted nitroalkene compounds were synthesised, three utilising 1,1-bis(methylsulfanyl)-2-nitroalkene (**162**) to furnish compounds based on an isoquinoline scaffold (**166**, **175-176**), and an additional seven compounds using 1,1-dichloro-2-nitroalkene (**186**) with piperidine and piperazine scaffolds (**187-193**) to further explore SAR. Although only moderate yields were observed, sufficient quantities of each compound were isolated for biological evaluation. Further work to optimise this reaction would be advantageous, particularly to scale-up compound synthesis to support any eventual *in vivo* work.

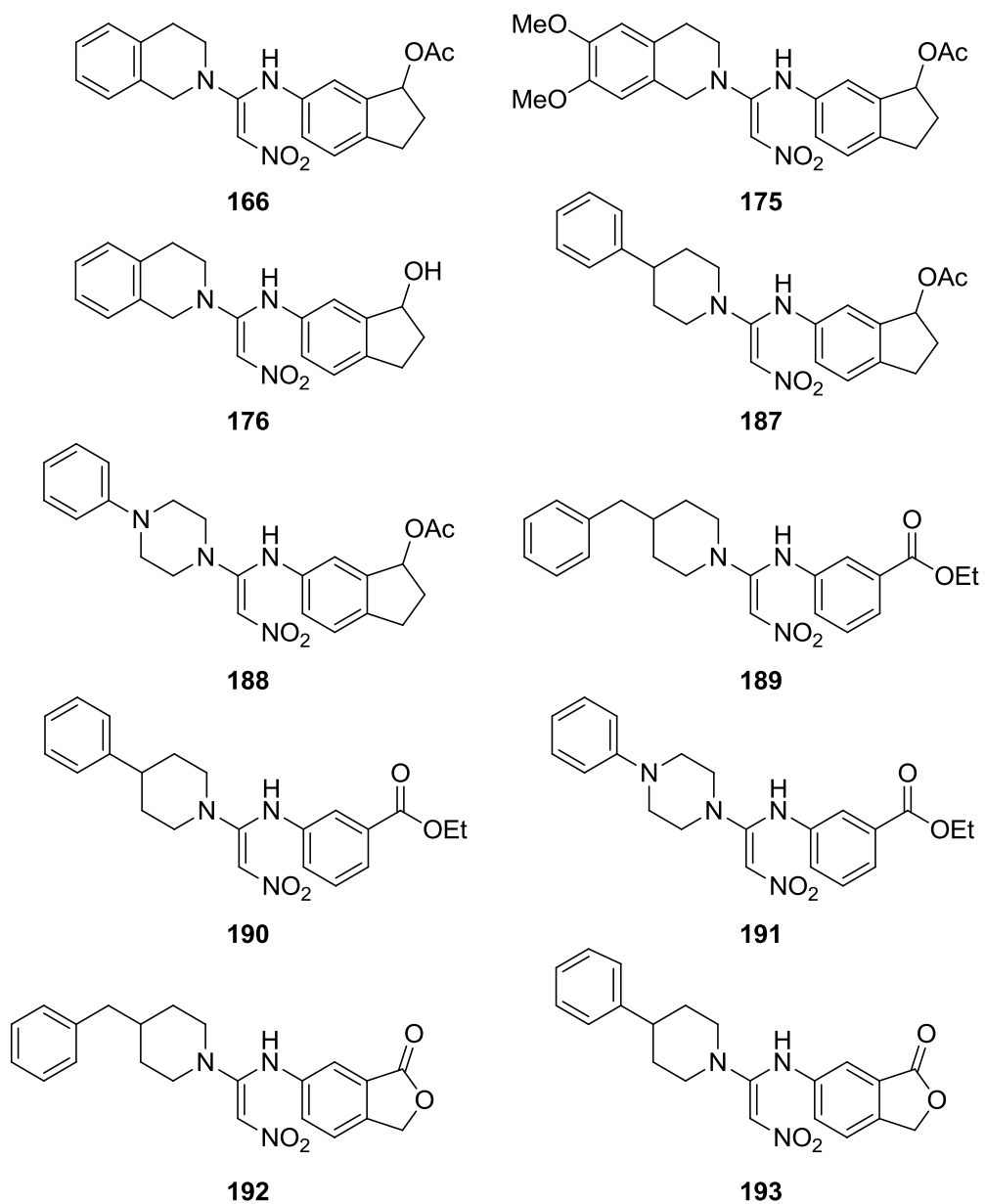
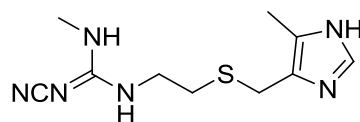


Figure 67: Novel *N,N'*-disubstituted nitroalkene compounds synthesised (166, 175-176, 187-193).

2.3 Linker modifications – Cyanoguanidines

Cyanoguanidines are a common motif in many drug compounds and are often used as bioisosteres, as exemplified by the development of Smith, Kline and French's (now GlaxoSmithKline) blockbuster H₂ antagonist cimetidine (**90**).¹⁷⁰ Cyanoguanidine was used bioisosterically to replace a thiourea with the result of modest pK_a change (from -1.2 to -0.4) but a great increase in potency and reduction in toxicity.¹⁹⁷



90

Figure 68: Cimetidine (**90**).

A cyanoguanidine moiety was therefore a good choice for an electron-withdrawing alternative to an amidine functional group. By analogy with the nitroalkene analogues, this group can be introduced by employing addition-elimination chemistry in this case using dimethyl cyanodithioimidocarbonate (**196**) and diphenyl cyanocarbonimidate (**197**).

As indicated in Table 22, monosubstitution of 1,2,3,4-tetrahydroisoquinolines (**116-117**) with dimethyl cyanodithioimidocarbonate (**196**) and diphenyl cyanocarbonimidate (**197**) was achieved in moderate to high yield by refluxing for 16 hours in dichloromethane (**198-201**, Table 22).

Compound	R	X	Solvent	Time (h)	Yield (%)
198	H	SMe	DCM	16	79
199	MeO	SMe	DCM	16	49
200	H	OPh	DCM	16	67
201	MeO	OPh	DCM	16	52

Table 22: Monosubstitution of tetrahydroisoquinolines **116** and **117**.

Crystals of phenyl *N*-cyano-6,7-dimethoxy-3,4-dihydro-2(1*H*)-isoquinolinecarboximidoate (**201**) were submitted for X-ray crystallographic analysis and the configuration of the cyano-imidate found to be *Z* (Figure 69).

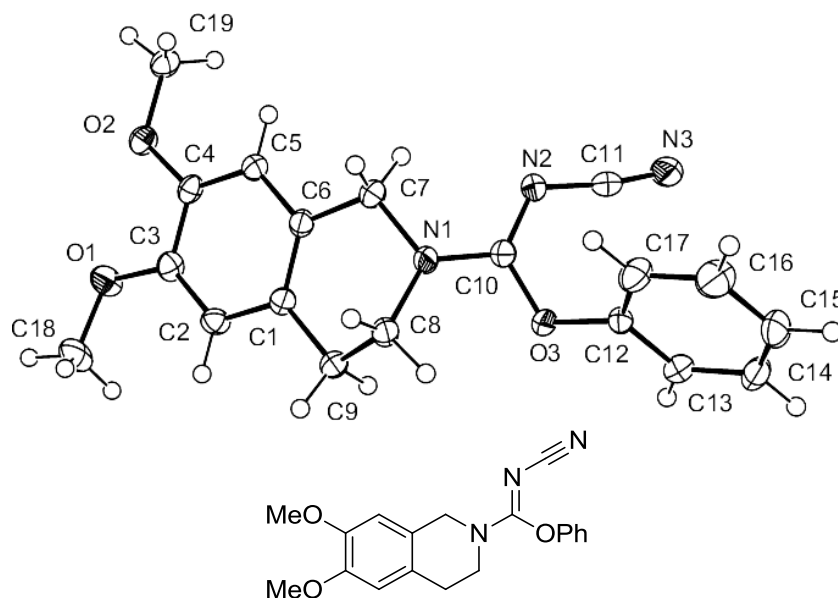


Figure 69: Crystal structure of cyano-6,7-dimethoxy-3,4-dihydro-2(1*H*)-isoquinolinecarboximidoate (**201**).

With the *Z*-monosubstituted products in hand, the second substitutions were carried out. These reactions were unsuccessful: only starting materials were observed by TLC and NMR even using a range of solvents and temperatures, microwave irradiation and using both methyl thiolate and phenolate leaving groups (Table 23).

R -substituted dimethyl cyanodithioimidocarbonate (198-201) + $\text{H}_2\text{N-Ar}$ (124-125) $\xrightarrow{\text{DCM, reflux}}$ R -substituted monosubstituted product (202-205)

Compound	R	Ar	X	Solvent	Time (h)	Yield (%)
202	H		SMe	DCM	96	-
	H		SMe	MeOH	96	-
	H		SMe	DMF	48	-
	H		SMe	DCE	96	-
	H		SMe	THF	96	-
	H		OPh	THF	1*	-
203	MeO		OPh	DCM	16	-
204	MeO		OPh	DCM	16	-
	MeO		OPh	MeOH	16	-
205	H		OPh	DCM	16	-

Table 23: Investigation of solvent effects on nucleophilic substitution of dimethyl cyanodithioimidocarbonate at reflux *microwave irradiation at 160 °C.

Phenolate was expected to be more easily displaced as it is a better leaving group than methyl thiolate as the anion can be stabilised by resonance. However, extended conjugation through the linker and poor nucleophilicity of the primary aromatic amines chosen may be contributing factors to the poor reactivity of these monosubstituted products (Figure 70).

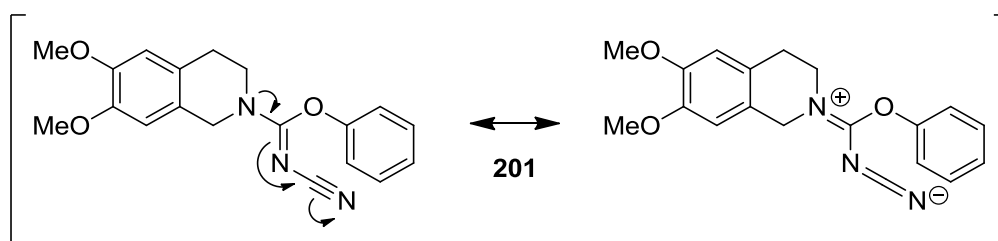


Figure 70: Resonance effects potentially contributing to poor reactivity of substrate **201**.

This work was carried out in tandem with the nitroalkene chemistry discussed previously (Section 2.2) and after successful synthesis of *N,N'*-disubstituted nitroalkene compounds was achieved by reversing the order of reactants this strategy was applied to the cyanoguanidines. The desired primary aromatic amine (**124-125**, **172**) was coupled to diphenyl cyanocarbonimidate (**197**) to give each monosubstituted product in moderate yield after flash chromatography (**206-208**).

Both propan-2-ol and dichloromethane were used for this reaction with little difference in yield (Table 24).

$\text{H}_2\text{N}-\text{Ar} + \text{PhO}-\overset{\text{NCN}}{\text{C}}=\text{OPh} \xrightarrow[16\text{ h}]{\text{reflux}} \text{PhO}-\overset{\text{NCN}}{\text{C}}=\text{N}-\text{Ar}$				
124-125. 172		197	206-208	
Compound	Ar	Solvent	Time (h)	Yield (%)
206		propan-2-ol	16	42
207		propan-2-ol	16	51
208		DCM	16	39

Table 24: Successful reaction conditions for monosubstitution of diphenyl cyanocarbonimide (**197**).

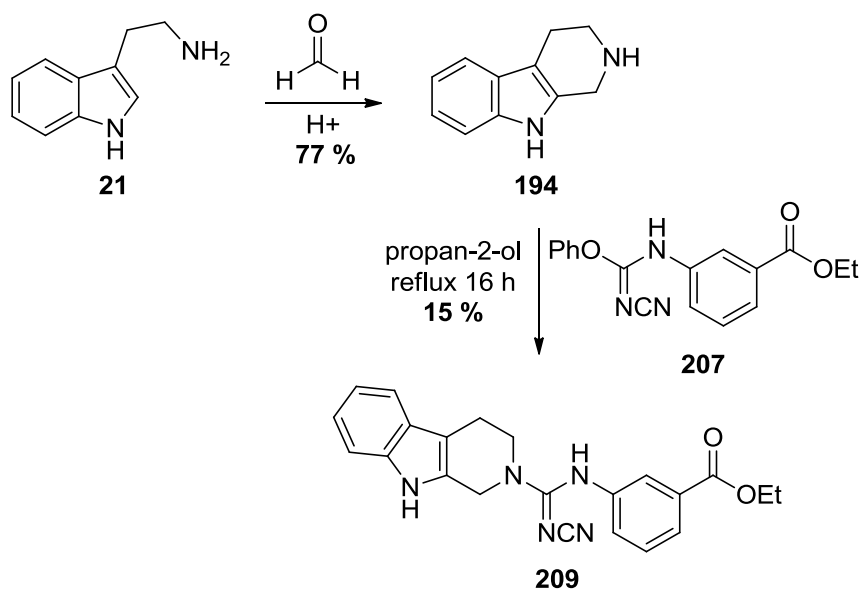
With these precursors in hand, the coupling of *N*-substituted phenyl cyanocarbonimidates (**206-208**) to unsubstituted and 6,7-dimethoxy substituted 1,2,3,4-tetrahydroisoquinolines (**116-117**) was carried out. After refluxing in propan-2-ol for 16 hours, three novel *N,N'*-disubstituted analogues were isolated in high yield after flash chromatography (**202-203** and **205**, Table 25).

$\text{PhO}-\overset{\text{NCN}}{\text{C}}=\text{N}-\text{Ar} + \text{R}-\text{C}_6\text{H}_3(\text{R})_2-\text{NH} \xrightarrow[16\text{ h}]{\text{reflux}} \text{R}-\text{C}_6\text{H}_3(\text{R})_2-\text{N}(\text{H})-\overset{\text{NCN}}{\text{C}}=\text{N}-\text{Ar}$					
206-208		R = MeO 116 H 117	202-203, 205		
Compound	Ar	R	Solvent	Time (h)	Yield (%)
202		H	propan-2-ol	24	71
203		MeO	propan-2-ol	24	70
205		H	propan-2-ol	24	74

Table 25: Successful synthesis of *N,N'*-disubstituted cyanoguanidine compounds (**202-203**, **205**).

Initial assay results (discussed in Chapter 3), indicated that this family of compounds was not sufficiently active to warrant further exploration. However, after the

unsuccessful preparation of a tetrahydro- β -carboline derived nitroalkene compound (Scheme 13 and Scheme 14), a corresponding cyanoguanidine analogue was successfully synthesised to investigate SAR. Additionally, information on hERG could be generated through the preparation of this analogue in the context of discrete structural modification. Tetrahydro- β -carboline **194** was coupled to the previously synthesised precursor **207** by refluxing in propan-2-ol for 16 hours to furnish tetrahydro- β -carboline derived cyanoguanidine analogue **209** in 15 % yield (Scheme 15).



Scheme 15: Synthesis of tetrahydro- β -carboline derived cyanoguanidine analogue (**209**).

Unfortunately, crystal growth proved unsuccessful after a number of attempts and X-ray analysis could not be carried out, therefore, the configuration of the cyanoguanidine moiety could not be assigned. However, conformational analysis using Gaussian¹⁸⁰ was carried out on compound **203** and the energy minimised structure is depicted below (Table 26). This energy minimised compound adopts a bent conformation, similar to the *N,N'*-disubstituted nitroalkene compounds, so these compounds may also be risky for hERG activity.¹⁴⁴ Again, the reduction in basicity by incorporation of the cyanoguanidine group may decrease hERG liability.

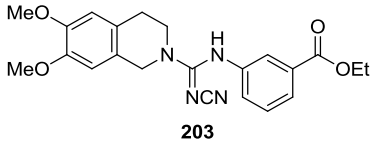
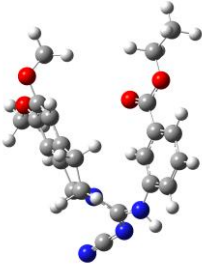
Compound	Energy minimised structure
 203	

Table 26: Conformational analysis of *N,N'*-disubstituted cyanoguanidine compound **203**.

2.3.1 Summary of *N,N'*-disubstituted cyanoguanidines

Overall, four novel *N,N'*-disubstituted cyanoguanidines were prepared in a similar fashion to the *N,N'*-disubstituted nitroalkene compounds in moderate to good yields.

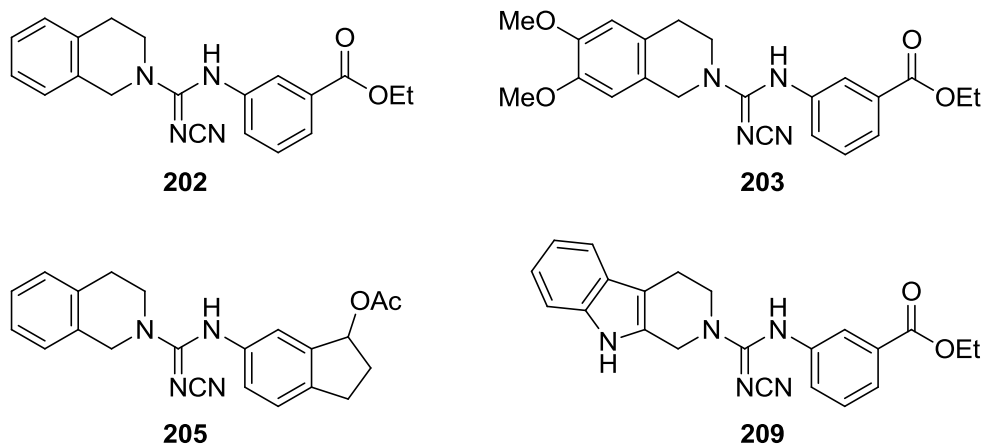


Figure 71: Summary of *N,N'*-disubstituted cyanoguanidines synthesised (**202-203**, **205** and **209**).

2.4 Linker modifications - Trifluoroethanimidamides

In the context of relatively small and electron-withdrawing amidine isosteres applicable to the programme of research, trifluoromethyl-linked compounds were of considerable interest. These represent alternative synthetic targets as a means of tuning pK_a with potentially desirable effects on hERG activity.

Historically, trifluoromethyl-containing compounds have been extremely popular in the pharmaceutical industry. This relatively small but highly electron-withdrawing substituent is used in drugs for a number of reasons: to introduce a powerful electron-withdrawing group, to increase lipophilicity, to decrease oxidative metabolism by increasing stability of drugs, or to enhance drug-protein interactions.^{198, 199} Examples of drugs containing trifluoromethyl groups include Eli Lilly's fluoxetine (Prozac™) (**210**), one of the world's most successful serotonin re-uptake inhibitors (SSRI) used mainly for depression and efavirenz (**211**), a non-nucleoside reverse transcriptase inhibitor (NNRTI) used to treat HIV-1.

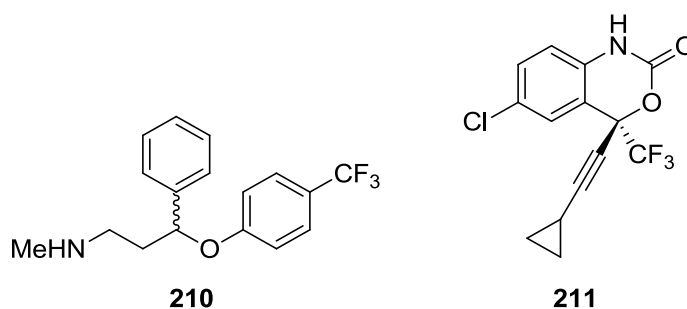
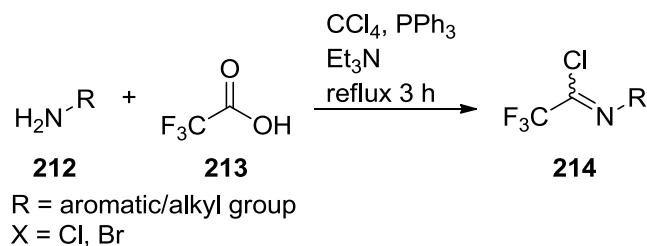


Figure 72: (\pm)-Fluoxetine (**210**) and efavirenz (**211**), examples of drugs containing trifluoromethyl substituents.

In recent years, the synthesis of N,N' -disubstituted trifluoromethyl-containing compounds has been simplified by the discovery of a one-pot procedure for the synthesis of trifluorinated imidoyl halides by Umeyama and co-workers which can tolerate a wide range of substrates.²⁰⁰ Such a protocol is therefore an attractive means of accessing trifluoromethyl-modified *serominic* compounds.

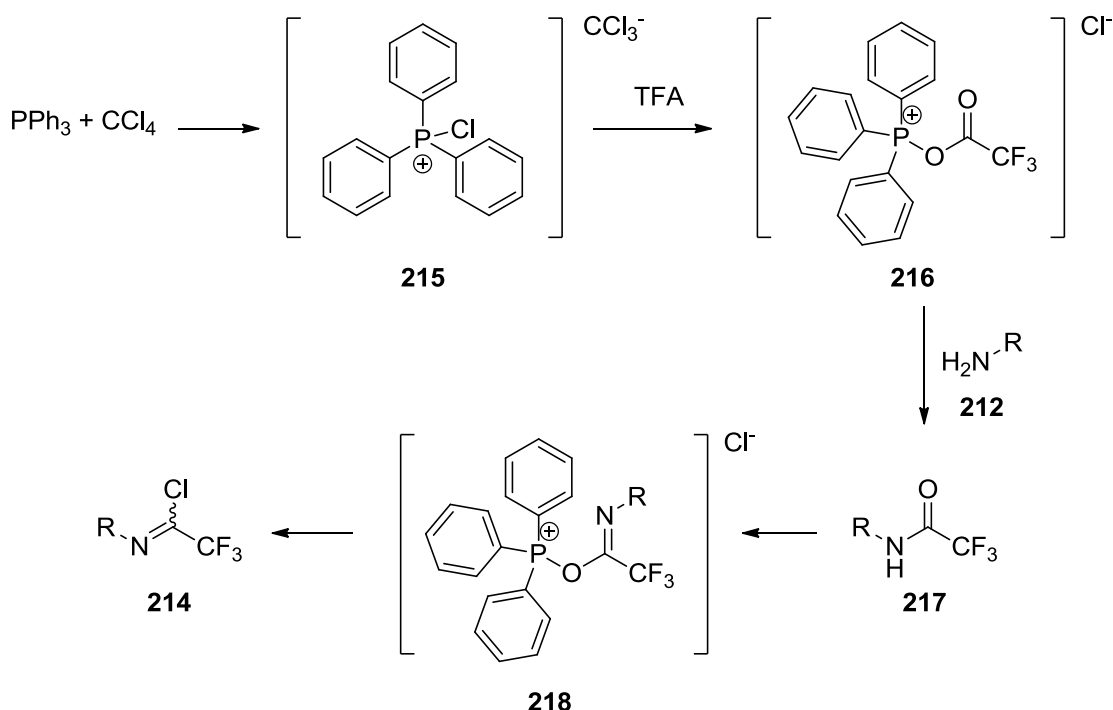
The trifluoro imidoyl chloride (**214**) is formed by refluxing trifluoroacetic acid (**213**) (TFA) and a primary amine (**212**) in carbon tetrachloride (or carbon tetrabromide to

prepare the corresponding bromide) in the presence of triethylamine and triphenylphosphine (Scheme 16).



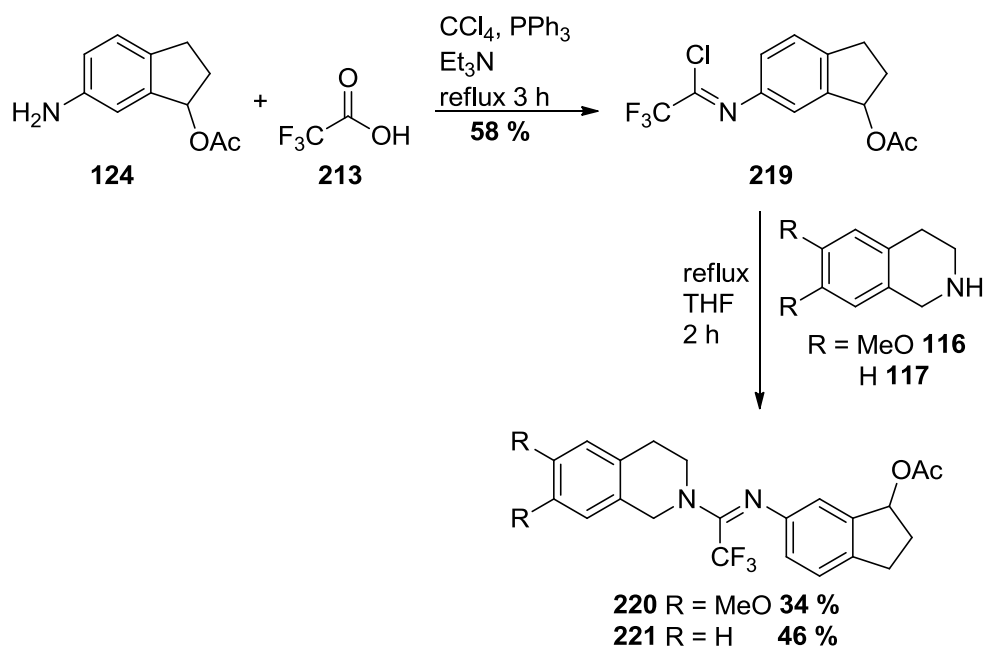
Scheme 16: One-pot synthesis of imidoyl halides (**214**).

Formation of chlorotriphenylphosphonium trichloromethide is postulated to be the initial step (**215**, Scheme 17). Nucleophilic attack on the phosphonium by trifluoroacetate forms the intermediate **216** which subsequently reacts with the primary amine **212** to form triphenylphosphine oxide and amide **217**. A final condensation is initiated upon nucleophilic attack of another molecule of chlorotriphenylphosphonium trichloromethide (**216**) to generate iminium intermediate **218** which then collapses to the trifluoro imidoyl chloride **214**, with the thermodynamically favourable formation of triphenylphosphine oxide.



Scheme 17: Proposed mechanism for imidoyl chloride formation.²⁰⁰

Returning to the synthesis of these target systems, the reactions were carried out according to the conditions described above using 6-amino-2,3-dihydro-1*H*-inden-1-yl acetate (**124**, Scheme 18) as the primary amine to give the corresponding imidoyl chloride (**219**) in 58 % yield. Nucleophilic substitution using both 1,2,3,4-tetrahydroisoquinoline (**116**) and 6,7-dimethoxy-1,2,3,4-tetrahydroisoquinoline (**117**) and furnished the desired trifluoroethanimidamide compounds in 34 and 46 % yields, respectively (**220-221**).



Scheme 18: Synthesis of trifluoroethanimidamide analogues (**220-221**).

The configuration of the trifluoroimidamides (**220-221**) was unable to be unambiguously assigned due to the lack of an X-ray structure. However, the *E* configuration may be favoured over the *Z* (as observed for the amidines, nitroalkenes and triazenes) in order to minimise steric repulsion (Figure 73). Each of the R groups is sterically bulky in comparison to a trifluoromethyl moiety which is approximately the size of an ethyl group.²⁰¹

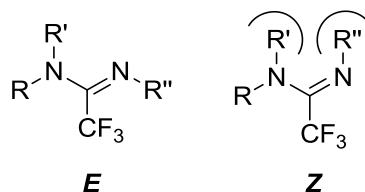


Figure 73: Proposed configuration of *N,N'*-disubstituted trifluoroimidamides based on relatively bulky R' and R'' groups.

Conformational analysis was carried out using Gaussian¹⁸⁰ on (*E*)-**220** and the energy-minimised structure is depicted below (Table 27). This energy-minimised compound adopts an almost staggered conformation with the 6,7-dimethoxy-1,2,3,4-tetrahydroisoquinoline group aligned perpendicular to the indanyl acetate group which may reduce the hERG liability of this family of compounds by hindering access to the binding site.

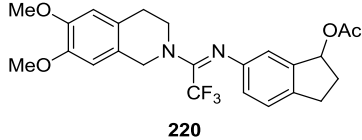
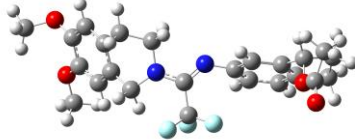
Compound	Energy minimised structure
 220	

Table 27: Conformational analysis of (*E*)-*N,N'*-disubstituted trifluoromethyl compound **220**.

2.4.1 Summary of *N,N'*-disubstituted trifluoroethylidene compounds

Overall two novel *N,N'*-disubstituted trifluoroethanimidamides were synthesised in a simple one-pot reaction (**220-221**).

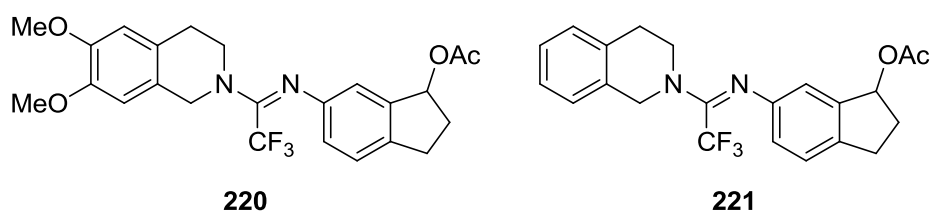


Figure 74: Novel *N,N'*-disubstituted trifluoroethanimidamides **220** and **221**.

2.5 Linker modifications – Hydrazides and ureas

Acyl derivatives of hydrazines, known as hydrazides, are frequently encountered motifs in drug discovery and are present in drugs such as the tuberculostatic isoniazid (**222**, Figure 75), the diuretic clopamid (**223**) and the anti-obesity CB1 inverse agonist rimonabant (**224**).

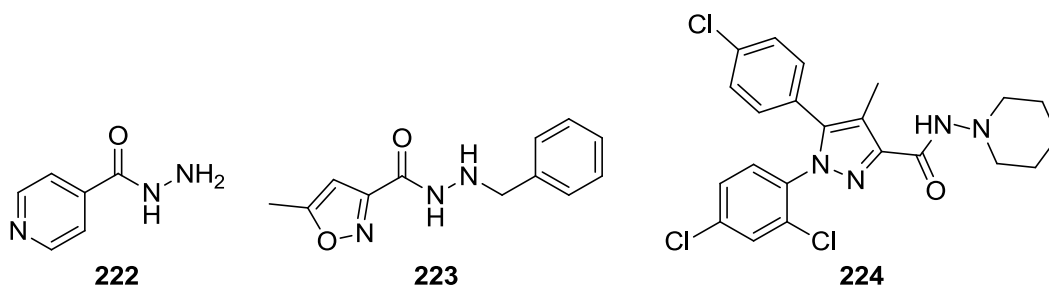


Figure 75: Compounds containing hydrazide functionalities, isoniazid (**222**), clopamid (**223**) and rimonabant (**224**).

In relation to the objectives of the research programme, introduction of hydrazide based linkers to replace the amidine linker functionality will reduce pK_a whilst additionally introducing a new hydrogen bond acceptor into the molecule. This decrease in basicity may be beneficial in terms of ameliorating hERG activity.

Hydrazides are readily prepared by simple coupling of a hydrazine and an acid functionality in the presence of an amide coupling agent and base (Figure 76). Amide coupling agent T3P was chosen as it had been used previously within the group and the water-soluble by-products were simple to remove on work-up.²⁰² Mechanistically, carboxylate **229** nucleophilically attacks a phosphonate group on T3P (**228**) which ring opens to give activated acid intermediate **230**. Nucleophilic attack of hydrazine **226** on this activated acid furnishes amide **231** and the water-soluble tri-phosphonate **232** (Figure 76).

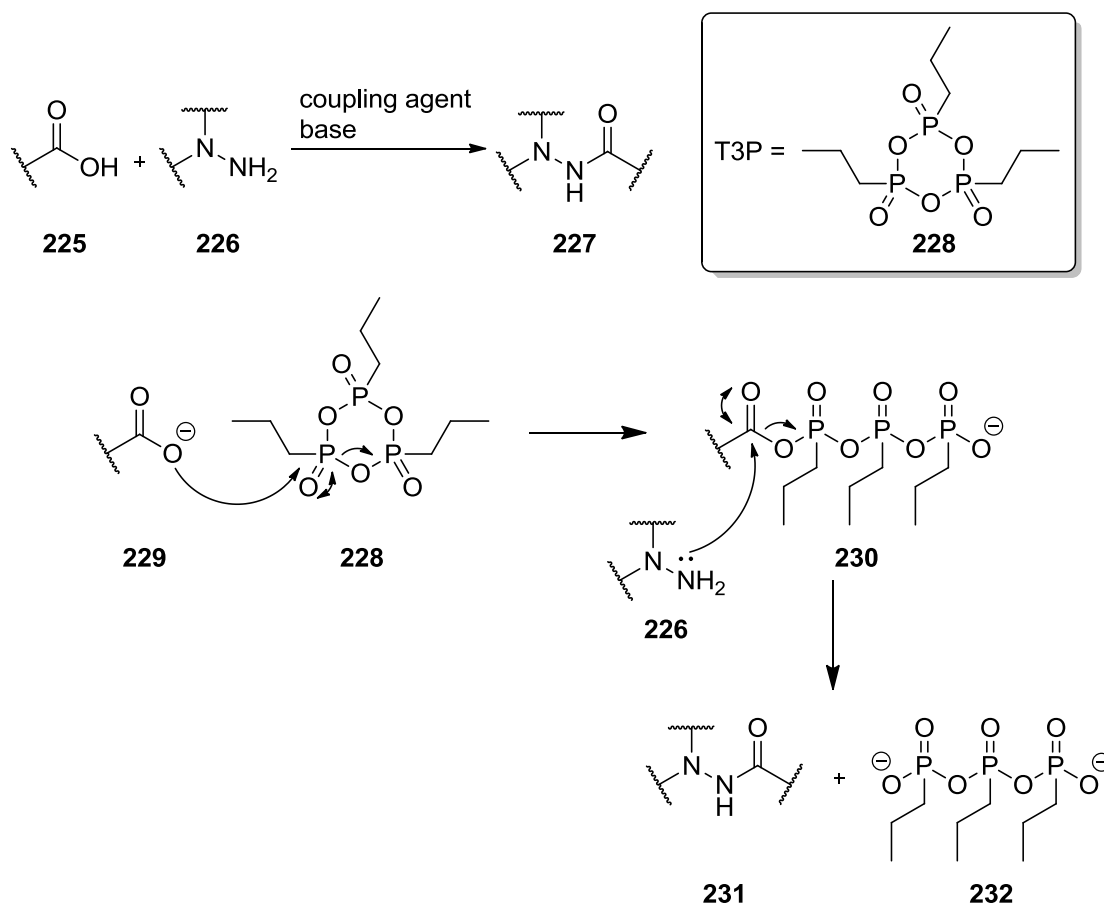
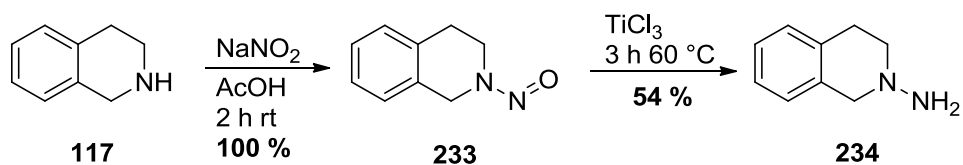


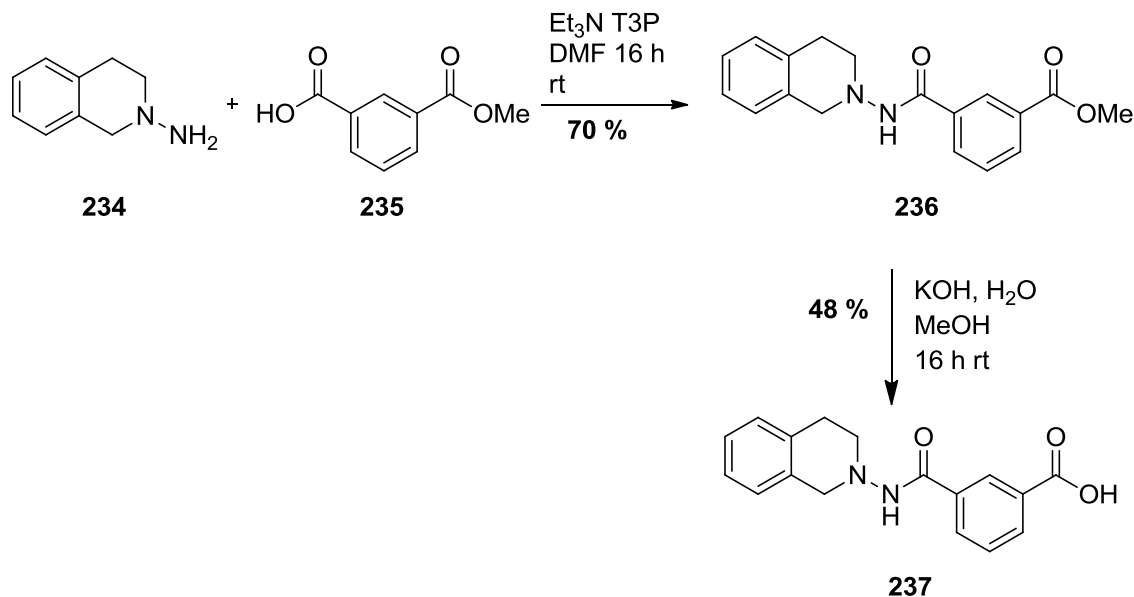
Figure 76: Mechanism of amide coupling using T3P.

Hydrazide analogues of the lead *serominic* series were synthesised using the above procedure by A. Cameron, a final-year undergraduate project student.²⁰³ Hydrazine **234** was synthesised by treating 1,2,3,4-tetrahydroisoquinoline (**117**) with sodium nitrite in the presence of acid to form the nitrosamine (**233**) in quantitative yield. The nitrosamine (**233**) was then reduced to the hydrazine derivative (**234**) using titanium (III) chloride.



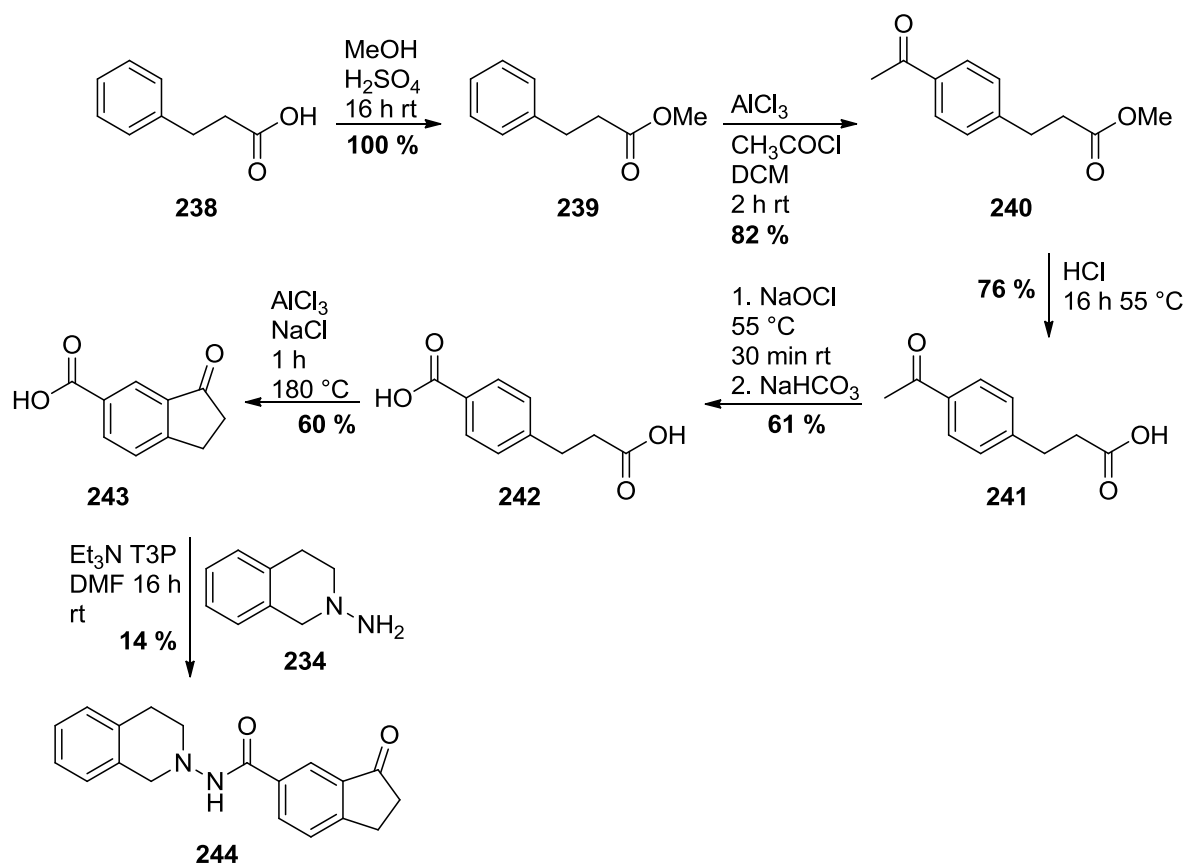
Scheme 19: Synthesis of hydrazine (**234**) from 1,2,3,4-tetrahydroisoquinoline (**117**).

With this compound in hand, it was coupled to commercially available 3-(methoxycarbonyl)benzoic acid (**235**) using T3P to give the desired hydrazide product (**236**) in 70 % yield after purification by flash chromatography. A sample of this methyl ester compound (**236**) was then hydrolysed using potassium hydroxide to furnish the corresponding carboxylic acid in 48 % yield (**237**).



Scheme 20: Synthesis of methyl ester (**236**) and carboxylic acid (**237**) hydrazide analogues.

The third hydrazide compound necessitated a longer synthesis. 1-Indanone-6-carboxylic acid (**243**, Scheme 20) was synthesised by esterification of the commercially available reagent, 2-phenylpropanoic acid (**238**), to form the methyl ester (**239**). Friedel-Crafts acylation using aluminium chloride and acetyl chloride then formed the 4-acetyl methyl ester (**240**) which was hydrolysed in the presence of hydrochloric acid to the carboxylic acid (**241**). The 4-acyl substituent was then oxidised using sodium hypochlorite to give the aromatic carboxylic acid (**242**). Finally, an intramolecular Friedel-Crafts cyclisation gave the desired 1-indanone-6-carboxylic acid (**243**) which was then coupled, as before, to hydrazine (**234**) using T3P to give the hydrazide (**244**) in 14 % yield.



Scheme 21: Synthesis of 1-indanone hydrazide derivative **244**.

Conformational analysis was carried out using Gaussian¹⁸⁰ on hydrazide compound **236** and the energy minimised structure is depicted below (Table 28). This energy minimised compound adopts a staggered conformation, similar to the trifluoromethyl compounds. The 1,2,3,4-tetrahydroisoquinoline group is aligned perpendicular to the methyl ester group which may hinder access to the hERG binding site and decrease hERG liability of this family of compounds compared to the amidine family.

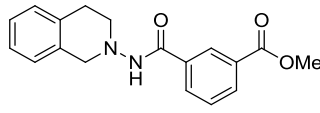
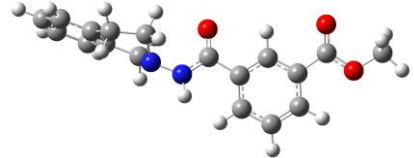
Compound	Energy minimised structure
 <p style="text-align: center;">236</p>	

Table 28: Conformational analysis of hydrazide compound **236**.

Ureas are also commonly used functional groups in drug discovery and feature in a number of drugs including Merck's hepatitis C protease inhibitor boceprevir (**245**), recently approved by the FDA (2011).²⁰⁴

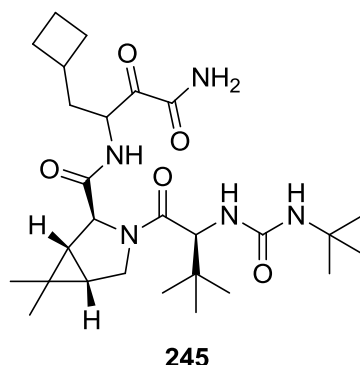
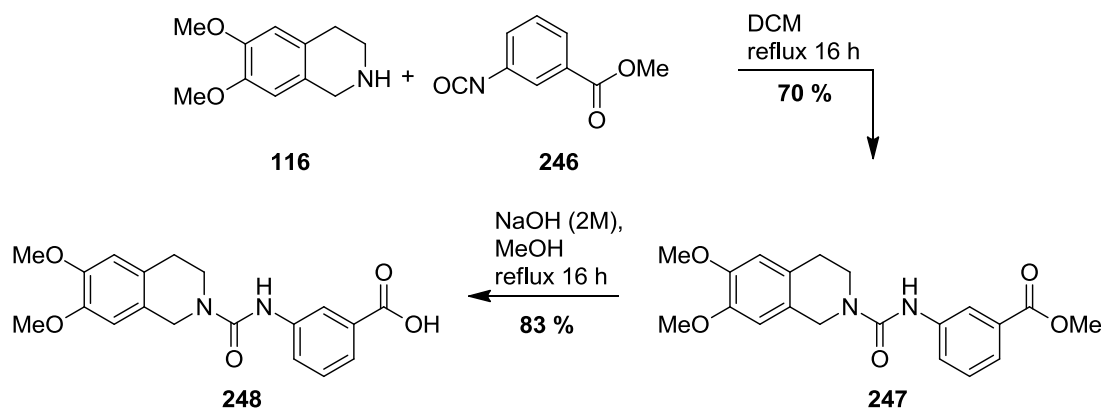


Figure 77: Drugs containing urea functionalities, boceprevir **245**.

Introduction of a urea functionality as an electron-withdrawing linker group in place of an amidine will significantly change the pK_a and provide an additional hydrogen bond acceptor to the molecule. Two urea compounds were synthesised by A. Rodriguez, an undergraduate student in the lab, by coupling the desired secondary amine to a commercially available isocyanate.²⁰⁵ 6,7-Dimethoxy-1,2,3,4-tetrahydroisoquinoline (**116**) was refluxed in dichloromethane with methyl 4-isocyanatobenzoate (**246**) for 16 h to precipitate urea **247** in 70 % yield. This was then hydrolysed using sodium hydroxide to furnish the corresponding carboxylic acid (**248**) in 83 % yield.



Scheme 22: Synthesis of methyl ester (**247**) and carboxylic acid urea derivatives (**248**).

Conformational analysis was carried out using Gaussian¹⁸⁰ on urea compound **247** and the energy minimised structure is depicted below (Table 29). This energy minimised compound adopts a bent conformation, which may actually increase likelihood of hERG binding but the decreased basicity of the central nitrogen may mitigate this.

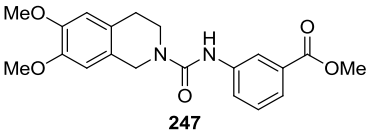
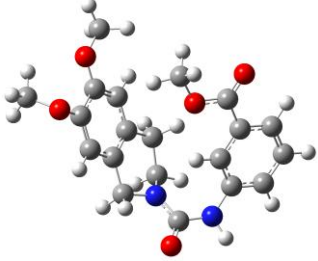
Compound	Energy minimised structure
 247	

Table 29: Conformational analysis of urea compound **247**.

2.5.1 Summary of synthesis of *N,N'*-disubstituted hydrazide and urea compounds

Overall, five new hydrazide and urea target compounds (**236-237**, **244**, **247-248**) were synthesised in moderate yield (Figure 78).

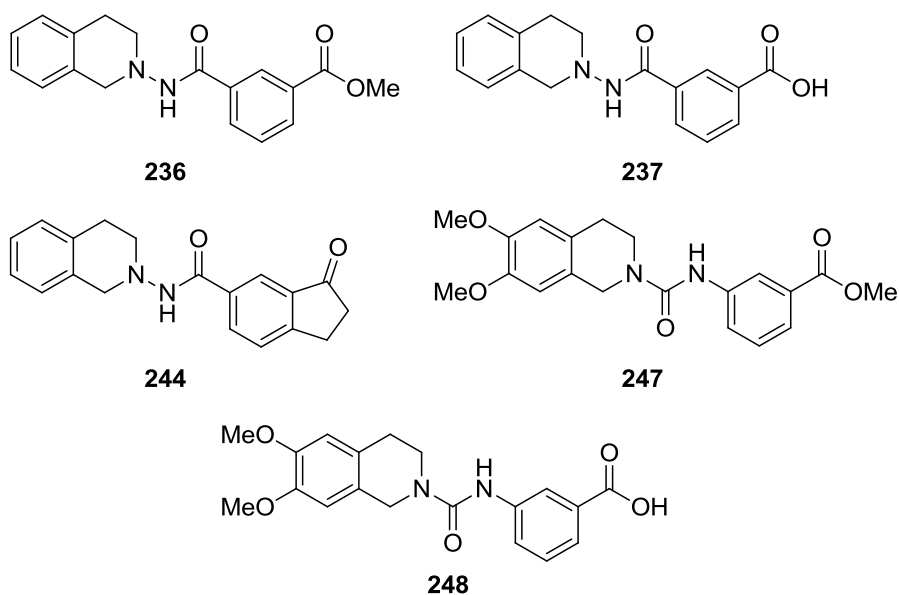


Figure 78: Five novel hydrazide and urea-linked compounds synthesised (**236-237**, **244**, **247-248**).

2.6 Linker modifications – Triazenes

Triazenes are well-known functional groups within the field of oncology as typified by compounds such as Bayer's alkylating agent, dacarbazine (**249**) and analogues of this type.²⁰⁶

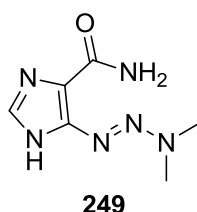
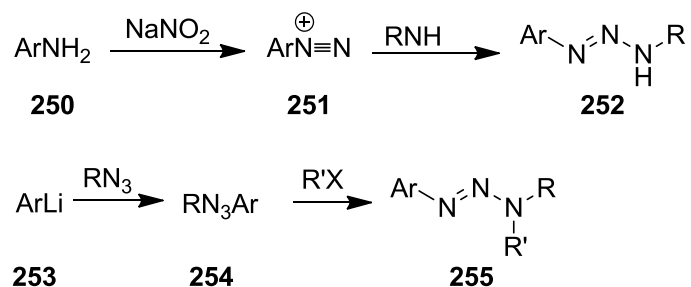


Figure 79: Anti-cancer drug dacarbazine (**249**), containing the triazene functional group.

Triazenes (**252**) are generally synthesised through diazotisation or utilising Grignard chemistry. Aryl triazenes can be synthesised from an aniline derivative (**250**), sodium nitrite and a primary or secondary amine, through a diazonium salt intermediate (**251**). Dialkyl triazenes (**255**) can be synthesised by reaction of an azide with a Grignard reagent or an alkyl lithium reagent (**253**, Scheme 23).



Scheme 23: General syntheses of triazene compounds (**252** and **255**).

It might be argued that triazenes are not appropriate functional groups for drugs because of their lability. The cytotoxicity of many triazene anti-tumour drugs is proposed to be mediated by their metabolism *in vivo* to more active metabolites.^{207, 208} However, a reasonable body of data has been collected on triazene stability and some have been shown to have sufficient stability in solution to be used as drugs. In acidic media, triazenes (**256**) undergo hydrolysis to the appropriate aryl diazonium salt (**257**) and amine (**258**) but rate of hydrolysis is significantly lower at physiological pH.²⁰⁹

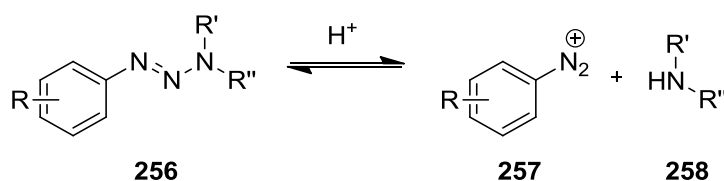
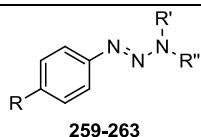


Figure 80: Hydrolysis of a triazene linker (**256**) under acidic conditions.

Connors *et al.* reported a range of half-lives from 11 min. to over 92 days on a small subset of structurally similar triazenes (Table 30). Compounds containing a dimethyl substituted N³ atom are relatively stable at physiological pH and 37 °C (**259-261**). However, substituting a methyl group for a hydrogen atom significantly decreases the half life of hydrolysis, to less than thirty min. under the same conditions (**262-263**).²⁰⁹



Number	R	R'	R''	Half-life (min)
259	CONH ₂	Me	Me	1.24 x 10 ⁵
260	CF ₃	Me	Me	1.33 x 10 ⁵
261	SO ₂ CH ₃	Me	Me	no decomposition observed
262	CONH ₂	Me	H	11
263	SO ₂ CH ₃	Me	H	25

Table 30: Half-life of hydrolysis at 37° C in pH 7.5 phosphate buffer.²⁰⁹

Nevertheless, interest was still strong in this functional group in terms of employing it as an isostere. Triazenes could reasonably be expected to be the most active family of compounds due to similar structural and geometrical properties to the amidine family but, importantly, with decreased pK_a values (amidine = 12¹⁶⁸) which could potentially reduce hERG activity. After consideration of the triazene compounds planned for synthesis, it was thought that their general structures were more likely to exhibit reasonable stabilities under physiological conditions (**264**, Figure 81).

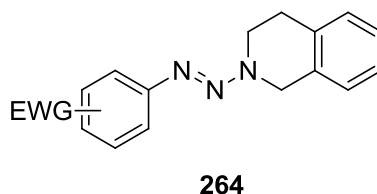
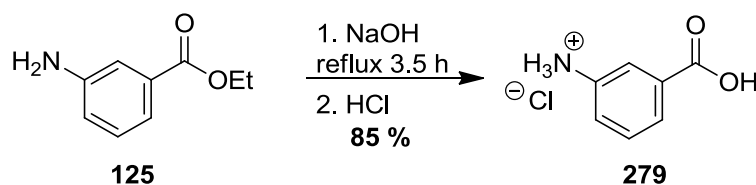


Figure 81: General structure of triazene compounds to be prepared (**264**).

Consequently, two triazene analogues were synthesised. An ethyl 3-amino benzoate derivative was synthesised in 75 % yield (**265**) by diazotisation of the primary aromatic amine (**266**) and subsequent coupling of 1,2,3,4-tetrahydroisoquinoline (**117**) by a final year undergraduate project student, L. Walker.²¹⁰ A 6-amino-2,3-dihydro-1*H*-inden-1-yl acetate analogue was later synthesised using the same procedure (**267**), and initial assay results suggested these compounds had potential *serominic* activity (Chapter 3). As a result, a more exploratory library was synthesised, including the 6,7-dimethoxy-1,2,3,4-tetrahydroisoquinoline analogue (**268**) which, upon purification, also yielded the hydroxyl derivative (**269**, Table 31).

The exploratory library focused on piperidine and piperazine analogues (**267-278**) and included carboxylic acid analogues (**277-276**) were also synthesised after hydrolysis of ethyl 3-amino benzoate (**125**) using sodium hydroxide yielded the corresponding acid (**279**) in 85 % yield (Scheme 24).



Scheme 24: Hydrolysis of ethyl 3-amino benzoate (**125**) to the corresponding carboxylate (**279**).

$\text{H}_2\text{N}-\text{Ar} \xrightarrow[30 \text{ min, } 0^\circ\text{C}]{1. \text{HCl, } 10 \text{ min}; 2. \text{NaNO}_2} \text{N}\equiv\text{N}^+\text{Ar} \text{Cl}^- \xrightarrow[0^\circ\text{C, } 4 \text{ h}]{\text{R, R', X, NH}} \text{R, R', X, N-N=N-Ar}$

124-125, 172 **266** **265, 267-269**

Compound	R	R'	X	Ar	Yield (%)
265	H	-	-		75
267	H	-	-		38
268	MeO	-	-		28
269	MeO	-	-		9

$\text{H}_2\text{N}-\text{Ar} \xrightarrow[30 \text{ min, } 0^\circ\text{C}]{1. \text{HCl, } 10 \text{ min}; 2. \text{NaNO}_2} \text{N}\equiv\text{N}^+\text{Ar} \text{Cl}^- \xrightarrow[0^\circ\text{C, } 4 \text{ h}]{\text{R', X, NH}} \text{R', X, N-N=N-Ar}$

124-125, 182, 279 **266** **270-278**

Compound	R	R'	X	Ar	Yield (%)
267	-	Ph	CH		21
271	-	Ph	N		18
272	-	Bn	CH		59
273	-	Ph	CH		45
274	-	Ph	N		25
277	-	Bn	CH		14
276	-	Ph	N		14
277	-	Bn	CH		45
278	-	Ph	N		5

Table 31: Synthesis of triazene compounds (**265, 267-278**).

A crystal of compound **277** was crystallised by slow evaporation of dichloromethane and submitted for X-ray analysis. This showed the compound existed only in its *E* configuration (Figure 82).

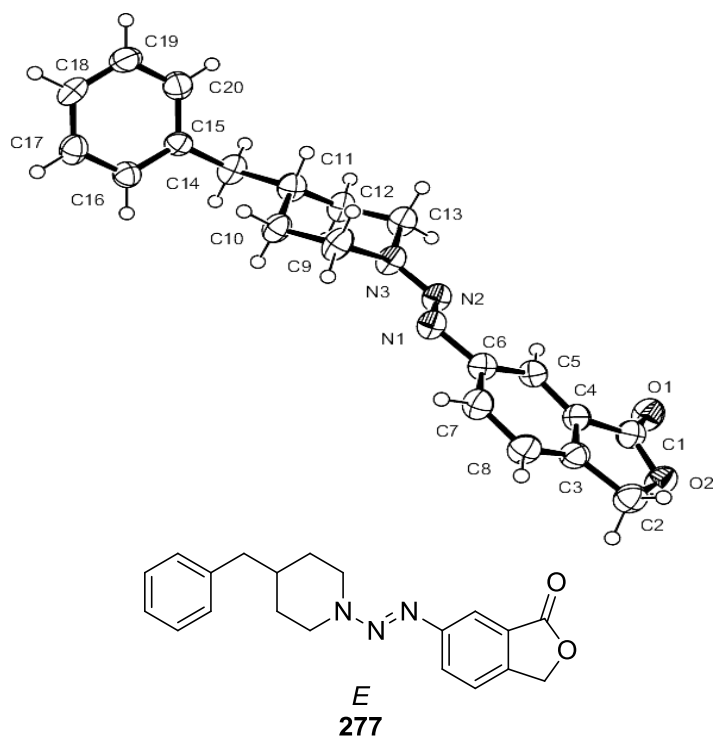


Figure 82: X-ray structure of compound **277** where the configuration across the triazene bond is *E*.

Although it might be expected that the configuration of these compounds would be dynamic, 2-D NOESY ^1H NMR supports the existence of *E* configuration only. No NOEs corresponding to *Z* configuration were observed experimentally (Figure 83 and Figure 84).

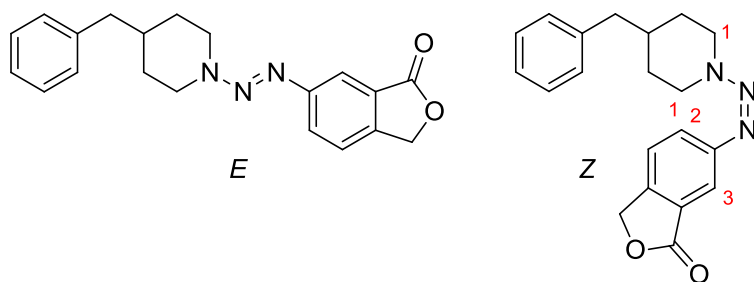


Figure 83: Potential NOEs (red) expected for *E* (none) and *Z* (1 and 2-3) configuration of triazene-linked compound **277**.

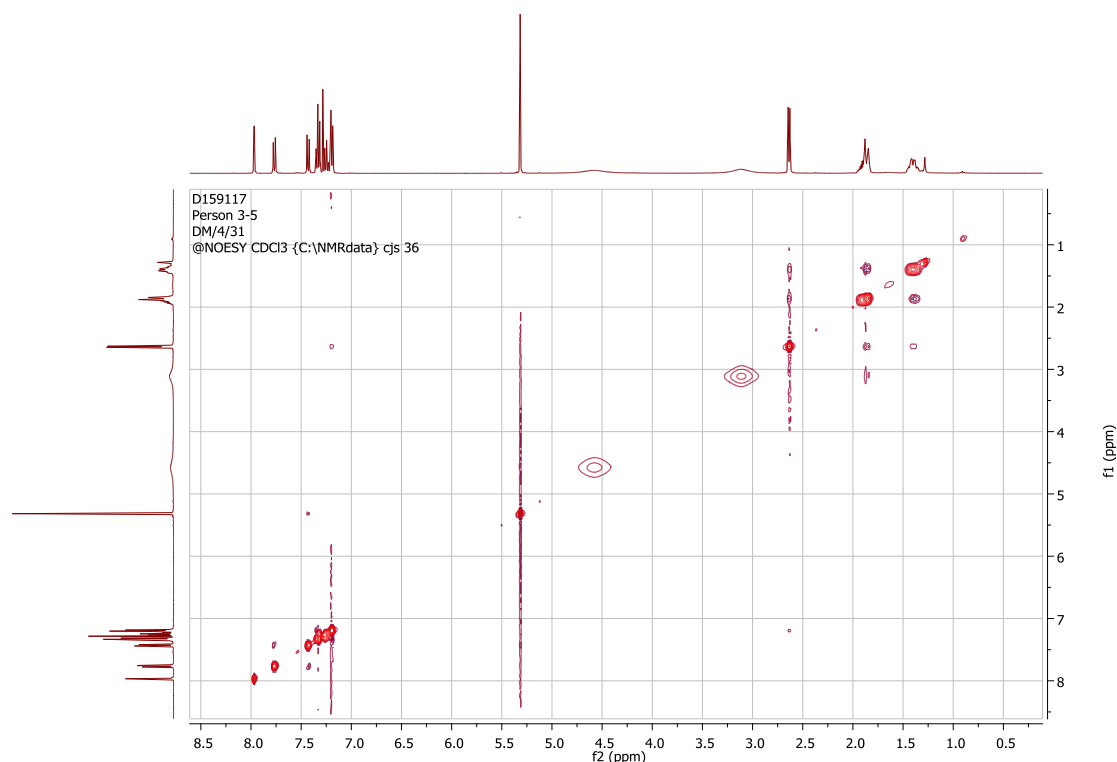


Figure 84: NOESY spectrum of triazene-linked compound **276** displaying no NOEs associated with *Z* configuration.

Conformational analysis was carried out using Gaussian¹⁸⁰ on triazene compound **268** and the energy minimised structure for *E* configuration is depicted below (Table 32). This energy minimised *E* compound adopts a planar conformation, similar to the amidine compounds. With the basic central nitrogen, these extended types of conformations are known to be high risk for hERG and therefore it would be expected that these compounds could have significant hERG liability.¹⁴⁴

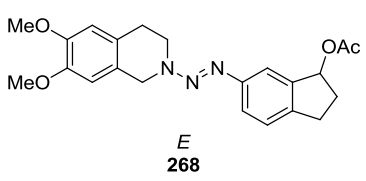
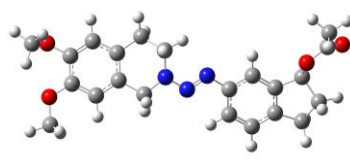
Compound	Energy minimised structure
 <i>E</i> 268	

Table 32: Conformational analysis of *E* triazene compound **268**.

2.6.1 Summary of triazene-linked compounds

To summarise, a number of novel triazenes were also synthesised in parallel to the compounds made for the second series of nitroalkenes, focusing mainly on *N*-heterocyclic changes as discussed previously in Section 2.2. These compounds were synthesised following the procedure described previously (Table 30) to furnish 13 novel triazene compounds overall within this phase of the programme (**265**, **267-278**, Figure 85). Furthermore, in terms of stability, compound **277** was observed to be bench-stable for over one year and stable in solution (CDCl₃) for at least two days. Further work to assess stability would be beneficial.

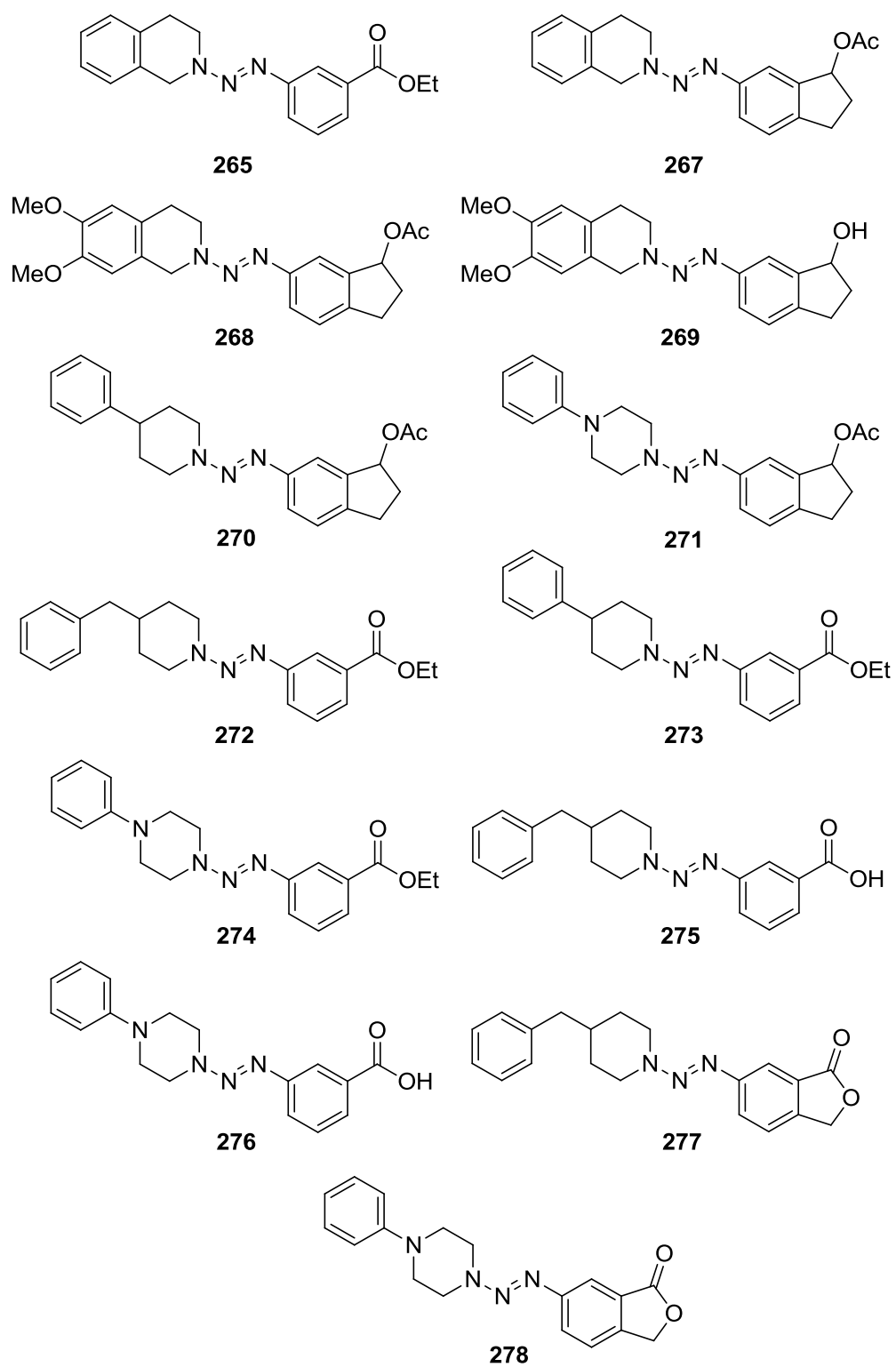


Figure 85: Summary of triazene compounds synthesised (265, 267-278).

2.7 Haloperidol analogues with potentially reduced hERG liability

As discussed in the introductory section, haloperidol (**5**) is a potent member of the butyrophenone class of typical antipsychotics. However, it is also a potent hERG blocker, with an IC_{50} value in the mid-nanomolar range³⁴ and evidence of QT prolongation in a number of patients has been observed.

It was thought that it may be possible to leverage the approach of linker modification adopted to the *serominic* series to potentially decrease hERG activity of established antipsychotics such as haloperidol (**5**) by inserting an EWG linker at an appropriate section (**280**) (Figure 86).

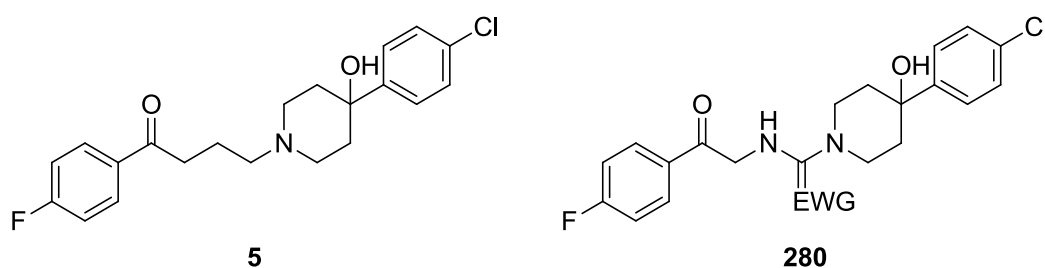


Figure 86: Haloperidol (**5**) and a haloperidol analogue with an EWG linker inserted (**280**).

Retrosynthetic analysis revealed two simple disconnections to give two commercially available substrates, 2-chloro-1-(4-fluorophenyl)ethanone (**281**) and 4-(4-chlorophenyl)piperidin-4-ol (**282**, Figure 87). Use of these substrates could provide wide scope to produce a number of target molecules with electron-withdrawing linkers.

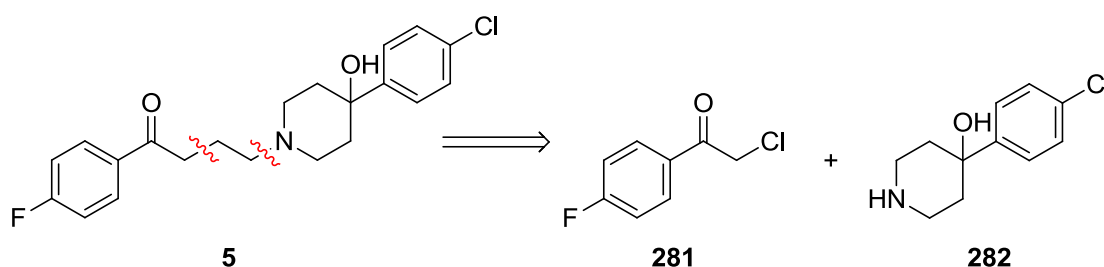
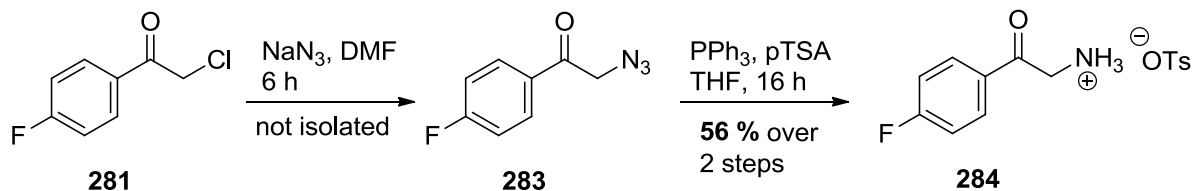


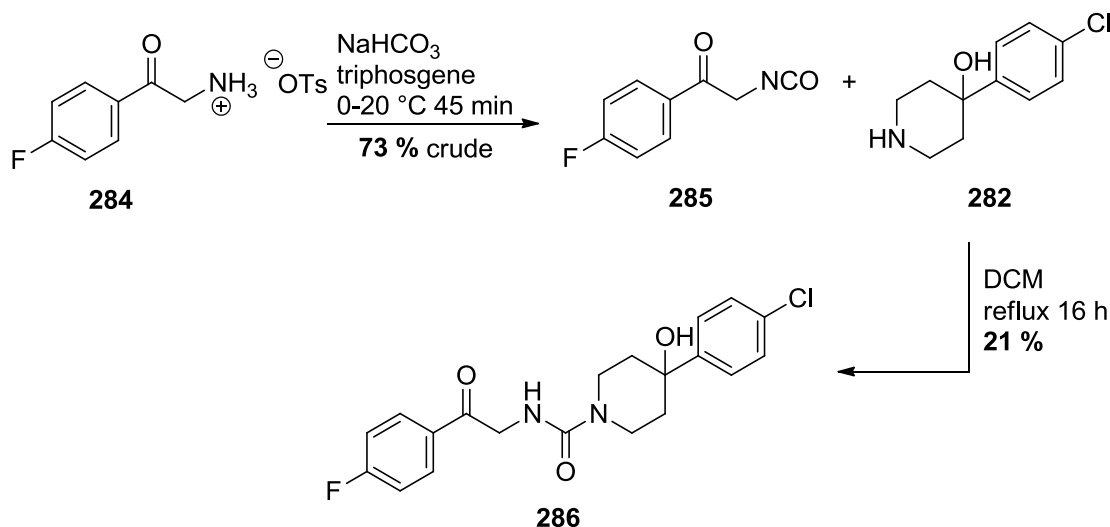
Figure 87: Retrosynthetic analysis of haloperidol (**5**).

First, functional group interconversion of 2-chloro-1-(4-fluorophenyl)ethanone (**281**) was carried out (Scheme 25). Azidation proceeded smoothly (**283**) and subsequent reduction utilising a modified Staudinger reaction furnished the requisite amine as the tosylate salt (**284**) in 56 % yield over two steps.²¹¹



Scheme 25: Functional group modification of 2-chloro-1-(4-fluorophenyl)ethanone (**281**).

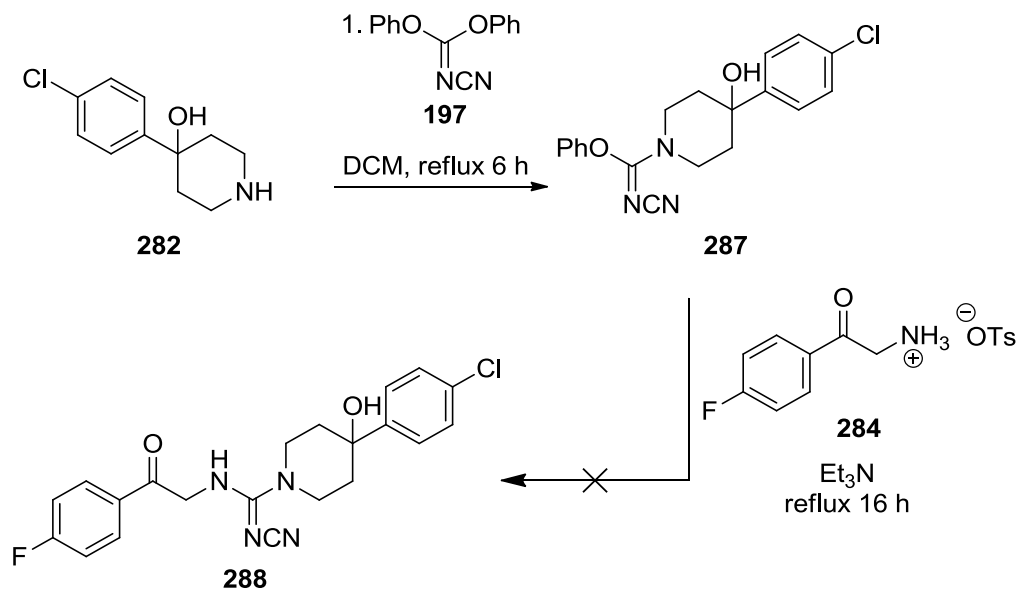
With this precursor in hand, haloperidol analogues with electron-withdrawing linkers could be synthesised. A urea-derived compound was synthesised by treating the previously prepared amine (**284**) with triphosgene, forming the isocyanate intermediate (**285**), which was then nucleophilically attacked by 4-(4-chlorophenyl)piperidin-4-ol (**282**) to furnish the desired urea (**286**, Scheme 26).



Scheme 26: Synthesis of urea derived haloperidol analogue (**286**).

Having developed a route to the urea derivative, a cyanoguanidine analogue was attempted. A one-pot reaction with addition of 4-(4-chlorophenyl)piperidin-4-ol (**282**) to diphenyl cyanocarbonimidate (**197**) under refluxing conditions for 6 h selectively yielded the monosubstituted product as observed by TLC. Amine **284** and triethylamine were then added and refluxing for an additional 16 h but there was

no further reaction and the *N,N'*-disubstituted cyanocarboximidamide product (**288**) could not be synthesised. Instead, the monosubstituted product was isolated in 67 % yield (**287**) after column chromatography and due to time constraints, this compound was taken forward for biological testing.



Scheme 27: Unsuccessful one-pot reaction for synthesis of *N,N'*-disubstituted cyanocarboximidamide (**288**).

2.7.1 Summary of haloperidol analogues

Overall, two novel haloperidol derivatives were synthesised and radioligand binding assays will ascertain if the addition of these linkers has an effect on the hERG activity compared to haloperidol. The primary pharmacology (retention of D₂ antagonism) was not investigated within this research programme but would be of interest for further work.

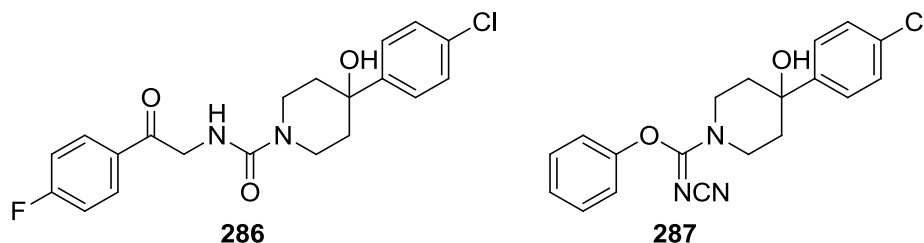


Figure 88: Haloperidol analogues synthesised **286-287**.

2.8 Summary of synthetic phase of research programme

Overall, 41 compounds incorporating six different linker groups, amidine, triazene, nitroalkene, hydrazide, urea and cyanoguanidine have been synthesised. A number of 5-HT₇ and M₄ responsive changes have been implemented to investigate SAR, alongside changes likely to reduce hERG activity (such as introduction of carboxylic acid functionalities). This approach should provide a good overview of the interaction between *serominic* and hERG pharmacology. The next stage of the research programme is biological evaluation. This was carried out at Strathclyde Institute of Pharmacy and Biomedical Sciences and involved membrane preparations, cell culturing and radioligand binding assays.

Chapter 3 - Biological results – 5-HT₇ and M₄

3.1 Biological results – 5-HT₇ and M₄

As previously reported, proof of concept was achieved for amidine-linked compounds with a *serominic* multi-receptor profile (5-HT₇ antagonism, M₄ agonism and low D₂ antagonism) as potential agents for use as schizophrenia therapeutics.¹¹⁹ However, despite the initial promise from an *in vivo* perspective, discovery of off-target hERG activity associated with the lead amidine series was of concern. After synthesis of a number of analogous compounds with a number of structural modifications to mitigate this undesirable off-target activity, biological assays to investigate whether *serominic* activity had been retained were carried out within the Strathclyde Institute of Pharmacy and Biomedical Sciences.

Radioligand binding assays were carried out in two series, **Series 1** comprised of 18 compounds with six different electron-withdrawing linker modifications: nitroalkene, cyanoguanidine, trifluoromethyl, urea, hydrazine and triazene systems. The focus of this series was to establish which pK_a modifying linkers could be introduced whilst retaining *serominic* activity. As stated previously, these linkers were designed to decrease hERG activity compared to the lead amidine series due to decreased basicity, therefore SAR at hERG was explored in tandem with their *serominic* profile. Additionally, a small number of M₄ responsive changes to further probe SAR were also investigated (Figure 89).

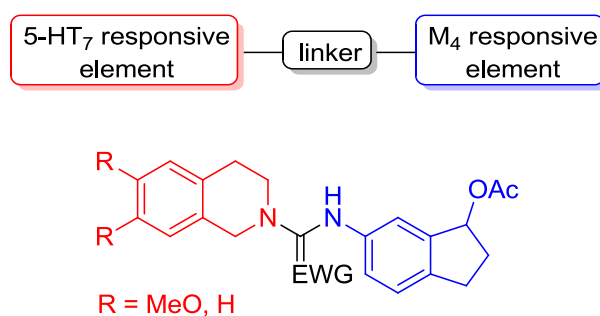


Figure 89: 5-HT₇ responsive fragment (red), and an M₄ responsive fragment (blue).

Initial assay results suggested that the triazene and nitroalkene systems retained the most promising *serominic* profiles (Chapter 3, Figure 90). Therefore, a more focused library, (*Series 2*) was synthesised, incorporating a number of changes to both 5-HT₇ and M₄ responsive elements of the molecular framework.

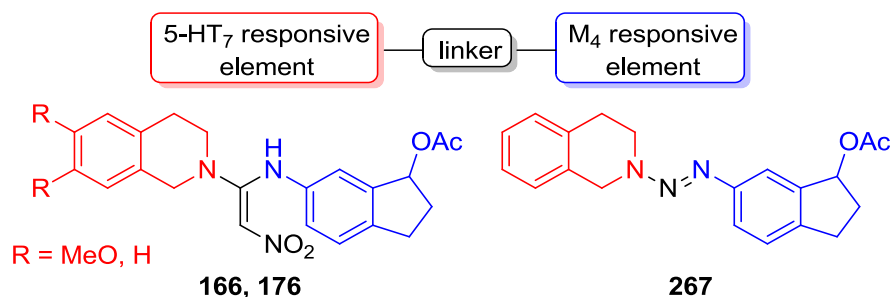


Figure 90: Electron-withdrawing linker compounds with promising *serominic* profiles, **166**, **176** and **267**.

4-Substituted piperidine and piperazine moieties, alongside a tetrahydro- β -carboline analogue were introduced in place of the 1,2,3,4-tetrahydroisoquinoline scaffold and additional M₄ responsive changes were implemented replacing the stereocentre with achiral H-bond acceptors.

3.1.1 Series 1 assay results

For *Series 1* biological assays, thalamic and striatal brain tissue from male Sprague-Dawley rats was dissected and used for 5-HT₇ and M₄ binding assays, respectively. The tissue was homogenised and stored in aliquots at -80 °C until use.

[³H]5-CT (3.1, Figure 91) was used to radiolabel 5-HT receptors in the thalamus utilising the approach of Stowe and Barnes.²¹² 5-CT (**288**) is a non-selective serotonin ligand and labels all 5-HT subtypes present in the thalamus: therefore, additional ligands are introduced to block other high density subtypes, such as 5-HT_{1A}. Specifically, (\pm)pindolol²¹³ (**289**) and WAY100635²¹⁴ (**290**) were used for this purpose. Thalamic tissue, radioligand, additional blocking ligands and test compounds were incubated for 2 h at 37 °C. To determine maximal binding, SB258741 (100 nM) (**291**), a 5-HT₇ selective antagonist,⁹¹ was used to fully displace radiolabelled 5-CT from 5-HT₇ (Figure 91) and drug binding was calculated as a percentage of this. The assay was carried out in triplicate and n (number of independent experiments) = 1.

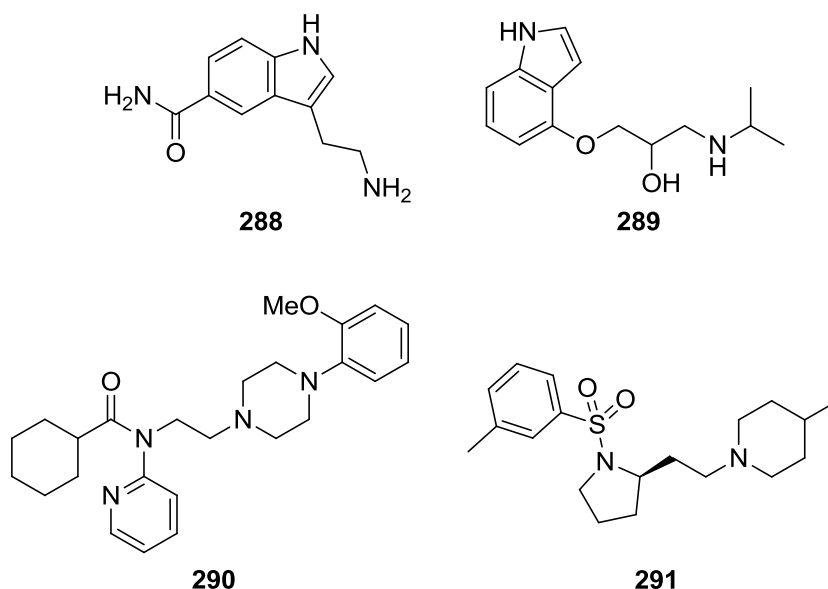


Figure 91: Ligands used in *Series 1* 5-HT₇ assay: [³H]5-CT (**288**), (±)pindolol (**289**), WAY100635 (**290**) and SB258741 (**291**).

Focusing on the M₄ assay, [³H]*N*-methylscopolamine (NMS) (**292**) was used to radiolabel muscarinic receptors in the striatum. Pirenzepine (**293**), a selective M₁ antagonist, was used to block M₁ receptors also present in the striatal tissue.²⁵ In a similar manner to the above, striatal tissue, radioligand, additional blocking ligands and test compounds were incubated for 30 min. at 30 °C. To determine maximal binding, PD102807 (250 nM) (**294**), a selective M₄ antagonist,²¹⁵ was used to fully displace radiolabelled NMS from M₄ (Figure 92) and drug binding was calculated as a percentage of this. Again, the assay was carried out in triplicate and n = 1.

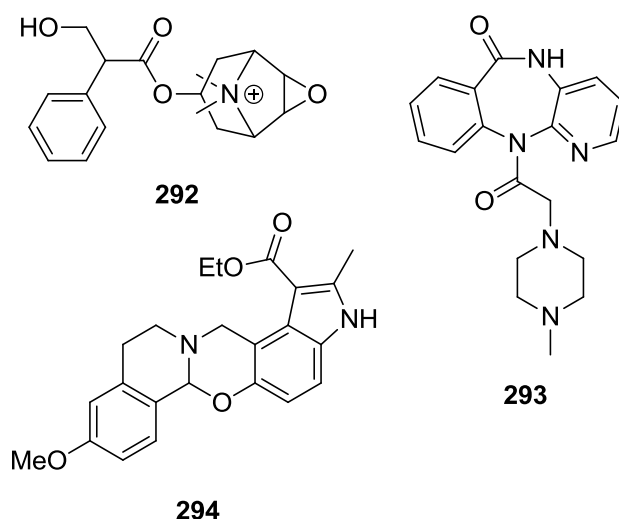
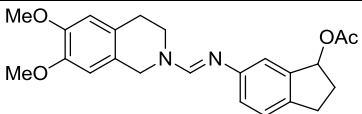
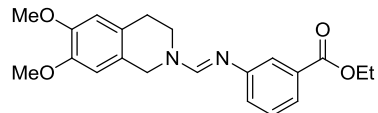
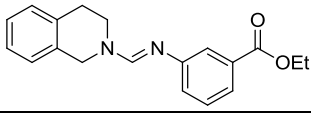
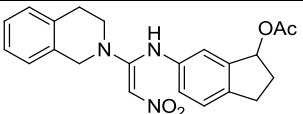
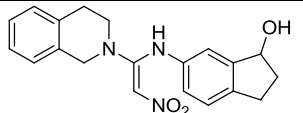
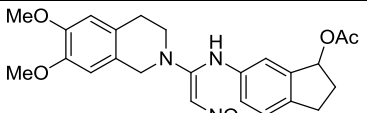
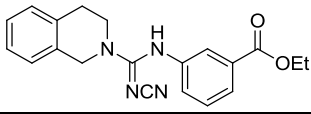
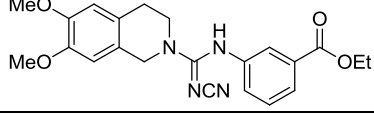


Figure 92: Ligands used in *Series 1* M₄ assay: [³H]NMS (**292**), pirenzepine (**293**) and PD102807 (**294**).

Unfortunately, high error margins were associated with the 5-HT₇ assay results which were attributed to either low density of receptors in the thalamic tissue that had been harvested or tissue degradation during the harvesting process. Consequently, at this stage the programme focused on compounds with linkers retaining activity at the M₄ receptor, which, based on previous experience within the group, was anticipated to be a more challenging goal to meet. In order to overcome the issue with thalamic tissue preparations, the subsequent set of 5-HT₇ assays was carried out using commercially available 5-HT₇ membrane preparations obtained from Perkin Elmer.

The test compounds screened and the percentage displacement of the radioligand [³H]NMS is shown below in Table 33. The general trends are depicted schematically in Figure 93.

Compound	Structure	% displacement of [³ H]NMS at 10 μM
53		> 100 ± 3
126		66 ± 6
127		> 100 ± 12
166		> 100 ± 3
175		42 ± 12
176		> 100 ± 18
202		32 ± 4
203		11 ± 4

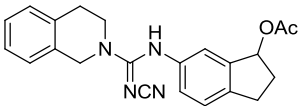
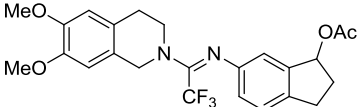
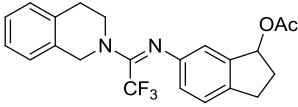
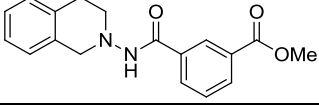
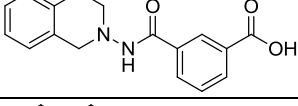
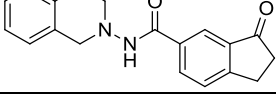
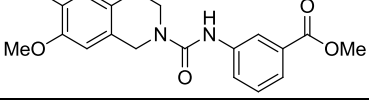
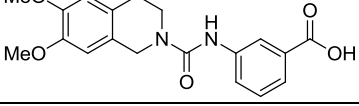
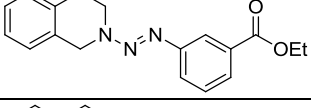
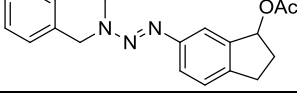
204		24 ± 7
220		17 ± 11
221		10 ± 12
236		43 ± 5
237		16 ± 12
244		28 ± 11
247		35 ± 17
248		54 ± 5
265		63 ± 10
267		> 100 ± 0.2

Table 33: Percentage displacement of [³H]NMS at 10 μM from striatal tissue by test compounds compared to maximal displacement by PD102807. Compounds displacing over 50 % of radiolabelled ligand are denoted in bold.

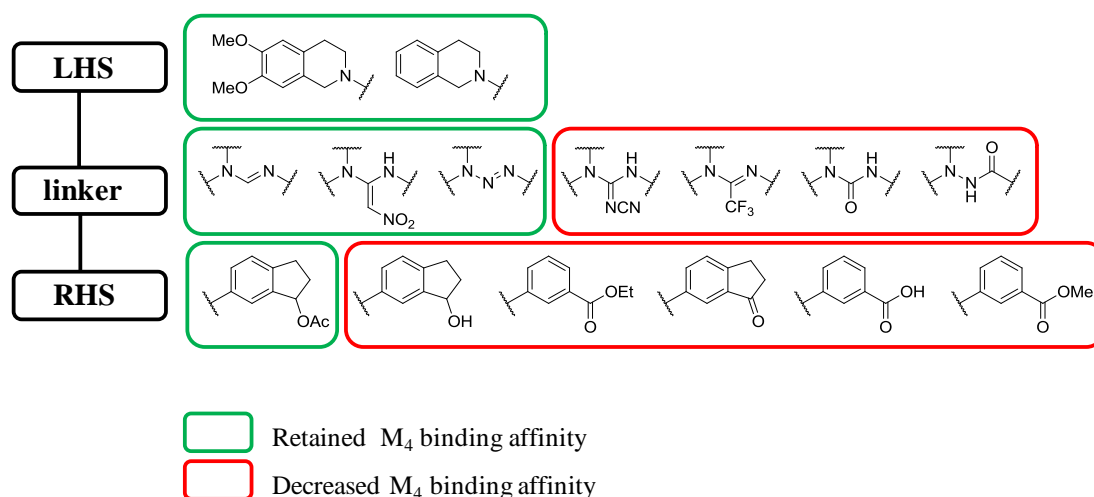


Figure 93: General SAR trends for M₄ binding of potentially *serominic* compounds.

Displacement of over 50 % of radiolabelled M₄ receptors at 10 μM was the criterion for an active compound (indicated in bold), however, it must be noted that some of the active compounds appeared to displace over 100 % of the radioligand. This was attributed to the radioligand binding to other proteins and receptors within the crude tissue membrane and the very high affinity test compounds (such as **53**) displacing these bound ligands alongside ligands labelling M₄ receptors. Based on this, a percentage displacement value of over 100 % is observed.

For the purposes of this research programme, it was assumed that the compounds were displacing M₄ primarily and candidate *serominic* analogues were chosen accordingly. The second, more focused, library was screened using commercially available membrane preparations consisting only of human serotonergic 5-HT₇ or muscarinic M₄ receptor subtypes to avoid this issue. To ensure the validity of these results, amidine **53** and triazene **267** were re-assayed at a later date using the purchased M₄ membrane preparation.

In the context of the M₄ binding assays, a number of general trends were apparent, detailed in Table 33. Amidine-linked compound **53** (used as a control) displayed significant M₄ activity (> 100 % displacement) as expected. Replacement of the chiral indanyl acetate (**53**) with achiral ethyl ester group (**126-127**, 66 % and > 100 % displacement, respectively) resulted in minimal loss of M₄ activity within the amidine family. This represented a significant result, suggesting that the chiral

indanyl acetate is not required for M₄ activity and the cheap, commercially available, achiral ethyl 3-aminobenzoate building block could be used as a potential replacement, reducing the number of synthetic steps.

Triazene containing compounds also performed well, with comparable potency to the amidine series. Compounds containing indanyl acetate or ethyl ester groups retained significant activity for M₄ (**265**, 63 % displacement and **267**, > 100 % displacement, respectively). The nitroalkenes (**166**, **175-176**), although structurally very different from amidine or triazene linkers, also showed highly encouraging activity at M₄ with both **176** and **166** exhibiting over 100 % displacement.

Introduction of cyanoguanidine (**202-204**, < 32 % displacement), trifluoromethyl (**220-221**, < 17 % displacement), urea (**247-248**, < 54 % displacement) or hydrazide (**236-237** and **244**, < 43 % displacement) linker systems generally reduced affinity for M₄ compared to the lead amidine compound (**53**, > 100 % displacement).

Substituent effects on the isoquinoline ring were minimal and M₄ activity had no correlation to substitution on the tetrahydroisoquinoline ring (as exemplified by **53** and **126**; **202-203**; **166** and **176**; and **220-221**): however, this is a limited SAR investigation.

Substituent effects at the indanyl acetate ring were also minimal, but appeared to be more related to the linker system in place. For example, both indanyl acetate and ethyl ester groups were very active in the triazene (**265** and **267**) and the nitroalkene (**166** and **176**) compounds, whereas other families incorporating these moieties, such as cyanoguanidines (**202-204**) and trifluoromethyl (**220-221**) had significantly lower activity. Additionally, hydrazides and urea families, featuring structurally similar units such as carboxylic acid, methyl ester and indanone displayed poor activity at M₄ underlining the role the linker moiety plays in contributing to activity.

To summarise, these results indicate that the linker is the most important feature within these compounds for activity at M₄ and suggests that a positive charge may be an essential requirement for significant activity at this receptor. Amidines (pK_a = 12)¹⁶⁸ and triazenes would be completely ionised at physiological pH, and the formal positive charge on the nitroalkene linker may mimic this, thus contributing to the M₄

activity of this non-basic system. Furthermore, it appears that the chiral indanyl acetate is not required for activity and therefore could be substituted for an achiral group.

On the whole, these results were considered to be very encouraging: two new potentially *seromimic* entities with the possibility of decreased synthetic complexity through the removal of the chiral centre were discovered within the triazene and nitroalkene families. The amidine series were still very active at M₄, but at this stage further exploration of SAR on these compounds was discontinued due to the propensity of this class of linker to have hERG affinity. General SAR trends are summarised in Figure 93 and a more extensive SAR was carried out in the second series of compounds.

3.1.2 Series 2 assay results

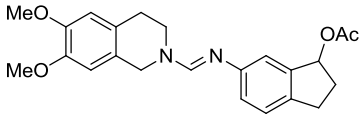
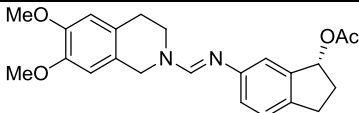
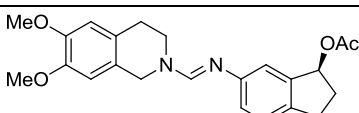
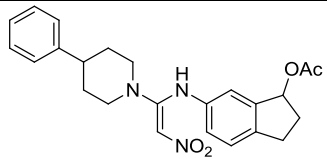
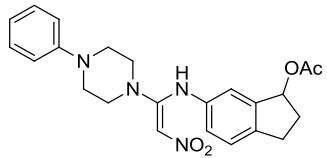
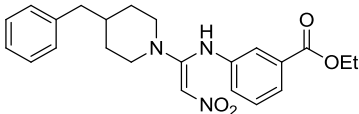
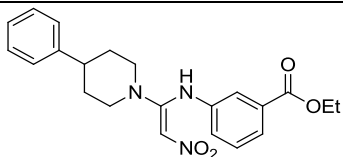
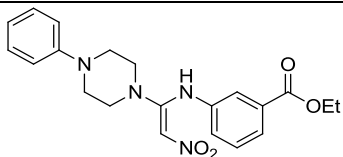
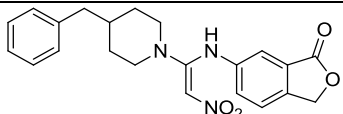
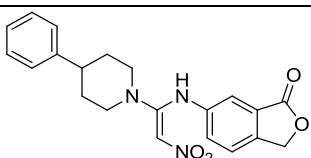
A second library, based on piperidine, piperazine and tetrahydro- β -carboline frameworks, was synthesised to further explore SAR in the serotonergic region and these compounds were also assessed for 5-HT₇ and M₄ binding affinity. Commercially available (PerkinElmer Membrane Target Systems™) CHO-K1 membranes expressing each receptor of interest were purchased, omitting the need for additional ligands to block unwanted receptor subtypes. These assays were carried out according to the recommended assay conditions supplied by PerkinElmer.^{216, 217}

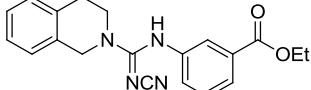
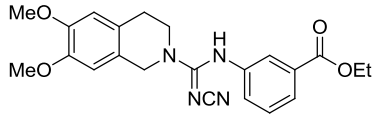
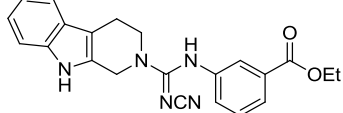
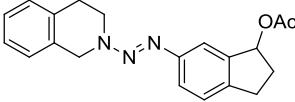
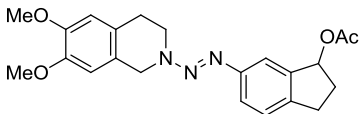
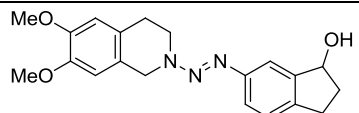
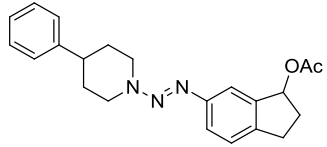
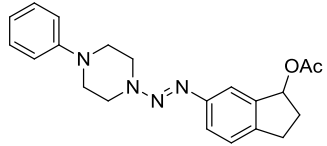
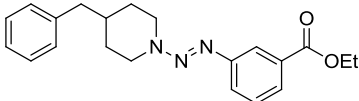
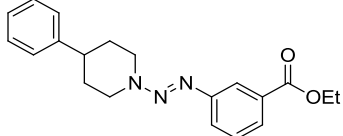
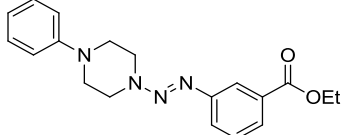
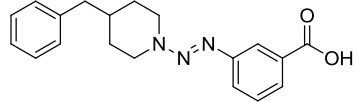
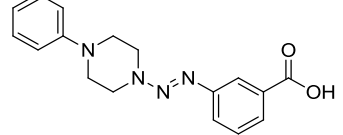
3.1.2.1 Single point assays

5-HT₇ binding was assessed by incubation of 5-HT₇ membrane and [³H]5-CT radioligand (0.5 nM), with the test compound (10 μ M). Membrane, radioligand and test compound was incubated for 2 h at 27 °C. Maximal binding was determined using SB258741 (100 nM)⁹¹ and drug binding was calculated as a percentage of this. The assay was carried out in triplicate and n=1.

M₄ binding was assessed in an analogous manner to 5-HT₇. M₄ membrane and [³H]NMS radioligand (0.1 nM) was incubated with the test compound (10 μ M). Membrane, radioligand and test compound was incubated for 2 h at 27 °C. Maximal binding was determined using PD102807 (250 nM)²¹⁵ and drug binding was

calculated as a percentage of this. The assay was carried out in triplicate and n=1. Percentage displacement of [³H]5-CT and [³H]NMS are tabulated below (Table 34).

Compound	Structure	% displacement of radioligand at 10 μM	
		[³ H]5-CT (5-HT ₇)	[³ H]NMS (M ₄)
53		70 ± 2	95 ± 3
(R)-isomer 154		73 ± 2	95 ± 2
(S)-isomer 155		64 ± 1	99 ± 1
187		6 ± 8	56 ± 8
188		8 ± 3	43 ± 8
189		11 ± 1	23 ± 7
190		5 ± 9	14 ± 8
191		3 ± 8	21 ± 4
192		21 ± 5	32 ± 5
193		14 ± 6	60 ± 13

202		25 ± 7	19 ± 10
203		5 ± 2	30 ± 7
209		38 ± 7	36 ± 4
267		50 ± 6	30 ± 7
268		26 ± 6	35 ± 5
269		32 ± 7	44 ± 3
270		65 ± 8	40 ± 7
271		98 ± 1	59 ± 1
272		18 ± 14	29 ± 14
273		15 ± 6	14 ± 10
274		36 ± 7	26 ± 10
275		7 ± 7	16 ± 4
276		41 ± 5	4 ± 2

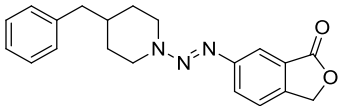
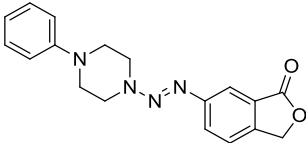
277		2 ± 5	31 ± 2
278		32 ± 2	26 ± 8

Table 34: Percentage displacement of [³H]5-CT and [³H]NMS at 10 μM from 5-HT₇ and M₄ membrane, respectively, by test compounds compared to maximal displacement by SB258741 and PD102807. Compounds displacing over 50 % of radiolabelled ligand at either receptor are denoted in bold.

3.1.2.2 5-HT₇ SAR

A number of compounds have significant activity at 5-HT₇, including both (*R*)- and (*S*)-enantiomers (**154-155**) of the racemic lead *serominic* compound (**53**), with all three compounds exhibiting similar affinity for 5-HT₇ (70, 64 and 73 % displacement, respectively).

Compounds within the triazene class displayed the most significant activity at 5-HT₇ with a 4-phenylpiperazine compound, **271** (98 % displacement), exhibiting much greater activity than the lead *serominic* compound **53** (70 % displacement). The corresponding 4-phenylpiperidine analogue **270** also demonstrated considerable activity (65 % displacement) but other substituted piperidine and 4-phenylpiperazine test compounds performed relatively poorly with displacement values under 40 % for the most part (**272-278**, **275-276**). Triazene compounds with an indanyl acetate unit were significantly more active (**270-271**) than analogous compounds with ethyl ester or carboxylic acid substituents (**272-274**, **275-276**). However, all triazenes containing a piperazine moiety (**271**, **274**, **278**, **276**) were more active than their piperidine analogues suggesting a favourable interaction between the 5-HT₇ receptor and the additional nitrogen present in piperazines.

The re-synthesised tetrahydroisoquinoline triazene compound from *Series 1*, **267**, displayed good activity at 5-HT₇ (50 % displacement), but upon substitution or hydrolysis of indanyl acetate, activity was lost (**268-269**, < 32 % displacement).

The nitroalkene family generally had poor affinity for 5-HT₇ (**187-193**, all < 21 % displacement), attributed directly to the presence of the linker as analogous triazene

compounds (nitroalkenes **187-188** and triazenes **270-271**) displayed significant 5-HT₇ activity.

Cyanoguanidine **209** (38 % displacement) with a tetrahydro- β -carboline substituent was more active at 5-HT₇ than both the substituted and unsubstituted tetrahydroisoquinoline analogues (**202-203**, < 25 % displacement) which may be attributed to its increased structural similarity to the endogenous ligand, serotonin.

3.1.2.3 M₄ SAR

Within the non-basic nitroalkene family, 4-phenylpiperidines **187** (56 % displacement) and **193** (60 % displacement) demonstrated considerable M₄ activity as observed within *Series 1*. **187** and **193** contain indanyl acetate and phthalide groups, respectively, whereas ethyl ester substituted analogues (**189-191**, < 23 % displacement) are much less active, although before in *Series 1* ethyl esters were tolerable for some linker families. This suggests that a hydrogen bond acceptor in locked position is favourable for piperidine and piperazine substituted nitroalkenes to bind to the M₄ receptor. Additionally, substitution of 4-phenylpiperidine (**187**, 56 % displacement) to 4-phenylpiperazine (**188**, 43 % displacement) and analogous 4-benzylpiperidine compounds (**192**, 32 % displacement) results in a loss of M₄ activity suggesting crosstalk between responsive elements.

Unfortunately, the lead nitroalkenes from *Series 1* could not be re-synthesised, even after extensive experimentation, to be re-assayed using the commercially available membrane preparations.

Triazene-linked piperazine **271** exhibits significant activity at M₄ (59 % displacement), but all other triazenes are much less active at M₄ (**270-278**, **275-276**, < 40 % displacement) suggesting that the increased activity of **271** is attributable to structural features other than the linker. The combination of the 4-phenylpiperazine and the indanyl acetate unit appears to deliver significant activity and underlines the importance of this wider SAR scan.

The generally diminished activity of the triazene compounds may be due to the slightly decreased basicity of the triazene nitrogen compared to the lead amidines (**53**

and **154-155**, > 95 % displacement), as a 60 % reduction in M₄ activity is observed between the structurally analogous amidine **53** and triazene **268**. Additionally, almost all M₄ activity is lost with the introduction of a carboxylic acid (**275-276**, < 16 % displacement) confirming that negatively charged elements are not tolerated well in M₄ receptors.^{152, 159} However, the negative charge on active nitroalkene compounds such as **187** and **193** is tolerated well within M₄ receptors indicating that position of charge may be important in binding.

No significant difference in M₄ binding is observed between the (*R*)- (95 % displacement) and (*S*)- (99 % displacement) *serominic* lead amidine enantiomers (**154-155**), suggesting that any interaction between the M₄ receptor and the indanyl acetate group is not dependent on stereochemistry.

To summarise, there appears to be no significant difference in binding to 5-HT₇ and M₄ by either enantiomer of the lead *serominic* amidine compounds (**53** and **154-155**). Compounds made within the nitroalkene family generally lack activity at both receptors with the exception of **187** and **193** which display significant M₄ activity.

Pleasingly however, one triazene compound displayed significant *serominic* activity, **271**, and a number of triazenes were active at only one receptor (**267** and **270**). Other compounds tested did not demonstrate significant activity at either receptor.

Upon consideration of the data for both 5-HT₇ and M₄, **53**, **154-155**, **187**, **270**, **271** and **274** were taken forward for competition binding assays to determine K_i values.

3.1.2.4 Competition binding assays

After the discovery that a number of compounds retained *serominic* activity after the introduction of a triazene or nitroalkene linker, the most active compounds from each sub-series were taken forward for additional competition binding assays **187**, **270**, **271** and **274**. Competition binding assays were also carried out for the enantio-enriched analogues of the *serominic* lead compound **154-155** and for the *serominic* lead **53** to compare to previously reported assay results. These followed the same procedure as for the single point assays but variation of the drug concentration (100, 10, 1, 0.1 μ M) allowed K_i values to be calculated from the Cheng–Prusoff equation

(see Appendix for IC₅₀ example graphs and equation).²¹⁸ The assay was carried out in triplicate and n = 3.

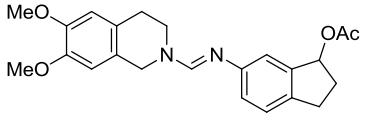
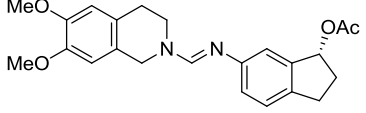
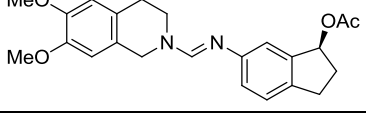
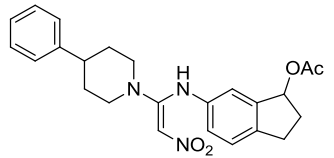
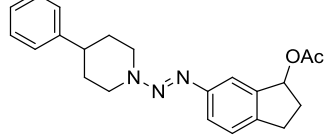
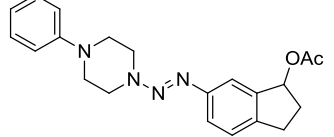
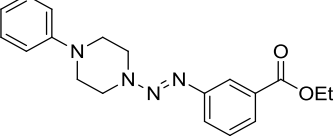
Structure	Compound	K _i (nM)	
		5-HT ₇	M ₄
	53	0.90 ± 0.03	0.47 ± 0.08
	(<i>R</i>)-isomer 154	0.85 ± 0.20	0.36 ± 0.07
	(<i>S</i>)-isomer 155	0.89 ± 0.06	0.11 ± 0.02
	187	-*	3.50 ± 1.18
	270	12.7 ± 1.09	75.0 ± 4.77
	271	0.22 ± 0.08	23.5 ± 1.17
	274	54.2 ± 1.77	-*

Table 35: K_i values for 5-HT₇ and M₄ for selected *serominic* compounds * = competition assay not carried out as single point assay < 50 % displacement.

Results from the competition binding assay confirmed the results from the single point assay. As can be seen in Table 35, there is no significant difference in 5-HT₇ and M₄ binding affinity between the (*S*)- lead *serominic* amidine (**155**, K_i 5-HT₇ 0.89 μM. M₄ 0.11 μM) compared to the (*R*)- lead *serominic* amidine (**154**, K_i 5-HT₇ 0.85 μM. M₄ 0.36 μM) or the racemic **53** (K_i 5-HT₇ 0.90 μM. M₄ 0.37 μM). This suggests that the geometry of the chiral acetate group is not an integral feature of the binding interaction with either receptor.

Within the triazene family, use of a piperidine or piperazine scaffold with an indanyl acetate unit retains significant activity at 5-HT₇, as exemplified by piperazine **271** (K_i 0.22 μ M) but this affinity is lost upon changing to an ethyl ester (**274**, K_i 54.2 μ M). M₄ affinity is modest for this family, perhaps due to the reduced pK_a and subsequent ionisation at physiological pH in comparison to the amidine series. However, piperazine **271** was significantly more active (K_i 23.5 μ M) than the piperidine analogue (**270**, K_i 75.0 μ M).

Interestingly, although nitroalkene **187** was inactive in 5-HT₇ assays (6 % displacement at 10 μ M), it displayed over 20-fold more potency for M₄ (K_i 3.5 μ M) when directly compared to the triazene analogue **270** (K_i 75.0 μ M). As the nitroalkene would be unprotonated at physiological pH, the positive charge on the nitro group may be playing a part in this increased affinity for M₄, as discussed previously.

Overall, a number of novel compounds with significant activity at each receptor of interest, 5-HT₇ and M₄, have been discovered in the series of compounds synthesised within the project. Compounds displaying the most promising *serominic* profiles are within the triazene family, **270** and **271**. These compounds have high affinity to 5-HT₇, comparable or better than the lead *serominic* amidine compounds (**53** and **154-155**) although with somewhat reduced potency at M₄. From consideration of their relative 5-HT₇ and M₄ activities in comparison to the progenitor compound **53**, **270** and **271** may be useful as tools to further explore and more precisely determine the role of the M₄ component to *in vivo* antipsychotic activity observed for the lead *serominic* amidines.

Chapter 4 - Biological results – hERG

4.1 Biological results – hERG

hERG activity was assessed using [³H]astemizole (**58**, Figure 94) with hERG transfected HEK293 cells (gifted by Dr. John Mitcheson, University of Leicester) maintained using a modified literature procedure by Chiu *et al.*²¹⁹

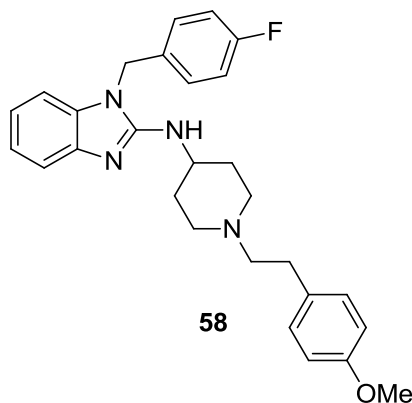


Figure 94: Astemizole (**58**).

Cell preparation, [³H]astemizole (1.5 nM) and test compound were incubated for 1 h at 25 °C. Maximal binding was determined using unlabelled astemizole (10 μM) and drug binding was calculated as a percentage of this. Compounds of interest were run in triplicate and n = 3.

4.1.1 Effects of linker modification on hERG activity

In the synthetic campaign a number of electron-withdrawing linkers were incorporated into the lead *serominic* amidine compound (**53**) to reduce the p*K*_a of the basic nitrogen. As previously discussed, reducing the basicity of hERG active compounds has been proven to be a useful strategy for reduction of hERG liability.¹⁵² **Series 1** consisted of a small library of compounds with six different electron-withdrawing linkers and a number of more discrete structural modifications. These compounds were assessed in a cell-based hERG radioligand binding assay and results are tabulated below (Table 36).

Compound	Structure	^a M ₄	^b hERG
53		> 100 ± 3	73 ± 5
126		66 ± 6	68 ± 3
127		> 100 ± 12	71 ± 3
166		> 100 ± 3	56 ± 6
175		42 ± 12	32 ± 2
176		> 100 ± 18	56 ± 5
202		32 ± 4	64 ± 5
203		11 ± 4	38 ± 2
204		24 ± 7	50 ± 5
220		17 ± 11	47 ± 1
221		10 ± 12	58 ± 4
236		43 ± 5	35 ± 4
237		16 ± 12	29 ± 19
244		28 ± 11	36 ± 3

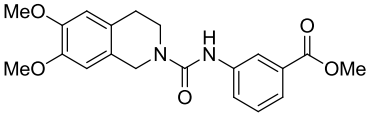
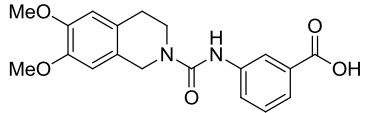
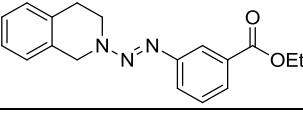
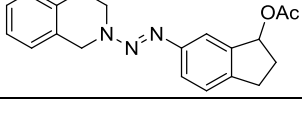
247		35 ± 17	30 ± 4
248		54 ± 5	20 ± 9
265		63 ± 10	71 ± 4
267		> 100 ± 0.2	71 ± 5

Table 36: Percentage displacement of ^a or ^b by test compounds compared to maximal displacement. ^a% displacement of [³H]NMS from rat brain tissue preparation at 10 μM. ^b% displacement of [³H]astemizole from hERG HEK293 cell preparation at 10 μM.

In general, all of the linker modifications were successful in attenuation of hERG compared to the lead amidine, **53**. However, due to the multiple parameters (linker, aryl amine substituent, heterocyclic substituent) that have been changed in some test compounds, reduction in hERG activity cannot be solely attributed to modification of linker.

Hydrazide (**236-237**, **244**, > 36 % displacement) and urea (**247-248**, > 30 % displacement) analogues in particular performed well and reduced hERG activity very significantly (30-50 %) compared to analogous amidine **53**. The strongly electron-withdrawing nitroalkene (**166**, **175-176**, 56 % displacement for both) and trifluoromethyl (**220-221**, 47 and 58 % displacement, respectively) linkers resulted in a smaller reduction of hERG activity (15-20 %) compared to the lead *serominic* amidine (**53**). One explanation for the decreased hERG activity from hydrazide and urea systems compared with nitroalkene and trifluoromethyl systems may be that the positive charge on the nitro group could be interacting with the hERG ion channel in the same way it was proposed earlier to interact with M₄. With regards to the trifluoromethyl family, favourable lipophilic interactions between the trifluoromethyl compounds and lipophilic sites on the hERG channel may increase the overall hERG activity of this family.

Cyanoguanidine results were varied, but hERG activity was reduced considerably for **203** (38 % displacement) compared to the amidine analogue **126** (68 %

displacement). Unsubstituted 1,2,3,4-tetrahydroisoquinoline amidine **204** (50 % displacement) also attenuated hERG activity compared to the 6,7-dimethoxy substituted analogue (**53**, 73 % displacement) but little change in hERG activity was observed for **202** (64 % displacement) compared with the analogous amidine compound (**127**, approximately 70 % displacement). This suggests that factors other than pK_a alone are directing hERG binding such as conformation or lipophilicity.

Compounds with a triazene linker offered limited hERG attenuation (**265-267**, approximately 70 % displacement) which was expected due to the very similar geometric and electronic structure of this family to the amidine class (**53**, **126-127**, approximately 70 % displacement).

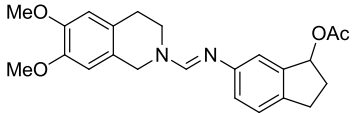
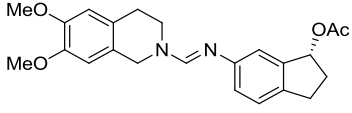
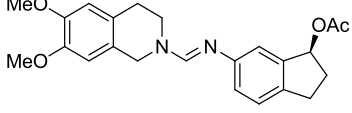
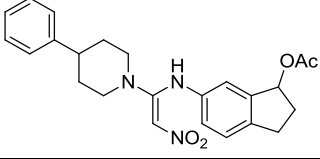
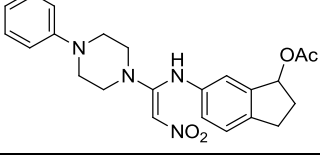
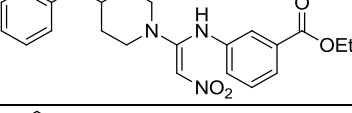
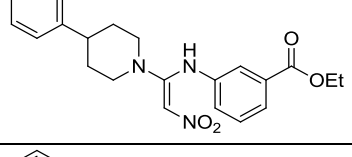
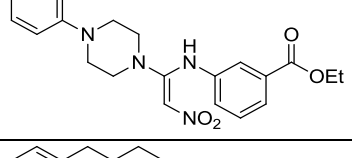
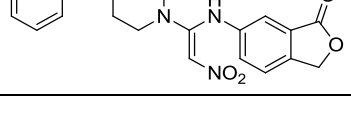
In the context of hERG binding, discrete structural modifications within linker families did not result in significant changes in binding within *Series 1*. However, the incorporation of a carboxylic acid, as seen in **237** and **248**, reduced hERG activity significantly. This was expected based on literature precedent.^{152, 159} Additionally, hydroxyl substituted indanyl nitroalkene **175** (32 % displacement) displayed significantly lower hERG activity than the indanyl acetate nitroalkenes **166** and **176** (54 % displacement for both) suggesting a possible interaction between the acetyl carbonyl and the hERG channel. Conversely, the introduction of a hydroxyl hydrogen bond donor increases polarity and may therefore destabilise interactions with the lipophilic binding site.

To summarise, a number of compounds from *Series 1* were of interest. In particular, cyanoguanidine **203** (38 % displacement), nitroalkene **175** (32 % displacement), hydrazides **236-237** and **244** (< 36 % displacement) and ureas **247-248** (< 30 % displacement) showed significantly low hERG liability compared to the lead *serominic* compound **53** (71 % displacement).

4.1.2 Effects of discrete structural modification on hERG activity

Compounds in *Series 2* focused mainly on investigating SAR of the triazene and nitroalkene families due to their potential *serominic* activity discussed in Chapter 3. As discussed previously, a number of nitroalkene and triazene compounds incorporating piperidine and piperazine moieties in place of the

tetrahydroisoquinoline framework were synthesised (**187**, **273-274**, **270-271**, **278** and **275-276**) alongside a tetrahydro- β -carboline cyanoguanidine derivative (**209**). In addition, the (*R*)- and (*S*)- enantiomers of the lead *serominic* amidine (**154-155**, respectively) were synthesised. Results from the hERG radioligand binding assay are tabulated below along with 5-HT₇ and M₄ data for comparison (Table 37).

Compound	Structure	^a 5-HT ₇	^b M ₄	^c hERG
53		70 ± 2	95 ± 3	73 ± 5
(<i>R</i>)-isomer 154		73 ± 2	95 ± 2	86 ± 3
(<i>S</i>)-isomer 155		64 ± 1	99 ± 1	77 ± 0.2
187		6 ± 8	56 ± 8	53 ± 16
188		8 ± 3	43 ± 8	54 ± 11
189		11 ± 1	23 ± 7	63 ± 5
190		5 ± 9	14 ± 8	33 ± 6
191		3 ± 8	21 ± 4	49 ± 2
192		21 ± 5	32 ± 5	44 ± 3

193		14 ± 6	60 ± 13	50 ± 7
202		25 ± 7	19 ± 10	64 ± 5
203		5 ± 2	30 ± 7	38 ± 3
209		38 ± 7	36 ± 4	68 ± 2
267		50 ± 6	30 ± 7	71 ± 5
268		26 ± 6	35 ± 5	68 ± 2
269		32 ± 7	44 ± 3	51 ± 17
270		65 ± 8	40 ± 7	77 ± 3
271		98 ± 1	59 ± 0.5	59 ± 8
272		18 ± 14	29 ± 14	58 ± 4
273		15 ± 6	14 ± 10	54 ± 6
274		36 ± 7	26 ± 10	65 ± 4

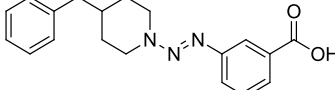
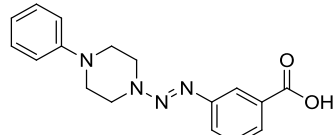
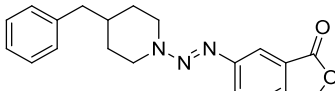
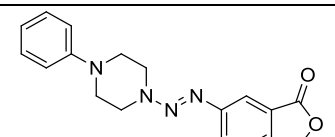
275		7 ± 7	16 ± 4	1 ± 6
276		41 ± 5	4 ± 2	6 ± 0.04
277		2 ± 5	31 ± 2	40 ± 10
278		32 ± 2	26 ± 8	19 ± 17

Table 37: Percentage displacement of ^a, ^b, or ^c by test compounds compared to maximal displacement. ^a% displacement of [³H]5-CT from human membrane preparation at 10 μM ^b% displacement of [³H]NMS from human membrane preparation at 10 μM. ^c% displacement of [³H]astemizole from hERG HEK293 cell preparation at 10 μM.

From consideration of the above data, a number of observations within *Series 2* can be made. The (*R*)- (**154**, 86 % displacement) and (*S*)- (**155**, 77 % displacement) amidines do not differ significantly with regard to hERG liability compared to the racemic lead *serominic* amidine (**53**, 73 % displacement).

Within the nitroalkene family, although discrete structural modifications such as 4-benzylpiperidine (**189**, **192**), 4-phenylpiperidine (**187**, **190**, **193**) and 4-phenylpiperazine (**188**, **191**), indanyl acetate (**187-188**), ethyl ester (**189-191**) and phthalide (**192-193**) were explored, most compounds reduced hERG activity by approximately 20 % (**187-193**, approximately 50 % displacement) compared to the lead *serominic* amidine (**53**). This suggests that the nitroalkene linker is playing an integral role in the attenuation of hERG activity. However, 4-phenylpiperidine substituted **190** in particular displayed low hERG activity (33 % displacement) although its acetate (**187**) and phthalide (**193**) counterparts were 20 % more active at hERG.

Triazene-linked compounds were comparatively less effective at attenuating hERG liability with a maximum reduction of approximately 10 % for most compounds (**270-274**, approximately 60 % displacement in each case). However, phthalide substituted compounds appreciably reduced activity at hERG, exemplified by **278**

with an impressive 19 % displacement compared to the ethyl ester equivalent **274** (65 % displacement) and the lead amidine compounds (**53** and **154-155**, approximately 70 % displacement), therefore providing support for discrete modifications as a hERG mitigating strategy in this series. Moreover, zwitterionic triazene-containing compounds also displayed low hERG activity (**275-276**, < 6 % displacement) confirming the utility of the zwitterion approach to minimising hERG activity.^{152, 159}

Discrete structural modifications within the cyanoguanidine series also resulted in a significant decrease in hERG activity. For example, unsubstituted tetrahydroisoquinoline or tetrahydro- β -carboline cyanoguanidine compounds demonstrated significant hERG activity (**202** and **209**, > 60 % displacement) compared to dimethoxy substituted cyanoguanidine **203** with 38 % displacement.

Overall, a general linker-dependent trend can be observed with regards to hERG activity, as depicted schematically in Figure 95.

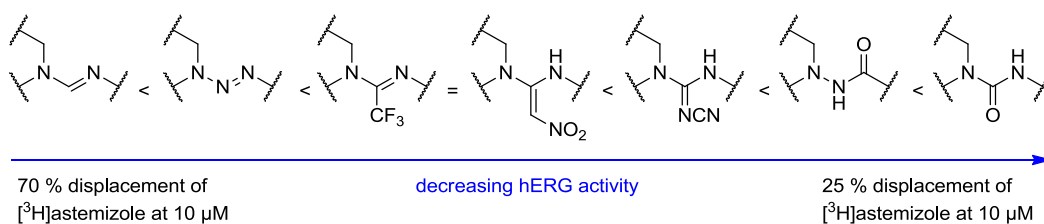


Figure 95: Effects of linker on hERG activity.

Other parameters such as discrete structural modifications can still play a major role in attenuation of hERG activity but the above diagram can be used as a general rule of thumb of the effect of a given linker on hERG liability.

4.1.3 Effects of clogP on hERG activity

As discussed earlier in Section 1.7, compounds with low clogP values are generally associated with decreased hERG liability compared to compounds which are more lipophilic in nature.^{144, 153} *Series 1* covers a range of clogP values (as calculated by ChemBioDraw Ultra) and these were plotted against hERG activity below (Figure 96).

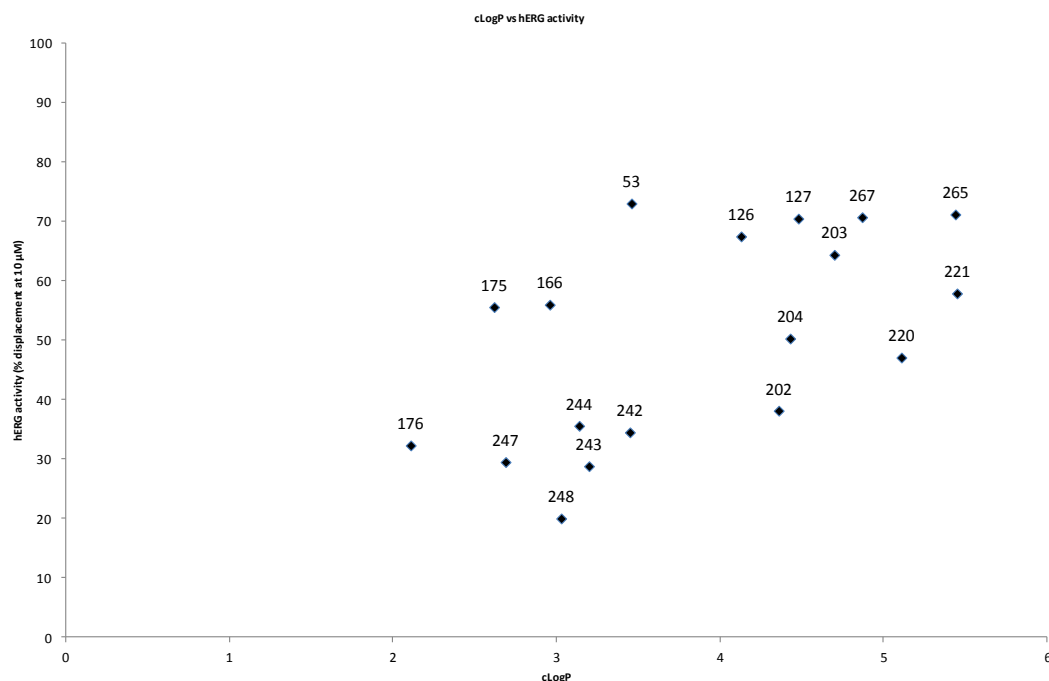


Figure 96: Plot of clogP vs hERG activity of *Series I* compounds.

With respect to clogP and hERG activity, a strong correlation was not observed within *Series I*, however, a general trend was apparent. A number of linker families with relatively low clogP values display corresponding low hERG activity such as the nitroalkene (**175**), hydrazides (**236-237** and **244**) and ureas (**247-248**). However, this is not observed in every system as the highly lipophilic trifluoromethyl-linked compounds (**220-221**), succeeded in reducing hERG activity by over 20 % compared to the lead *serominic* amidine. This suggests that other factors such as structural modifications, pK_a or conformation may play a larger role in hERG affinity for this series than lipophilicity. Indeed, this is in accord with literature findings which indicate where correlation with clogP is low, then discrete structural modifications may be a more appropriate strategy for reduction of hERG liability.¹⁵²

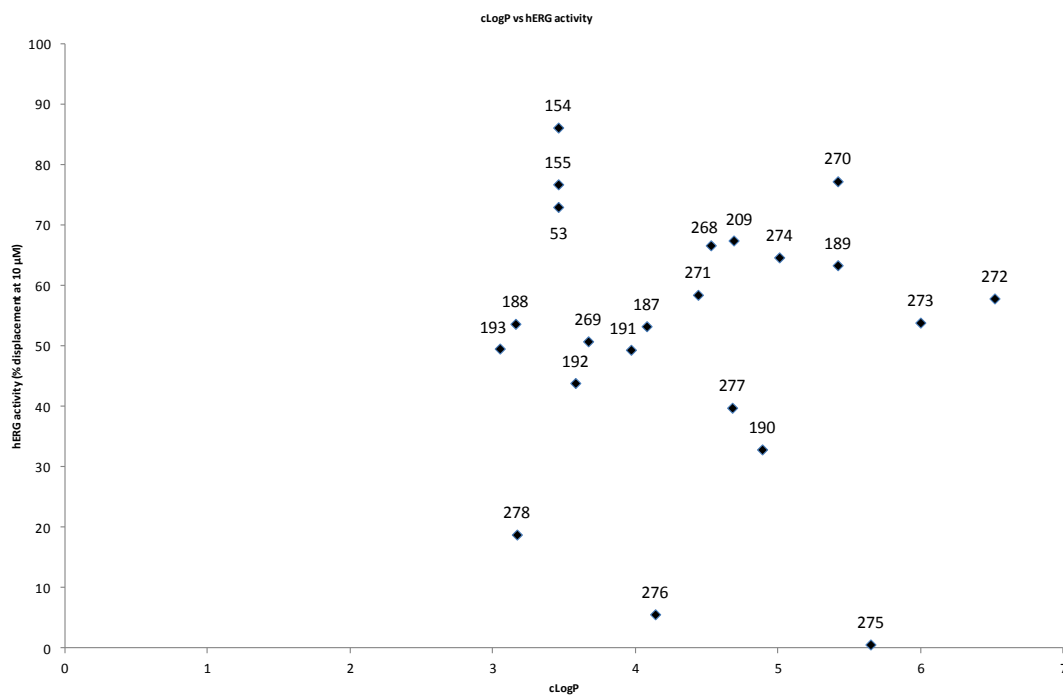


Figure 97: Plot of clogP vs hERG activity of *Series 2* compounds.

No compelling trend was observed within *Series 2* (Figure 97). Within this dataset, a number of compounds displayed unexpected results. Triazene **278** (clogP 3.17, 19 % displacement) has significantly lower hERG activity than the lead *seromonic* compound **53** (clogP 3.46, 73 % displacement), in contrast to the rest of the compounds within the triazene family (**270-274** and **277**, clogP > 4, > 40 % displacement). This may be a clogP mediated effect, but is more likely to be due to an interplay between structural modifications and clogP.

Similarly, nitroalkene **190**, triazene **277** and cyanoguanidine **203** also have low hERG liability but clogP values between 4 and 5, this indicates that, like in *Series 1*, discrete structural modification has a greater effect on hERG activity in *Series 2*. This is further supported by the mitigating effect of introducing an acidic functionality even with relatively high clogP values (**275-276**, clogP 4.14 and 5.65 respectively, > 10 % displacement).

Overall, it appears that lipophilicity as measured by clogP does not play a global controlling role in hERG activity within the families of compounds discussed between *Series 1* and *Series 2*. This is not surprising as literature examples normally report correlations when clogP has increased or decreased by at least one log unit

without significant difference to other parameters such as pK_a .^{152, 153} Although there is a range of $clogP$ values within compounds this normally accompanied by the change of another variable therefore results are difficult to attribute to $clogP$ alone. Consequently, other factors such as pK_a and discrete structural modifications appear to be much more effective for mitigation of hERG activity within this range of compounds.

4.1.4 Conformational analysis and potential implications for hERG activity

Introduction of electron-withdrawing groups, as discussed above, is a valuable tool for mitigation of hERG liability through tuning of pK_a . Reduction of hERG activity, however, cannot unequivocally be assigned to incorporation of linkers which tune pK_a as conformational changes may influence the propensity of the compound to bind to the hERG channel as well as affecting other physicochemical properties.¹⁴⁴

In the context of hERG liability through conformation alone, Aronov compiled a simple schematic to gauge how hERG active a drug is likely to be based on conformation (Figure 98).¹⁴⁴ The lead *serominic* amidine has a central basic nitrogen with high potential for hERG blockade according to the diagram, which is observed experimentally. Although efforts have been made to reduce the basicity of this nitrogen, aromatic π - π and hydrophobic interactions also play a key role in hERG activity and may have a large contribution to hERG affinity for a number of compounds.

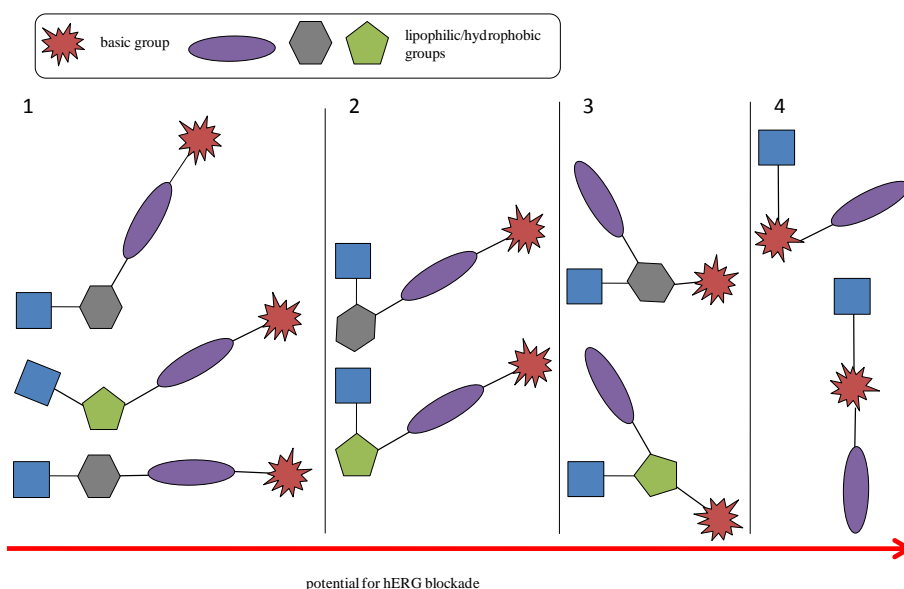
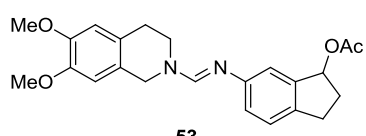
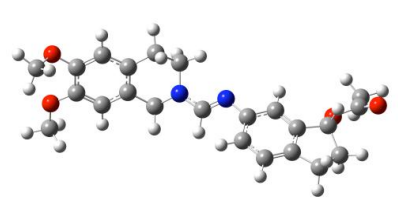
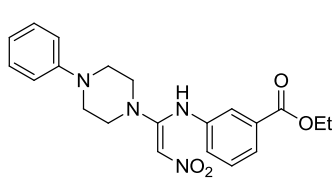
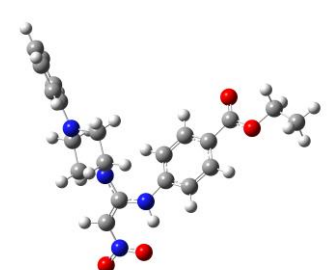


Figure 98: Diagram depicting potential for hERG blockade based on conformation of test compound.¹⁴⁴ Adapted from reference ¹⁴⁴.

Based on the above, conformational analysis was carried out using Gaussian.¹⁸⁰ An example from each family of linker was chosen, lowest energy conformation assessed and compared with experimental hERG data (Table 38). The lowest energy conformations were then overlaid against each other to directly compare the conformational differences (Figure 99).

Compound	Energy minimised structure	hERG ^a
 <p>53</p>		73 ± 5
 <p>191</p>		49 ± 2

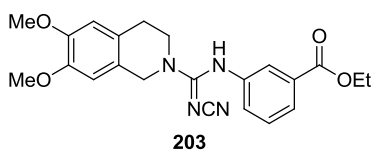
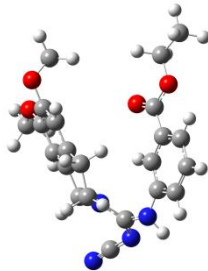
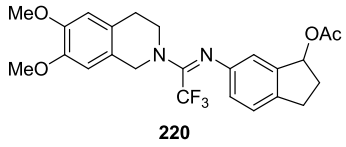
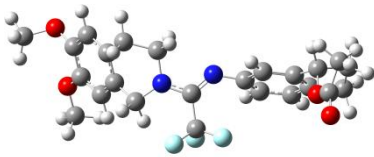
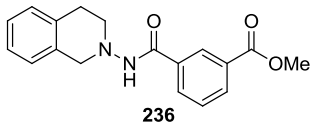
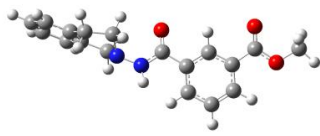
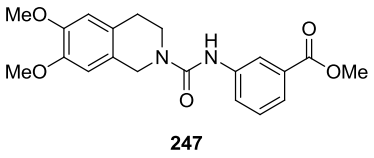
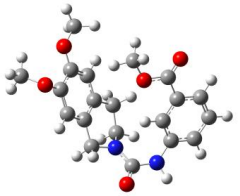
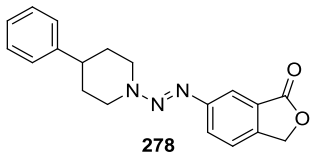
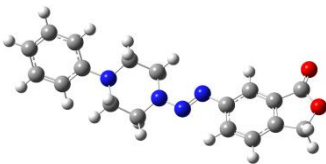
 <p>203</p>		38 ± 2
 <p>220</p>		47 ± 1
 <p>236</p>		35 ± 4
 <p>247</p>		30 ± 4
 <p>278</p>		19 ± 17

Table 38: Lowest energy conformation of selected compounds from each linker family. ^a% displacement of [³H]astemizole from hERG HEK293 cell preparation at 10 μM.

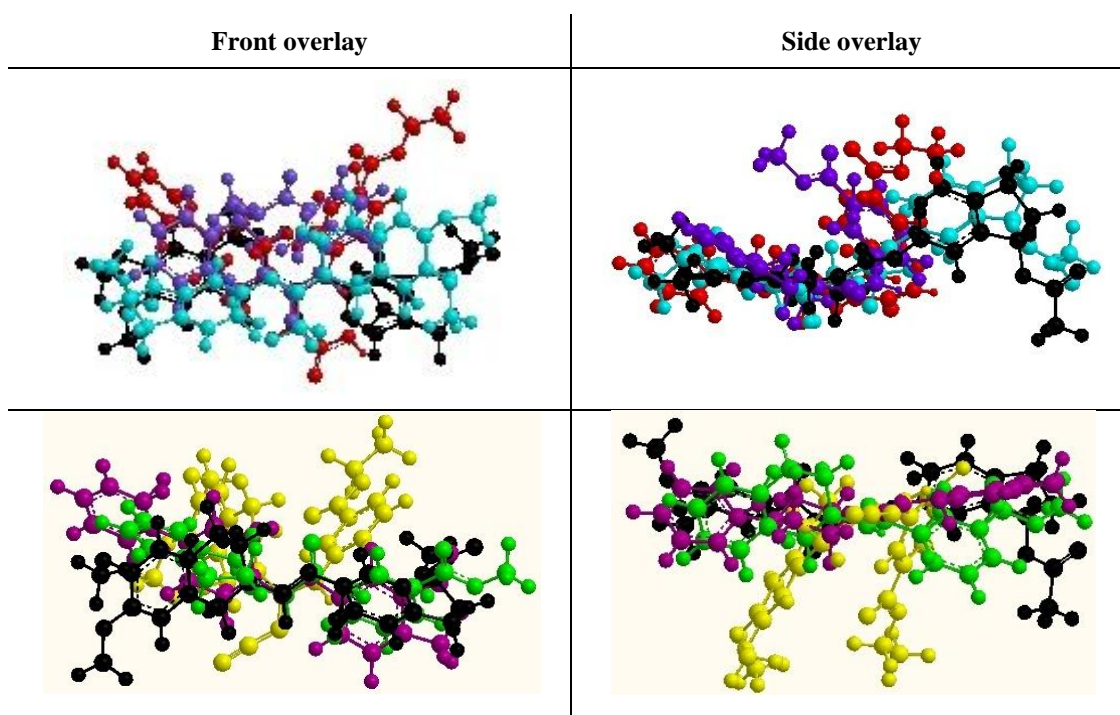


Figure 99: Front and side overlay of lowest energy conformations. Top row - Amidine **53** (black) overlaid with nitroalkene **191** (red), trifluoromethyl **220** (blue) and urea **247** (purple). Bottom row – Amidine **53** (black overlaid with cyanoguanidine **203** (yellow), triazene **278** (pink) and hydrazide **236** (green).

Linker families with high hERG liability such as amidines and triazenes have fairly planar, linear conformations with a central positively charged nitrogen atom. This is consistent with the hERG pharmacophoric model discussed previously (depicted schematically in Figure 98) and may contribute to the increased hERG activity associated with these compounds (> 70 % displacement generally). However, triazene **278** (pink) in particular displays extremely low hERG activity (19 % displacement) suggesting that it may adopt a binding conformation where it cannot be accommodated in the putative binding site of the channel in the same manner as the other triazene compounds. Furthermore, trifluoromethyl (blue) and hydrazide-linked (green) compounds are fairly planar but have reduced hERG activity (47 and 35 % displacement, respectively) compared to the lead amidine (black) (73 % displacement) indicating that the reduced basicity of these compounds is playing a role and preventing binding interactions.

The nitroalkene (red) adopts a bent conformation, which although regarded as high-risk for hERG liability, it displays significantly decreased hERG activity (49 % displacement) in comparison to the lead amidine (73 % displacement) (Table 38).

This is also observed for the cyanoguanidine (yellow) and urea (purple) compounds (38 and 30 % displacement, respectively) which also adopt bent conformations, suggesting that their less basic or neutral central nitrogen atom may hinder electrostatic interaction with the hERG binding site.

It must be noted that it is not known at this stage whether the compounds are binding when the channel pore is open or closed and further work utilising electrophysiological patch clamp assays would be required to investigate this.

The conformational studies carried out only offer limited insight to hERG binding and correlation to hERG data is somewhat irregular, however, reducing the basicity of the central nitrogen does, in general, have a negative effect on hERG binding. It is likely that a number of parameters, such as lipophilicity, acidity and conformation have a complex interplay and as a result, hERG activity cannot be easily predicted without recourse to more sophisticated data modelling techniques.

4.1.5 Haloperidol analogues with reduced hERG liability

In order to further investigate applicability of linker modification as a tool to mitigate hERG activity, electron-withdrawing linkers were incorporated into a known ‘hERG active’ compound. Haloperidol was selected as an easily disconnected molecule with significant hERG activity³⁴ and cyanoguanidine and urea analogues synthesised (Table 39).

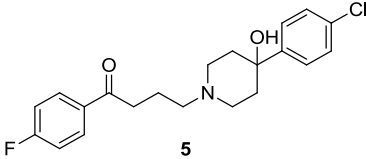
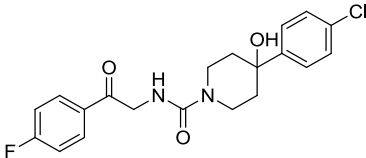
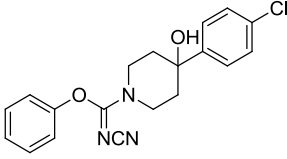
Compound	displacement of [³ H]astemizole from hERG cells ^a
 5	80 ± 2
 286	67 ± 2
 287	39 ± 9

Table 39: Comparison of hERG activity between haloperidol and hERG optimised haloperidol analogues. ^a% displacement of [³H]astemizole from hERG HEK293 cell preparation at 10 μM.

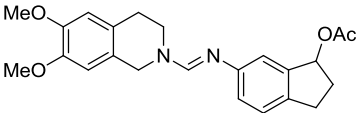
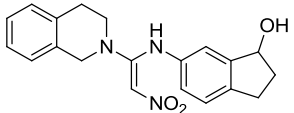
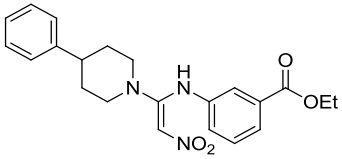
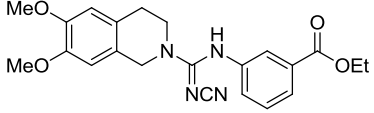
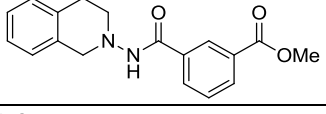
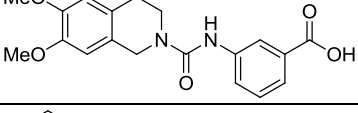
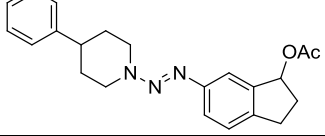
Both analogues successfully reduced hERG activity of haloperidol, particularly the cyanoguanidine analogue which reduced hERG activity significantly from 80 % to 39 %. It would be of great interest to synthesise the full cyanoguanidine analogue and directly compare the hERG results. However, it does appear that simple insertion of an electron-withdrawing group to reduce basicity is a useful method to reduce hERG activity within this small class of haloperidol analogues.

Further work to compare pharmacology (e.g. D₂ antagonism) between haloperidol analogues of this type would more fully investigate the effect of hERG mitigating electron-withdrawing linker introduction, which could potentially be applied to a number of known hERG active compounds.

4.1.6 Summary of biological assay results

To summarise, a range of novel compounds has been synthesised and SAR of 5-HT₇ and M₄ explored. A number of the synthesised compounds have significant affinity at one or both of the receptors of interest. Additionally, hERG SAR has been explored and introduction of electron-withdrawing linker groups such as hydrazides, ureas and nitroalkenes appears to be a valuable tool to mitigate undesirable hERG activity (Table 40). Pathfinder compounds such as **270** have also been discovered, where M₄ requirement for antipsychotic activity could be probed.

Overall, **271** is the best exemplar of a compound with affinity for both 5-HT₇ and M₄, with reduced hERG activity compared to the original lead *serominic* compound. Functional assays and *in vivo* testing will provide additional information to whether this compound or others have potential for application in the field of schizophrenia therapeutics.

Compound	Structure	5-HT ₇ ^a	M ₄ ^b	hERG ^c	clogP
53		70 ± 2	95 ± 3	73 ± 5	3.46
175		-	42 ± 12	32 ± 2	2.11
190		5 ± 9	14 ± 8	33 ± 6	4.89
203		5	11	38	4.48
236		-	43 ± 5	35 ± 4	3.45
248		-	54 ± 5	20 ± 9	3.03
270		65 ± 8	40 ± 7	77 ± 3	5.42

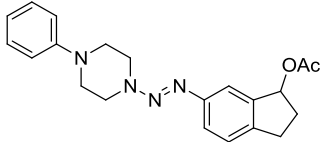
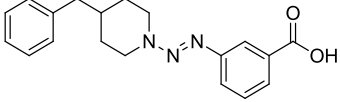
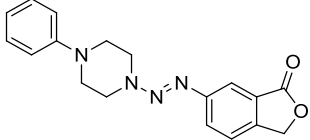
271		98 ± 1	59 ± 0.5	59 ± 8	4.44
275		7 ± 7	16 ± 4	1 ± 6	5.65
278		32 ± 2	26 ± 8	19 ± 17	3.17

Table 40: Selected compounds, their 5-HT₇, M₄, and hERG activities at 10 μM and clogP values.

Chapter 5 - Conclusions and further work

Initially, the compounds synthesised were based on a previously synthesised amidine lead compound with *serominic* activity (**53**) which displayed undesirable hERG activity.¹¹⁹ Non-basic linkers (triazene, nitroalkene, urea, hydrazide and trifluoromethyl) were incorporated into the structural motif to mitigate potential hERG activity and explore SAR at 5-HT₇ and M₄.

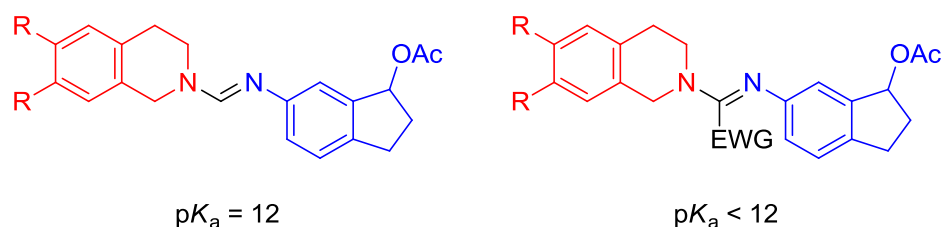


Figure 100: Compounds with electron-withdrawing linkers based on previously made *serominic* compound **53**. 5-HT₇ responsive elements are highlighted in blue, M₄ responsive elements are highlighted in red.

After a range of compounds were synthesised, muscarinic M₄ single point binding assay results indicated that the nitroalkene and triazene classes had *serominic* potential (Chapter 3). This led to a series focused mainly on triazene and nitroalkene SAR, utilising piperidines and piperazines in place of the tetrahydroisoquinoline moiety and investigating other aromatic groups in place of the chiral indanyl acetate, whilst retaining the general scaffold that previously afforded *serominic* activity.

The previously made lead compound (**53**) was also synthesised asymmetrically using CBS-reduction to obtain enantio-enriched compounds to investigate the effect of chirality on binding. Finally, analogues of the potent typical antipsychotic haloperidol with reduced hERG activity were also synthesised.

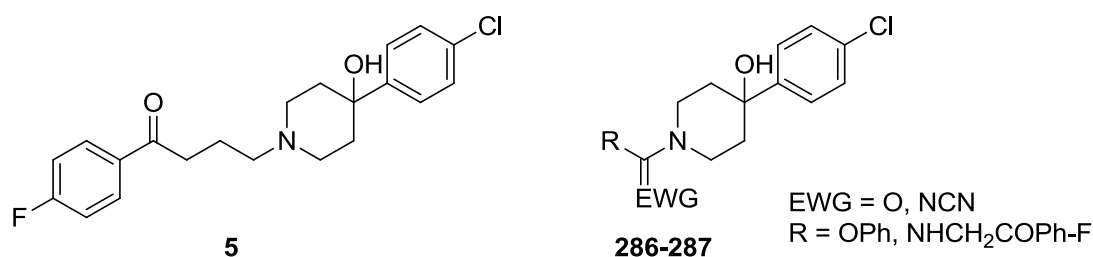


Figure 101: Haloperidol (**5**) and haloperidol analogues (**286-287**) with electron-withdrawing linkers inserted to reduce hERG activity.

5.1.2 Biological assays

Three radioligand binding assays were successfully developed and executed throughout the research programme: 5-HT₇, M₄ and hERG. 5-HT₇ and M₄ assays for *Series 1* were prepared from rat membrane initially but high error associated with the 5-HT₇ data meant this data was not reproducible. Consequently, commercially available human receptor membrane was purchased for the second series of assays. hERG however, was grown directly from cell cultures and after tissue preparation was used in hERG radioligand binding assays. Despite significant efforts, a D₂ radioligand binding assay was unable to be developed, attributed to poor membrane or radioisotope quality. Therefore, a full receptor screen would be useful for novel compounds of interest, alongside functional assays to ascertain antagonism or agonism.

From the biological data, it was clear that it was challenging to retain *seromimic* activity whilst introducing electron-withdrawing linkers as it appeared that a positive charge was associated with M₄ potency, however, triazene and nitroalkene linkers seemed promising.

After further exploration of SAR, one compound in particular, triazene **271** displayed exceptional activity at both receptors. Further biological evaluation of **271** would be beneficial, such as D₂ radioligand binding assays and functional assays for each.

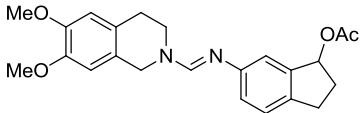
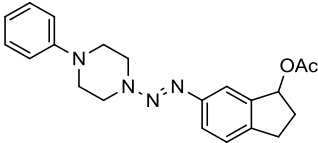
Number	Compound	5-HT ₇ ^a	M ₄ ^b	hERG ^c
53		70 ± 2	95 ± 3	73 ± 5
271		98 ± 1	59 ± 0.5	59 ± 8

Table 41: Lead amidine **53** and potentially seromimic triazene **271**. ^a% displacement of [³H]5-CT from human membrane preparation at 10 μM. ^b% displacement of [³H]NMS from human membrane preparation at 10 μM. ^c% displacement of [³H]astemizole from hERG HEK293 cell preparation at 10 μM.

Stability studies would also be useful, especially as it was observed that the 4-benzylpiperidine triazene **278** compound was shelf-stable in a closed container for over a year and was stable for at least two days in CDCl_3 .

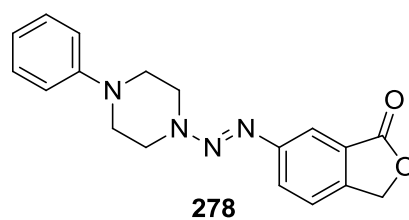


Figure 102: Shelf-stable triazene **278**.

Overall, a range of compounds displayed significant activity for one or both receptors (Table 42). It was also apparent that compounds containing an indanyl acetate group generally displayed higher activity for both receptors compared to compounds with analogous groups. As a number of compounds have very different affinities for 5-HT_7 and M_4 , assuming they displayed antipsychotic potential *in vivo*, some could be used as tool compounds to further validate the role either 5-HT_7 or M_4 plays in the antipsychotic effect e.g. comparing **53** with **270** to investigate the role of M_4 .

Compound	Structure	5-HT_7	M_4	hERG
53		70 ± 2^a	95 ± 3^b	73 ± 5^c
(<i>R</i>)-isomer 154		73 ± 2^a	95 ± 2^b	86 ± 3^c
(<i>S</i>)-isomer 155		64 ± 1^a	99 ± 1^b	77 ± 0.2^c
166		-*	$> 100 \pm 3^d$	56 ± 6^c
176		-*	$> 100 \pm 18^d$	56 ± 5^c

187		6 ± 8^a	56 ± 8^b	53 ± 16^c
193		14 ± 6^a	60 ± 13^b	50 ± 7^c
203		5 ± 2^a	30 ± 7^b	38 ± 3^c
237		-*	16 ± 12^d	29 ± 19^c
248		-*	54 ± 5^d	20 ± 9^c
265		-*	63 ± 10^d	71 ± 5^c
267		50 ± 6^a	30 ± 7^b	71 ± 5^c
270		65 ± 8^a	40 ± 7^b	77 ± 3^c
271		98 ± 1^a	59 ± 0.5^b	59 ± 8^c
278		32 ± 2^a	26 ± 8^b	19 ± 17^c

Table 42: Selected compounds displaying significant activity for 5-HT₇, M₄ and/or low affinity for hERG.. ^a% displacement of [³H]5-CT from human membrane preparation at 10 μM. ^b% displacement of [³H]NMS from human membrane preparation at 10 μM. ^c% displacement of [³H]astemizole from hERG HEK293 cell preparation at 10 μM. ^d% displacement of [³H]NMS from rat brain tissue preparation at 10 μM. *5-HT₇ data using rat brain tissue not reproducible.

Although the electron-withdrawing linkers generally did not improve *serominic* activity significantly compared to the lead *serominic* compound **53**, they were very successful at decreasing hERG activity. However, it is difficult to assert whether the reduction in hERG activity is due to introduction of the linker, or the concomitant change in clogP or p*K*_a. Moreover, hERG activity seems to be significantly affected by discrete functional changes, as exemplified by **278** (19 % displacement) (Table 42). Furthermore, the utility of the zwitterionic strategy for mitigation of hERG has been shown, in accordance with literature (**248** and **237**, 20 % and 29 % displacement, respectively).^{152, 153, 159}

Compounds containing urea (**248**, 20 % displacement), hydrazide (**237**, 29 % displacement) and cyanoguanidine (**203**, 38 % displacement) linkers were the least hERG active, reasoned to be an interplay between the introduction of a non-basic central nitrogen and conformationally favouring a bent (or perpendicular in the case of hydrazide) shape instead of a more linear conformation.

Unfortunately, this reduction in hERG affinity generally went hand in hand with a reduction in receptor affinity. There is a lack of hERG activity in the urea and hydrazide series' in particular and this may be due to low polarisability.

This was further supported by urea and cyanoguanidine haloperidol analogues where hERG was successfully mitigated compared to haloperidol (Table 43).

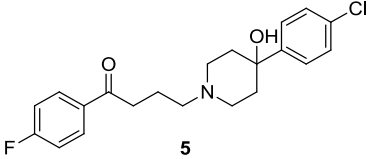
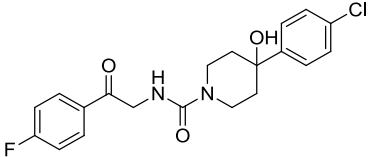
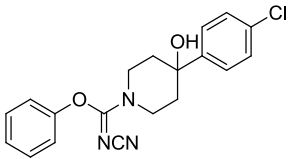
Compound	hERG ^a
 5	80 ± 2
 286	67 ± 2
 287	39 ± 9

Table 43: Incorporation of electron-withdrawing linkers to haloperidol mitigates hERG significantly.
^a% displacement of [³H]astemizole from hERG HEK293 cell preparation at 10 μM.

To summarise, triazene and nitroalkene-linked compounds still retained *serominic* activity compared to the lead amidine. Improving the relative potency (e.g. 10-fold) of these series' could lead to a potential drug candidate. Additionally, if potency was increased substantially in the triazenes, nitroalkenes or indeed the amidines, their hERG activity may not be a major issue as relative hERG activity versus therapeutic activity would become important. This is exemplified by haloperidol, a potent hERG blocker still used extensively for schizophrenia due to its potency. Additionally, further work such as enantioselective synthesis of **271** would be of interest, to investigate both the impact on *serominic* activity and hERG activity.

Improving potency could be achieved in a number of ways and further work on SAR where the linkers are not the primary target of modification could be of interest. For example, introduction of a flexible carboxylic acid, introduction of an oxygen atom in the tetrahydroisoquinoline ring or replacement of the aromatic ring in the tetrahydroisoquinoline with a pyridine ring could all be beneficial strategies in regards to reduction of hERG activity, whilst still retaining the template required for *serominic* activity (**289-291**).

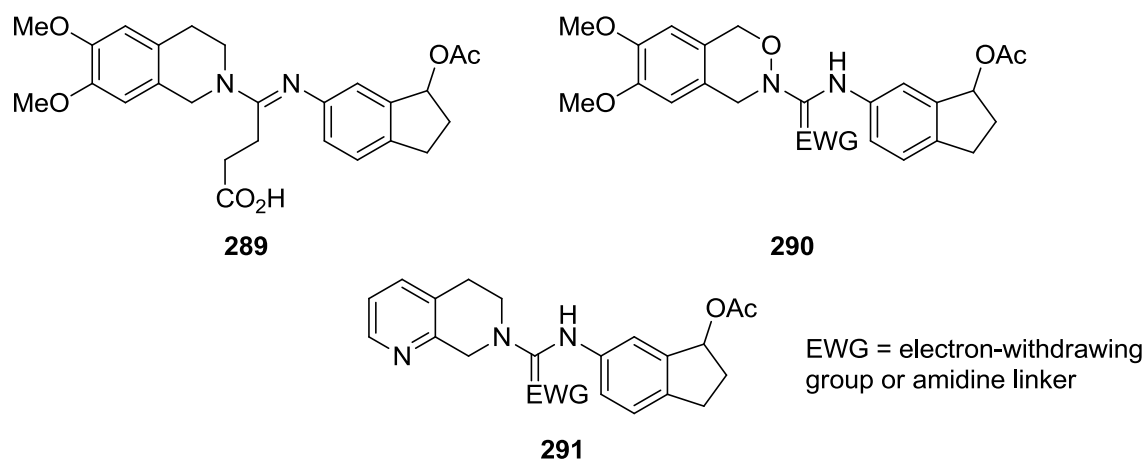


Figure 103: Structural changes with the potential to ameliorate hERG activity through zwitterionic effect (**289**) or through reduction in basicity (**290-291**).

Additionally, retaining the indanyl acetate that appears to be required for activity but further modifying the 5-HT₇ responsive element could explore SAR more extensively. For example, a hybridisation strategy could be introduced by incorporation of scaffolds from other well-known antipsychotic drugs such as olanzapine (**10**, Figure 104) and risperidone (**11**, Figure 105).

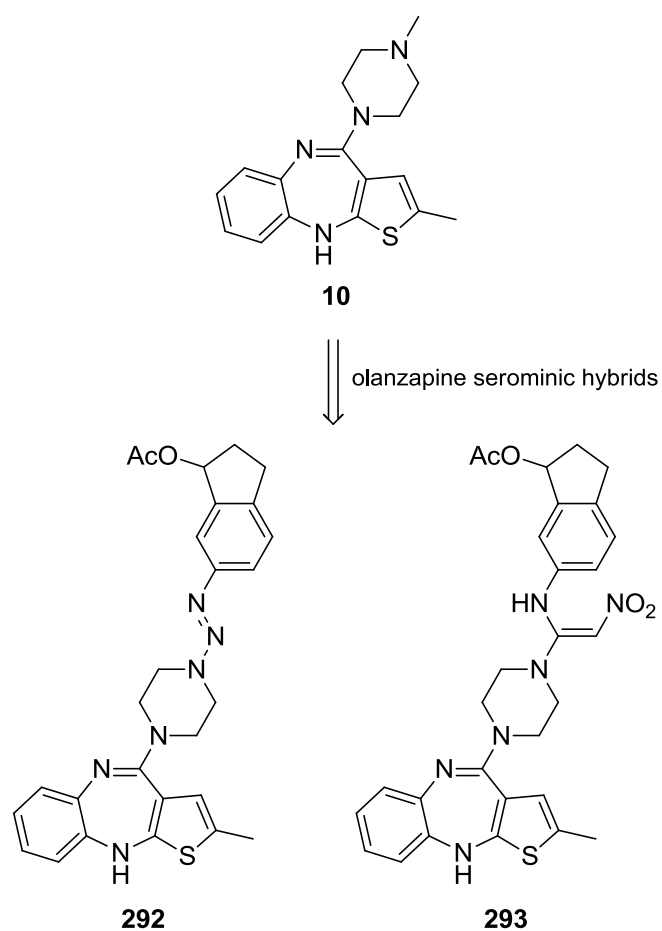


Figure 104: Hybridisation strategy using olanzapine (**10**), triazene and nitroalkene linkers and an indanyl acetate moiety (**292-293**).

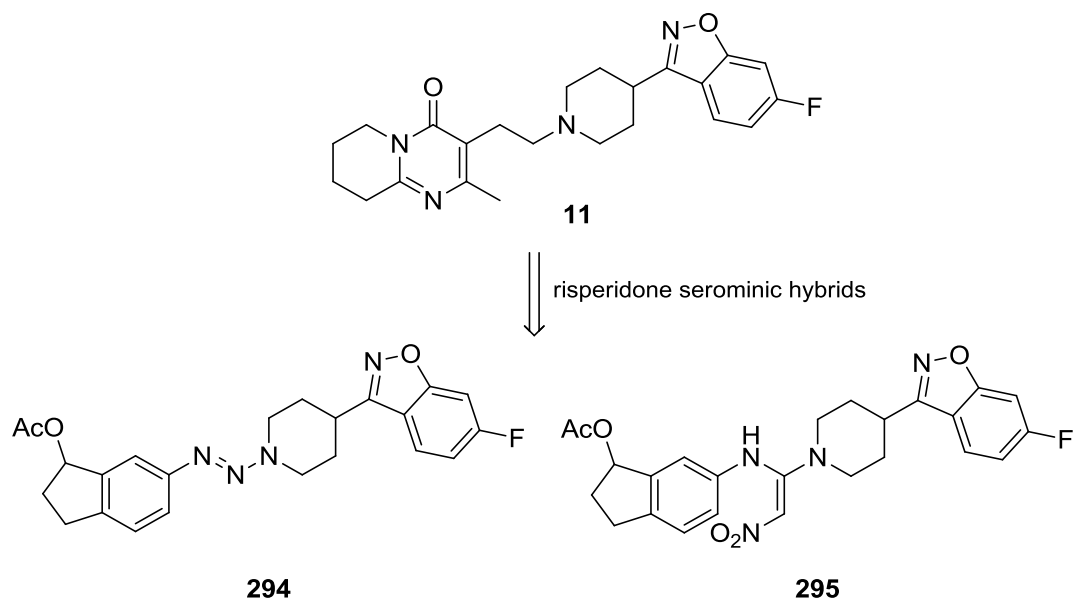


Figure 105: Hybridisation strategy using risperidone (**11**), triazene and nitroalkene linkers and an indanyl acetate moiety (**294-295**).

Overall, the *serominic* concept still has great potential, within the triazene and nitroalkene series', to provide a novel treatment for schizophrenia. A number of novel pathfinder compounds with promising multi-receptor profiles have been designed, synthesised and evaluated in radioligand binding assays. Further work may provide evidence for the utility of these multi-ligands as a new generation of antipsychotic therapies.

Chapter 6 - Experimental

6.1 Experimental

6.1.1 General

Anhydrous solvents were obtained from a Puresolv purification system from Innovative Technologies. All other reagents were used as supplied.

Removal of solvents was carried out by evaporation using a rotary evaporator at reduced pressure (*ca.* 70 mbar) unless otherwise stated.

Microwave reactions were carried out using a Biotage Initiator Eight apparatus.

Reaction progress was monitored by thin layer chromatography (TLC) carried out using pre-coated silica plates (Alugram[®] Sil G/UV₂₅₄). Visualisation of TLC plates was achieved by UV (254 nm) and/or vanillin dip.

Flash column chromatography was performed according to the procedure of Still²²⁰ *et al.* using silica gel (230-400 mesh).

Melting points were performed on Reichert 7905 hot stage melting point apparatus and are uncorrected.

Nuclear magnetic resonance (NMR) (¹H, ¹³C, ¹⁹F) spectra were recorded on Bruker Spectrospin AV3 or DRX500 spectrometer. Chemical shifts are quoted relative to the solvent in parts per million and coupling constants (*J* =) are given in Hz. The following abbreviations were used: s = singlet; d = doublet; t = triplet; q = quartet; m = multiplet; dd = doublet of doublets, bs = broad singlet.

Infra red spectra were recorded on a Perkin Elmer FT-IR spectrometer as a KBr disc or as a film on a NaCl plate or recorded neat on an ATR Microlab PAL spectrometer.

Mass spectra were recorded at the University of Strathclyde using a Jeol JMS AX505 mass spectrometer in low resolution mass spectrometry (LRMS) or high resolution mass spectrometry (HRMS) by Orbitrap. Both methods use electrospray ionisation (ESI).

Reverse phase high performance liquid chromatography (HPLC) was carried out on a Waters system with a Waters 1525 Binary HPLC pump and a Waters 2487 dual λ

absorbance detector at 254 nM using a C18 Luna column with the following gradient (Table 44).

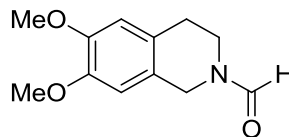
Time (min)	% A	% B	Flow rate (mL/min)
0.00	70	30	6
25.00	50	50	6
30.00	30	70	6
35.00	70	30	6
40.00	70	30	6
40.10	70	30	6

Table 44: HPLC conditions where A = acetonitrile and B = water.

Liquid chromatography-mass spectrometry (LCMS) was carried out on an Agilent LCMS 6130 APCI.

Final compounds taken forward for biological assay were at least 95 % pure as determined by HPLC or LCMS. The purity of the amidine-linked compounds and some triazene-linked compounds could not be ascertained due to product degradation on the column however their NMR spectra are collated in the Appendix.

6.1.2 Synthesis

Preparation of 6,7-dimethoxy-3,4-dihydroisoquinoline-2(1H)-formamide²²¹
(118)

6,7-Dimethoxy-1,2,3,4-tetrahydroisoquinoline hydrochloride (500 mg, 2.18 mmol) was dissolved in methanol (10 mL) at room temperature. Triethylamine (221 mg, 0.3 mL, 2.18 mmol) and methyl formate (131 mg, 2.18 mmol) were added and the solution heated under reflux for 16 h. The solvent was evaporated under reduced pressure and the residue purified by flash chromatography (ethyl acetate 100 %) to give two rotamers (major: minor ratio 1.5:1) of the title compound **118** as a white solid (163 mg, 34 %).

δ_{H} NMR (500 MHz, CDCl_3): 2.79-2.85 (2H, m, CH_2), 3.64 (major) 3.79 (minor) [2H, 2 x t, $J = 6.0$ (major), 6.0 (minor) CH_2], 3.87 (6H, 2 x s, 2 x MeO), 4.48 (minor) 4.62 (major) [2H, 2 x s, CH_2], 6.59 (minor) 6.61 (major) [1H, 2 x s, ArH], 6.61 (major) 6.64 (minor) [1H, 2 x s, ArH], 8.20 (major) 8.26 (minor) [1H, 2 x s, CHO].

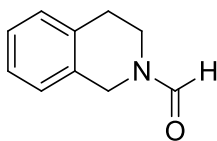
δ_{C} NMR (125 MHz, CDCl_3): 27.4 (minor) 29.1 (major), 37.9 (minor) 41.8 (major), 43.3 (major) 46.9 (minor), 55.9, 108.7 (minor) 109.2 (major), 111.5 (major) 111.8 (minor), 123.5 (major) 123.9 (minor), 125.3 (major) 126.2 (minor), 147.7, 148.0, 161.1 (minor) 161.5 (major).

LRMS (ESI): $[\text{M} + \text{H}^+]$ $\text{C}_{12}\text{H}_{16}\text{NO}_3^+$; calc. 222.11, found 222.20.

IR ν_{max} (ATR): 2934, 2870, 2835, 1673, 1658, 1444, 1114, 849 cm^{-1} .

Melting point: 127-129 °C (lit. 129-130²²², 126-127²²³ °C).

^1H NMR data obtained were consistent with those of previously characterised and published product.²²¹

Preparation of 3,4-dihydro-2(1H)-isoquinolineformamide²²¹ (119)

A solution of 1,2,3,4-tetrahydroisoquinoline (500 mg, 3.76 mmol) and methyl formate (226 mg, 3.76 mmol) in methanol (4 mL) was heated to 160 °C for 1 h using a Biotage microwave apparatus. The solvent was evaporated under reduced pressure and the residue purified by flash chromatography (hexane: ethyl acetate, 1:1) to give two rotamers (major: minor ratio 1.6:1) of the title compound **119** (463 mg, 77 %) as a pale yellow oil.

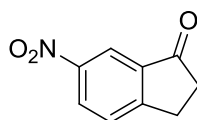
δ_{H} NMR (500 MHz, CDCl_3): 2.87-2.93 (2H, m, CH_2), 3.66 (major) 3.80 (minor) [2H, 2 x t, $J = 6.0$ (major), 6.0 (minor), CH_2], 4.55 (minor) 4.70 (major) [2H, 2 x s, CH_2], 7.10-7.22 (4H, m, ArH), 8.21 (major) 8.27 (minor) [1H, 2 x s, CHO].

δ_{C} NMR (125 MHz, CDCl_3): 27.9 (minor) 29.7 (major), 37.9 (minor) 42.2 (major), 43.2 (major) 47.2 (minor), 125.9 (minor) 126.6 (major), 126.4 (minor) 126.7 (major), 126.6 (major) 127.0 (minor), 128.9 (major) 129.1 (minor), 131.8 (major) 132.3 (minor), 133.6 (major) 134.4 (minor), 161.2 (minor) 161.7 (major).

LRMS (ESI): $[\text{M} + \text{H}^+]$ $\text{C}_{10}\text{H}_{12}\text{NO}^+$; calc. 162.09, found 162.20.

IR ν_{max} (ATR): 2910, 2859, 1671, 1638, 1431, 1395, 1196, 735 cm^{-1} .

^1H NMR data obtained were consistent with those of previously characterised and published product.²²¹

Preparation of 6-nitro-1-indanone²²¹ (121)

A solution of 1-indanone (2.0 g, 15.2 mmol) in concentrated sulfuric acid (20 mL) was cooled in an acetone-dry ice bath to $-15\text{ }^{\circ}\text{C}$. A solution of potassium nitrate (1.8 g, 17.8 mmol) in concentrated sulfuric acid (8 mL) was added via a dropping funnel maintaining an internal temperature of $-10 \pm 5\text{ }^{\circ}\text{C}$. After stirring at $0\text{ }^{\circ}\text{C}$ for 1 h, the mixture was poured into ice and stirred for a further 30 min. The resulting solid was filtered, washed with water and air dried. Purification by flash chromatography (hexane:ethyl acetate 4:1) gave the title compound **121** (1.32 g, 49 %) as a pale yellow solid.

δ_{H} NMR (500 MHz, CDCl_3): 2.54-2.56 (2H, m, CH_2), 3.08 (2H, t, $J = 6.0$, CH_2), 7.50 (1H, d, $J = 8.5$, ArH), 7.92 (1H, d, $J = 2.0$, ArH), 8.06 (1H, dd, $J = 8.5, 2.0$, ArH).

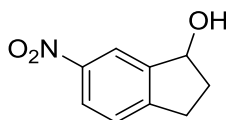
δ_{C} NMR (125 MHz, CDCl_3): 25.8, 36.2, 117.8, 127.6, 128.1, 137.4, 146.9, 160.8, 204.0.

LRMS (ESI): $[\text{M} + \text{H}^+]$ $\text{C}_9\text{H}_8\text{NO}_3^+$; calc. 178.05, found 178.10.

IR ν_{max} (ATR): 3099, 2932, 1712, 1597, 1530, 1339, 1077, 739 cm^{-1} .

Melting point: 74-75 $^{\circ}\text{C}$ (lit. 74 $^{\circ}\text{C}$).²²⁴

^1H NMR data obtained were consistent with those of previously characterised and published product.²²¹

Preparation of 6-nitro-1-indanol²²¹ (122)

A solution of 6-nitro-1-indanone (2 g, 11.3 mmol) in methanol (15 mL) was cooled in an ice-water bath and sodium borohydride (428 mg, 11.3 mmol) added in 3 portions. The reaction was continued at room temperature for 90 min. and quenched using hydrochloric acid (2 M, 20 mL). The methanol was removed by rotary evaporation and the residue partitioned between dichloromethane and water. The organic phase was then dried over magnesium sulfate, filtered and concentrated to give the title compound **122** as a brown solid (1.93 g, 96 %).

δ_{H} NMR (500 MHz, CDCl_3): 2.02-2.09 (2H, m and bs, 1H of CH_2 and OH), 2.58-2.64 (1H, m, 1H of CH_2), 2.88-2.94 (1H, m, 1H of CH_2), 3.11-3.17 (1H, m, 1H of CH_2), 5.32 (1H, t, $J = 6.5$, CHOH), 7.38 (1H, d, $J = 8.0$, ArH), 8.14 (1H, dd, $J = 8.5$, 2.0, ArH), 8.25 (1H, d, $J = 1.5$, ArH).

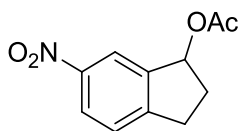
δ_{C} NMR (125 MHz, CDCl_3): 30.2, 36.4, 75.7, 119.9, 124.1, 125.7, 146.9, 147.8, 151.1.

LRMS (ESI): $[\text{M} + \text{H}^+]$ $\text{C}_9\text{H}_{10}\text{NO}_3^+$; calc. 179.06, $[\text{M} + \text{H}^+]$ not observed.

IR ν_{max} (KBr): 3269, 2946, 2840, 1918, 1518, 1348, 1043, 738 cm^{-1} .

Melting point: 74-75 °C (lit. 74 °C).²²⁵

^1H NMR data obtained were consistent with those of previously characterised and published product.²²¹

Preparation of 6-nitro-2,3-dihydro-1*H*-inden-1-yl acetate²²¹ (123)

Acetic anhydride (6 mL) was added to a solution of 6-nitro-1-indanol (1.93 g, 10.8 mmol) in pyridine (20 mL) at 0 °C and stirred at room temperature for 16 h under nitrogen. Most of the solvent was evaporated under reduced pressure and the residue partitioned with diethyl ether and washed with hydrochloric acid (2M, 30 mL). The organic layer was then dried over magnesium sulfate, filtered and concentrated to give the title compound **123** as brown oil (2.35 g, 99 %).

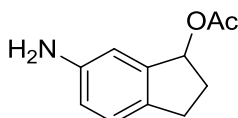
δ_{H} NMR (500 MHz, CDCl_3): 2.10 (3H, s, CH_3), 2.17-2.19 (1H, m, 1H of CH_2), 2.56-2.62 (1H, m, 1H of CH_2), 2.92-2.98 (1H, m, 1H of CH_2), 3.13-3.19 (1H, m, 1H of CH_2), 6.18 (1H, dd, $J = 7.0, 4.0$, CHOCOCH_3), 7.38 (1H, d, $J = 8.5$, ArH), 8.12 (1H, dd, $J = 8.5, 2.0$, ArH), 8.20 (1H, d, $J = 1.5$, ArH).

δ_{C} NMR (125 MHz, CDCl_3): 21.3, 30.5, 32.8, 77.1, 121.2, 124.6, 125.6, 143.1, 147.7, 152.0, 171.0.

LRMS (ESI): $[\text{M} + \text{H}^+]$ $\text{C}_{11}\text{H}_{12}\text{NO}_4^+$; calc. 221.07, $[\text{M} + \text{H}^+]$ not observed.

IR ν_{max} (NaCl): 2942, 1754, 1523, 1351, 1126, 897 cm^{-1} .

^1H NMR data obtained were consistent with those of previously characterised and published product.²²¹

Preparation of 6-amino-2,3-dihydro-1*H*-inden-1-yl acetate²²¹ (124)

Activated palladium on carbon (Pd/C) (50 % w/w, 277 mg) was added under a stream of nitrogen to a cooled solution of 6-nitro-2,3-dihydro-1*H*-inden-1-yl acetate

(550 mg, 2.49 mmol) in aqueous methanol (5: 0.5 methanol: water, 5.5 mL). Sodium borohydride (480 mg, 12.5 mmol) was added portion-wise and the mixture stirred at room temperature for 5 min. The methanol was evaporated under reduced pressure and the residue partitioned with dichloromethane and water. The organic layer was then washed with NaOH (2M), dried with magnesium sulfate, filtered and concentrated. The resulting residue was then purified by flash chromatography (hexane:ethyl acetate 4:1) to afford the title compound **124** (265 mg, 56 %) as a pale brown oil.

δ_{H} NMR (500 MHz, CDCl_3) : 2.07-2.10 (4H, m, CH_3 and 1H of CH_2), 2.44-2.51 (1H, m, 1H of CH_2), 2.74-2.80 (1H, m, 1H of CH_2), 2.97-3.03 (1H, m, 1H of CH_2), 3.65 (2H, bs, NH_2), 6.12 (1H, dd, $J = 7.0, 3.5$, CHOCOCH_3), 6.65 (1H, dd, $J = 8.0, 2.0$, ArH), 6.76 (1H, d, $J = 1.5$, ArH), 7.06 (1H, d, $J = 8.0$, ArH).

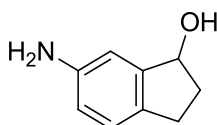
δ_{C} NMR (125 MHz, CDCl_3): 21.6, 29.6, 32.8, 78.7, 112.1, 116.7, 125.5, 134.5, 142.5, 145.6, 171.4.

LRMS (ESI): $[\text{M} + \text{H}^+]$ $\text{C}_{11}\text{H}_{14}\text{NO}_2^+$; calc. 192.10, found 192.20

IR ν_{max} (ATR): 3400, 3344, 2916, 2865, 1738, 1619, 1492, 1228, 1021, 722 cm^{-1} .

^1H NMR data obtained were consistent with those of previously characterised and published product.²²¹

Preparation of 6-amino-1-indanol (**172**)



The title compound 6-amino-1-indanol (**172**) was isolated as a by-product in the purification of 6-amino-2,3-dihydro-1*H*-inden-1-yl acetate (**124**) as a brown-beige solid (150 mg).

δ_{H} NMR (500 MHz, CDCl_3): 1.87-1.93 (1H, m, 1H of CH_2), 2.43-2.49 (1H, m, 1H of CH_2), 2.67-2.73 (1H, m, 1H of CH_2), 2.90-2.95 (1H, m, 1H of CH_2), 3.08 (2H, bs,

NH₂), 5.13 (1H, t, $J = 6.0$, CHOH), 6.61 (1H, q, $J = 8.0, 2.5$, ArH), 6.72 (1H, d, $J = 2.5$, ArH), 7.03 (1H, d, $J = 8.0$, ArH). Note: OH peak not observed by ¹H NMR.

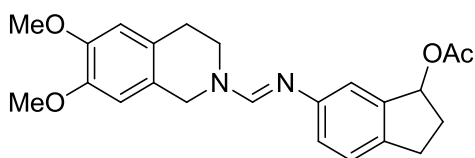
δ_C NMR (125 MHz, CDCl₃): 28.9, 36.4, 76.5, 110.8, 115.8, 125.4, 135.3, 145.3, 146.3.

IR ν_{\max} (KBr): 3348, 2937, 2852, 1621, 1493, 1330, 805 cm⁻¹.

LRMS (ESI): [M + H⁺] C₉H₁₂NO⁺; calc. 150.09, [M + H⁺] not observed.

Melting point: 106-109 °C.

Preparation of (*E*)-6-[[*(6,7*-dimethoxy-3,4-dihydro-2(*1H*)-isoquinolinyl)methylidene]amino]-2,3-dihydro-1*H*-inden-1-yl acetate²²¹ (53**)**



A solution of 6,7-dimethoxy-3,4-dihydroisoquinoline-2(*1H*)-formamide (200 mg, 0.91 mmol) and phosphoryl chloride (280 mg, 1.82 mmol) in dry dichloromethane (10 mL) was stirred for 30 min. at room temperature under nitrogen. 6-Amino-2,3-dihydro-1*H*-inden-1-yl acetate (135 mg, 0.71 mmol) was added and the reaction mixture stirred for a further 4 h. The solution was partitioned with dichloromethane and washed with sodium hydroxide (2M). The organic layer was then dried with magnesium sulfate, filtered and concentrated under reduced pressure and purification by flash chromatography (hexane:ethyl acetate 3:1 and 1 % triethylamine) afforded the title compound **53** as a yellow oil (46 mg, 19 %).

δ_H NMR (400 MHz, CDCl₃): 2.06-2.11 (4H, m, 1H of CH₂ and CH₃), 2.49-2.51 (1H, m, 1H of CH₂), 2.80-2.88 (3H, m, 1H of CH₂ and CH₂), 3.02-3.07 (1H, m, 1H of CH₂), 3.68 (2H, bs, CH₂), 3.85 (3H, s, MeO), 3.87 (3H, s, MeO), 4.67 (2H, bs, CH₂), 6.18 (1H, dd, $J = 6.8, 3.6$, CHOCOCH₃), 6.64 (2H, s, ArH), 6.96 (1H, dd, $J = 8.0, 2.0$, ArH), 7.02 (1H, s, ArH), 7.16 (1H, d, $J = 8.0$, ArH), 7.71 (1H, s, CHN).

δ_{C} NMR (100 MHz, CDCl_3): 21.4, 29.6, 29.6, 32.7, 44.8, 46.5, 56.0, 78.5, 109.1, 111.6, 117.3, 122.7, 124.6, 125.1, 125.9, 138.5, 142.0, 147.7, 147.8, 150.9, 152.4, 171.1.

IR ν_{max} (ATR): 2924, 2850, 2743, 1728, 1627, 1605, 1247, 1111 cm^{-1} .

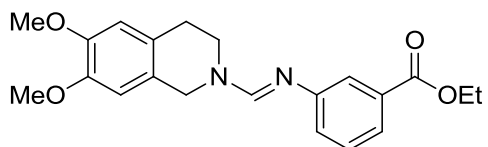
LRMS (ESI): $[\text{M} + \text{H}^+]$ $\text{C}_{23}\text{H}_{27}\text{N}_2\text{O}_4^+$; calc. 395.20, found 395.20.

HRMS (ESI): $[\text{M} + \text{H}^+]$ $\text{C}_{23}\text{H}_{27}\text{N}_2\text{O}_4^+$; calc. 395.1965, found 395.1964.

^1H NMR data obtained were consistent with those of previously characterised and published product.²²¹

Purity: Purity could not be determined by HPLC. See appendix for ^1H NMR.

Preparation of (*E*)-ethyl 3-[(6,7-dimethoxy-3,4-dihydro-2(1*H*)-isoquinolinyl)methylidene]amino]benzoate (126**)**



A solution of 6,7-dimethoxy-3,4-dihydroisoquinoline-2-(1*H*)-formamide (200 mg, 0.91 mmol) and phosphoryl chloride (280 mg, 1.82 mmol) in dry dichloromethane (10 mL) was stirred for 30 min. at room temperature under nitrogen. Ethyl 3-amino benzoate (150 mg, 0.91 mmol) was added and the reaction mixture stirred for a further 4 h. The solution was partitioned with dichloromethane and washed with sodium hydroxide (2M). The organic layer was then dried with magnesium sulfate, filtered and concentrated under reduced pressure and purification by flash chromatography (hexane:ethyl acetate, 3:1 and 1 % triethylamine) afforded the title compound **126** as a colourless oil (108 mg, 32 %).

δ_{H} NMR (400 MHz, CDCl_3): 1.39 (3H, t, $J = 7.2$, OCH_2CH_3), 2.88 (2H, t, $J = 5.6$, CH_2), 3.65 (2H, bs, CH_2), 3.86 (3H, s, MeO), 3.87 (3H, s, MeO), 4.37 (2H, q, $J = 7.2$, OCH_2CH_3), 4.73 (2H, bs, CH_2), 6.64 (2H, bs, ArH), 7.19 (1H, dd, $J = 8.0, 1.2$,

ArH), 7.33 (1H, t, $J = 7.6$, ArH), 7.65 (1H, s, ArH), 7.69-7.71 (1H, m, ArH), 7.74 (1H, s, CHN).

δ_{C} NMR (100 MHz, CDCl_3): 14.5, 29.9, 45.0, 46.8, 56.1, 61.0, 109.4, 111.7, 121.7, 123.9, 124.5, 126.5, 129.1, 131.5, 147.9, 152.2, 152.9, 167.05.

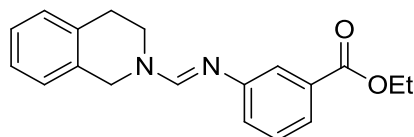
IR ν_{max} (ATR): 2926, 2848, 2835, 1711, 1621, 1256, 1210, 1103 cm^{-1} .

LRMS (ESI): $[\text{M} + \text{H}^+]$ $\text{C}_{21}\text{H}_{25}\text{N}_2\text{O}_4^+$; calc. 369.18 found 369.60.

HRMS (ESI): $[\text{M} + \text{H}^+]$ $\text{C}_{21}\text{H}_{25}\text{N}_2\text{O}_4^+$; calc. 369.1809, found 369.1806.

Purity: Purity could not be determined by HPLC. See appendix for ^1H NMR.

Preparation of (*E*)-ethyl 3-[[3,4-dihydro-2(1*H*)-isoquinolinyl)methylidene)amino]benzoate (127**)**



A solution of 3,4-dihydroisoquinoline-2(1*H*)-formamide (150 mg, 0.93 mmol) and phosphoryl chloride (280 mg, 1.82 mmol) in dry dichloromethane (10 mL) was stirred for 30 min. at room temperature under nitrogen. Ethyl 3-aminobenzoate (154 mg, 0.93 mmol) was added and the reaction mixture stirred for a further 4 h. The solution was partitioned with dichloromethane and water and washed with sodium hydroxide (2M). The organic layer was then dried with magnesium sulfate, filtered and concentrated under reduced pressure and purification by flash chromatography (hexane: ethyl acetate, 6:1 and 1 % TEA) afforded the title compound **127** as a transparent yellow oil (141 mg, 50 %).

δ_{H} NMR (400 MHz, CDCl_3): 1.40 (3H, t, $J = 7.2$, OCH_2CH_3), 2.96 (2H, t, $J = 6.0$, CH_2), 3.67 (2H, bs, CH_2), 4.38 (2H, q, $J = 7.2$, OCH_2CH_3), 4.81 (2H, bs, CH_2), 7.18-7.22 (5H, m, ArH), 7.34 (1H, t, $J = 8.0$, ArH), 7.67 (1H, s, ArH), 7.71-7.73 (1H, m, ArH), 7.75 (1H, s, CHN).

δ_{C} NMR (100 MHz, CDCl_3) 14.4, 29.7, 45.3, 46.5, 60.9, 121.6, 123.8, 126.4, 126.6, 128.1, 128.9, 129.0, 129.6, 131.3, 131.9, 132.2, 152.0, 152.8, 166.9.

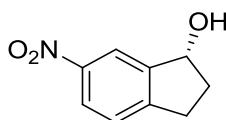
IR ν_{max} (ATR): 2980, 2935, 2900, 2864, 1715, 1666, 1631, 1288, 1275 cm^{-1} .

LRMS (ESI): $[\text{M} + \text{H}^+]$ $\text{C}_{19}\text{H}_{21}\text{N}_2\text{O}_2^+$; calc. 309.16, found 309.33.

HRMS (ESI): $[\text{M} + \text{H}^+]$ $\text{C}_{19}\text{H}_{21}\text{N}_2\text{O}_2^+$; calc. 309.1598, found 309.1597.

Purity: Purity could not be determined by HPLC. See appendix for ^1H NMR.

Preparation of (*R*)-6-nitro-2,3-dihydro-1*H*-inden-1-ol²²⁶ (142)



Formation of (*S*)-(-)-2-methyl-oxazaborolidine complex

A flask containing (*S*)-(-)-2-methyl-oxazaborolidine (200 mg, 0.72 mmol) in dry hexane (4 mL) was stirred under nitrogen and borane-methane sulfide (84 μL , 0.84 mmol) was added neat via syringe over a few min. The solution was stirred for 30 min. at room temperature and then diluted with dry hexane (8 mL) over 1 h. The reaction was aged for 1 h, cooled to -10 $^{\circ}\text{C}$ and aged for a further 2 h. The mother liquor was decanted and the resulting white solid washed with dry hexane (3 x 1 mL) and dried under vacuum for 1 h.

Preparation of (*R*)-6-nitro-2,3-dihydro-1*H*-inden-1-ol

A flask containing (*S*)-(-)-2-methyl-oxazaborolidine complex (33 mg, 0.11 mmol) in dry dichloromethane was stirred under nitrogen, borane-methane sulfide (227 μL , 2.27 mmol, 10 equiv.) added and the solution cooled to -20 $^{\circ}\text{C}$. A solution of 6-nitro-1-indanone (300 mg, 1.7 mmol) in dry dichloromethane (2 mL) was added over 10 min. and the reaction stirred at -20 $^{\circ}\text{C}$ for 2 h. The mixture was then poured into a flask with methanol (20 mL) at -20 $^{\circ}\text{C}$ and warmed to room temperature then reduced in volume (to approximately 5 mL) by distillation (x 2). The resulting

brown residue was rotary evaporated to dryness to give the title compound **142** as a brown gummy solid (300 mg, 99 %).

δ_{H} NMR (400 MHz, CDCl_3): 1.98-2.03 (1H, m, 1H of CH_2), 2.49-2.57 (1H, m, 1H of CH_2), 2.80-2.88 (1H, m, 1H of CH_2), 3.02-3.10 (1H, m, 1H of CH_2), 3.66 (1H, bs, OH), 5.24 (1H, t, $J = 6.4$, CHOH), 7.30 (1H, d, $J = 8.0$, ArH), 8.01 (1H, dd, $J = 8.0$, 2.0, ArH), 8.13 (1H, d, $J = 1.6$, ArH).

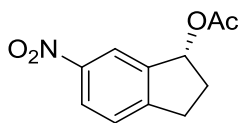
δ_{C} NMR (100 MHz, CDCl_3): 29.4, 35.4, 74.7, 119.1, 123.1, 125.4, 146.2, 146.7, 150.6.

IR ν_{max} (KBr): 3419, 2952, 1614, 1518, 1346, 738 cm^{-1} .

HRMS (ESI): $[\text{M} + \text{H}^+]$ $\text{C}_9\text{H}_{10}\text{NO}_3^+$; calc. 180.0655, $[\text{M} + \text{H}^+]$ not observed.

$\alpha_{\text{D}} = -50.5$ ($c = 0.0125$, 20 °C, CHCl_3).

Preparation of (*R*)-6-nitro-2,3-dihydro-1*H*-inden-1-yl acetate (**148**)



Acetic anhydride (1 mL) was added to a solution of (*R*)-6-nitro-2,3-dihydro-1*H*-inden-1-ol (150 mg, 0.84 mmol) in pyridine (1 mL) at 0 °C and stirred at room temperature for 16 h under nitrogen. The solution was partitioned with diethyl ether and washed with hydrochloric acid (2M). The organic layer was then dried over magnesium sulfate, filtered and concentrated to give **148** as viscous brown oil (164 mg, 88 %).

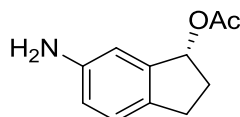
δ_{H} NMR (400 MHz, CDCl_3): 2.11 (3H, s, CH_3), 2.17-2.24 (1H, m, 1H of CH_2), 2.59-2.68 (1H, m, 1H of CH_2), 2.95-3.03 (1H, m, 1H of CH_2), 3.16-3.24 (1H, m, 1H of CH_2), 6.22 (1H, dd, $J = 7.2$, 4.4, CHOCOCH_3), 7.42 (1H, d, $J = 8.4$, ArH), 8.18 (1H, dd, $J = 8.4$, 2.0, ArH), 8.26 (1H, d, $J = 2.0$, ArH).

δ_{C} NMR (100 MHz, CDCl_3): 20.6, 29.4, 32.1, 76.5, 120.5, 123.9, 124.9, 142.4, 147.0, 151.3, 170.3.

HRMS (ESI): $[\text{M} + \text{H}^+]$ $\text{C}_{11}\text{H}_{12}\text{NO}_4^+$; calc. 222.0761, $[\text{M} + \text{H}^+]$ not observed.

$\alpha_{\text{D}} = +18.8$ ($c = 0.085$, 20 °C, CHCl_3).

Preparation of (*R*)-6-amino-2,3-dihydro-1*H*-inden-1-yl acetate (**150**)



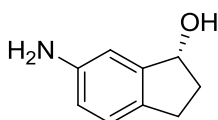
A solution of (*R*)-6-nitro-2,3-dihydro-1*H*-inden-1-yl acetate (164 mg, 0.74 mmol) in aqueous methanol (5: 0.5 methanol: water, 5.5 mL) was cooled in an ice-water bath and activated palladium on carbon added (17 mg, 10 % w/w) under a stream of nitrogen. Sodium borohydride (140 mg, 3.7 mmol, 5 equiv.) was added slowly and the reaction stirred for 10 min. after addition. The mixture was filtered through Kieselguhr, methanol removed by rotary evaporation, and the residue partitioned with dichloromethane and water. The organic layer was then dried over magnesium sulfate, filtered and evaporated under reduced pressure. The residue was purified by flash chromatography (hexane:ethyl acetate 3:1) to afford the title compound **150** as a yellow oil (35 mg, 25 %).

δ_{H} NMR (400 MHz, CDCl_3): 2.07-2.12 (4H, s, CH_3 and 1H of CH_2), 2.44-2.53 (1H, m, 1H of CH_2), 2.75-2.82 (1H, m, 1H of CH_2), 2.98-3.05 (1H, m, 1H of CH_2), 3.64 (2H, bs, NH_2), 6.14 (1H, dd, $J = 7.2, 3.6$, CHOCOCH_3), 6.66 (1H, dd, $J = 8.0, 2.4$, ArH), 6.77 (1H, d, $J = 2.0$, ArH), 7.06 (1H, d, $J = 8.0$, ArH).

δ_{C} NMR (100 MHz, CDCl_3): 21.4, 29.3, 32.6, 78.5, 111.9, 116.4, 125.3, 134.3, 142.2, 145.4, 171.2.

HRMS (ESI): $[\text{M} + \text{H}^+]$ $\text{C}_{11}\text{H}_{14}\text{NO}_3^+$; calc. 192.1019, $[\text{M} + \text{H}^+]$ not observed.

$\alpha_{\text{D}} = +43.6$ ($c = 0.80$, 20 °C, CHCl_3).

Preparation of (*R*)-6-amino-2,3-dihydro-1*H*-inden-1-ol (152**)**

(*R*)-6-amino-2,3-dihydro-1*H*-inden-1-ol was obtained as a by-product in the column chromatography of (*R*)-6-amino-2,3-dihydro-1*H*-inden-1-yl acetate (**150**). Slow evaporation of a dichloromethane solution afforded small yellow-beige crystals (90 mg, 0.61 mmol) of title compound **152** a sample of which was submitted for X-ray analysis.

δ_{H} NMR (400 MHz, CDCl_3): 1.91-1.96 (2H, m, 1H of CH_2 and OH), 2.44-2.52 (1H, m, 1H of CH_2), 2.68-2.76 (1H, m, 1H of CH_2), 2.91-2.98 (1H, m, 1H of CH_2), 3.64 (2H, bs, NH_2), 5.15 (1H, t, $J = 6.0$, CHOH), 6.24 (1H, dd, $J = 8.0, 2.4$, ArH), 6.75 (1H, d, $J = 2.0$, ArH), 7.04 (1H, d, $J = 8.0$, ArH).

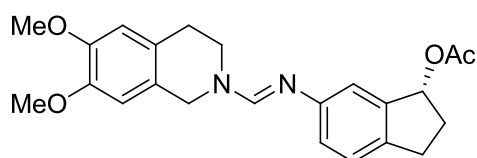
δ_{C} NMR (100 MHz, CDCl_3): 28.4, 36.0, 76.1, 110.2, 115.2, 124.9, 132.7, 144.9, 145.8.

IR ν_{max} (ATR): 3388, 3301, 2962, 2922, 2852, 1615, 1496, 1049 cm^{-1} .

HRMS (ESI): $[\text{M} + \text{H}^+]$ $\text{C}_9\text{H}_{12}\text{NO}^+$; calc. 150.0913, $[\text{M} + \text{H}^+]$ not observed.

Melting point: 126-129 $^{\circ}\text{C}$.

α_{D} = - 48.8 ($c = 0.135$, 20 $^{\circ}\text{C}$, CHCl_3).

Preparation of (*R,E*)-6-(((6,7-dimethoxy-3,4-dihydroisoquinolin-2(1*H*)-yl)methylene)amino)-2,3-dihydro-1*H*-inden-1-yl acetate (154**)**

A solution of 6,7-dimethoxy-3,4-dihydroisoquinoline-2(1*H*)-formamide (40 mg, 0.18 mmol) and phosphoryl chloride (33 mg, 0.22 mmol) in dry dichloromethane (4 mL)

was stirred for 30 min. at room temperature under nitrogen. (*R*)-6-Amino-2,3-dihydro-1*H*-inden-1-yl acetate (35 mg, 0.18 mmol) was added and the reaction mixture stirred for a further 4 h. The solution was partitioned with dichloromethane and washed with sodium hydroxide (2M). The organic layer was then dried with magnesium sulfate, filtered and concentrated. Purification by flash chromatography (hexane:ethyl acetate 2:1 and 0.1 % triethylamine) afforded the title compound **154** as a pale yellow oil (20 mg, 28 %).

δ_{H} NMR (400 MHz, CDCl_3): 2.08-2.15 (4H, m, 1H of CH_2 and CH_3), 2.50-2.54 (1H, m, 1H of CH_2), 2.83-2.91 (3H, m, 1H of CH_2 and CH_2), 3.05-3.08 (1H, m, 1H of CH_2), 3.71 (2H, bs, CH_2), 3.88 (3H, s, MeO), 3.89 (3H, s, MeO), 4.73 (2H, bs, CH_2), 6.20 (1H, dd, $J = 5.6, 2.8$, CHOCOCH_3), 6.67 (2H, s, ArH), 7.06 (2H, bs, ArH), 7.20 (1H, d, $J = 6.4$, ArH), 7.73 (1H, s, CHN).

δ_{C} NMR (100 MHz, CDCl_3): 21.4, 29.6, 32.7, 56.0, 78.5, 109.2, 111.6, 117.3, 122.8, 125.1, 138.6, 142.0, 147.8, 147.9, 152.0, 152.3, 171.1. Note: 3 x CH_2 not observed by ^{13}C NMR due to fast relaxation.

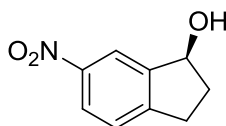
IR ν_{max} (ATR): 2926, 2835, 1716, 1632, 1228, 726 cm^{-1} .

LRMS (ESI): $[\text{M} + \text{H}^+]$ $\text{C}_{23}\text{H}_{27}\text{N}_2\text{O}_4^+$; calc. 395.1965, found 395.13.

HRMS (ESI): $[\text{M} + \text{H}^+]$ $\text{C}_{23}\text{H}_{27}\text{N}_2\text{O}_4^+$; calc. 395.1965, found 395.1962.

$\alpha_{\text{D}} = + 35.1$ ($c = 0.35$, 20 °C, CHCl_3).

Purity: Purity could not be determined by HPLC. See appendix for ^1H NMR.

Preparation of (S)-6-nitro-2,3-dihydro-1H-inden-1-ol²²⁶ (143)*Preparation of (R)-(+)-2-methyl-oxazaborolidine complex*

A flask containing (R)-(+)-2-methyl-oxazaborolidine (200 mg, 0.72 mmol) in dry hexane (4 mL) was stirred under nitrogen and borane-methane sulfide (84 μ L, 0.84 mmol) was added neat via syringe over a few min. The solution was stirred for 30 min. at room temperature and then diluted with dry hexane (8 mL) over 1 h. The reaction was aged for 1 h, cooled to -10 °C and aged for a further 2 h. The mother liquor was decanted and the resulting white solid washed with dry hexane (3 x 1 mL) and dried under reduced pressure for 1 h. This was taken forward to the next stage without characterisation.

Preparation of (S)-6-nitro-2,3-dihydro-1H-inden-1-ol

A flask containing (R)-(+)-2-methyl-oxazaborolidine complex (33 mg, 0.11 mmol) in dry DCM was stirred under nitrogen, borane-methane sulfide (227 μ L, 2.27 mmol, 10 equiv.) added and the solution cooled to -20 °C. A solution of 6-nitro-1-indanone (300 mg, 1.7 mmol) in dry DCM (2 mL) was added over 10 min. and the reaction stirred at -20 °C for 2 h. The mixture was then poured into a flask with methanol (20 mL) at -20 °C and warmed to room temperature. The solution was then reduced in volume (to approximately 5 mL) by distillation (x 2). The resulting brown residue was rotary evaporated to dryness to give the title compound **143** as a brown gummy solid (290 mg, 94 %).

δ_{H} NMR (500 MHz, CDCl_3): 2.00-2.09 (1H, m, 1H of CH_2), 2.55-2.61 (2H, m, 1H of CH_2 and OH), 2.85-2.92 (1H, m, 1H of CH_2), 3.08-3.14 (1H, m, 1H of CH_2), 5.29 (1H, t, $J = 6.5$, CHOH), 7.35 (1H, d, $J = 8.5$, ArH), 8.10 (1H, dd, $J = 8.0, 2.0$, ArH), 8.21 (1H, d, $J = 1.5$, ArH).

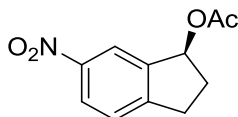
δ_{C} NMR (125 MHz, CDCl_3): 30.0, 36.1, 75.4, 119.7, 123.8, 125.4, 146.7, 147.5, 150.9.

IR ν_{\max} (**KBr**): 3401, 2949, 1611, 1519, 1346, 739 cm^{-1} .

HRMS (ESI): $[\text{M} + \text{H}^+]$ $\text{C}_9\text{H}_{10}\text{NO}_3^+$; calc. 180.0655, $[\text{M} + \text{H}^+]$ not observed.

α_{D} = + 45.5 ($c = 0.0125$, 20 °C, CHCl_3).

Preparation of (*S*)-6-nitro-2,3-dihydro-1*H*-inden-1-yl acetate (**149**)



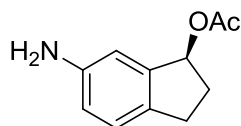
Acetic anhydride (1 mL) was added to a solution of (*S*)-6-nitro-2,3-dihydro-1*H*-inden-1-ol (150 mg, 0.84 mmol) in pyridine (1 mL) at 0 °C and stirred at room temperature for 16 h under nitrogen. The mixture was partitioned with diethyl ether and washed with hydrochloric acid (2M). The organic layer was then dried over magnesium sulfate, filtered and concentrated to give **149** as viscous brown oil (170 mg, 92 %).

δ_{H} **NMR** (400 MHz, CDCl_3): 2.09 (3H, s, CH_3), 2.14-2.22 (1H, m, 1H of CH_2), 2.56-2.65 (1H, m, 1H of CH_2), 2.93-3.00 (1H, m, 1H of CH_2), 3.14-3.22 (1H, m, 1H of CH_2), 6.20 (1H, dd, $J = 7.2, 4.4$, CHOCOCH_3), 7.40 (1H, d, $J = 8.4$, ArH), 8.18 (1H, dd, $J = 8.4, 2.4$, ArH), 8.22 (1H, d, $J = 2.0$, ArH).

δ_{C} **NMR** (100 MHz, CDCl_3): 20.6, 29.8, 32.1, 76.5, 120.4, 123.9, 124.9, 142.4, 146.9, 151.4, 170.3.

HRMS (ESI): $[\text{M} + \text{H}^+]$ $\text{C}_{11}\text{H}_{12}\text{NO}_4^+$; calc. 222.0761, $[\text{M} + \text{H}^+]$ not observed.

α_{D} = - 14.6 ($c = 0.245$, 20 °C, CHCl_3).

Preparation of (S)-6-amino-2,3-dihydro-1H-inden-1-yl acetate (151)

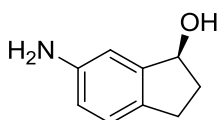
A solution of (S)-6-nitro-2,3-dihydro-1H-inden-1-yl acetate (170 mg, 0.77 mmol) in aqueous methanol (5: 0.5 methanol: water, 5.5 mL) was cooled in an ice-water bath and activated palladium on carbon added (17 mg, 10 % w/w) under a stream of nitrogen. Sodium borohydride (146 mg, 3.9 mmol) was added slowly and the reaction stirred for 5 min. after addition. The mixture was filtered through Kieselguhr, methanol removed by rotary evaporation and the residue partitioned with dichloromethane and water. The organic layer was then dried with magnesium sulfate, filtered and concentrated. The residue was purified using flash chromatography (hexane:ethyl acetate 3:1) to afford the title compound **151** as a yellow oil (58 mg, 39 %).

δ_{H} NMR (400 MHz, CDCl_3): 2.07-2.11 (4H, s, CH_3 and 1H of CH_2), 2.44-2.53 (1H, m, 1H of CH_2), 2.74-2.82 (1H, m, 1H of CH_2), 2.80-2.99 (1H, m, 1H of CH_2), 3.65 (2H, bs, NH_2), 6.14 (1H, dd, $J = 7.2, 4.0$, CHOCOCH_3), 6.66 (1H, dd, $J = 8.0, 2.4$, ArH), 6.77 (1H, d, $J = 2.4$, ArH), 7.06 (1H, d, $J = 8.0$, ArH).

δ_{C} NMR (100 MHz, CDCl_3): 21.4, 29.3, 32.6, 78.5, 111.9, 116.4, 125.3, 134.3, 142.3, 145.4, 171.2.

HRMS (ESI): $[\text{M} + \text{H}^+]$ $\text{C}_9\text{H}_{10}\text{NO}_3^+$; calc. 192.1019, $[\text{M} + \text{H}^+]$ not observed.

$\alpha_{\text{D}} = -57.1$ ($c = 1.1$, 20°C , CHCl_3).

Preparation of (*S*)-6-amino-2,3-dihydro-1*H*-inden-1-ol (153**)**

The title compound **153** was obtained as a by-product in the column chromatography of (*R*)-6-amino-2,3-dihydro-1*H*-inden-1-yl acetate (**151**) as a white solid (50 mg, 0.34 mmol).

δ_{H} NMR (400 MHz, CDCl_3): 1.88-1.96 (1H, m, 1H of CH_2), 2.44-2.52 (1H, m, 1H of CH_2), 2.68-2.76 (1H, m, 1H of CH_2), 2.91-2.98 (1H, m, 1H of CH_2), 3.52 (2H, bs, NH_2), 5.15 (1H, t, $J = 6.0$, CHOH), 6.24 (1H, dd, $J = 8.0, 2.4$, ArH), 6.75 (1H, d, $J = 2.0$, ArH), 7.04 (1H, d, $J = 8.0$, ArH).

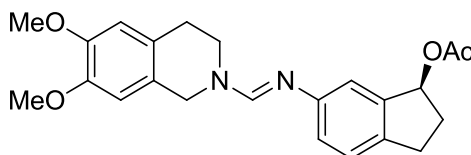
δ_{C} NMR (100 MHz, CDCl_3): 28.4, 36.0, 76.1, 110.2, 115.3, 124.9, 132.7, 144.9, 145.8.

IR ν_{max} (ATR): 3379, 3305, 2958, 2913, 2852, 1610, 1487, 1039, 816 cm^{-1} .

HRMS (ESI): $[\text{M} + \text{H}^+]$ $\text{C}_9\text{H}_{12}\text{NO}^+$; calc. 150.0913, $[\text{M} + \text{H}^+]$ not observed.

Melting point: 128-130 $^{\circ}\text{C}$.

$\alpha_{\text{D}} = +28.8$ ($c = 0.135$, 20 $^{\circ}\text{C}$, CHCl_3).

Preparation of (*S,E*)-6-(((6,7-dimethoxy-3,4-dihydroisoquinolin-2(1*H*)-yl)methylene)amino)-2,3-dihydro-1*H*-inden-1-yl acetate (155**)**

Procedure as for **154** but using 6,7-dimethoxy-3,4-dihydroisoquinoline-2(1*H*)-formamide (67 mg, 0.30 mmol), phosphoryl chloride (55 mg, 0.36 mmol) and (*S*)-6-amino-2,3-dihydro-1*H*-inden-1-yl acetate (58 mg, 0.30 mmol). After the reaction mixture was stirred for 4 h, the solution was partitioned with dichloromethane and

water and washed with sodium hydroxide (1 M). The organic layer was then dried with magnesium sulfate, filtered and concentrated and purification of the residue by flash chromatography (hexane:ethyl acetate 2:1 and 1 % triethylamine) afforded the title compound **155** as a pale yellow oil (40 mg, 33 %).

δ_{H} NMR (500 MHz, CDCl_3): 2.08-2.15 (4H, m, 1H of CH_2 and CH_3), 2.49-2.53 (1H, m, 1H of CH_2), 2.82-2.90 (3H, m, 1H of CH_2 and CH_2), 3.04-3.08 (1H, m, 1H of CH_2), 3.70 (2H, bs, CH_2), 3.87 (3H, s, MeO), 3.88 (3H, s, MeO), 4.70 (2H, bs, CH_2), 6.20 (1H, dd, $J = 7.0, 4.0$, CHOCOCH_3), 6.64 (2H, s, ArH), 7.00 (1H, dd, $J = 8.0, 2.0$, ArH), 7.04 (1H, d, $J = 2.0$ ArH), 7.18 (1H, d, $J = 8.0$, ArH), 7.76 (1H, s, CHN).

δ_{C} NMR (125 MHz, CDCl_3): 21.4, 29.6, 32.7, 56.0, 78.5, 109.2, 111.6, 117.3, 122.8, 125.1, 138.5, 142.0, 147.9, 147.8, 150.8, 152.4, 171.2. Note: 3 x CH_2 not observed by ^{13}C NMR due to fast relaxation.

IR ν_{max} (ATR): 2935, 2838, 1724, 1627, 1231, 719 cm^{-1} .

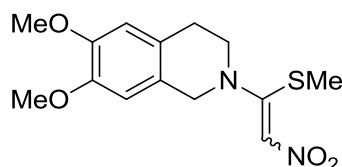
LRMS (ESI): $[\text{M} + \text{H}^+]$ $\text{C}_{23}\text{H}_{27}\text{N}_2\text{O}_4^+$; calc. 395.20, found 395.20.

HRMS (ESI): $[\text{M} + \text{H}^+]$ $\text{C}_{23}\text{H}_{27}\text{N}_2\text{O}_4^+$; calc. 395.1965, found 395.1957.

$\alpha_{\text{D}} = -26.2$ ($c = 1.0$, 20°C , CHCl_3).

Purity: Purity could not be determined by HPLC. See appendix for ^1H NMR.

Preparation of 6,7-dimethoxy-2-[1-(methylsulfanyl)-2-nitroethenyl]-1,2,3,4-tetrahydroisoquinoline (**164**)



A solution of 6,7-dimethoxy-1,2,3,4-tetrahydroisoquinoline hydrochloride (200 mg, 0.87 mmol), 1,1-bis(methylsulfanyl)-2-nitroalkene (145 mg, 0.87 mmol) and triethylamine (180 mg, 0.25 mL, 1.78 mmol) in dichloromethane (10 mL) was

heated under reflux for 16 h. The solvent was removed under reduced pressure and purification of the resulting residue by flash chromatography (hexane: ethyl acetate, 2:1) afforded the title compound **164** as a viscous orange oil (165 mg, 61 %).

δ_{H} NMR (500 MHz, CDCl_3): 2.42 (3H, s, SMe), 2.87 (2H, t, $J = 6.0$, CH_2), 3.76 (3H, s, MeO), 3.78 (3H, s, MeO), 3.84 (2H, t, $J = 6.0$, CH_2), 4.51 (2H, s, CH_2), 6.49 (1H, s, CHNO_2), 6.58 (1H, s, ArH), 6.66 (1H, s, ArH).

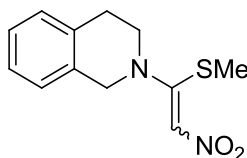
δ_{C} NMR (125 MHz, CDCl_3): 17.8 (SMe), 28.9, 50.0, 55.2, 56.2, 108.9, 111.4, 124.2, 125.3, 148.3, 148.4, 166.6.

IR ν_{max} (NaCl): 3122, 3000, 2933, 2837, 1611, 1516, 1380, 1111 cm^{-1} .

LRMS (ESI): $[\text{M} + \text{H}^+]$ $\text{C}_{14}\text{H}_{19}\text{N}_2\text{O}_4\text{S}^+$; calc. 311.11, found 311.13.

HRMS (ESI): $[\text{M} + \text{H}^+]$ $\text{C}_{14}\text{H}_{19}\text{N}_2\text{O}_4\text{S}^+$; calc. 311.1060, found 311.1058.

Preparation of 2-[1-(methylsulfanyl)-2-nitroethenyl]-1,2,3,4-tetrahydroisoquinoline (**165**)



A solution of 1,2,3,4-tetrahydroisoquinoline (1 g, 7.52 mmol) and 1,1-bis(methylsulfanyl)-2-nitroalkene (1.24 g, 7.52 mmol) in dichloromethane (10 mL) was heated under reflux for 16 h. The solvent was removed under reduced pressure and purification of the resulting residue by flash chromatography (hexane: ethyl acetate, 3:1) afforded the title compound **165** as a yellow-green oil (920 mg, 49 %).

δ_{H} NMR (500 MHz, CDCl_3): 2.47 (3H, s, SMe), 2.99 (2H, t, $J = 6.0$, CH_2), 3.89 (2H, t, $J = 6.0$, CH_2), 4.62 (2H, s, CH_2), 6.72 (1H, s, CHNO_2), 7.03-7.05 (1H, m, ArH), 7.14-7.16 (1H, m, ArH), 7.17-7.20 (2H, m, ArH).

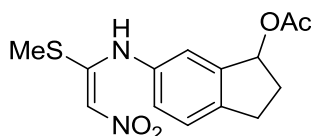
δ_{C} NMR (125 MHz, CDCl_3): 17.7, 29.2, 49.8, 55.1, 111.3, 126.1, 126.9, 127.3, 128.5, 132.3, 133.5, 166.5.

IR ν_{\max} (NaCl): 3118, 3023, 2927, 2849, 1666, 1538, 1392 cm^{-1} .

LRMS (ESI): $[\text{M} + \text{H}^+]$ $\text{C}_{12}\text{H}_{15}\text{N}_2\text{O}_2\text{S}^+$; calc. 251.09, found 251.07.

HRMS (ESI): $[\text{M} + \text{H}^+]$ $\text{C}_{12}\text{H}_{15}\text{N}_2\text{O}_2\text{S}^+$; calc. 251.0849, found 251.0846.

Preparation of (*E*)-6-[[1-(methylsulfanyl)-2-nitroethenyl]amino]-2,3-dihydro-1*H*-inden-1-yl acetate (171**)**



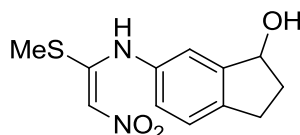
A solution of 6-amino-2,3-dihydro-1*H*-inden-1-yl acetate (150 mg, 0.79 mmol) and 1,1-bis(methylsulfanyl)-2-nitroalkene (130 mg, 0.79 mmol) was heated under reflux in dichloromethane (2 mL) for 16 h. Removal of solvent under reduced pressure then flash chromatography of the resulting residue (hexane:ethyl acetate 4:1 then 3:1) afforded the title compound **171** as an orange oil (160 mg, 66 %). Slow evaporation of the oil in dichloromethane afforded orange crystals, a sample from which was submitted for X-ray crystallography.

δ_{H} NMR (400 MHz, CDCl_3): 2.08 (3H, s, CH_3), 2.10-2.18 (1H, m, 1H of CH_2), 2.37 (3H, s, SMe), 2.51-2.60 (1H, m, 1H of CH_2) 2.86-2.94 (1H, m, 1H of CH_2), 3.08-3.16 (1H, m, 1H of CH_2), 6.16-6.19 (1H, m, CHOCOCH_3), 6.68 (1H, s, CHNO_2), 7.21 (1H, dd, $J = 8.0, 2.0$, ArH), 7.30-7.37 (2H, m, ArH), 11.77 (1H, bs, NH).

δ_{C} NMR (100 MHz, CDCl_3): 14.7, 21.2, 30.0, 32.5, 75.4, 107.7, 123.3, 125.6, 126.8, 134.8, 142.8, 144.6, 163.8, 171.0.

IR ν_{\max} (NaCl): 3365, 3154, 2925, 2851, 1731, 1552, 1347, 1237, 1040 cm^{-1} .

LRMS (ESI): $[\text{M} + \text{H}^+]$ $\text{C}_{14}\text{H}_{17}\text{N}_2\text{O}_4\text{S}^+$; calc. 309.09, found 309.13.

Preparation of (*E*)-6-[[1-(methylsulfanyl)-2-nitroethenyl]amino]-1-indanol (173)

A solution of 6-amino-1-indanol (100 mg, 0.67 mmol) and 1,1-bis(methylsulfanyl)-2-nitroalkene (111 mg, 0.67 mmol) was heated under reflux in dichloromethane (4 mL) for 16 h. The solvent was evaporated under reduced pressure and methanol (4 mL) added. The resulting precipitate was filtered off and the mother liquor concentrated to give the title compound **173** as a pale yellow solid (130 mg, 73 %).

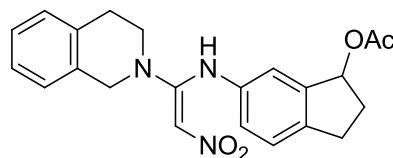
δ_{H} NMR (400 MHz, CDCl_3): 1.91-2.00 (1H, m, 1H of CH_2), 2.34 (3H, s, SMe), 2.46-2.54 (1H, m, 1H of CH_2) 2.75-2.83 (1H, m, 1H of CH_2), 2.98-3.04 (1H, m, 1H of CH_2), 5.27, (1H, t, $J = 6.4$, CHOH), 6.67 (1H, s, CHNO_2), 7.12 (1H, dd $J = 8.0$, 1.6, ArH), 7.24-7.29 (2H, m, ArH), 11.78 (1H, bs, NH). Note: OH peak not observed by ^1H NMR.

δ_{C} NMR (100 MHz, CDCl_3): 14.8, 29.7, 36.1, 75.8, 107.6, 122.1, 125.7, 125.9, 134.8, 143.7, 147.1, 164.5.

IR ν_{max} (KBr): 3260, 3147, 2997, 2924, 1554, 1341, 1204, 1058, 932 cm^{-1} .

HRMS (ESI): $[\text{M} + \text{H}^+]$ $\text{C}_{12}\text{H}_{15}\text{N}_2\text{O}_3\text{S}^+$; calc. 267.0798, found 267.0803.

Melting point: 138-139 $^{\circ}\text{C}$.

Preparation of (*E*)-6-[[3,4-dihydro-2(1*H*)-isoquinolinyl(nitro)methyl]amino]-2,3-dihydro-1*H*-inden-1-yl acetate (166)

A solution of (*E*)-6-[[1-(methylsulfanyl)-2-nitroethenyl]amino]-2,3-dihydro-1*H*-inden-1-yl acetate (55 mg, 0.18mmol) and 1,2,3,4-tetrahydroisoquinoline (24 mg,

0.18 mmol) in propan-2-ol (3 mL) was heated under reflux for 16 h. The solvent was removed under reduced pressure and the residue purified by flash chromatography (hexane:ethyl acetate 3:1), followed by HPLC purification, to afford the title compound **166** as an orange oil (10.3 mg, 14 %).

δ_{H} NMR (500 MHz, CDCl_3): 1.99 (3H, s, CH_3), 2.06-2.15 (1H, m, 1H of CH_2), 2.50-2.56 (1H, m, 1H of CH_2), 2.81-2.90 (3H, m, 1H of CH_2 and CH_2), 3.06-3.12 (1H, m, 1H of CH_2), 3.45-3.53 (2H, m, CH_2), 4.30 (2H, s, CH_2), 6.10-6.12 (1H, m, CHOCOCH_3), 6.80 (1H, s, CHNO_2), 6.99-7.00 (1H, m, ArH), 7.09-7.13 (2H, m, ArH), 7.19-7.25 (4H, m, ArH), 11.19 (1H, bs, NH).

δ_{C} NMR (125 MHz, CDCl_3): 21.2, 27.9, 29.8, 32.5, 46.5, 50.0, 75.4, 107.7, 119.7, 123.4, 125.9, 126.2, 126.8, 127.4, 128.5, 131.6, 133.7, 137.7, 141.9, 142.9, 157.6, 171.0.

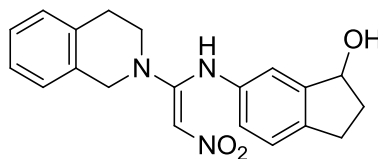
IR ν_{max} (ATR): 3040, 2935, 2861, 1715, 1559, 1428, 1182, 1131 cm^{-1} .

LRMS (ESI): $[\text{M} + \text{H}^+]$ $\text{C}_{22}\text{H}_{24}\text{N}_3\text{O}_4^+$; calc. 394.18, found 394.33.

HRMS (ESI): $[\text{M} + \text{H}^+]$ $\text{C}_{22}\text{H}_{24}\text{N}_3\text{O}_4^+$; calc. 394.1761, found 394.1759.

Purity: 95 %, HPLC t_{R} 7.85 min.

Preparation of (*E*)-6-[[1-(3,4-dihydro-2(1*H*)-isoquinolinyl)(nitro)methyl]amino]-2,3-dihydro-1*H*-indanol (**175**)



A solution of (*E*)-6-[[1-(methylsulfanyl)-2-nitroethenyl]amino]-2,3-dihydro-1*H*-indanol (98 mg, 0.37 mmol) and 1,2,3,4-tetrahydroisoquinoline (49 mg, 0.37 mmol) in propan-2-ol (3 mL) was heated under reflux for 16 h. The solvent was removed under reduced pressure and the residue purified by flash chromatography

(hexane:ethyl acetate 1:1), followed by HPLC purification, to afford the title compound **175** as an orange oil (24.7 mg, 19 %).

δ_{H} NMR (500 MHz, CDCl_3 , 50 °C): 1.92 (1H, bs, 1H of CH_2), 2.49 (1H, bs, 1H of CH_2), 2.79 (1H, m, 1H of CH_2), 2.97-3.06 (3H, m, 1H of CH_2 and CH_2), 3.97 (2H, bs, CH_2), 4.94 (1H, bs, 1H of CH_2), 5.19 (1H, bs, 1H of CH_2), 5.65 (1H, bs, CHOH), 7.07 (1H, s, CHNO_2), 7.15-7.29 (7H, m, ArH), 7.65 (1H, bs, NH). Note: OH peak not observed by ^1H NMR.

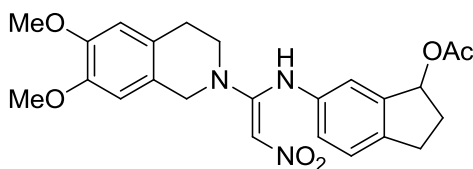
IR ν_{max} (ATR): 3245, 2930, 2864, 1536, 1314, 1193, 1135 cm^{-1} .

LRMS (ESI): $[\text{M} + \text{H}^+]$ $\text{C}_{20}\text{H}_{24}\text{N}_3\text{O}_3^+$; calc. 352.17, found 352.27.

HRMS (ESI): $[\text{M} + \text{H}^+]$ $\text{C}_{20}\text{H}_{24}\text{N}_3\text{O}_3^+$; calc. 352.1656, found 352.1653.

Purity: > 95 %, HPLC t_{R} 13.68 min.

Preparation of (*E*)-6-[[6,7-dimethoxy-3,4-dihydro-2(1*H*)-isoquinolinyl](nitro)methyl]amino}-2,3-dihydro-1*H*-inden-1-yl acetate (176**)**



A solution of 6-[[*E*]-1-(methylsulfanyl)-2-nitroethenyl]amino}-2,3-dihydro-1*H*-inden-1-yl acetate (50 mg, 0.16 mmol) and 6,7-dimethoxy 1,2,3,4-tetrahydroisoquinoline (32 mg, 0.16 mmol) in propan-2-ol (2 mL) was heated under reflux for 16 h. The solvent was removed under reduced pressure and the residue purified by flash chromatography (hexane:ethyl acetate 1:1) to afford the title compound **176** as an orange oil (25 mg, 38 %).

δ_{H} NMR (400 MHz, CDCl_3): 2.02 (3H, s, CH_3), 2.09-2.17 (1H, m, 1H of CH_2), 2.50-2.58 (1H, m, 1H of CH_2), 2.72-2.76n (2H, m, CH_2) 2.84-2.91 (1H, m, 1H of CH_2), 3.06-3.13 (1H, m, 1H of CH_2), 3.44-3.54 (2H, m, CH_2), 3.82 (3H, s, MeO), 3.84 (3H, s, MeO), 4.22 (2H, s, CH_2), 6.13 (1H, dd, $J = 7.2, 4.0$, CHOCOCH_3), 6.44 (1H, s,

ArH), 6.59 (1H, s, ArH), 6.78 (1H, s, CHNO₂), 7.11 (1H, dd, $J = 8.0, 2.0$, ArH), 7.22 (1H, d, $J = 1.6$, ArH), 7.27 (1H, d, $J = 8.0$, ArH), 11.17 (1H, bs, NH).

δ_{C} NMR (100 MHz, CDCl₃): 21.2, 27.3, 29.8, 32.5, 46.5, 49.8, 56.0, 77.9, 103.3, 108.9, 111.2, 119.6, 123.3, 123.4, 125.4, 125.9, 137.7, 141.8, 142.9, 148.0, 148.3, 157.5, 171.0.

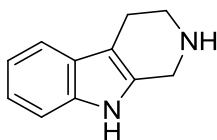
IR ν_{max} (ATR): 2963, 2840, 1737, 1517, 1368, 1122 cm⁻¹.

LRMS (ESI): [M + H⁺] C₂₄H₂₈N₃O₆⁺; calc. 454.20, found 454.19.

HRMS (ESI): [M + H⁺] C₂₄H₂₈N₃O₆⁺; calc. 454.1973, found 454.1970.

Purity: > 99 %, HPLC t_{R} 16.85 min.

Preparation of 2,3,4,9-tetrahydro-1H- β -carboline²²⁷ (**180**)



A solution of tryptamine (770 mg, 4.8 mmol) and paraformaldehyde (144 mg, 4.8 mmol) in water (12 mL) and sodium acetate buffer (pH 5.8, 8 mL) was heated under reflux for 4 h. The solid was filtered off, methanol added and mixture basified using sodium hydroxide (2M, pH 14). The resulting suspension was filtered and the title compound **180** precipitated out of the filtrate (636 mg, 77 %).

δ_{H} NMR (400 MHz, DMSO-d₆): 2.76-2.79 (2H, tt, $J = 5.6, 1.6$, CH₂), 3.20 (2H, t, $J = 5.6$, CH₂), 4.04 (2H, d, $J = 2.8$, CH₂), 7.09-7.18 (2H, m, ArH), 7.31 (1H, t, $J = 8.0$, ArH), 7.49 (1H, d, $J = 7.2$, ArH), 7.78 (1H, bs, NH). Note: One NH peak not observed by ¹H NMR.

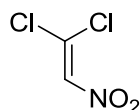
δ_{C} NMR (100 MHz, DMSO-d₆): 22.0, 42.7, 43.4, 108.3, 110.2, 117.4, 118.9, 121.0, 127.1, 132.3, 135.2.

IR ν_{max} (ATR): 3297, 3060, 2878, 1446, 1306, 870 cm⁻¹.

LRMS (ESI): $[M + H^+]$ $C_{11}H_{13}N_2^+$; calc. 173.11, found 173.00.

Melting point: 203-205 °C. Lit. 200-202 °C.²²⁸

Preparation of 1,1-dichloro-2-nitroethane²²⁹ (186)



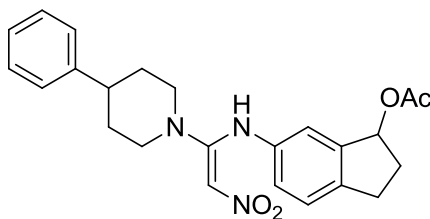
Concentrated hydrochloric acid (24.16g, 35 %) was cooled to 15 °C and concentrated nitric acid (14.3 mL, 69 %) added dropwise over 30 min. After the addition was complete, the reaction was stirred at 15 °C for 2 h and nitrogen blown over the reaction for 20 min to rid the solution of NO_x gases. 1,1-dichloroethylene (14.0 mL, 0.177 mmol) was then added to the reaction dropwise over 30 min and stirred for 5 h. The organic layer was separated, warmed to 80 °C and stirred for 2.5 h. Water (84 mL) was then added and the reaction heated to 83 °C for 6 h. The organic layer was then separated and concentrated to give the title compound **186** as a yellow-green oil (7.024 g, 28 %).

δ_H NMR (400 MHz, $CDCl_3$): 7.63 (1H, s, $CHNO_2$).

δ_C NMR (100 MHz, $CDCl_3$): 135.9, 136.0.

IR ν_{max} (NaCl): 1603, 1534, 1344 cm^{-1} .

HRMS (ESI): $[M + H^+]$ $C_2HCl_2NO_2^+$; calc. 140.9384, $[M + H^+]$ not observed.

Preparation of (*E*)-6-((2-nitro-1-(4-phenylpiperidin-1-yl)vinyl)amino)-2,3-dihydro-1*H*-inden-1-yl acetate (187**)**

1,1-Dichloro-2-nitroalkene (45 mg, 0.32 mmol, 1.1 equiv.) and 6-amino-2,3-dihydro-1*H*-inden-1-yl acetate (56 mg, 0.29 mmol) were added to a flask containing a mixture of dichloromethane:sat. aqueous potassium carbonate (3:1 mL) at 4 °C and stirred for 90 min. 4-Phenylpiperidine (47 mg, 0.29 mmol) was then added and the reaction mixture stirred for a further 4 h. The solution was partitioned with dichloromethane and water, the organic layer dried with magnesium sulfate, then filtered and concentrated under reduced pressure. The residue was then purified by flash chromatography (hexane:ethyl acetate 3:1 then 4:1) to give the title compound **187** as a brown gum (17 mg, 14 %).

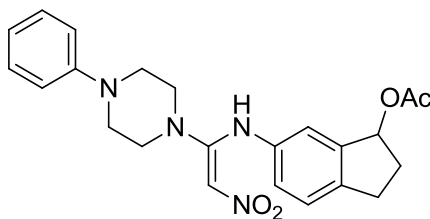
δ_{H} NMR (500 MHz, CDCl_3): 1.64-1.76 (2H, m, CH_2), 1.82-1.85 (2H, m, CH_2), 2.03 (3H, s, CH_3), 2.11-2.18 (1H, m, 1H of CH_2), 2.50-2.57 (1H, m, 1H of CH_2), 2.66-2.73 (1H, m, CH), 2.84-2.98 (3H, m, 1H of CH_2 and CH_2), 3.06-3.12 (1H, m, 1H of CH_2), 3.69-3.74 (2H, m, CH_2), 6.17 (1H, dd, $J = 7.0, 3.0$ CHOCO CH_3), 6.71 (1H, s, CHNO $_2$), 7.12 (1H, dd, $J = 8.0, 2.0$, ArH), 7.18-7.34 (7H, m, ArH), 11.18 (1H, s, NH).

δ_{C} NMR (125 MHz, CDCl_3): 21.2, 29.8, 32.3, 32.4, 32.5, 42.0, 49.2, 49.3, 78.0, 103.7, 119.0, 122.8, 125.8, 126.6, 126.6, 128.7, 137.6, 141.7, 142.9, 144.3, 157.6, 171.1.

IR ν_{max} (ATR): 3140, 2919, 2829, 1729, 1573, 1362, 1220, 1185 cm^{-1} .

HRMS (ESI): $[\text{M} + \text{H}^+]$ $\text{C}_{24}\text{H}_{28}\text{N}_3\text{O}_4^+$; calc. 422.2074, found 422.2073.

Purity: 96 %, HPLC t_{R} 25.78 min.

Preparation of (*E*)-6-((2-nitro-1-(4-phenylpiperazin-1-yl)vinyl)amino)-2,3-dihydro-1*H*-inden-1-yl acetate (188**)**

Compound **188** was prepared similarly to **187** using 1,1-dichloro-2-nitroalkene (45 mg, 0.32 mmol, 1.1 equiv.) and 6-amino-2,3-dihydro-1*H*-inden-1-yl acetate (56 mg, 0.29 mmol) and 4-phenylpiperazine (47 mg, 0.29 mmol). The solution was partitioned with dichloromethane and water, the organic layer dried with magnesium sulfate, then filtered and concentrated under reduced pressure. The residue was then purified by flash chromatography (hexane: ethyl acetate, 2:1 then 3:1) to give the title compound **188** as a light brown gum (13 mg, 9 %).

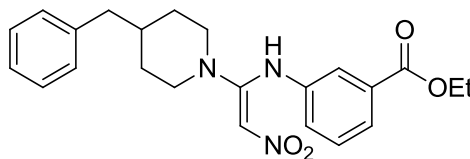
δ_{H} NMR (400 MHz, CDCl_3): 1.96 (3H, s, CH_3), 2.10-2.19 (1H, m, 1H of CH_2), 2.51-2.59 (1H, m, 1H of CH_2), 2.85-2.92 (1H, m, 1H of CH_2), 3.07-3.17 (5H, m, 1H of CH_2 and 2 x CH_2), 3.37 (4H, t, $J = 5.2$, 2 x CH_2), 6.16 (1H, dd, $J = 6.8, 4.0$, CHOCOCH_3), 6.70 (1H, s, CHNO_2), 6.88-6.95 (3H, m, ArH), 7.15 (1H, dd, $J = 8.0, 2.0$, ArH), 7.27-7.31 (3H, m, ArH), 7.35 (1H, s, $J = 2.0$, ArH), 11.12 (1H, s, NH).

δ_{C} NMR (100 MHz, CDCl_3): 21.1, 29.8, 32.4, 42.1, 48.4, 77.9, 103.6, 116.5, 119.4, 120.9, 123.1, 125.9, 129.3, 137.3, 142.1, 143.0, 150.4, 157.5, 171.0.

IR ν_{max} (ATR): 3120, 2939, 2829, 1735, 1559, 1369, 1218, 1183, 1015 cm^{-1} .

HRMS (ESI): $[\text{M} + \text{H}^+]$ $\text{C}_{23}\text{H}_{27}\text{N}_4\text{O}_4^+$; calc. 423.2027, found 423.2023.

Purity: 98 %, HPLC t_{R} 16.99 min.

Preparation of (*E*)-ethyl 3-((1-(4-benzylpiperidin-1-yl)-2-nitrovinyl)amino)benzoate (189**)**

Compound **189** was prepared similarly to **187** using 1,1-dichloro-2-nitroalkene (186 mg, 1.32 mmol, 1.1 equiv.) and ethyl 3-aminobenzoate (200 mg, 1.2 mmol) and 4-benzylpiperidine (210 mg, 1.2 mmol). The solution was partitioned with dichloromethane and water, the organic layer dried with magnesium sulfate, then filtered and concentrated under reduced pressure. The residue was then purified by flash chromatography (hexane: ethyl acetate, 5:1 then 7:1) to give the title compound **189** as a brown gum (100 mg, 21 %).

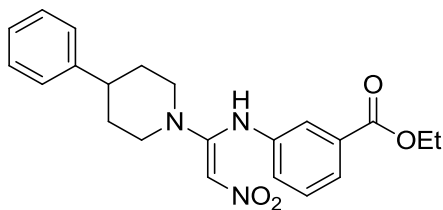
δ_{H} NMR (400 MHz, CDCl_3): 1.20-1.31 (2H, m, CH_2), 1.40 (3H, t, $J = 7.2$, OCH_2CH_3), 1.65 (2H, d, $J = 12.0$, CH_2), 1.72-1.77 (1H, m, CH), 2.55 (2H, d, $J = 7.2$, CH_2), 2.81 (2H, dt, $J = 12.8, 2.0$, CH_2), 3.58 (2H, d, $J = 13.2$, CH_2), 4.43 (2H, q, $J = 7.2$, OCH_2CH_3), 6.68 (1H, s, CHNO_2), 7.11 (2H, dd, $J = 6.8, 1.6$, ArH), 7.20-7.23 (1H, m, ArH), 2.73-2.34 (4H, m, ArH), 7.46 (1H, t, $J = 8.0$, ArH), 7.86 (1H, d, $J = 8.4$, ArH), 11.15 (1H, s, NH).

δ_{C} NMR (100 MHz, CDCl_3): 13.9, 30.6, 37.2, 42.1, 48.5, 60.9, 103.5, 121.8, 125.3, 125.8, 125.8, 127.9, 128.5, 129.2, 131.5, 138.8, 138.8, 156.8, 165.2.

IR ν_{max} (ATR): 3008, 2907, 2848, 1720, 1559, 1282, 1246, 1054 cm^{-1} .

HRMS (ESI): $[\text{M} + \text{H}^+]$ $\text{C}_{23}\text{H}_{28}\text{N}_3\text{O}_4^+$; calc. 410.2074 found 410.2067.

Purity: 95 %, HPLC t_{R} 24.07 min.

Preparation of (*E*)-ethyl 3-((2-nitro-1-(4-phenylpiperidin-1-yl)vinyl)amino)benzoate (190**)**

Compound **190** was prepared similarly to **187** using 1,1-dichloro-2-nitroalkene (93 mg, 0.67 mmol, 1.1 equiv.) and ethyl 3-aminobenzoate (100 mg, 0.6 mmol) and 4-phenylpiperidine (97 mg, 0.6 mmol). The solution was partitioned with dichloromethane and water, the organic layer dried with magnesium sulfate, then filtered and concentrated under reduced pressure. The residue was then purified by flash chromatography (hexane: ethyl acetate, 5:1 then 4:1) to give the title compound **190** as a yellow gum (55 mg, 23 %).

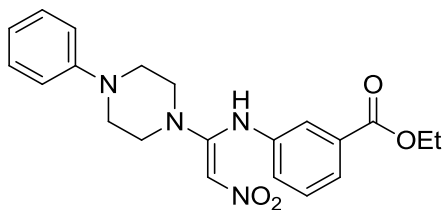
δ_{H} NMR (500 MHz, CDCl_3): 1.41 (3H, t, $J = 7.0$, OCH_2CH_3), 1.70-1.74 (2H, m, CH_2), 1.83 (2H, d, $J = 11.0$, CH_2), 2.72 (1H, m, CH), 2.95-3.01 (2H, m, CH_2), 3.71 (2H, dd, $J = 11.0, 2.0$, CH_2), 4.41 (2H, q, $J = 7.0$, OCH_2CH_3), 6.73 (1H, s, CHNO_2), 7.17-7.49 (6H, m, ArH), 7.48 (1H, t, $J = 8.0$, ArH), 7.86 (1H, dt, $J = 8.0, 1.0$, ArH), 7.96 (1H, t, $J = 2.0$, ArH), 11.13 (1H, bs, NH).

δ_{C} NMR (125 MHz, CDCl_3): 14.3, 32.2, 42.1, 49.3, 61.5, 104.2, 122.4, 125.9, 126.4, 126.6, 126.8, 126.9, 128.6, 128.7, 129.8, 132.0, 139.3, 157.4.

IR ν_{max} (ATR): 3005, 2982, 2926, 2857, 1712, 1569, 1360, 1285, 1207, 748 cm^{-1} .

HRMS (ESI): $[\text{M} + \text{H}^+]$ $\text{C}_{22}\text{H}_{26}\text{N}_3\text{O}_4^+$; calc. 396.1918, found 396.1924.

Purity: 97 %, HPLC t_{R} 21.42 min

Preparation of (*E*)-ethyl 3-((2-nitro-1-(4-phenylpiperazin-1-yl)vinyl)amino)benzoate (191**)**

Compound **191** was prepared similarly to **187** using 1,1-dichloro-2-nitroalkene (186 mg, 1.32 mmol, 1.1 equiv.) and ethyl 3-aminobenzoate (200 mg, 1.2 mmol) and 4-phenylpiperazine (194 mg, 1.2 mmol). The solution was partitioned with dichloromethane and water, the organic layer dried with magnesium sulfate, then filtered and concentrated under reduced pressure. The residue was then purified by flash chromatography (hexane: ethyl acetate, 5:1 then 4:1) to give the title compound **191** as a brown gum (51 mg, 11 %).

δ_{H} NMR (500 MHz, CDCl_3): 1.32 (3H, t, $J = 7.0$, OCH_2CH_3), 3.11 (4H, m, 2 x CH_2), 3.33 (4H, m, 2 x CH_2), 4.33 (2H, q, $J = 7.0$, OCH_2CH_3), 6.63 (1H, s, CHNO_2), 6.79-6.95 (3H, m, ArH), 7.19-7.40 (4H, m, ArH), 7.8 (1H, d, $J = 7.5$, ArH), 7.90 (1H, d, $J = 1.5$, ArH), 11.00 (1H, bs, NH).

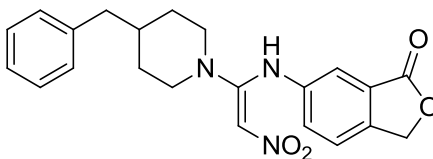
δ_{C} NMR (125 MHz, CDCl_3): 14.1, 48.3, 48.5, 61.5, 104.1, 116.6, 121.0, 122.6, 126.0, 126.6, 129.3, 129.9, 132.1, 139.0, 150.3, 157.4, 157.4.

IR ν_{max} (ATR): 3012, 2976, 2930, 2855, 1712, 1574, 1373, 1280, 1006, 748 cm^{-1} .

HRMS (ESI): $[\text{M} + \text{H}^+]$ $\text{C}_{21}\text{H}_{25}\text{N}_4\text{O}_4^+$; calc. 397.1870, found 397.1865.

Purity: > 99 %, HPLC t_{R} 19.32 min.

Preparation of (*E*)-6-((1-(4-benzylpiperidin-1-yl)-2-nitrovinyl)amino)isobenzofuran-1(3*H*)-one (192**)**



Compound **192** was prepared similarly to **187** using 1,1-dichloro-2-nitroalkene (78 mg, 0.6 mmol, 1.1 equiv.) and 6-amino phthalide (75 mg, 0.5 mmol) and 4-benzylpiperidine (86 mg, 0.5 mmol). The solution was partitioned with dichloromethane and water, the organic layer dried with magnesium sulfate, then filtered and concentrated under reduced pressure. The residue was then purified by flash chromatography (hexane: ethyl acetate, 2.5:1 then 4:1) to afford the title compound **192** as a light brown gum (65 mg, 27 %).

δ_{H} NMR (500 MHz, CDCl_3): 1.26-1.29 (2H, m, CH_2), 1.65 (2H, d, $J = 13.5$, CH_2), 1.72-1.76 (1H, m, CH), 2.55 (2H, d, $J = 7.5$, CH_2), 2.81-2.88 (2H, m, CH_2), 3.54 (2H, d, $J = 13.5$, CH_2), 5.32 (2H, s, CH_2), 6.67 (1H, s, CHNO_2), 7.09-7.30 (5H, ArH), 7.44-7.51 (2H, m, ArH), 7.65 (1H, d, $J = 2.0$, ArH), 11.13 (1H, s, NH).

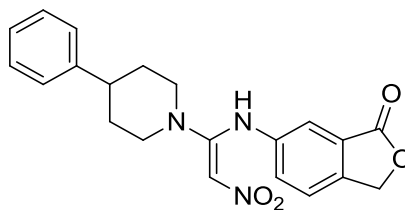
δ_{C} NMR (100 MHz, CDCl_3): 31.2, 37.7, 42.5, 49.1, 69.6, 104.3, 117.1, 123.6, 126.3, 127.6, 128.4, 128.4, 129.0, 139.3, 140.5, 142.8, 156.9, 170.2.

IR ν_{max} (ATR): 3137, 2919, 2852, 1755, 1578, 1312, 1442, 1207, 1000, 748 cm^{-1} .

HRMS (ESI): $[\text{M} + \text{H}^+]$ $\text{C}_{22}\text{H}_{24}\text{N}_3\text{O}_4^+$; calc. 394.1761, found 394.1756.

Purity: 96 %, HPLC t_{R} 15.42 min.

Preparation of (*E*)-6-((2-nitro-1-(4-phenylpiperidin-1-yl)vinyl)amino)isobenzofuran-1(3*H*)-one (193)



Compound **193** was prepared similarly to **187** using 1,1-dichloro-2-nitroalkene (78 mg, 0.6 mmol, 1.1 equiv.) and 6-aminophthalide (75 mg, 0.5 mmol) and 4-phenylpiperidine (81 mg, 0.5 mmol). The solution was partitioned with dichloromethane and water, the organic layer dried with magnesium sulfate, then filtered and concentrated under reduced pressure. The residue was then purified by flash chromatography (hexane: ethyl acetate, 2.5:1 then 4:1) to afford the title compound **193** as a yellow gum (15 mg, 8 %).

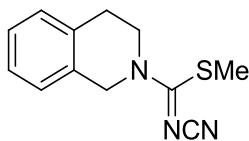
δ_{H} NMR (500 MHz, CDCl_3): 1.87 (2H, d, $J = 12.5$, CH_2), 1.98 (1H, d, $J = 12.5$, CH), 2.71-2.80 (2H, m, CH_2 and CH), 3.00-3.06 (2H, m, CH_2), 3.69 (2H, d, $J = 13.5$, CH_2), 5.33 (2H, s, CH_2), 6.74 (1H, s, CHNO_2), 7.15-7.41 (5H, ArH), 7.50-7.54 (2H, m, ArH), 7.50 (1H, d, $J = 1.5$, ArH), 11.14 (1H, s, NH).

δ_{C} NMR (125 MHz, CDCl_3): 32.4, 42.1, 49.5, 69.6, 104.4, 117.2, 123.6, 126.3, 127.64, 128.4, 128.4, 129.0, 139.3, 140.5, 142.8, 156.9, 170.2.

IR ν_{max} (ATR): 3001, 2926, 2855, 1755, 1660, 1574, 1302, 1215, 998, 745 cm^{-1} .

HRMS (ESI): $[\text{M} + \text{H}^+]$ $\text{C}_{21}\text{H}_{22}\text{N}_3\text{O}_4^+$; calc. 380.1605, found 380.1599.

Purity: 83 %, HPLC t_{R} 12.63 min.

Preparation of methyl *N*-cyano-3,4-dihydro-2(1*H*)-isoquinolinecarbimidothioate (198)

1,2,3,4-Tetrahydroisoquinoline (500 mg, 3.76 mmol) was added to dimethyl cyanodithioimidocarbonate (550 mg, 3.76 mmol) in dichloromethane (10 mL) and heated under reflux for 16 h. The solvent was removed under reduced pressure and the resulting residue purified by flash chromatography (hexane:ethyl acetate 2:1) to afford **198** as a yellow oil (682 mg, 79 %).

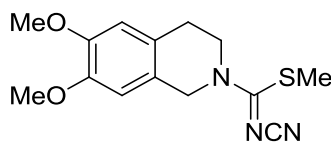
δ_{H} NMR (500 MHz, CDCl_3): 2.71 (3H, s, SMe), 2.87 (2H, t, $J = 6.0$, CH_2), 3.91 (2H, t, $J = 6.0$, CH_2), 4.81 (2H, s, CH_2), 7.03-7.05 (1H, m, ArH), 7.09-7.12 (1H, m, ArH), 7.13-7.15 (2H, m, ArH).

δ_{C} NMR (125 MHz, CDCl_3): 16.1, 28.6, 46.5, 49.9, 115.1, 126.1, 126.7, 127.2, 128.2, 131.6, 133.8, 168.8.

IR ν_{max} (NaCl): 3468, 3025, 2931, 2178, 1689, 1542, 1225, 752 cm^{-1} .

LRMS (ESI): $[\text{M} + \text{H}^+]$ $\text{C}_{12}\text{H}_{14}\text{N}_3\text{S}^+$; calc. 232.09, found 232.20.

HRMS (ESI): $[\text{M} + \text{H}^+]$ $\text{C}_{12}\text{H}_{14}\text{N}_3\text{S}^+$; calc. 232.0903, found 232.0910.

Preparation of methyl *N*-cyano-6,7-dimethoxy-3,4-dihydro-2(1*H*)-isoquinolinecarbimidothioate (199)

A solution of 6,7-dimethoxy-1,2,3,4-tetrahydroisoquinoline hydrochloride (200 mg, 0.87 mmol), dimethyl cyanodithioimidocarbonate (127 mg, 0.87 mmol) and triethylamine (180 mg, 0.25 mL, 1.78 mmol) in dichloromethane (10 mL) was heated

under reflux for 16 h. Cooling to room temperature precipitated the title compound **199** out of solution as a white solid (125 mg, 49 %).

δ_{H} NMR (500 MHz, CDCl_3): 2.69 (3H, s, SMe), 2.78 (2H, t, $J = 6.0$, CH_2), 3.75 (3H, s, MeO), 3.76 (3H, s, MeO), 3.90 (2H, t, $J = 6.0$, CH_2), 4.74 (2H, s, CH_2), 6.51 (1H, s, ArH), 6.56 (1H, s, ArH).

δ_{C} NMR (125 MHz, CDCl_3): 16.2, 28.4, 46.7, 49.9, 56.0, 109.0, 111.2, 115.2, 123.5, 125.8, 148.2, 148.3, 169.0.

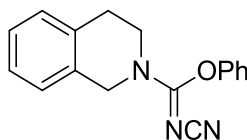
IR ν_{max} (NaCl): 3424, 2992, 2935, 2828, 2179, 1560, 1221, 750 cm^{-1} .

LRMS (ESI): $[\text{M} + \text{H}^+]$ $\text{C}_{14}\text{H}_{18}\text{N}_3\text{O}_2\text{S}^+$; calc. 292.11, found 292.23.

HRMS (ESI): $[\text{M} + \text{H}^+]$ $\text{C}_{14}\text{H}_{18}\text{N}_3\text{O}_2\text{S}^+$; calc. 292.1114, found 292.1130.

Melting point: 103-106 $^{\circ}\text{C}$.

Preparation of (Z)-phenyl N-cyano-3,4-dihydro-2(1H)-isoquinolinecarboximidoate (**200**)



A solution of 1,2,3,4-tetrahydroisoquinoline (200 mg, 1.5 mmol) and diphenyl cyanocarbonimidate (358 mg, 1.5 mmol) in dichloromethane (5 mL) was heated under reflux for 16 h. The solvent was removed under reduced pressure and the resulting residue purified by flash chromatography (hexane:ethyl acetate 3:1) to afford the title compound **200** as a yellow-green solid (279 mg, 67 %).

δ_{H} NMR (500 MHz, CDCl_3): 2.98 (2H, bs, CH_2), 3.91 (2H, bs, CH_2), 4.83 (2H, bs, CH_2), 7.12-7.14 (3H, m, ArH), 7.21-7.27 (4H, m, ArH), 7.39-7.42 (2H, m, ArH).

δ_{C} NMR (125 MHz, CDCl_3): 28.6, 43.8, 47.7, 113.2, 118.8, 126.0, 126.4, 127.0, 127.5, 128.6, 130.2, 131.5, 133.8, 152.4, 157.7.

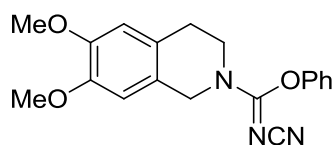
IR ν_{\max} (NaCl): 3424, 3048, 2928, 2185, 1620, 1580, 1455, 1203, 751 cm^{-1} .

LRMS (ESI): $[\text{M} + \text{H}^+]$ $\text{C}_{17}\text{H}_{16}\text{N}_3\text{O}^+$; calc. 278.13, found 278.33.

HRMS (ESI): $[\text{M} + \text{H}^+]$ $\text{C}_{17}\text{H}_{16}\text{N}_3\text{O}^+$; calc. 278.1288, found 278.1289.

Melting point: 72-74 $^{\circ}\text{C}$.

Preparation of (Z)-phenyl N-cyano-6,7-dimethoxy-3,4-dihydro-2(1H)-isoquinolinecarboximidoate (201)



A solution of 6,7-dimethoxy-1,2,3,4-tetrahydroisoquinoline (100 mg, 0.44 mmol), diphenyl cyanocarbonimidate (105 mg, 0.44 mmol) and triethylamine (133 mg, 0.18 mL, 1.3 mmol) in dichloromethane (2.5 mL) was heated under reflux for 16 h. The solvent was evaporated under reduced pressure and the residue partitioned with ethyl acetate and water. Slow evaporation of ethyl acetate gave the title compound **201** as colourless crystals, a sample from which was submitted for X-ray crystallography (79 mg, 52 %).

δ_{H} NMR (500 MHz, CDCl_3): 2.91 (2H, bs, CH_2), 3.86-3.88 (8H, m, 2 x MeO and CH_2) 4.79 (2H, bs, CH_2), 6.63 (1H, bs, ArH), 6.68 (1H, s, ArH), 7.12 (2H, d, $J = 7.5$, ArH), 7.27 (1H, t, $J = 7.5$, ArH), 7.42 (2H, t, $J = 7.5$, ArH).

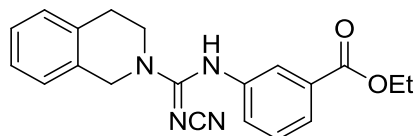
δ_{C} NMR (500 MHz, CDCl_3): 28.5, 43.9, 47.6, 56.2, 109.2, 111.5, 113.4, 119.1, 123.3, 126.2, 130.3, 148.4, 148.5, 152.5, 157.9.

IR ν_{\max} (KBr): 3421, 3063, 2996, 2938, 2186, 1626, 1594, 1267, 1107, 755 cm^{-1} .

LRMS (ESI): $[\text{M} + \text{H}^+]$ $\text{C}_{19}\text{H}_{20}\text{N}_3\text{O}_3^+$; calc. 338.15, found 338.27.

HRMS (ESI): $[\text{M} + \text{H}^+]$ $\text{C}_{19}\text{H}_{20}\text{N}_3\text{O}_3^+$; calc. 338.1499, found 338.1451.

Melting point: 129-131 $^{\circ}\text{C}$.

Preparation of ethyl 3-[[cyanoimino (3,4-dihydro-2(1H)-isoquinolinyl)methyl]amino]benzoate (202)

A solution of ethyl 3-(cyanoimino)(phenoxy)methyl]aminobenzoate (40 mg, 0.13 mmol) and 1,2,3,4-tetrahydroisoquinoline (20 mg, 0.15 mmol) in propan-2-ol (3 mL) was heated under reflux for 16 h. The solvent was removed under reduced pressure and the resulting residue purified by flash chromatography (hexane:ethyl acetate 2:1) to afford the title compound **202** as a white gum (65 mg, 71 %).

δ_{H} NMR (400 MHz, CDCl_3): 1.36 (3H, t, $J = 6.8$, OCH_2CH_3), 2.87 (2H, t, $J = 5.6$, CH_2), 3.67 (2H, t, $J = 5.6$, CH_2), 4.35 (2H, q, $J = 7.2$, OCH_2CH_3), 4.50 (2H, s, CH_2), 6.98 (1H, d, $J = 6.4$, ArH), 7.13-7.20 (3H, m, ArH), 7.27-7.29 (1H, m, ArH), 7.40 (1H, t, $J = 8.0$, ArH), 7.71 (1H, t, $J = 2.0$, ArH), 7.79 (1H, d, $J = 6.4$, 1.2, ArH), 7.91 (1H, s, NH).

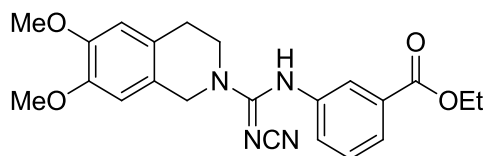
δ_{C} NMR (100 MHz, CDCl_3): 14.3, 28.1, 45.1, 49.1, 61.3, 117.4, 121.6, 125.1, 125.7, 126.2, 126.6, 127.2, 128.6, 129.7, 131.8, 131.9, 133.9, 139.0, 159.4, 165.8.

IR ν_{max} (ATR): 2963, 2932, 2857, 2169, 1707, 1523, 1288 cm^{-1} .

LRMS (ESI): $[\text{M} + \text{H}^+]$ $\text{C}_{20}\text{H}_{20}\text{N}_4\text{O}_2\text{Na}^+$; calc. 371.15, found 371.47 ($\text{M} + \text{Na}^+$).

HRMS (ESI): $[\text{M} + \text{H}^+]$ $\text{C}_{20}\text{H}_{21}\text{N}_4\text{O}_2^+$; calc. 349.1659, found 349.1656.

Purity: 97 %, LCMS t_{R} 27.0 min.

Preparation of ethyl 3-[[cyanoimino](6,7-dimethoxy-3,4-dihydro-2(1H)-isoquinolinyl)methyl]amino}benzoate (203)

A solution of ethyl 3-(cyanoimino)(phenoxy)methyl]amino benzoate (70 mg, 0.23 mmol) and 6,7-dimethoxy-1,2,3,4-tetrahydroisoquinoline (44 mg, 0.23 mmol) in propan-2-ol (1 mL) was heated under reflux for 16 h. The solvent was removed under reduced pressure and the resulting residue purified by flash chromatography (hexane:ethyl acetate 2:1) to afford the title compound **203** as an opaque white oil (65 mg, 70 %).

δ_{H} NMR (400 MHz, CDCl_3): 1.36 (3H, t, $J = 7.2$, OCH_2CH_3), 2.79 (2H, t, $J = 6.0$, CH_2), 3.67 (2H, t, $J = 6.0$, CH_2), 3.79 (3H, s, MeO), 3.84 (3H, s, MeO), 4.34 (2H, q, $J = 7.2$, OCH_2CH_3), 4.41 (2H, s, CH_2), 6.43 (1H, s, ArH), 6.59 (1H, s, ArH), 7.26-7.28 (1H, m, ArH), 7.39 (1H, t, $J = 7.6$, ArH), 7.71 (1H, s, ArH), 7.78 (1H, d, $J = 7.6$, ArH), 7.91 (1H, s, NH).

δ_{C} NMR (100 MHz, CDCl_3): 13.7, 27.2, 44.6, 48.3, 55.5, 60.8, 108.5, 110.8, 116.9, 121.1, 123.2, 124.6, 124.9, 125.3, 129.0, 131.3, 138.6, 147.4, 149.6, 158.5, 165.4.

IR ν_{max} (ATR): 2922, 2857, 2171, 1715, 1508, 1265, 1113, 747 cm^{-1} .

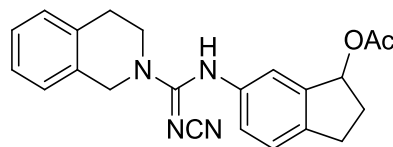
LRMS (ESI): $[\text{M} + \text{H}^+]$ $\text{C}_{22}\text{H}_{25}\text{N}_4\text{O}_4^+$; calc. 409.19, found 409.60.

HRMS (ESI): $[\text{M} + \text{H}^+]$ $\text{C}_{22}\text{H}_{25}\text{N}_4\text{O}_4^+$; calc. 409.1870, found 409.1867.

Melting point: 131-135 $^{\circ}\text{C}$.

Purity: 95 %, HPLC t_{R} 25.81 min.

Preparation of 6-[(cyanoimino)(3,4-dihydro-2(1H)-isoquinolinyl)methyl]amino}-2,3-dihydro-1H-inden-1-yl acetate (205)



A solution of 6-(cyanoimino)(phenoxy)methyl]amino-2,3-dihydro-1H-inden-1-yl acetate (45 mg, 0.13 mmol) and 1,2,3,4-tetrahydroisoquinoline (20 mg, 0.15 mmol) in propan-2-ol was heated under reflux for 16 h. The solvent was removed under reduced pressure and the resulting residue purified by flash chromatography (hexane:ethyl acetate 4:1-1:1) to afford the title compound **205** as a gum (37 mg, 74 %).

δ_{H} NMR (500 MHz, CDCl_3): 2.01 (3H, s, CH_3), 2.09-2.13 (1H, m, 1H of CH_2), 2.48-2.56 (1H, m, 1H of CH_2), 2.82-2.88 (3H, m, 1H of CH_2 and CH_2), 3.04-3.10 (1H, m, 1H of CH_2), 3.59-3.67 (2H, m, CH_2), 4.48 (2H, d, $J = 9.0$, CH_2), 6.10 (1H, dd, $J = 7.0, 3.5$, CHOCOCH_3), 6.98-7.03 (2H, m, ArH), 7.10-7.13 (2H, m, ArH), 7.17-7.19 (2H, m, ArH), 7.23 (1H, d, $J = 8.0$, ArH), 7.50 (1H, s, NH).

δ_{C} NMR (125 MHz, CDCl_3): 21.2, 28.1, 29.7, 32.6, 45.1, 49.0, 78.0, 117.8, 118.5, 122.2, 125.8, 126.2, 126.6, 127.1, 128.5, 132.1, 134.0, 137.4, 141.1, 142.8, 159.8, 171.0.

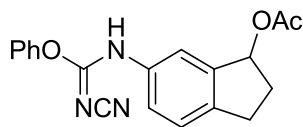
IR ν_{max} (ATR): 3220, 2932, 2857, 2167, 1715, 1519, 1213, 747 cm^{-1} .

LRMS (ESI): $[\text{M} + \text{H}^+]$ $\text{C}_{22}\text{H}_{22}\text{N}_4\text{O}_2\text{Na}^+$; calc. 397.16, found 397.26 ($\text{M} + \text{Na}^+$).

HRMS (ESI): $[\text{M} + \text{H}^+]$ $\text{C}_{22}\text{H}_{23}\text{N}_4\text{O}_2^+$; calc. 375.1816, found 375.1813.

Melting point: 101-105 $^{\circ}\text{C}$.

Purity: 98 %, LCMS t_{R} 26.3 min.

Preparation of 6-(cyanoimino)(phenoxy)methyl]amino-2,3-dihydro-1H-inden-1-yl acetate (206)

A solution of diphenyl cyanocarbonimidate (93 mg, 0.39 mmol) and 6-amino-2,3-dihydro-1H-inden-1-yl acetate in propan-2-ol (3 mL) was heated under reflux for 16 h. The solvent was removed under reduced pressure and the residue purified by flash chromatography (hexane:ethyl acetate 2:1) to afford **206** as a brown solid (55 mg, 42 %).

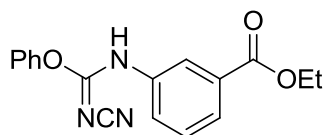
δ_{H} NMR (500 MHz, CDCl_3): 2.05 (3H, s, CH_3), 2.11-2.15 (1H, m, 1H of CH_2) 2.50-2.57 (1H, m, 1H of CH_2), 2.84-2.90 (1H, m, 1H of CH_2), 3.07-3.13 (1H, m, 1H of CH_2), 6.16 (1H, dd, $J = 7.0, 3.5$, CHOCOCH_3), 7.13-7.15 (2H, m, ArH), 7.27-7.33 (3H, m, ArH), 7.39-7.45 (3H, m, ArH), 9.10 (1H, bs, NH).

δ_{C} NMR (125 MHz, CDCl_3): 21.3, 29.9, 32.6, 78.0, 114.7, 121.0, 121.4, 124.6, 125.4, 126.8, 129.7, 134.0, 142.3, 142.9, 151.1, 161.8, 171.1.

IR ν_{max} (NaCl): 3449, 3284, 3177, 2963, 2854, 2204, 1732, 1641, 1488, 1240 cm^{-1} .

HRMS (ESI): $[\text{M} + \text{H}^+]$ $\text{C}_{19}\text{H}_{18}\text{N}_3\text{O}_3^+$; calc. 336.1343, found 336.1351.

Melting point: 175-177 $^{\circ}\text{C}$.

Preparation of ethyl 3-(cyanoimino)(phenoxy)methyl]amino benzoate (207)

A solution of ethyl 3-aminobenzoate (75 mg, 0.46 mmol) and diphenyl cyanocarbonimidate (109 mg, 0.46 mmol) was heated under reflux for 16 h in propan-2-ol. The solution was concentrated under reduced pressure and the resulting

residue partitioned with dichloromethane. Hydrochloric acid (2M) was added until the solution was acidic (pH 4) and the organic layer dried with magnesium sulfate, filtered and concentrated. The title compound **207** precipitated upon addition of ethyl acetate as a white solid. Hexane was added to the filtrate to yield additional product (199 mg, 51 %).

δ_{H} NMR (500 MHz, CDCl_3): 1.40 (3H, t, $J = 7.0$, OCH_2CH_3), 4.40 (2H, q, $J = 7.0$, OCH_2CH_3) 7.17 (2H, d, $J = 8.0$, ArH), 7.33 (1H, t, $J = 7.5$, ArH), 7.42-7.49 (3H, m, ArH), 7.62 (1H, d, $J = 7.5$, ArH), 7.93-7.95 (1H, m, ArH), 8.07 (1H, s, ArH), 8.78 (1H, bs, NH).

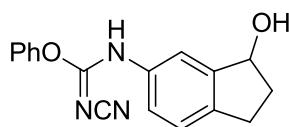
δ_{C} NMR (125 MHz, CDCl_3): 14.3, 61.4, 114.3, 121.4, 124.3, 127.0, 127.4, 127.5, 129.3, 129.8, 131.8, 135.6, 150.9, 161.5, 165.7.

IR ν_{max} (KBr): 3408, 3073, 2975, 2952, 2211, 1724, 1657, 1221, 753 cm^{-1} .

HRMS (ESI): $[\text{M} + \text{H}^+]$ $\text{C}_{17}\text{H}_{16}\text{N}_3\text{O}_3^+$; calc. 310.1186, found 310.1190.

Melting point: 167-168 $^{\circ}\text{C}$.

Preparation of phenyl *N'*-cyano-*N*-(3-hydroxy-2,3-dihydro-1*H*-inden-5-yl)imidocarbamate (**208**)



A solution of diphenyl cyanocarbonimidate (160 mg, 0.67 mmol) and 6-amino-1-indanol (100 mg, 0.67 mmol) in dichloromethane (5 mL) was heated under reflux for 16 h. The mixture was concentrated and the title compound **208** precipitated as a white solid upon slow addition of dichloromethane (75 mg, 39 %).

δ_{H} NMR (400 MHz, CDCl_3): 1.95-2.04 (1H, m, 1H of CH_2), 2.52-2.60 (1H, m, 1H of CH_2) 2.79-2.87 (1H, m, 1H of CH_2), 3.02-3.10 (1H, m, 1H of CH_2), 5.28 (1H, t, $J = 6.4$, CHOH), 7.14-7.16 (2H, d, $J = 8.0$, ArH), 7.21-7.24 (1H, m, ArH), 7.29-7.34

(2H, m, ArH), 7.42-7.46 (3H, m, ArH), 7.79 (1H, bs, NH). Note: OH peak not observed by ^1H NMR.

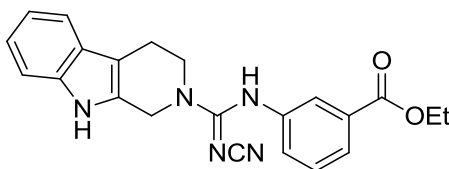
δ_{C} NMR (100 MHz, CDCl_3): 28.9, 35.8, 75.6, 113.3, 119.0, 120.9, 123.2, 125.1, 126.5, 129.3, 133.1, 141.6, 145.9, 150.4. Note: $\text{C}=\text{NCN}$ signal not observed by ^{13}C NMR due to fast relaxation.

IR ν_{max} (KBr): 3380, 3029, 2966, 2940, 2220, 1657, 1492, 1205 cm^{-1} .

HRMS (ESI): $[\text{M} + \text{H}^+]$ $\text{C}_{17}\text{H}_{16}\text{N}_3\text{O}_2^+$; calc. 294.1237, found 294.1234.

Melting point: 176-178 $^{\circ}\text{C}$.

Preparation of ethyl 3-(*N'*-cyano-2,3,4,9-tetrahydro-1*H*-pyrido[3,4-*b*]indole-2-carboximidamido)benzoate (209)



A solution of 2,3,4,9-tetrahydro-1*H*- β -carboline (30 mg, 0.17 mmol) and ethyl 3-(cyanoimino)(phenoxy)methyl]amino benzoate (53 mg, 0.17 mmol) was heated under reflux in propan-2-ol (5 mL) for 16 h. The solvent was removed under reduced pressure and the resulting residue purified by flash chromatography (hexane:ethyl acetate 2:1) to afford the title compound **209** as an orange gum (10 mg, 15 %).

δ_{H} NMR (500 MHz, CDCl_3): 1.33 (3H, t, $J = 7.0$, OCH_2CH_3), 2.79 (2H, t, $J = 5.5$, CH_2), 3.80 (2H, t, $J = 5.5$, CH_2), 4.32 (2H, q, $J = 7.0$, OCH_2CH_3), 4.58 (2H, s, CH_2), 7.11 (1H, t, $J = 7.5$, ArH), 7.18 (1H, t, $J = 8.0$, ArH), 7.29-7.31 (2H, m, ArH), 7.43 (2H, q, $J = 8.0$, ArH), 7.54 (1H, bs, NH), 7.76 (1H, t, $J = 2.0$, ArH), 7.82 (1H, d, $J = 8.0$, ArH), 7.96 (1H, bs, NH).

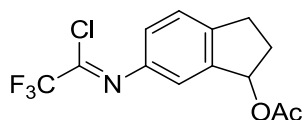
δ_{C} NMR (125 MHz, CDCl_3): 14.2, 29.7, 45.6, 46.2, 61.4, 103.0, 108.6, 111.0, 116.5, 117.2, 118.1, 119.9, 121.7, 122.3, 125.1, 126.1, 128.5, 129.8, 136.3, 138.8, 160.0, 165.7.

IR ν_{max} (ATR): 2926, 2857, 2162, 1716, 1571, 1520, 1080, 739 cm^{-1} .

HRMS (ESI): $[\text{M} + \text{H}^+]$ $\text{C}_{22}\text{H}_{22}\text{N}_5\text{O}_2$; calc. 388.1768, found 388.1768.

Purity: 95 %, HPLC t_{R} 25.67 min.

Preparation of 6-[[1-chloro-2,2,2-trifluoroethylidene]amino]-2,3-dihydro-1H-inden-1-yl acetate (**219**)

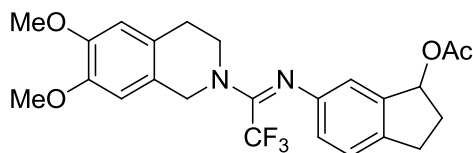


A flask containing triphenylphosphine (354 mg, 1.35 mmol) was cooled in an ice bath and trifluoroacetic acid (33 μL , 0.45 mmol), triethylamine (76 μL , 0.54 mmol) and carbon tetrachloride (518 μL , 5.35 mmol) added. After stirring for 10 min. a solution of 6-amino-2,3-dihydro-1H-inden-1-yl acetate (85 mg, 0.45 mmol) in carbon tetrachloride (218 μL , 2.25 mmol) was added and the reaction mixture heated under reflux for 3 h. The resulting solid was filtered off and the filtrate concentrated to give the title compound as a yellow oil **219** (78 mg, 58 %).

δ_{H} NMR (500 MHz, CDCl_3): 2.08 (3H, s, CH_3), 2.13-2.19 (1H, m, 1H of CH_2), 2.53-2.60 (1H, m, 1H of CH_2), 2.88-2.94 (1H, m, 1H of CH_2), 3.10-3.16 (1H, m, 1H of CH_2), 6.21 (1H, dd, $J = 7.0, 3.0$, CHOCOCH_3), 7.07 (1H, dd, $J = 8.0, 2.0$, ArH), 7.22 (1H, s, $J = 2.0$, ArH), 7.33-7.35 (1H, d, $J = 8.0$, ArH).

δ_{C} NMR (125 MHz, CDCl_3): 21.2, 30.0, 32.4, 77.9, 118.3, 119.3 ($^1J_{\text{C-F}} = 225$ Hz), 121.9, 125.4, 142.0, 142.4, 143.9, 160.6 ($^2J_{\text{C-F}} = 46$ Hz), 171.0.

δ_{F} NMR (376 MHz, CDCl_3): -71.5 (CF_3).

Preparation of 6-[[1-(6,7-dimethoxy-3,4-dihydro-2(1H)-isoquinoliny)-2,2,2-trifluoroethylidene]amino]-2,3-dihydro-1H-inden-1-yl acetate (220)

A solution of 6-[[1-chloro-2,2,2-trifluoroethylidene]amino]-2,3-dihydro-1H-inden-1-yl acetate (38 mg, 0.13 mmol) and 6,7-dimethoxy-1,2,3,4-tetrahydroisoquinoline (36 mg, 0.19 mmol) was heated under reflux in dry THF (2 mL) under nitrogen for 2.5 h. The solvent was removed under reduced pressure and the resulting residue purified by small scale flash chromatography (hexane:ethyl acetate 7:1) using a Pasteur pipette to afford the title compound **220** as a yellow-orange oil (20 mg, 34 %).

δ_{H} NMR (400 MHz, CDCl_3): 2.05 (3H, s, CH_3), 2.05-2.11 (1H, m, 1H of CH_2), 2.48-2.52 (1H, m, 1H of CH_2), 2.83-2.87 (3H, m, 1H of CH_2 and CH_2), 3.02-3.10 (1H, m, 1H of CH_2), 3.66 (2H, bs, CH_2), 3.84 (3H, s, MeO), 3.87 (3H, s, MeO), 4.48 (2H, bs, CH_2), 6.16 (1H, dd, $J = 7.2, 4.0$, CHOCOCH_3), 6.53 (1H, bs, ArH), 6.64 (1H, s, ArH), 6.71 (1H, d, $J = 7.6$, ArH), 6.81 (1H, s, ArH), 7.14 (1H, d, $J = 7.6$, ArH).

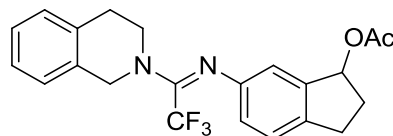
δ_{C} NMR (125 MHz, CDCl_3): 21.3, 28.3, 29.6, 32.5, 45.0, 48.7, 56.0, 78.4, 109.2, 111.4, 116.5, 120.7, 124.7, 129.3, 133.2, 133.7, 141.7, 146.9, 147.8, 147.9, 156.0 ($^2J_{\text{C-F}} = 56$ Hz), 171.1. Note: CF_3 signal not observed by ^{13}C NMR due to fast relaxation.

δ_{F} NMR (376 MHz, CDCl_3): -74.2 (CF_3).

IR ν_{max} (ATR): 2930, 2851, 1731, 1511, 1241, 1146, 1040, 759 cm^{-1} .

HRMS (ESI): $[\text{M} + \text{H}^+]$ $\text{C}_{24}\text{H}_{26}\text{F}_3\text{N}_2\text{O}_4^+$; calc. 463.1839, found 463.1836.

Purity: Purity could not be determined by HPLC. See appendix for ^1H NMR.

Preparation of 6-{{1-(3,4-dihydro-2(1*H*)-isoquinolinyl)-2,2,2-trifluoroethylidene}amino}-2,3-dihydro-1*H*-inden-1-yl acetate (221)

A solution of 6-{{1-chloro-2,2,2-trifluoroethylidene}amino}-2,3-dihydro-1*H*-inden-1-yl acetate (40 mg, 0.13 mmol) and 1,2,3,4-tetrahydroisoquinoline (17 mg, 0.13 mmol) was heated under reflux in dry THF (2 mL) under nitrogen for 2.5 h. The solvent was removed under reduced pressure and the resulting residue purified by small scale flash chromatography (100 % hexane) using a Pasteur pipette to afford the title compound **221** as a pale brown oil (24 mg, 46 %).

δ_{H} NMR (500 MHz, CDCl_3): 2.05 (3H, s, CH_3), 2.07-2.11 (1H, m, 1H of CH_2), 2.49-2.52 (1H, m, 1H of CH_2), 2.84-2.86 (1H, m, 1H of CH_2), 2.95 (2H, bs, CH_2), 3.03-3.09 (1H, m, 1H of CH_2), 3.69 (2H, bs, CH_2), 4.56 (2H, bs, CH_2), 6.16 (1H, dd, $J = 7.0, 3.0$, CHOCOCH_3), 6.72 (1H, d, $J = 7.0$, ArH), 6.82 (1H, s, ArH), 7.06 (1H, bs, ArH), 7.14-7.21 (4H, m, ArH).

δ_{C} NMR (125 MHz, CDCl_3): 21.3, 28.8, 29.6, 32.5, 44.9, 48.9, 78.4, 116.5, 120.5, 120.7, 124.7, 126.4, 126.7, 128.6, 132.9, 134.1, 138.2, 141.7, 146.9, 171.1. Note: CF_3 and $\text{C}=\text{N}$ signal not observed by ^{13}C NMR due to fast relaxation.

δ_{F} NMR (376 MHz, CDCl_3): -75.7 (CF_3).

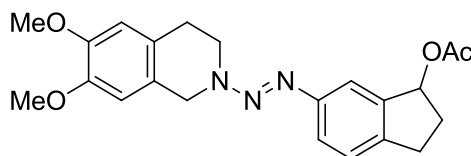
IR ν_{max} (ATR): 2935, 2864, 1739, 1647, 1245, 1191, 747 cm^{-1} .

LRMS (ESI): $[\text{M} + \text{H}^+]$ $\text{C}_{22}\text{H}_{22}\text{F}_3\text{N}_2\text{O}_2^+$; calc. 403.16, found 403.47.

HRMS (ESI): $[\text{M} + \text{H}^+]$ $\text{C}_{22}\text{H}_{22}\text{F}_3\text{N}_2\text{O}_2^+$; calc. 403.1628, found 403.1623.

Purity: Purity could not be determined by HPLC. See appendix for ^1H NMR.

Preparation of (*E*)-((6,7-dimethoxy-3,4-dihydroisoquinolin-2-1*H*-yl)diazenyl)-2,3-dihydro-1*H*-inden-1-yl acetate (268**)**



A solution of 6-amino-2,3-dihydro-1*H*-inden-1-yl acetate (75 mg, 0.39 mmol) in hydrochloric acid (1 mL, 2M) was stirred for 10 min. at 0 °C. Sodium nitrite (34 mg, 0.49 mmol, 1.25 equiv.) in water (0.5 mL) was added dropwise, maintaining the internal temperature of the flask at 0 ± 4 °C. After completion of the addition, the reaction was stirred at 0 °C for 30 min. The resulting diazonium salt solution was then added dropwise to a suspension of 6,7-dimethoxy-1,2,3,4-tetrahydroisoquinoline (75 mg, 0.39 mmol) in sodium hydroxide (1 mL, 2M) maintaining the internal temperature at 0 ± 4 °C. After stirring for 4 h at 0 °C the solution was partitioned with diethyl ether, the organic layer dried with magnesium sulfate and concentrated under reduced pressure. Purification of the resulting residue by flash chromatography (hexane:ethyl acetate 3:1) afforded the title compound **268** as a viscous brown oil (42 mg, 28 %)

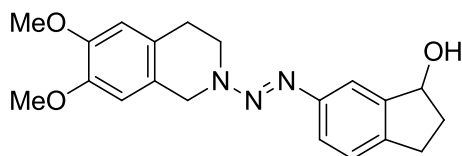
δ_{H} NMR (400 MHz, CDCl₃): 2.09 (3H, s, CH₃), 2.11-2.17 (1H, m, 1H of CH₂), 2.49-2.59 (1H, m, 1H of CH₂), 2.84-2.92 (1H, m, 1H of CH₂), 3.00 (2H, t, *J* = 6.0, CH₂), 3.07-3.15 (1H, m, 1H of CH₂), 3.89 (3H, s, MeO), 3.90 (3H, s, MeO), 4.10 (2H, t, *J* = 6.0, CH₂), 4.88 (2H, s, CH₂), 6.24 (1H, dd, *J* = 6.8, 3.6, CHOCOCH₃), 6.70 (1H, s, ArH), 6.72 (1H, s, ArH), 7.26 (1H, d, *J* = 8.0, ArH), 7.44 (1H, dd, *J* = 8.0, 1.6, ArH), 7.52 (1H, s, ArH).

δ_{C} NMR (100 MHz, CDCl₃): 20.8, 29.3, 32.2, 47.6, 55.5, 77.8, 109.2, 110.9, 116.6, 121.5, 124.5, 126.1, 128.3, 141.2, 141.3, 147.4, 147.5, 149.7, 170.6. Note: 2 x CH₂ peaks not observed by ¹³C NMR due to fast relaxation.

IR ν_{max} (ATR): 2924, 2829, 1729, 1375, 1232, 1025, 745 cm⁻¹.

HRMS (ESI): [M + H⁺] C₂₂H₂₆N₃O₄⁺; calc. 396.1918, found 396.1915.

Purity: Purity could not be determined by HPLC. See appendix for ¹H NMR.

Preparation of (*E*)-((6,7-dimethoxy-3,4-dihydroisoquinolin-2(1*H*)-yl)diazenyl)-2,3-dihydro-1*H*-inden-1-ol (269**)**

The title compound **269** was obtained from the chromatographic purification as a by-product in the synthesis of ((6,7-dimethoxy-3,4-dihydroisoquinolin-2(1*H*)-yl)diazenyl)-2,3-dihydro-1*H*-inden-1-yl acetate (**268**). It was isolated as a brown oil (12 mg, 9 %).

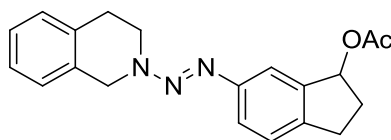
δ_{H} NMR (400 MHz, CDCl_3): 1.77 (1H, bs, OH), 1.97-2.02 (1H, m, 1H of CH_2), 2.50-2.55 (1H, m, 1H of CH_2), 2.79-2.87 (1H, m, 1H of CH_2), 3.02 (2H, t, $J = 6.0$, CH_2), 3.04-3.10 (1H, m, 1H of CH_2), 3.90 (6H, 2 x s, 2 x MeO), 4.10 (2H, t, $J = 6.0$, CH_2), 4.89 (2H, s, CH_2), 5.27 (1H, t, $J = 6.0$, CH), 6.70 (1H, s, ArH), 6.74 (1H, s, ArH), 7.24 (1H, d, $J = 8.0$, ArH), 7.38 (1H, dd, $J = 8.0, 1.6$, ArH), 7.56 (1H, s, ArH).

δ_{C} NMR (100 MHz, CDCl_3): 24.4, 29.3, 35.4, 41.0, 43.3, 55.5, 76.0, 108.7, 111.0, 118.7, 123.0, 123.6, 124.4, 127.7, 127.9, 147.9, 148.4.

IR ν_{max} (ATR): 3325, 2924, 2837, 1358, 1140, 1032, 741 cm^{-1} .

HRMS (ESI): $[\text{M} + \text{H}^+]$ $\text{C}_{20}\text{H}_{24}\text{N}_3\text{O}_3^+$; calc. 354.1812, found 354.1809.

Purity: Purity could not be determined by HPLC. See appendix for ^1H NMR.

Preparation of (*E*)-((3,4-dihydroisoquinolin-2(1*H*)-yl)diazenyl)-2,3-dihydro-1*H*-inden-1-yl acetate (267**)**

Compound **267** was prepared similarly to **268** using 6-amino-2,3-dihydro-1*H*-inden-1-yl acetate (65 mg, 0.34 mmol), 1,2,3,4-tetrahydroisoquinoline (45 mg, 0.34 mmol)

and sodium nitrite (29 mg, 0.43 mmol, 1.25 equiv.). The residue was purified by flash chromatography (hexane:ethyl acetate 3:1) to afford the title compound **267** as a light brown oil (42 mg, 38 %)

δ_{H} NMR (400 MHz, CDCl_3): 2.10 (3H, s, CH_3), 2.12-2.15 (1H, m, 1H of CH_2), 2.53-2.60 (1H, m, 1H of CH_2), 2.85-2.93 (1H, m, 1H of CH_2), 3.10 (2H, t, $J = 6.0$, CH_2), 3.14-3.16 (1H, m, 1H of CH_2), 4.13 (2H, t, $J = 6.0$, CH_2), 4.97 (2H, s, CH_2), 6.24 (1H, dd, $J = 6.8, 3.6$, CHOCOCH_3), 7.23-7.28 (5H, m, ArH), 7.45 (1H, dd, $J = 8.4, 2.0$, ArH), 7.53 (1H, d, $J = 1.6$, ArH).

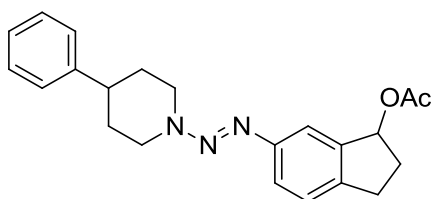
δ_{C} NMR (125 MHz, CDCl_3): 21.4, 29.8, 32.7, 48.6, 78.3, 117.1, 122.0, 125.0, 125.6, 126.7, 128.4, 129.0, 132.6, 134.8, 141.5, 141.8, 150.2, 171.1. Note: 2 x CH_2 peaks not observed by ^{13}C NMR due to fast relaxation.

IR ν_{max} (ATR): 3025, 2935, 2848, 1725, 1360, 1233, 1157, 748 cm^{-1} .

HRMS (ESI): $[\text{M} + \text{H}^+]$ $\text{C}_{20}\text{H}_{22}\text{N}_3\text{O}_2^+$; calc. 336.1707, found 336.1702.

Purity: Purity could not be determined by HPLC. See appendix for ^1H NMR.

Preparation of (*E*)-((4-phenylpiperidin-1-yl)diazenyl)-2,3-dihydro-1*H*-inden-1-yl acetate (**270**)



Compound **270** was prepared similarly to **268** using 6-amino-2,3-dihydro-1*H*-inden-1-yl acetate (75 mg, 0.39 mmol), 4-phenylpiperidine (63 mg, 0.39 mmol) and sodium nitrite (34 mg, 0.49 mmol, 1.25 equiv.). The residue was purified by flash chromatography (hexane:ethyl acetate 3:1) to afford the title compound **270** as a viscous brown oil (30 mg, 21 %)

δ_{H} NMR (400 MHz, CDCl_3): 1.86-1.89 (2H, m, CH_2), 2.02-2.05 (2H, m, CH_2), 2.10 (3H, s, CH_3), 2.12-2.15 (1H, m, 1H of CH_2), 2.52-2.60 (1H, m, 1H of CH_2), 2.79-2.92 (2H, m, 1H of CH_2 and CH), 3.08-3.21 (3H, m, 1H of CH_2 and CH_2), 4.71 (2H, d, $J = 12.0$, CH_2), 6.24 (1H, dd, $J = 6.8, 2.8$, CHOCOCH_3), 7.22-7.26 (4H, m, ArH), 7.34-7.37 (2H, m, ArH), 7.43-7.45 (1H, m, ArH), 7.53 (1H, s, ArH).

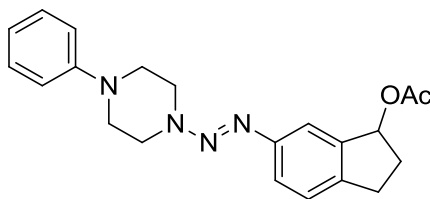
δ_{C} NMR (125 MHz, CDCl_3): 20.9, 29.3, 32.2, 42.1, 43.9, 47.4, 77.8, 116.6, 121.5, 124.5, 126.0, 126.3, 128.1, 141.3, 141.4, 144.8, 149.5, 170.6.

IR ν_{max} (ATR): 2958, 2906, 2848, 1741, 1439, 1343, 1239, 1086, 712 cm^{-1} .

HRMS (ESI): $[\text{M} + \text{H}^+]$ $\text{C}_{22}\text{H}_{26}\text{N}_3\text{O}_2^+$; calc. 364.2020, found 364.2017.

Purity: Purity could not be determined by HPLC. See appendix for ^1H NMR.

Preparation of (*E*)-((4-phenylpiperazin-1-yl)diazenyl)-2,3-dihydro-1*H*-inden-1-yl acetate (**271**)



Compound **271** was prepared similarly to **268** using 6-amino-2,3-dihydro-1*H*-inden-1-yl acetate (75 mg, 0.39 mmol), 4-phenylpiperazine (63 mg, 0.39 mmol) and sodium nitrite (34 mg, 0.49 mmol, 1.25 equiv.). The residue was purified by flash chromatography (hexane:ethyl acetate 3:1) to afford the title compound **271** as a viscous light brown oil (25 mg, 18 %)

δ_{H} NMR (500 MHz, CDCl_3): 2.09 (3H, s, CH_3), 2.11-2.14 (1H, m, 1H of CH_2), 2.52-2.58 (1H, m, 1H of CH_2), 2.85-2.91 (1H, m, 1H of CH_2), 3.08-3.13 (1H, m, 1H of CH_2), 3.37 (4H, t, $J = 4.5$, 2 x CH_2), 3.95 (4H, t, $J = 4.5$, 2 x CH_2), 6.22 (1H, dd, $J = 7.0, 3.5$, CHOCOCH_3), 6.93 (1H, t, $J = 7.0$, ArH), 7.01 (2H, dd, $J = 8.0, 1.0$, ArH), 7.25 (1H, s, ArH), 7.32 (2H, t, $J = 7.5$, ArH), 7.43 (1H, dd, $J = 8.0, 2.0$, ArH), 7.52 (1H, s, ArH).

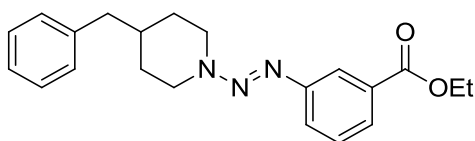
δ_{C} NMR (125 MHz, CDCl_3): 21.3, 30.2, 32.3, 42.5, 48.9, 78.4, 119.1, 124.8, 125.4, 125.6, 126.7, 128.8, 129.0, 130.0, 141.1, 144.4, 171.1.

IR ν_{max} (ATR): 2909, 2812, 1738, 1599, 1364, 1241, 1015, 739 cm^{-1} .

HRMS (ESI): $[\text{M} + \text{H}^+]$ $\text{C}_{21}\text{H}_{25}\text{N}_4\text{O}_2^+$; calc. 365.1972, found 365.1970.

Purity: Purity could not be determined by HPLC. See appendix for ^1H NMR.

Preparation of (*E*)-ethyl 3-((4-benzylpiperidin-1-yl)diazenyl)benzoate (**272**)



Compound **272** was prepared similarly to **268** using ethyl 3-aminobenzoate (48 mg, 0.29 mmol), 4-benzylpiperidine (50 mg, 0.29 mmol) and sodium nitrite (26 mg, 0.36 mmol, 1.25 equiv.). The residue was purified by flash chromatography (hexane:ethyl acetate 7:1) to afford the title compound **272** as a yellow oil (62 mg, 59 %).

δ_{H} NMR (400 MHz, CDCl_3): 1.35-1.45 (5H, m, OCH_2CH_3 and CH_2), 1.83-1.95 (3H, m, CH_2 and CH), 2.63 (2H, d, $J = 7.2$, CH_2), 3.08 (2H, bs, CH_2), 4.41 (2H, q, $J = 7.2$, OCH_2CH_3), 4.58 (2H, bs, CH_2), 7.20 (2H, d, $J = 7.2$, ArH), 7.22-7.28 (1H, m, ArH), 7.34 (2H, t, $J = 7.6$, ArH), 7.42 (1H, t, $J = 7.6$, ArH), 7.63-7.65 (1H, m, ArH), 7.85-7.88 (1H, m, ArH), 8.12-8.13 (1H, t, $J = 1.6$, ArH).

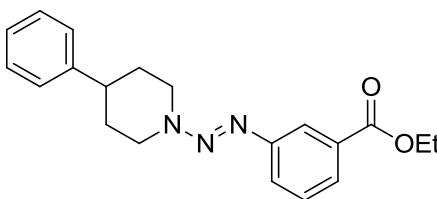
δ_{C} NMR (100 MHz, CDCl_3): 13.9, 30.9, 37.6, 42.3, 46.6, 60.4, 121.2, 124.4, 125.6, 126.1, 127.9, 128.3, 128.6, 130.8, 139.5, 150.5, 166.2.

IR ν_{max} (ATR): 2980, 2921, 2852, 1714, 1578, 1357, 1265, 1094 cm^{-1} .

LRMS (ESI): $[\text{M} + \text{H}^+]$ $\text{C}_{21}\text{H}_{26}\text{N}_3\text{O}_2^+$; calc. 352.20, found 352.20.

HRMS (ESI): $[\text{M} + \text{H}^+]$ $\text{C}_{21}\text{H}_{26}\text{N}_3\text{O}_2^+$; calc. 352.2020, found 352.2016.

Purity: Purity could not be determined by HPLC. See appendix for ^1H NMR.

Preparation of (*E*)-ethyl 3-((4-phenylpiperidin-1-yl)diazenyl)benzoate (273)

Compound **273** was prepared similarly to **268** using ethyl 3-aminobenzoate (48 mg, 0.29 mmol), 4-phenylpiperidine (47 mg, 0.29 mmol) and sodium nitrite (25 mg, 0.36 mmol, 1.25 equiv.). The residue was purified by flash chromatography (hexane:ethyl acetate 7:1) to afford the title compound **273** as a pale yellow oil (43 mg, 45 %).

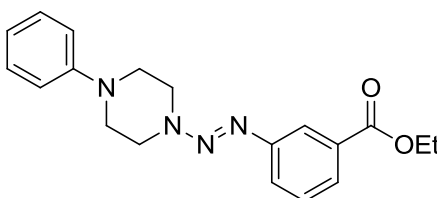
δ_{H} NMR (400 MHz, CDCl_3): 1.43 (3H, t, $J = 7.2$, OCH_2CH_3), 1.82-1.94 (2H, m, CH_2), 2.06 (2H, d, $J = 12.8$, CH_2), 2.83-2.90 (1H, m, CH), 3.23 (2H, bs, CH_2), 4.42 (2H, q, $J = 7.2$, OCH_2CH_3), 4.75 (2H, bs, CH_2), 7.26-7.28 (3H, m, ArH), 7.34-7.38 (2H, m, ArH), 7.44 (1H, t, $J = 8.0$, ArH), 7.66-7.69 (1H, m, ArH), 7.87-7.90 (1H, m, ArH), 8.16 (1H, m, ArH).

δ_{C} NMR (100 MHz, CDCl_3): 14.5, 32.9, 42.8, 47.4, 61.1, 121.9, 125.1, 126.8, 126.9, 126.9, 128.8, 129.0, 131.5, 145.3, 151.1, 166.9.

IR ν_{max} (ATR): 2921, 2826, 1746, 1582, 1360, 1219, 1038 cm^{-1} .

HRMS (ESI): $[\text{M} + \text{H}^+]$ $\text{C}_{20}\text{H}_{24}\text{N}_3\text{O}_2^+$; calc. 338.1863, found 338.1860.

Purity: Purity could not be determined by HPLC. See appendix for ^1H NMR.

Preparation of (*E*)-ethyl 3-((4-phenylpiperazin-1-yl)diazenyl)benzoate (274)

Compound **274** was prepared similarly to **268** using ethyl 3-aminobenzoate (48 mg, 0.29 mmol), 4-phenylpiperazine (47 mg, 0.29 mmol) and sodium nitrite (25 mg, 0.36

mmol, 1.25 equiv.). The residue was purified by flash chromatography (hexane:ethyl acetate 5:1) to afford the title compound **274** as a yellow oil (24 mg, 25 %).

δ_{H} NMR (400 MHz, CDCl_3): 1.43 (3H, t, $J = 7.2$, OCH_2CH_3), 3.40 (4H, t, $J = 5.2$, 2 x CH_2), 4.02 (4H, t, $J = 5.2$, 2 x CH_2), 4.42 (2H, q, $J = 7.2$, OCH_2CH_3), 6.93-6.97 (1H, m, ArH), 7.01 (2H, d, $J = 7.6$, ArH), 7.31-7.35 (2H, m, ArH), 7.45 (1H, t, $J = 8.0$, ArH), 7.66-7.69 (1H, m, ArH), 7.89-7.92 (1H, m, ArH), 8.16 (1H, t, $J = 1.6$, ArH).

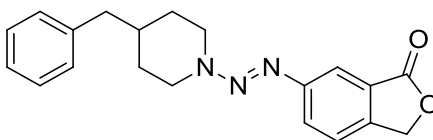
δ_{C} NMR (125 MHz, CDCl_3): 13.9, 46.8, 48.7, 60.5, 116.4, 120.1, 121.4, 124.6, 126.6, 128.4, 128.8, 130.8, 150.0, 150.4, 166.1.

IR ν_{max} (ATR): 2891, 2859, 2826, 1694, 1567, 1319, 1254, 973 cm^{-1} .

HRMS (ESI): $[\text{M} + \text{H}^+]$ $\text{C}_{19}\text{H}_{23}\text{N}_4\text{O}_2^+$; calc. 339.1816, found 339.1816.

Purity: Purity could not be determined by HPLC. See appendix for ^1H NMR.

Preparation of (*E*)-((4-benzylpiperidin-1-yl)diazenyl)isobenzofuran-1(3*H*)-one (**277**)



Compound **277** was prepared similarly to **268** using 6-aminophthalide (50 mg, 0.34 mmol), 4-benzylpiperidine (60 mg, 0.34 mmol) and sodium nitrite (30 mg, 0.43 mmol, 1.25 equiv.). The residue was purified by flash chromatography (hexane:ethyl acetate 6:1) to afford the title compound **277** as an opaque white gum (51 mg, 45 %).

δ_{H} NMR (400 MHz, CDCl_3): 1.36-1.45 (2H, m, CH_2), 1.84-1.94 (3H, m, CH_2 and CH), 2.64 (2H, d, $J = 6.8$, CH_2), 3.12 (2H, bs, CH_2), 4.58 (2H, bs, CH_2), 5.32 (2H, s, CH_2), 7.20 (2H, d, $J = 8.0$, ArH), 7.23-7.26 (1H, m, ArH), 7.31-7.35 (2H, m, ArH), 7.44 (1H, d, $J = 8.0$, ArH), 7.76 (1H, dd, $J = 8.0, 1.6$, ArH), 7.97 (1H, d, $J = 1.6$, ArH).

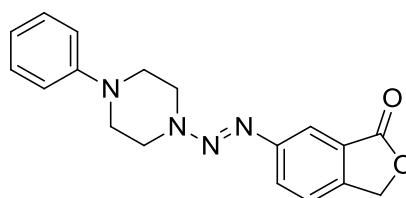
δ_{C} NMR (100 MHz, CDCl_3): 30.9, 37.5, 42.3, 69.1, 115.8, 121.7, 125.7, 126.1, 127.0, 127.9, 128.6, 139.4, 142.5, 151.8, 170.8. Note: 2 x CH_2 peaks not observed by ^{13}C NMR due to fast relaxation.

IR ν_{max} (ATR): 2924, 2863, 1767, 1580, 1355, 1220, 1049 cm^{-1} .

HRMS (ESI): $[\text{M} + \text{H}^+]$ $\text{C}_{20}\text{H}_{22}\text{N}_3\text{O}_2^+$; calc. 336.1707, found 336.1703.

Purity: > 99 %, HPLC t_{R} 29.85 min.

Preparation of (*E*)-((4-phenylpiperazin-1-yl)diazenyl)isobenzofuran-1(3*H*)-one (278)



Compound **278** was prepared similarly to **268** using 6-aminophthalide (50 mg, 0.34 mmol), 4-phenylpiperazine (55 mg, 0.34 mmol) and sodium nitrite (30 mg, 0.43 mmol, 1.25 equiv.). The residue was purified by flash chromatography (hexane:ethyl acetate 6:1) to afford the title compound **278** as an opaque white gum (5 mg, 5 %).

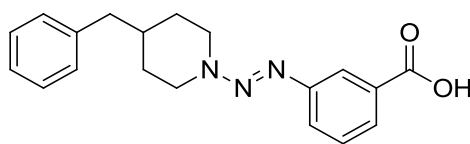
δ_{H} NMR (400 MHz, CDCl_3): 3.41 (4H, t, $J = 5.6$, 2 x CH_2), 4.04 (4H, t, $J = 5.6$, 2 x CH_2), 5.34 (2H, s, CH_2), 6.96 (1H, t, $J = 7.2$, ArH), 7.01 (2H, d, $J = 7.6$, ArH), 7.33 (2H, t, $J = 7.6$, ArH), 7.47 (1H, d, $J = 8.4$, ArH) 7.82-7.80 (1H, dd, $J = 8.0$, 1.6, ArH), 8.01 (1H, d, $J = 1.6$, ArH).

δ_{C} NMR (125 MHz, CDCl_3): 29.7, 49.2, 69.6, 116.7, 116.9, 120.7, 122.3, 126.7, 127.7, 129.3, 143.5, 150.8, 151.8, 171.2.

IR ν_{max} (ATR): 2997, 2924, 2826, 1744, 1591, 1351, 1232, 1036 cm^{-1} .

HRMS (ESI): $[\text{M} + \text{H}^+]$ $\text{C}_{18}\text{H}_{19}\text{N}_4\text{O}_2^+$; calc. 323.1503, found 323.1500.

Purity: > 99 %, HPLC t_{R} 25.99 min.

Preparation of (*E*)-3-((4-benzylpiperidin-1-yl)diazenyl)benzoic acid (275)

Compound **275** was prepared similarly to **268** using 3-aminobenzoic acid hydrochloride (75 mg, 0.43 mmol), 4-benzylpiperidine (74 mg, 0.43 mmol) and sodium nitrite (37 mg, 0.54 mmol, 1.25 equiv.). The residue was purified by flash chromatography (hexane:ethyl acetate 5:1 then 3:1) to afford the title compound **275** as pale brown gum (20 mg, 14 %).

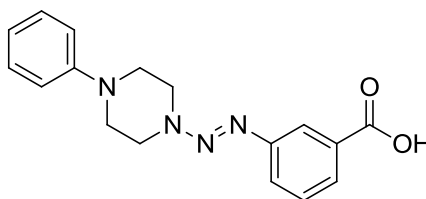
δ_{H} NMR (400 MHz, CDCl_3): 1.28-1.31 (2H, m, CH_2), 1.84-1.92 (3H, m, CH_2 and CH), 2.63 (2H, d, $J = 6.8$, CH_2), 3.10 (2H, bs, CH_2), 4.59 (2H, bs, CH_2), 7.19-7.27 (3H, m, ArH), 7.34 (2H, t, $J = 7.6$, ArH), 7.45 (1H, t, $J = 7.6$, ArH), 7.67-7.70 (1H, m, ArH), 7.92 (1H, dt, $J = 8.0, 1.6$, ArH), 8.19 (1H, t, $J = 1.6$, ArH). Note: OH peak not observed by ^1H NMR.

δ_{C} NMR (100 MHz, CDCl_3): 30.9, 37.6, 42.3, 121.6, 125.4, 125.6, 126.6, 127.9, 128.4, 128.6, 129.7, 139.5, 150.6, 171.1. Note: 2 x CH_2 peaks not observed by ^{13}C NMR due to fast relaxation.

IR ν_{max} (ATR): 3250, 2922, 2852, 1675, 1295, 1146, 762 cm^{-1} .

HRMS (ESI): $[\text{M} + \text{H}^+]$ $\text{C}_{19}\text{H}_{22}\text{N}_3\text{O}_2^+$; calc. 324.1707, found 324.1706.

Purity: 96 %, HPLC t_{R} 26.48 min.

Preparation of (*E*)-3-((4-phenylpiperazin-1-yl)diazenyl)benzoic acid (276**)**

Compound **276** was prepared similarly to **268** using 3-aminobenzoic acid hydrochloride (75 mg, 0.43 mmol), 4-phenylpiperazine (70 mg, 0.43 mmol) and sodium nitrite (37 mg, 0.54 mmol, 1.25 equiv.). The residue was purified by flash chromatography (hexane:ethyl acetate 2:1) to give the title compound **276** as a brown gum (18 mg, 14 %).

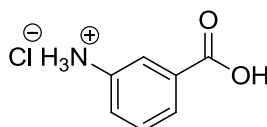
δ_{H} NMR (400 MHz, CDCl_3): 3.41 (4H, t, $J = 5.2$, CH_2), 4.03 (4H, t, $J = 5.2$, CH_2), 6.96 (1H, t, $J = 7.2$, ArH), 7.03 (2H, d, $J = 8.0$, ArH), 7.34 (2H, dt, $J = 8.4$, 1.2, ArH), 7.49 (1H, t, $J = 8.4$, ArH), 7.73 (1H, d, $J = 8.4$, ArH), 7.97 (1H, d, $J = 7.6$, ArH), 8.24 (1H, s, ArH).

δ_{C} NMR (100 MHz, CDCl_3): 29.2, 48.7, 116.5, 120.2, 121.8, 125.6, 127.2, 128.5, 128.8, 150.1, 150.4, 171.1. One peak not observed by ^{13}C NMR due to fast relaxation.

IR ν_{max} (ATR): 3242, 2919, 2852, 1677, 1597, 1147, 754 cm^{-1} .

HRMS (ESI): $[\text{M} + \text{H}^+]$ $\text{C}_{17}\text{H}_{18}\text{N}_4\text{O}_2^+$; calc. 311.1503, found 311.1500.

Purity: 98 %, HPLC t_{R} 12.12 min.

Preparation of 3-aminobenzoic acid (279**)**

Ethyl 3-aminobenzoate (1.021g, 6.19 mmol) was stirred in ethanol (4 mL) and a solution of sodium hydroxide (550 mg, 13.75 mmol) in water (10 mL) added. The

mixture was heated until reflux for 3.5 h then cooled to 0 °C in an ice-water bath. Hydrochloric acid (2M) was added whilst stirring to precipitate the title compound **279** as a beige solid which was then filtered and dried at 60 °C in a drying pistol for 2 h (913 mg, 85 %).

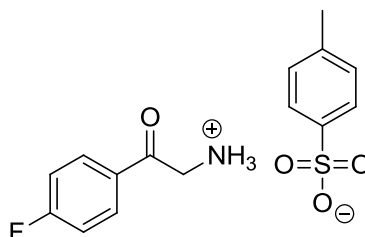
δ_{H} NMR (500 MHz, DMSO- d_6): 7.51-7.57 (2H, m, ArH), 7.82-7.84 (2H, m, ArH), 9.83 (3H, bs, NH_3). Note: OH peak not observed by ^1H NMR.

δ_{C} NMR (125 MHz, DMSO- d_6): 123.6, 127.3, 128.1, 130.5, 132.6, 134.4, 166.8.

IR ν_{max} (KBr): 2888, 2552, 1687, 1314, 1284, 752 cm^{-1} .

HRMS (ESI): $[\text{M} + \text{H}^+]$ $\text{C}_7\text{H}_8\text{NO}_2^+$; calc. 138.0550, found 138.0550.

Preparation of 2-amino-1-(4-fluorophenyl)ethanone tosylate²¹¹ (**284**)



2-Chloro-1-(4-fluorophenyl)ethanone (3 g, 17.3 mmol) was cooled to 0 °C in DMF (13 mL) and sodium azide (1.35g, 20.82 mmol, 1.2 equiv.) added portion-wise. The reaction was stirred at room temperature for 6 h then the mixture poured into cold ethyl acetate and water. The organic layer was dried with magnesium sulfate and concentrated. The azide residue was then added to triphenylphosphine (4.54g, 17.3 mmol, 1 equiv.) and *para*-toluenesulfonic acid (9.88g, 52.02 mmol, 3 equiv.) then stirred at room temperature for 16 h in THF (15 mL). Filtration afforded the title compound **284** as a pale brown solid (3.15g, 56 % over two steps).

δ_{H} NMR (400 MHz, DMSO- d_6): 2.92 (3H, s, CH_3), 4.61 (2H, s, CH_2), 7.12 (2H, d, $J = 8.0$, ArH), 7.43-7.49 (4H, m, ArH), 8.10-8.14 (2H, m, ArH), 8.22 (3H, bs, NH_3^+).

δ_{C} NMR (125 MHz, DMSO- d_6): 20.7, 44.9, 116.2 ($^2J_{\text{C-F}} = 22.5$ Hz), 125.5, 128.0, 130.5, 131.4 ($^3J_{\text{C-F}} = 10.1$ Hz), 137.6, 145.6, 165.7 ($^1J_{\text{C-F}} = 254.0$ Hz), 191.7.

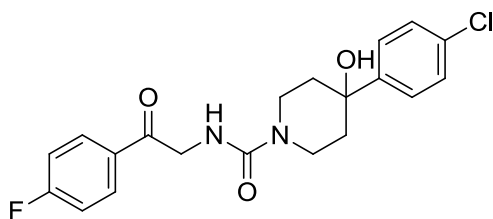
δ_{F} NMR (376 MHz, DMSO- d_6): -103.7 (F-Ph).

IR ν_{max} (KBr): 3070, 2892, 2635, 1697, 1598, 1253, 1038, 686 cm^{-1} .

LRMS (ESI): $[\text{M} + \text{H}^+]$ $\text{C}_8\text{H}_9\text{FNO}^+$; calc. 154.1, found 154.1.

^1H and ^{13}C NMR data obtained were consistent with those of previously characterised and published product.²¹¹

Preparation of 4-(4-chlorophenyl)-*N*-(2-(4-fluorophenyl)-2-oxoethyl)-4-hydroxypiperidine-1-carboxamide (**286**)



Triphosgene (15 mg, 0.05 mmol, 0.34 equiv.) was added to a solution of 2-amino-1-(4-fluorophenyl)ethanone tosylate (50 mg, 0.15 mmol) in dichloromethane (1 mL) and sat. aqueous sodium hydrogen carbonate (1 mL) at 0 °C, under vigorous stirring. The reaction was stirred for 15 min. then left to reach room temperature for 30 min. The reaction mixture was partitioned with ethyl acetate and the organic layer dried with magnesium sulfate and concentrated under reduced pressure to give the intermediate crude isocyanate as a pale yellow solid (20 mg, 73 %). This was then added to a solution of 4-(4-chlorophenyl)-4-piperidinol (24 mg, 0.11 mmol) in dichloromethane (4 mL) and heated under reflux for 16 h. The resulting solution was acidified with dilute hydrochloric acid (2M, pH 4), partitioned with dichloromethane, the organic layer dried with magnesium sulfate, filtered and concentrated under reduced pressure. Flash chromatography of the residue (ethyl acetate:hexane, 1:1) afforded the title compound **286** as a yellow oil (9 mg, 21 %).

δ_{H} NMR (400 MHz, CDCl_3): 1.80 (3H, d, $J = 12.8$, CH_2 and OH), 2.02-2.09 (2H, m, CH_2), 3.40 (2H, dt, $J = 13.2, 2.4$, CH_2), 4.00 (2H, dd, $J = 13.2, 2.4$, CH_2), 4.77 (2H,

d, $J = 4.4$, CH₂), 5.65 (1H, t, $J = 4.0$, NH), 7.20 (2H, dt, $J = 8.6$, 2.0, ArH), 7.33-7.37 (2H, m, ArH), 7.40-7.45 (2H, m, ArH), 8.03-8.06 (2H, m, ArH).

δ_{C} NMR (100 MHz, CDCl₃): 37.5, 39.8, 47.4, 70.8, 115.7 ($^2J_{\text{C-F}} = 22.1$ Hz), 125.4, 125.5, 128.1, 128.2, 130.2 ($^3J_{\text{C-F}} = 9.1$ Hz), 132.7, 145.8, 156.5, 165.8 ($^1J_{\text{C-F}} = 256.6$ Hz), 193.5.

δ_{F} NMR (376 MHz, CDCl₃): -103.2 (F-Ph).

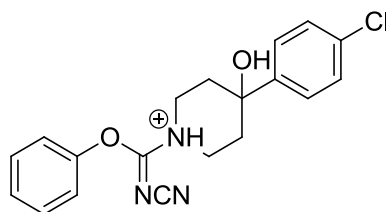
IR ν_{max} (ATR): 3414, 2924, 1627, 1598, 1412, 1230, 828 cm⁻¹.

LRMS (ESI): [M + H⁺] C₂₀H₂₁ClFN₂O₃⁺; calc. 391.1, found 391.1.

HRMS (ESI): [M + H⁺] C₂₀H₂₁ClFN₂O₃⁺; calc. 391.1219, found 391.1213.

Purity: > 99 %, LCMS t_{R} 12.91 min.

Preparation of phenyl 4-(4-chlorophenyl)-N-cyano-4-hydroxypiperidine-1-carbimide (287)



A solution of diphenyl cyanocarbonimide (57 mg, 0.24 mmol) and 4-(4-chlorophenyl)piperidin-4-ol (50 mg, 0.24 mmol) were heated under reflux in dichloromethane (3 mL) for 6 h. 2-Amino-1-(4-fluorophenyl)ethanone tosylate (78 mg, 0.24 mmol) and triethylamine (34 μL , 0.24 mmol, 1 equiv.) were added and the reaction heated under reflux for 16 h. The solvent was evaporated under reduced pressure and the residue purified by flash chromatography (hexane:ethyl acetate 2:1) to afford only the title compound **287** as a viscous yellow oil (60 mg, 67 %).

δ_{H} NMR (400 MHz, CDCl₃): 1.84 (2H, d, $J = 12.8$, CH₂), 2.00 (2H, d, $J = 2.8$, CH₂), 3.01 (1H, bs, OH), 3.54 (2H, dt, $J = 13.8$, 2.8, CH₂), 4.26 (2H, bs, CH₂), 7.07-7.10 (2H, m, ArH), 7.22-7.26 (1H, t, $J = 6.4$, ArH), 7.33-7.42 (6H, m, ArH).

δ_C NMR (100 MHz, $CDCl_3$): 37.34, 41.9, 69.9, 113.0, 117.9, 125.3, 125.6, 128.1, 129.6, 132.7, 145.2, 152.0, 156.9.

IR ν_{max} (ATR): 3392, 2922, 2190, 1446, 1028, 748 cm^{-1} .

HRMS (ESI): $[M + H^+]$ $C_{19}H_{19}ClN_3O_2^+$; calc. 356.1160, found 356.1157.

Purity: > 99 %, HPLC t_R 14.76 min.

6.1.3 Materials and methods for bioassays

Rat tissue preparation

Male Sprague-Dawley rats (250-300 g) were euthanised, brains removed and thalami and striata dissected by Prof. Judy Pratt. Each was homogenised in 50 volumes of 50 mM Tris·HCl pH 7.4 buffer using a Brinkman Polytron and the homogenate centrifuged using a Beckman Coulter Optima L-70K Ultracentrifuge at 25,000 rpm for 15 min. at 4 °C. The pellet was resuspended in the same volume of fresh buffer and centrifuged again. This procedure was repeated a final time and the resulting pellet resuspended in 50 volumes of fresh buffer and stored in 1 mL aliquots at -80 °C.

5-HT₇ receptor binding assay using rat thalamic tissue²³⁰

The final thalamic tissue concentration was approximately 4 mg/assay tube. Assays were carried out in an incubation buffer consisting of Tris·HCl pH 7.4 (50 mM), Na·EDTA (0.5 mM) and MgSO₄ (10 mM). The radioligand used was [³H]5-CT (0.5 nM, 200 µL;) in the presence of pindolol (100 µM, 200 µL) and WAY100635 (10 nM, 200 µL). Non-specific binding was defined with SB258741 (100 nM, 200 µL). Buffer was added to each assay tube to make the overall volume 2 mL. The assay tubes were incubated for 2 h at 37 °C, after which time the tube contents were rapidly filtered, under vacuum, through GF/B filters and washed with ice-cold buffer (2 mL x 5). The radioactivity retained on the filters (pre-soaked in 0.5 % PEI) was measured by counting in scintillation fluid (4 mL, Tri-Carb 1500 Packard; Emulsifier Safe).

Competition binding assays were determined using at least 5 concentrations of each drug of interest.

M₄ receptor binding assay using rat striatal tissue

The final striatal tissue concentration was approximately 4 mg/assay tube. Assays were carried out in an incubation buffer consisting of Tris·HCl pH 7.4 (50 mM), Na·EDTA (0.5 mM) and MgSO₄ (10 mM). The radioligand used was [³H]NMS (0.1 nM, 200 µL) in the presence of pirenzepine (50 nM, 200 µL). Non-specific binding was defined with PD102807 (250 nM, 200 µL). Buffer was added to each assay tube

to make the overall volume 2 mL. The assay tubes were incubated for 30 min at 30 °C, after which time the tube contents were rapidly filtered, under vacuum, through GF/B filters and washed with ice-cold buffer (2 mL x 5). The radioactivity retained on the filters (pre-soaked in 0.5 % PEI) was measured by counting in scintillation fluid (4 mL, Tri-Carb 1500 Packard; Emulsifier Safe).

Competition binding assays were determined using at least 5 concentrations of each drug of interest.

5-HT₇ receptor binding assay using human 5-HT₇ receptor membrane

Human 5-HT₇ receptor (CHO-K1) was purchased from Perkin Elmer and membranes diluted 1:200 to give a final membrane concentration of 17 µg/assay tube. Binding assays were performed in 550 µL total volume according to the following conditions; Membranes (1:200 dilution, 500 µL), [³H]5-CT (0.5 nM, 25 µL), incubation buffer (Tris·HCl pH 7.4 (50 mM), Na·EDTA (0.5 mM) and MgSO₄ (10 mM), 25 µL) for total binding, SB258741 (100 nM, 25 µL) for non-specific binding or drug compound (10 µM, 25 µL) for single point assay. The tubes were incubated for 2 h at 27 °C after which time the tube contents were rapidly filtered, under vacuum, through GF/B filters and washed with ice-cold wash buffer (2 mL x 5, Tris·HCl pH 7.4 (50 mM)). The radioactivity retained on the filters (pre-soaked in 0.5 % PEI) was measured by counting in scintillation fluid (4 mL, Tri-Carb 1500 Packard; Emulsifier Safe).

Competition binding assays were determined using at least 5 concentrations of each drug of interest.

M₄ receptor binding assay using human M₄ receptor membrane

Human M₄ receptor (CHO-K1) was purchased from Perkin Elmer and membranes diluted 1:200 to give a final membrane concentration of 24 µg/assay tube (500 µL). Binding assays were performed in 550 µL total volume according to the following conditions: Membranes (1:200 dilution, 500 µL), [³H]NMS (0.1 nM, 25 µL), incubation buffer (PBS pH 7.4, 25 µL) for total binding, PD102807 (250 nM, 25 µL) for non-specific binding or drug compound (10 µM, 25 µL) for single point assay. The tubes were incubated for 2 h at 27 °C after which time the tube contents were

rapidly filtered, under vacuum, through GF/B filters and washed with ice-cold wash buffer (2 mL x 5, Tris-HCl pH 7.4 (50 mM), 154 mM NaCl). The radioactivity retained on the filters (pre-soaked in 0.5 % PEI) was measured by counting in scintillation fluid (4 mL, Tri-Carb 1500 Packard; Emulsifier Safe).

Competition binding assays were determined using at least 5 concentrations of each drug of interest.

Preparation of hERG cells

hERG transfected HEK293 cells were kindly gifted from Dr. John Mitcheson, University of Leicester. Cell cultures were maintained in Gibco® Dulbecco's Modified Eagle Medium (D-MEM) + GlutaMAX-1™ medium supplemented with 10 % fetal bovine serum, 1 % penicillin-streptomycin and 0.8 % Geneticin® in a Sanyo humidified incubator (37 °C, 5 % CO₂) under the supervision of Dr. Ben Pickard. Once at 80-90 % confluency, the cells were lifted using PBS based, enzyme free, Cell Dissociation Buffer. The cell suspension was centrifuged at 1000 rpm for 5 min. and the supernatant discarded. The pellet was resuspended in ice-cold Tris-HCl pH 7.4 (20 mM) with 1 % phenylmethylsulfonyl fluoride (PMSF). The cells were homogenised using a Brinkman Polytron and the homogenate centrifuged using a Beckman Coulter Optima L-70K Ultracentrifuge or a L-100 XP Ultracentrifuge at 200,000 g for 40 min. at 4 °C, resuspended in buffer (10 mM HEPES, pH 7.4, 130 mM NaCl, 5 mM KCl, 0.8 mM MgCl₂, 10 mM glucose, 0.1 % BSA), aliquots quick-frozen in liquid N₂ and stored at – 80 °C.

hERG cell binding assay

Binding assays were performed in 300 µL total volume according to the following conditions: Cells (~400,000 cells per tube, 100 µL), [³H]astemizole (1.5 nM, 100 µL), buffer (10 mM HEPES, pH 7.4, 130 mM NaCl, 5 mM KCl, 0.8 mM MgCl₂, 10 mM glucose, 0.1 % BSA, 100 µL) for total binding, astemizole (10 µM, 100 µL) for non-specific binding or drug compound (10 µM, 100 µL) for single point assay. The tubes were incubated for 1 h at 25 °C after which time the tube contents were rapidly filtered, under vacuum, through GF/B filters and washed with ice-cold incubation buffer (2 mL x 5, see above). The radioactivity retained on the filters (pre-soaked in

0.5 % PEI) was measured by counting in scintillation fluid (4 mL, Tri-Carb 1500 Packard; Emulsifier Safe).

Competition binding assays were determined using at least 5 concentrations of each drug of interest.

Chapter 7 – References

1. D. M. Taylor, *Schizophrenia in Focus*, 1st edn., Pharmaceutical Press, Great Britain, 2006.
2. R. Kuhn and C. H. Cahn, *History of Psychiatry*, 2004, **15**, 361-366.
3. M. J. Tueth, *J. Emerg. Med.*, 1995, **13**, 805-809.
4. F. Lopez-Munoz, C. Alamo, G. Rubio and E. Cuenca, *Prog. Neuro-Psychopharmacol. Biol. Psychiat.*, 2004, **28**, 205-208.
5. A. P. Association, *American Psychiatric Association: Diagnostic and Statistical Manual of Mental Disorders*, 4th Edition, Text Revision edn., Washington D.C., 2000.
6. M. D. Jibson, I. D. Glick and R. Tandon, *Focus*, 2004, **2**, 17-30.
7. J. Addington and D. Addington, *Schiz. Res.*, **5**, 51-59.
8. J. Addington, D. Addington and E. Maticka-Tyndale, *Schiz. Res.*, 1991, **5**, 123-134.
9. N. C. Andreasen, *Schiz. Bull.*, 1985, **11**, 380-389.
10. N. C. Andreasen and S. Olsen, *Arch. Gen. Psychiat.*, 1982, **39**, 789-794.
11. W. G. Rosen, R. C. Mohs, C. A. Johns, N. S. Small, K. S. Kendler, T. B. Horvath and K. L. Davis, *Psychiat. Res.*, 1984, **13**, 277-284.
12. J. M. Gold and P. D. Harvey, *Psychiat. Clin. North Am.*, 1993, **16**, 295-312.
13. R. J. Wyatt, R. C. Alexander, M. F. Egan and D. G. Kirch, *Schiz. Res.*, 1988, **1**, 3-18.
14. E. Q. Wu, H. G. Birnbaum, L. Shi, D. E. Ball, R. C. Kessler, M. Moulis and J. Aggarwal, *J. Clin. Psychiat.*, 2005, **66**, 1122-1129.
15. H. Häfner, W. a. d. Heiden, S. Behrens, W. F. Gattaz, M. Hambrecht, W. Löffler, K. Maurer, P. Munk-Jørgensen, B. Nowotny, A. Riecher-Rössler and A. Stein, *Schiz. Bull.*, 1998, **24**, 99-113.
16. M. Tsuang, *Biol. Psychiat.*, 2000, **47**, 210-220.
17. I. I. Gottesman and J. Shields, *Schiz. Bull.*, 1976, **2**, 360-401.
18. L. L. Heston, *Br. J. Psychiat.*, 1966, **112**, 819-825.
19. N. Craddock, M. C. O'Donovan and M. J. Owen, *J. Med. Genet.*, 2005, **42**, 193-204.
20. P. B. Mortensen, C. B. Pedersen, T. Westergaard, J. Wohlfahrt, H. Ewald, O. Mors, P. K. Andersen and M. Melbye, *New Engl. J. Med.*, 1999, **340**, 603-608.
21. J. J. McGrath, M. R. Pemberton, J. L. Welham and R. M. Murray, *Schiz. Res.*, 1994, **14**, 1-8.
22. S. Andréasson, A. Engström, P. Allebeck and U. Rydberg, *The Lancet*, 1987, **330**, 1483-1486.
23. M. Bleuler and W. A. Stoll, *Ann. N.Y. Acad. Sci.*, 1955, **61**, 167-173.
24. T. W. Stone, ed., *Neuropharmacology*, 1st edn., 1995.
25. H. P. Rang and M. M. Dale, *Pharmacology*, Sixth edn., 2007.
26. L. Farde, A.-L. Nordstrom, F.-A. Wiesel, S. Pauli, C. Halldin and G. Sedvall, *Arch. Gen. Psychiat.*, 1992, **49**, 538-544.
27. D. E. Casey, *Schiz. Res.*, 1991, **4**, 109-120.
28. F. López-Muñoz and C. Alamo, *Brain Res. Bull.*, 2009, **79**, 130-141.
29. G. D. Tollefson and T. M. Sanger, *Am. J. Psychiat.*, 1997, **154**, 466-474.

30. D. J. Palao, A. Arauxo, M. Brunet, M. Marquez, M. Bernardo, J. Ferrer and E. Gonzalez-Monclus, *Prog. Neuro-Psychopharmacol. Biol. Psychiat.*, 1994, **18**, 155-164.
31. P. M. Haddad and A. Wieck, *Drugs*, 2004, **64**, 2291-2314.
32. K. Gao, D. E. Kemp, S. J. Ganocy, P. Gajwani, G. Xia and J. R. Calabrese, *J. Clin. Psychopharmacol.*, 2008, **28**, 203-209.
33. L.-M. Gunne and S. Bárány, *Psychopharmacol.*, 1976, **50**, 237-240.
34. A. N. Katchman, J. Koerner, T. Tosaka, R. L. Woosley and S. N. Ebert, *J. Pharmacol. Exp. Ther.*, 2006, **316**, 1098-1106.
35. A. Carlsson and M. Lindqvist, *Acta. Pharmacol. Toxicol.*, 1963, **20**, 140-144.
36. G. L. Patrick, *An Introduction to Medicinal Chemistry*, Oxford University Press, 2005.
37. A. Carlsson, *Biosci. Rep.*, 2001, **2**, 484-493.
38. I. Creese, D. Burt and S. Snyder, *Science*, 1976, **192**, 481-483.
39. P. Seeman, T. Lee, M. Chau-Wong and K. Wong, *Nature*, 1976, **261**, 717-719.
40. T. C. Manschrek, J. A. Laughery, C. C. Weisstein, D. Allen, B. Humblestone, M. Neville, H. Podlewski and N. Mitra, *Yale J. Biol. Med.*, 1988, **61**, 115-122.
41. B. Angrist, G. Sathanathan, S. Wilk and S. Gershon, *J. Psychiat. Res.*, 1974, **11**, 13-23.
42. A. Breier, T.-P. Su, R. Saunders, R. E. Carson, B. S. Kolachana, A. de Bartolomeis, D. R. Weinberger, N. Weisenfeld, A. K. Malhotra, W. C. Eckelman and D. Pickar, *Proc. Natl. Acad. Sci. U.S.A.*, 1997, **94**, 2569-2574.
43. J. Arnt, *Eur. J. Pharmacol.*, 1995, **283**, 55-62.
44. C. C. Tenn, P. J. Fletcher and S. Kapur, *Schiz. Res.*, 2003, **64**, 103-114.
45. M. Laruelle, A. Abi-Dargham, C. H. van Dyck, R. Gil, C. D. D'Souza, J. Erdos, E. McCance, W. Rosenblatt, C. Fingado, S. S. Zoghbi, R. M. Baldwin, J. P. Seibyl, J. H. Krystal, D. S. Charney and R. B. Innis, *Proc. Natl. Acad. Sci.*, 1996, **93**, 9235-9240.
46. A. Abi-Dargham, R. Gil, J. Krystal, R. M. Baldwin, J. P. Seibyl, M. Bowers, C. H. van Dyck, D. S. Charney, R. B. Innis and M. Laruelle, *Am. J. Psychiat.*, 1998, **155**, 761-767.
47. A. Breier, R. W. Buchanan, B. Kirkpatrick and O. R. Davis, *Am. J. Psychiat.*, 1994, **151**, 20-26.
48. M. A. Lee, K. Jayathilake and H. Y. Meltzer, *Schiz. Res.*, 1999, **37**, 1-11.
49. D. E. Casey, *Psychopharmacol.*, 1989, **99**, S47-S53.
50. K. Kuoppasalmi, R. Rimon, H. Naukkarinen, S. Lang, A. Sandqvist and E. Leinonen, *Schiz. Res.*, 1993, **10**, 29-32.
51. H. Y. Meltzer, *Psychopharmacol.*, 1989, **99**, S18-S27.
52. A. Safferman, J. A. Lieberman, J. M. Kane, S. Szymanski and B. Kinon, *Schiz. Bull.*, 1991, **17**, 247-261.
53. J. M. J. Alvir, J. A. Lieberman, A. Z. Safferman, J. L. Schwimmer and J. A. Schaaf, *New Engl. J. Med.*, 1993, **329**, 162-167.
54. M. D. Jibson and R. Tandon, *J. Psychiat. Res.*, 1998, **32**, 215-228.
55. C. M. Beasley, S. H. Hamilton, A. M. Crawford, M. A. Dellva, G. D. Tollefson, P. V. Tran, O. Blin and J.-N. Beuzen, *Euro. Neuropsychopharmacol.*, 1997, **7**, 125-137.

56. S. Leucht, G. Pitschel-Walz, D. Abraham and W. Kissling, *Schiz. Res.*, 1999, **35**, 51-68.
57. C. M. Beasley, M. A. Dellva, R. N. Tamura, H. Morgenstern, W. M. Glazer, K. Ferguson and G. D. Tollefson, *Br. J. Psychiat.*, 1999, **174**, 23-30.
58. S. R. David, C. C. Taylor, B. J. Kinon and A. Breier, *Clin. Ther.*, 2000, **22**, 1085-1096.
59. S. R. Marder and R. C. Meibach, *Am. J. Psychiat.*, 1994, **151**, 825-835.
60. P. F. Buckley, *Curr. Med. Res. Opin.*, 2004, **20**, 1357-1363.
61. J. Peuskens and C. G. G. Link, *Acta Psychiat. Scand.*, 1997, **96**, 265-273.
62. M. Atmaca, M. Kuloglu, E. Tezcan, H. Canatan and O. Gecici, *Arch. Med. Res.*, 2002, **33**, 562-565.
63. S. G. Potkin, M. Cohen and J. Panagides, *J. Clin. Psychiat.*, 2007, **68**, 1492-1500.
64. J. S. Kim, H. H. Kornhuber, W. Schmid-Burgk and B. Holzmüller, *Neurosci. Lett.*, 1980, **20**, 379-382.
65. W. O. Faustman, M. Bardgett, K. F. Faull, A. Pfefferbaum and J. G. Csernansky, *Biol. Psychiat.*, 1999, **45**, 68-75.
66. K. L. R. Jansen, *J. Psychoactive Drugs*, 2000, **32**, 419-433.
67. R. Allen and S. Young, *Am. J. Psych.*, 1978, **135**, 1081-1084.
68. E. D. Luby, B. D. Cohen, G. Rosenbaum, J. S. Gottlieb and R. Kelley, *Arch. Neur. Psych.*, 1959, **81**, 363-369.
69. A. K. Malhotra, C. M. Adler, S. D. Kennison, I. Elman, D. Pickar, A. Clifton and A. Breier, *Neuropsychopharmacol.*, 1997, **17**, 141-150.
70. J. H. Krystal, L. P. Karper, J. P. Seibyl, G. K. Freeman, R. Delaney, J. D. Bremner, G. R. Heninger, M. B. Bowers, Jr and D. S. Charney, *Arch. Gen. Psychiat.*, 1994, **51**, 199-214.
71. A. K. Malhotra, C. M. Adler, S. D. Kennison, I. Elman, D. Pickar and A. Breier, *Biol. Psychiat.*, 1997, **42**, 664-668.
72. S. M. Cochran, M. Kennedy, C. E. McKerchar, L. J. Steward, J. A. Pratt and B. J. Morris, *Neuropsychopharmacol.*, 2003, **28**, 265-275.
73. M. Chatterjee, S. Ganguly, M. Srivastava and G. Palit, *Behav. Brain Res.*, 2011, **216**, 247-254.
74. J. T. Coyle and G. Tsai, *Psychopharmacol.*, 2004, **174**, 32-38.
75. D. C. Javitt, I. Zylberman, S. R. Zukin and U. Heresco-Levy, *Am. J. Psychiat.*, 1994, **151**, 1234-1236.
76. U. Heresco-Levy, M. Ermilov, P. Lichtenberg, G. Bar and D. C. Javitt, *Biol. Psychiat.*, 2004, **55**, 165-171.
77. B. Moghaddam and B. W. Adams, *Science*, 1998, **281**, 1349-1352.
78. S. T. Patil, L. Zhang, F. Martenyi, S. L. Lowe, K. A. Jackson, B. V. Andreev, A. S. Avedisova, L. M. Bardenstein, I. Y. Gurovich, M. A. Morozova, S. N. Mosolov, N. G. Neznanov, A. M. Reznik, A. B. Smulevich, V. A. Tochilov, B. G. Johnson, J. A. Monn and D. D. Schoepp, *Nat. Med.*, 2007, **13**, 1102-1107.
79. B. J. Kinon, L. Zhang, B. A. Millen, O. O. Osuntokun, J. E. Williams, S. Kollack-Walker, K. Jackson, L. Kryzhanovskaya and N. Jarkova, *J. Clin. Psychopharmacol.*, 2011, **31**, 349-355.
80. D. Hoyer, J. P. Hannon and G. R. Martin, *Pharmacol. Biochem. Behav.*, 2002, **71**, 533-554.

81. D. Hoyer, D. E. Clarke, J. R. Fozard, P. R. Hartig, G. R. Martin, E. J. Mylecharane, P. R. Saxena and P. P. Humphrey, *Pharmacol. Rev.*, 1994, **46**, 157-203.
82. A. Meneses, *Neurosci. Biobehav. R.*, 1999, **23**, 1111-1125.
83. L. Irwin, *Biol. Psychiat.*, 1998, **44**, 151-162.
84. R. A. Glennon, M. Titeler and J. D. McKenney, *Life Sci.*, 1984, **35**, 2505-2511.
85. R. A. Glennon, S. M. Liebowitz and E. C. Mack, *J. Med. Chem.*, 1978, **21**, 822-825.
86. R. A. Glennon, S. M. Liebowitz and G. M. Anderson, *J. Med. Chem.*, 1980, **23**, 294-299.
87. R. A. Glennon and P. K. Gessner, *J. Med. Chem.*, 1979, **22**, 428-432.
88. R. A. Glennon, R. Raghupathi, P. Bartyzel, M. Teitler and S. Leonhardt, *J. Med. Chem.*, 1992, **35**, 734-740.
89. H. Y. Meltzer, S. Matsubara and J. C. Lee, *J. Pharmacol. Exp. Ther.*, 1989, **251**, 238-246.
90. J. A. Bard, J. Zgombick, N. Adham, P. Vaysse, T. A. Branchek and R. L. Weinshank, *J. Biol. Chem.*, 1993, **268**, 23422-23426.
91. B. Pouzet, *CNS Drug Reviews*, 2002, **8**, 90-100.
92. P. B. Hedlund and J. G. Sutcliffe, *Trend. Pharmacol. Sci.*, 2004, **25**, 481-486.
93. J. Neill, B. Grayson, D. N. C. Jones, J. J. Hagan and D. R. Thomas, *Schiz. Res.*, 2006, **81 (suppl)**, 37-308.
94. B. Pouzet, M. Didriksen and J. Arnt, *Pharmacol. Biochem. Behav.*, 2002, **71**, 655-665.
95. A. Schotte, P. Janssen, W. Gommeren, W. Luyten, P. Gompel, A. Lesage, K. Loore and J. Leysen, *Psychopharmacol.*, 1996, **124**, 57-73.
96. M. Horiguchi, M. Huang and H. Y. Meltzer, *J. Pharmacol. Exp. Ther.*, 2011, **338**, 605-614.
97. M. P. Caulfield and N. J. M. Birdsall, *Pharmacol. Rev.*, 1998, **50**, 279-290.
98. H. Neubauer, D. Sundland and S. Gershon, *J. Nerv. Ment. Dis.*, 1966, **142**, 265-277.
99. M. H. Schubert, K. A. Young and P. B. Hicks, *Biol. Psychiat.*, 2006, **60**, 530-533.
100. E. Scarpini, P. Schelterns and H. Feldman, *The Lancet Neurology*, 2003, **2**, 539-547.
101. H. E. Shannon, K. Rasmussen, F. P. Bymaster, J. C. Hart, S. C. Peters, M. D. B. Swedberg, L. Jeppesen, M. J. Sheardown, P. Sauerberg and A. Fink-Jensen, *Schiz. Res.*, 2000, **42**, 249-259.
102. M. B. Andersen, A. Fink-Jensen, L. Peacock, J. Gerlach, F. Bymaster, J. A. Lundbaek and T. Werge, *Neuropsychopharmacol.*, 2003, **28**, 1168-1175.
103. M. L. Woolley, H. J. Carter, J. E. Gartlon, J. M. Watson and L. A. Dawson, *Eur. J. Pharmacol.*, 2009, **603**, 147-149.
104. F. P. Bymaster, D. O. Calligaro, J. F. Falcone, R. D. Marsh, N. A. Moore, N. C. Tye, P. Seeman and D. T. Wong, *Neuropsychopharmacol.*, 1996, **14**, 87-96.
105. J. M. Rusted and D. M. Warburton, *Psychopharmacol.*, 1988, **96**, 145-152.
106. R. C. Petersen, *Psychopharmacol.*, 1977, **52**, 283-289.
107. R. Morphy and Z. Rankovic, *J. Med. Chem.*, 2005, **48**, 6523-6543.

108. R. Morphy, C. Kay and Z. Rankovic, *Drug Discov. Today*, 2004, **9**, 641-651.
109. B. L. Roth, S. C. Craigo, M. S. Choudhary, A. Uluer, F. J. Monsma, Y. Shen, H. Y. Meltzer and D. R. Sibley, *J. Pharmacol. Exp. Ther.*, 1994, **268**, 1403-1410.
110. M. Shahid, G. Walker, S. Zorn and E. Wong, *J. Psychopharmacol.*, 2009, **23**, 65-73.
111. H. R. Howard, J. A. Lowe, T. F. Seeger, P. A. Seymour, S. H. Zorn, P. R. Maloney, F. E. Ewing, M. E. Newman, A. W. Schmidt, J. S. Furman, G. L. Robinson, E. Jackson, C. Johnson and J. Morrone, *J. Med. Chem.*, 1996, **39**, 143-148.
112. R. M. Carnahan, B. C. Lund and P. J. Perry, *Pharmacotherapy*, 2001, **21**, 717-730.
113. Z. Rankovic and R. Morphy, eds., *Lead Generation Approaches In Drug Discovery*, John Wiley & Sons, Inc., 2010.
114. J. Kane, G. Honigfeld, J. Singer and H. Meltzer, *Arch. Gen. Psychiat.*, 1988, **45**, 789-796.
115. A. Ücok and W. Gaebel, *World Psychiat.*, 2008, **7**, 58-62.
116. K. J. Stanhope, N. R. Mirza, M. J. Bickerdike, J. L. Bright, N. R. Harrington, M. B. Hesselink, G. A. Kennett, S. Lightowler, M. J. Sheardown, R. Syed, R. L. Upton, G. Wadsworth, S. M. Weiss and A. Wyatt, *J. Pharmacol. Exp. Ther.*, 2001, **299**, 782-792.
117. X. P. Zeng, F. Le and E. Richelson, *Eur. J. Pharmacol.*, 1997, **321**, 349-354.
118. S. H. Zorn, S. B. Jones, K. M. Ward and D. R. Liston, *Eur. J. Pharmacol.: Mol. Pharmacol.*, 1994, **269**, R1-R2.
119. C. J. Suckling, J. A. Murphy, A. I. Khalaf, S.-z. Zhou, D. E. Lizos, A. N. van Nhien, H. Yasumatsu, A. McVie, L. C. Young, C. McCraw, P. G. Waterman, B. J. Morris, J. A. Pratt and A. L. Harvey, *Bioorg. Med. Chem. Lett.*, 2007, **17**, 2649-2655.
120. J. W. Warmke and B. Ganetzky, *Proc. Nat. Acad. Sci.*, 1994, **91**, 3438-3442.
121. J. Mitcheson, J. Chen, M. Lin, C. Culberson and M. Sanguinetti, *Proc. Nat. Acad. Sci. U.S.A.*, 2000, **97**, 12329-12333.
122. D. A. Doyle, J. M. Cabral, R. A. Pfuetzner, A. Kuo, J. M. Gulbis, S. L. Cohen, B. T. Chait and R. MacKinnon, *Science*, 1998, **280**, 69-77.
123. Y. Jiang, A. Lee, J. Chen, V. Ruta, M. Cadene, B. T. Chait and R. MacKinnon, *Nature*, 2003, **423**, 33-41.
124. S. B. Long, E. B. Campbell and R. MacKinnon, *Science*, 2005, **309**, 897-903.
125. R. MacKinnon, *Angew. Chem. Int. Ed.*, 2004, **43**, 4265-4277.
126. L. Heginbotham, Z. Lu, T. Abramson and R. MacKinnon, *Biophys. J.*, 1994, **66**, 1061-1067.
127. *The PyMOL Molecular Graphics System, Version 1.3, Schrödinger, LLC.*
128. M. E. Curran, I. Splawski, K. W. Timothy, G. M. Vincen, E. D. Green and M. T. Keating, *Cell*, 1995, **80**, 795-803.
129. V. Sami, *The Lancet*, 1999, **354**, 1625-1633.
130. M. C. Sanguinetti and M. Tristani-Firouzi, *Nature*, 2006, **440**, 463-469.
131. P. L. Hedley, P. Jørgensen, S. Schlamowitz, R. Wangari, J. Moolman-Smook, P. A. Brink, J. K. Kanters, V. A. Corfield and M. Christiansen, *Human Mutation*, 2009, **30**, 1486-1511.
132. A. M. Brown and D. Rampe, *Pharm. News*, 2000, **7**, 15-20.

133. M. Recanatini, E. Poluzzi, M. Masetti, A. Cavalli and F. De Ponti, *Med. Res. Rev.*, 2005, **25**, 133-166.
134. H. Suessbrich, S. Waldegger, F. Lang and A. E. Busch, *FEBS Lett.*, 1996, **385**, 77-80.
135. C. R. Scherer, C. Lerche, N. Decher, A. T. Dennis, P. Maier, E. Ficker, A. E. Busch, B. Wollnik and K. Steinmeyer, *Br. J. Pharmacol.*, 2002, **137**, 892-900.
136. S.-H. Jo, H.-K. Hong, S. H. Chong, H. S. Lee and H. Choe, *Pharmacol. Res.*, 2009, **60**, 429-437.
137. A. A. Paul, H. J. Witchel and J. C. Hancox, *Biochem. Biophys. Res. Comm.*, 2001, **280**, 1243-1250.
138. S.-Y. Lee, Y.-J. Kim, K.-T. Kim, H. Choe and S.-H. Jo, *Br. J. Pharmacol.*, 2006, **148**, 499-509.
139. S. Kongsamut, J. Kang, X.-L. Chen, J. Roehr and D. Rampe, *Eur. J. Pharmacol.*, 2002, **450**, 37-41.
140. P. Ball, *J. Antimicrob. Chemother.*, 2000, **45**, 557-559.
141. D. Fernandez, A. Ghanta, G. W. Kauffman and M. C. Sanguinetti, *J. Biol. Chem.*, 2004, **279**, 10120-10127.
142. P. S. Spector, M. E. Curran, M. T. Keating and M. C. Sanguinetti, *Circ. Res.*, 1996, **78**, 499-503.
143. D. del Camino, M. Holmgren, Y. Liu and G. Yellen, *Nature*, 2000, **403**, 321-325.
144. A. M. Aronov, *Drug Discovery Today*, 2005, **10**, 149-155.
145. M. C. Sanguinetti and J. S. Mitcheson, *Trends Pharmacol. Sci.*, 2005, **26**, 119-124.
146. R. A. Pearlstein, R. J. Vaz, J. Kang, X.-L. Chen, M. Preobrazhenskaya, A. E. Shchekotikhin, A. M. Korolev, L. N. Lysenkova, O. V. Miroshnikova, J. Hendrix and D. Rampe, *Bioorg. Med. Chem. Lett.*, 2003, **13**, 1829-1835.
147. R. Pearlstein, R. Vaz and D. Rampe, *J. Med. Chem.*, 2003, **46**, 2017-2022.
148. A. Cavalli, E. Poluzzi, F. De Ponti and M. Recanatini, *J. Med. Chem.*, 2002, **45**, 3844-3853.
149. S. Ekins, K. V. Balakin, N. Savchuk and Y. Ivanenkov, *J. Med. Chem.*, 2006, **49**, 5059-5071.
150. A. M. Aronov and B. B. Goldman, *Bioorg. Med. Chem.*, 2004, **12**, 2307-2315.
151. S. Ekins, W. J. Crumb, R. D. Sarazan, J. H. Wikel and S. A. Wrighton, *J. Pharmacol. Exp. Ther.*, 2002, **301**, 427-434.
152. C. Jamieson, E. M. Moir, Z. Rankovic and G. Wishart, *J. Med. Chem.*, 2006, **49**, 5029-5046.
153. M. J. Waring and C. Johnstone, *Bioorg. Med. Chem. Lett.*, 2007, **17**, 1759-1764.
154. R. J. Vaz, Z. Gao, J. Pribish, X. Chen, J. Levell, L. Davis, E. Albert, M. Brollo, A. Ugolini, D. M. Cramer, J. Cairns, K. Sides, F. Liu, J. Kwong, J. Kang, S. Rebello, M. Elliot, H. Lim, V. Chellaraj, R. W. Singleton and Y. Li, *Bioorg. Med. Chem. Lett.*, 2004, **14**, 6053-6056.
155. D. A. Price, D. Armour, M. de Groot, D. Leishman, C. Napier, M. Perros, B. L. Stammen and A. Wood, *Bioorg. Med. Chem. Lett.*, 2006, **16**, 4633-4637.

156. O. Irie, T. Kosaka, M. Kishida, J. Sakaki, K. Masuya, K. Konishi, F. Yokokawa, T. Ehara, A. Iwasaki, Y. Iwaki, Y. Hitomi, A. Toyao, H. Gunji, N. Teno, G. Iwasaki, H. Hirao, T. Kanazawa, K. Tanabe, P. C. Hiestand, M. Malcangio, A. J. Fox, S. J. Bevan, M. Yaqoob, A. J. Culshaw, T. W. Hart and A. Hallett, *Bioorg. Med. Chem. Lett.*, 2008, **18**, 5280-5284.
157. D. Rampe, B. Wible, A. M. Brown and R. C. Dage, *Mol. Pharmacol.*, 1993, **44**, 1240-1245.
158. X. Zhang, H. Hufnagel, T. Markotan, J. Lanter, C. Cai, C. Hou, M. Singer, E. Opas, S. McKenney, C. Crysler, D. Johnson and Z. Sui, *Bioorg. Med. Chem. Lett.*, 2011, **21**, 5577-5582.
159. B.-Y. Zhu, Z. J. Jia, P. Zhang, T. Su, W. Huang, E. Goldman, D. Tumas, V. Kadambi, P. Eddy, U. Sinha, R. M. Scarborough and Y. Song, *Bioorg. Med. Chem. Lett.*, 2006, **16**, 5507-5512.
160. A. U. Rao, A. Palani, X. Chen, Y. Huang, R. G. Aslanian, R. E. West Jr, S. M. Williams, R.-L. Wu, J. Hwa, C. Sondey and J. Lachowicz, *Bioorg. Med. Chem. Lett.*, 2009, **19**, 6176-6180.
161. H. Bregman, H. N. Nguyen, E. Feric, J. Ligutti, D. Liu, J. S. McDermott, B. Wilenkin, A. Zou, L. Huang, X. Li, S. I. McDonough and E. F. DiMauro, *Bioorg. Med. Chem. Lett.*
162. J. T. Sisko, T. J. Tucker, M. T. Bilodeau, C. A. Buser, P. A. Ciecko, K. E. Coll, C. Fernandes, J. B. Gibbs, T. J. Koester, N. Kohl, J. J. Lynch, X. Mao, D. McLoughlin, C. M. Miller-Stein, L. D. Rodman, K. W. Rickert, L. Sepp-Lorenzino, J. M. Shipman, K. A. Thomas, B. K. Wong and G. D. Hartman, *Bioorg. Med. Chem. Lett.*, 2006, **16**, 1146-1150.
163. D. G. Brown, D. L. Maier, M. A. Sylvester, T. N. Hoerter, E. Menhaji-Klotz, C. C. Lasota, L. T. Hirata, D. E. Wilkins, C. W. Scott, S. Trivedi, T. Chen, D. J. McCarthy, C. M. Maciag, E. J. Sutton, J. Cumberledge, D. Mathisen, J. Roberts, A. Gupta, F. Liu, C. S. Elmore, C. Alhambra, J. R. Krumrine, X. Wang, P. J. Ciaccio, M. W. Wood, J. B. Campbell, M. J. Johansson, J. Xia, X. Wen, J. Jiang, X. Wang, Z. Peng, T. Hu and J. Wang, *Bioorg. Med. Chem. Lett.*, 2011, **21**, 3399-3403.
164. S. D. Kuduk, R. K. Chang, C. N. Di Marco, D. R. Pitts, T. J. Greshock, L. Ma, M. Wittmann, M. A. Seager, K. A. Koeplinger, C. D. Thompson, G. D. Hartman, M. T. Bilodeau and W. J. Ray, *J. Med. Chem.*, 2011, **54**, 4773-4780.
165. D. A. Nugiel, J. R. Krumrine, D. C. Hill, J. R. Damewood, P. R. Bernstein, C. D. Sobotka-Briner, J. Liu, A. Zacco and M. E. Pierson, *J. Med. Chem.*, 2010, **53**, 1876-1880.
166. J. D. Hughes, J. Blagg, D. A. Price, S. Bailey, G. A. DeCrescenzo, R. V. Devraj, E. Ellsworth, Y. M. Fobian, M. E. Gibbs, R. W. Gilles, N. Greene, E. Huang, T. Krieger-Burke, J. Loesel, T. Wager, L. Whiteley and Y. Zhang, *Bioorg. Med. Chem. Lett.*, 2008, **18**, 4872-4875.
167. P. D. Leeson and B. Springthorpe, *Nat. Rev. Drug Discov.*, 2007, **6**, 881-890.
168. J. Clayden, N. Greeves, S. Warren and P. Wothers, *Organic Chemistry*, 1st edn., Oxford University Press, United States, 2001.
169. R. W. Brimblecombe, W. A. M. Duncan, G. J. Durant, C. R. Ganellin, M. E. Parsons and J. W. Black, *Br. J. Pharmacol.*, 2010, **160**, S52-S53.
170. H. K. M. Molinder, *J. Clin. Gastroenterol.*, 1994, **19**, 248-254.

171. J. W. Black, W. A. Duncan, C. J. Durant, C. R. Ganellin and E. M. Parsons, *Nature*, 1972, **236**, 385-390.
172. J. W. Black, *Angew. Chem. Int. Ed.*, 1989, **28**, 886-894.
173. R. A. Gray, *Phytopathol.*, 1955, **45**, 281-285.
174. F. Arcamone, S. Penco, P. Orezzi, V. Nicolella and A. Pirelli, *Nature*, 1964, **203**, 1064-1065.
175. C. J. Suckling, *Future Med. Chem.*, 2012, **4**, 971-989.
176. E. A. Steck, K. E. Kinnamon, D. S. Rane and W. L. Hanson, *Exp. Parasitol.*, 1981, **52**, 404-413.
177. R. D. Pearson and E. L. Hewlett, *Ann. Intern. Med.*, 1985, **103**, 782.
178. I. Kline, M. Gang, D. D. Tyrer, J. M. Venditti, E. W. Artis and A. Goldin, *Cancer Chemother. Rep.*, 1972, **3**, 1-69.
179. A. Pinner and F. Klein, *Ber. Dtsch. Chem. Ges.*, 1877, **10**, 1889-1897.
180. *Gaussian, Inc.*
181. M. E. Franks, G. R. Macpherson and W. D. Figg, *The Lancet*, 2004, **363**, 1802-1811.
182. *Top 200 Brand Name Drugs by US Retail Sales in 2010*, [http://cbc.arizona.edu/njardarson/group/sites/default/files/Top%202000%20Br and-name%20Drugs%20by%20US%20Retail%20Sales%20in%202010sm_0.pdf](http://cbc.arizona.edu/njardarson/group/sites/default/files/Top%202000%20Br%20and%20name%20Drugs%20by%20US%20Retail%20Sales%20in%202010sm_0.pdf), Accessed 03/02/2012.
183. A. Hirao, S. Itsuno, S. Nakahama and N. Yamazaki, *J. Chem. Soc., Chem. Commun.*, 1981, 315-317.
184. E. J. Corey, R. K. Bakshi and S. Shibata, *J. Am. Chem. Soc.*, 1987, **109**, 5551-5553.
185. E. J. Corey, R. K. Bakshi, S. Shibata, C. P. Chen and V. K. Singh, *J. Am. Chem. Soc.*, 1987, **109**, 7925-7926.
186. E. J. Corey and C. J. Helal, *Angew. Chem. Int. Ed.*, 1998, **37**, 1986-2012.
187. T. G. Bonner and J. C. Lockhart, *J. Chem. Soc.*, 1958, 3858-3861.
188. J. Kazius, R. McGuire and R. Bursi, *J. Med. Chem.*, 2004, **48**, 312-320.
189. J. C. Spain, *Ann. Rev. Microbiol.*, 1995, **49**, 523-555.
190. Y. Soro, F. Bamba, S. Siaka and J.-M. Coustard, *Tetrahedron Lett.*, 2006, **47**, 3315-3319.
191. H. He, M. Liu, Z. Zheng, Y. Liu, J. Xiao, R. Su, C. Hu, J. Li and S. Li, *Molecules*, 2006, **11**, 393-402.
192. J.-M. Contreras, Y. M. Rival, S. Chayer, J.-J. Bourguignon and C. G. Wermuth, *J. Med. Chem.*, 1999, **42**, 730-741.
193. K. Matsuno, T. Nakajima, M. Ichimura, N. A. Giese, J.-C. Yu, N. A. Lokker, J. Ushiki, S.-i. Ide, S. Oda and Y. Nomoto, *J. Med. Chem.*, 2002, **45**, 4513-4523.
194. *EP Pat.*, 2 186 802 A1, 2008.
195. A. Pictet and T. Spengler, *Ber. Dtsch. Chem. Ges.*, 1911, **44**, 2030-2036.
196. G. Tatsui, *J. Pharm. Soc. Jpn.*, 1928, **48**, 453-459.
197. G. J. Durant, J. C. Emmett, C. R. Ganellin, P. D. Miles, M. E. Parsons, H. D. Prain and G. R. White, *J. Med. Chem.*, 1977, **20**, 901-906.
198. W. K. Hagmann, *J. Med. Chem.*, 2008, **51**, 4359-4369.
199. S. Purser, P. R. Moore, S. Swallow and V. Gouverneur, *Chem. Soc. Rev.*, 2008, **37**, 320-330.

200. K. Uneyama, K. Tamura, H. Mizukami, K. Maeda and H. Watanabe, *J. Org. Chem.*, 1993, **58**, 32-35.
201. M. Jagodzinska, F. Huguenot, G. Candiani and M. Zanda, *ChemMedChem*, 2009, **4**, 49-51.
202. H. Wissmann and H.-J. Kleiner, *Angew. Chem. Int. Ed.*, 1980, **19**, 133-134.
203. A. Cameron, MSci thesis, University of Strathclyde, 2010.
204. *FDA Approves Merck's VICTRELIS™ (boceprevir), First-in-Class Oral Hepatitis C Virus (HCV) Protease Inhibitor*, http://www.merck.com/newsroom/news-release-archive/prescription-medicine-news/2011_0513.html, Accessed 12/04/2012.
205. A. Rodriguez, 2009.
206. F. Marchesi, M. Turriziani, G. Tortorelli, G. Avvisati, F. Torino and L. De Vecchis, *Pharmacol. Res.*, 2007, **56**, 275-287.
207. A. Gescher and M. D. Threadgill, *Pharmacol. Ther.*, 1987, **32**, 191-205.
208. A. Gescher, J. A. Hickman, R. J. Simmonds, M. F. G. Stevens and K. Vaughan, *Biochem. Pharmacol.*, 1981, **30**, 89-93.
209. T. A. Connors, P. M. Goddard, K. Merai, W. C. J. Ross and D. E. V. Wilman, *Biochem. Pharmacol.*, 1976, **25**, 241-246.
210. L. Walker, MSci thesis, University of Strathclyde, 2010.
211. J. Holub, K. O'Toole-Colin, A. Getzel, A. Argenti, M. Evans, D. Smith, G. Dalglish, S. Rifat, D. Wilson, B. Taylor, U. Miott, J. Glersaye, K. Lam, B. McCranor, J. Berkowitz, R. Miller, J. Lukens, K. Krumpe, J. Gupton and B. Burnham, *Molecules*, 2004, **9**, 134-157.
212. R. L. Stowe and N. M. Barnes, *Neuropharmacol.*, 1998, **37**, 1611-1619.
213. A. Newman-Tancredi, C. Chaput, S. Gavaudan, L. Verrielle and M. J. Millan, *Neuropsychopharmacol.*, 1998, **18**, 395-398.
214. A. Fletcher, E. A. Forster, D. J. Bill, G. Brown, I. A. Cliffe, J. E. Hartley, D. E. Jones, A. McLenachan, K. J. Stanhope, D. J. P. Critchley, K. J. Childs, V. C. Middlefell, L. Lanfumey, R. Corradetti, A.-M. Laporte, H. Gozlan, M. Hamon and C. T. Dourish, *Behav. Brain Res.*, 1995, **73**, 337-353.
215. J. Gross, C. E. Augelli-Szafran, S. Czeche, T. Friebe, J. C. Jaen, J. R. Penrose-Yi, R. D. Schwarz, E. Mutschler and G. Lambrecht, *Life Sci. Pharmacol. Lett.*, 1997, **60**, 1168-1168.
216. *human Muscarinic M4 Receptor*, http://www.perkinelmer.com/Content/TDLotSheet/RBHM4M400UA_598-506-A.pdf, Accessed 21/02/2012.
217. *human Serotonin 5-HT7 Receptor*, http://www.perkinelmer.com/Content/TDLotSheet/6110512400UA_594-194-A.pdf, Accessed 21/02/2012.
218. C. Yung-Chi and W. H. Prusoff, *Biochem. Pharmacol.*, 1973, **22**, 3099-3108.
219. P. J. S. Chiu, K. F. Marcoe, S. E. Bounds, C.-H. Lin, J.-J. Feng, A. Lin, F.-C. Cheng, W. J. Crumb and R. Mitchell, *J. Pharmacol. Sci.*, 2004, **95**, 311-319.
220. W. C. Still, M. Kahn and A. Mitra, *J. Org. Chem.*, 1978, **43**, 2923-2925.
221. *U.S. Pat.*, 20060199978, 2004.
222. L. K. Lukanov, A. P. Venkov and N. M. Mollov, *Synthesis*, 1987, **11**, 1031-1032.
223. S. Ruchirawat, M. Chaisupakitsin, N. Patranuwatana, J. L. Cashaw and V. E. Davis, *Synth. Commun.*, 1984, **14**, 1221-1228.

224. R. J. Murray and N. H. Cromwell, *J. Org. Chem.*, 1976, **41**, 3540-3545.
225. R. D. Haworth and D. Woodcock, *J. Chem. Soc.*, 1947, 95-96.
226. L. C. Xavier, J. J. Mohan, D. J. Mathre, A. S. Thompson, J. D. Carroll, E. G. Corley and R. Desmond, *Org. Synth. Coll.*, 1998, **9**, 676-687.
227. Y. Li and S. R. Prakash, *J. Labelled Compd. Radiopharm.*, 2005, **48**, 323-330.
228. J. Gynther, *Acta Chem. Scand., Ser. B*, 1988, **B42**, 433-441.
229. *Eur. Pat.*, 08826943.6, 2010.
230. A. J. Sleight, C. Carolo, N. Petit, C. Zwingelstein and A. Bourson, *Mol. Pharmacol.*, 1995, **47**, 99-103.

Chapter 8 - Appendix

8.1 Crystal data

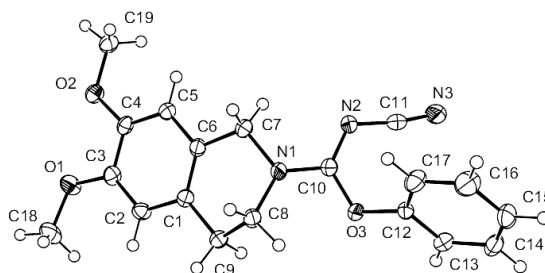


Table 1. Crystal data and structure refinement for suck0809.

Identification code	suck0809	
Empirical formula	C ₁₉ H ₁₉ N ₃ O ₃	
Formula weight	337.37	
Temperature	123(2) K	
Wavelength	0.71073 Å	
Crystal system	Triclinic	
Space group	P-1	
Unit cell dimensions	a = 7.9879(3) Å	α = 69.318(4)°.
	b = 9.6089(4) Å	β = 74.217(4)°.
	c = 12.3324(5) Å	γ = 89.564(3)°.
Volume	848.06(6) Å ³	
Z	2	
Density (calculated)	1.321 Mg/m ³	
Absorption coefficient	0.091 mm ⁻¹	
F(000)	356	
Crystal size	0.20 x 0.08 x 0.04 mm ³	
Theta range for data collection	2.66 to 27.99°.	
Index ranges	-10 ≤ h ≤ 10, -12 ≤ k ≤ 12, -16 ≤ l ≤ 16	
Reflections collected	15378	
Independent reflections	15378 [R(int) = 0.0000]	
Completeness to theta = 27.99°	99.9 %	
Absorption correction	Semi-empirical from equivalents	
Max. and min. transmission	1.00000 and 0.86023	
Refinement method	Full-matrix least-squares on F ²	
Data / restraints / parameters	15378 / 0 / 229	

Goodness-of-fit on F^2	1.077
Final R indices [$I > 2\sigma(I)$]	$R1 = 0.0497$, $wR2 = 0.1095$
R indices (all data)	$R1 = 0.0677$, $wR2 = 0.1136$
Largest diff. peak and hole	0.286 and $-0.345 \text{ e.}\text{\AA}^{-3}$

Table 2. Atomic coordinates ($\times 10^4$) and equivalent isotropic displacement parameters ($\text{\AA}^2 \times 10^3$) for suck0809. $U(\text{eq})$ is defined as one third of the trace of the orthogonalized U^{ij} tensor.

	x	y	z	$U(\text{eq})$
O(1)	7720(1)	7660(1)	-1387(1)	33(1)
O(2)	6599(1)	5265(1)	533(1)	28(1)
O(3)	14248(1)	8469(1)	2579(1)	28(1)
N(1)	12850(1)	7039(1)	1936(1)	26(1)
N(2)	12134(1)	6491(1)	3982(1)	27(1)
N(3)	11987(2)	7044(1)	5817(1)	40(1)
C(1)	11090(1)	7795(1)	149(1)	21(1)
C(2)	10162(1)	8212(1)	-720(1)	24(1)
C(3)	8688(1)	7351(1)	-575(1)	25(1)
C(4)	8084(1)	6045(1)	462(1)	22(1)
C(5)	8993(1)	5627(1)	1311(1)	22(1)
C(6)	10507(1)	6493(1)	1153(1)	22(1)
C(7)	11482(2)	5912(1)	2093(1)	29(1)
C(8)	13891(1)	7831(1)	676(1)	26(1)
C(9)	12719(1)	8745(1)	-30(1)	26(1)
C(10)	13060(1)	7293(1)	2881(1)	23(1)
C(11)	12142(2)	6864(1)	4919(1)	29(1)
C(12)	15435(1)	8337(1)	3263(1)	22(1)
C(13)	15788(1)	9574(1)	3516(1)	25(1)
C(14)	17025(2)	9536(1)	4120(1)	30(1)
C(15)	17881(2)	8272(1)	4465(1)	35(1)
C(16)	17518(2)	7047(1)	4201(1)	40(1)
C(17)	16290(2)	7070(1)	3591(1)	32(1)
C(18)	8522(2)	8770(2)	-2558(1)	37(1)
C(19)	5906(2)	3989(1)	1614(1)	30(1)

Table 3. Bond lengths [\AA] and angles [$^{\circ}$] for suck0809.

O(1)-C(3)	1.3770(13)
O(1)-C(18)	1.4327(13)
O(2)-C(4)	1.3745(12)
O(2)-C(19)	1.4293(13)
O(3)-C(10)	1.3578(13)
O(3)-C(12)	1.4089(12)
N(1)-C(10)	1.3237(13)
N(1)-C(8)	1.4684(13)
N(1)-C(7)	1.4693(13)
N(2)-C(10)	1.3071(13)
N(2)-C(11)	1.3276(14)
N(3)-C(11)	1.1540(14)
C(1)-C(6)	1.3841(14)
C(1)-C(2)	1.4087(15)
C(1)-C(9)	1.5149(14)
C(2)-C(3)	1.3777(15)
C(2)-H(2)	0.9500
C(3)-C(4)	1.4086(15)
C(4)-C(5)	1.3770(14)
C(5)-C(6)	1.4021(14)
C(5)-H(5)	0.9500
C(6)-C(7)	1.5131(15)
C(7)-H(7A)	0.9900
C(7)-H(7B)	0.9900
C(8)-C(9)	1.5156(15)
C(8)-H(8A)	0.9900
C(8)-H(8B)	0.9900
C(9)-H(9A)	0.9900
C(9)-H(9B)	0.9900
C(12)-C(17)	1.3788(15)
C(12)-C(13)	1.3795(15)
C(13)-C(14)	1.3835(16)
C(13)-H(13)	0.9500
C(14)-C(15)	1.3804(17)
C(14)-H(14)	0.9500

C(15)-C(16)	1.3790(17)
C(15)-H(15)	0.9500
C(16)-C(17)	1.3848(17)
C(16)-H(16)	0.9500
C(17)-H(17)	0.9500
C(18)-H(18A)	0.9800
C(18)-H(18B)	0.9800
C(18)-H(18C)	0.9800
C(19)-H(19A)	0.9800
C(19)-H(19B)	0.9800
C(19)-H(19C)	0.9800
C(3)-O(1)-C(18)	115.95(9)
C(4)-O(2)-C(19)	116.34(8)
C(10)-O(3)-C(12)	118.90(8)
C(10)-N(1)-C(8)	124.85(9)
C(10)-N(1)-C(7)	120.66(9)
C(8)-N(1)-C(7)	114.49(8)
C(10)-N(2)-C(11)	121.78(10)
C(6)-C(1)-C(2)	118.90(10)
C(6)-C(1)-C(9)	120.85(9)
C(2)-C(1)-C(9)	120.24(10)
C(3)-C(2)-C(1)	120.88(10)
C(3)-C(2)-H(2)	119.6
C(1)-C(2)-H(2)	119.6
O(1)-C(3)-C(2)	124.78(10)
O(1)-C(3)-C(4)	115.45(9)
C(2)-C(3)-C(4)	119.77(10)
O(2)-C(4)-C(5)	124.79(10)
O(2)-C(4)-C(3)	115.61(9)
C(5)-C(4)-C(3)	119.59(10)
C(4)-C(5)-C(6)	120.53(10)
C(4)-C(5)-H(5)	119.7
C(6)-C(5)-H(5)	119.7
C(1)-C(6)-C(5)	120.31(10)
C(1)-C(6)-C(7)	122.45(10)
C(5)-C(6)-C(7)	117.21(10)
N(1)-C(7)-C(6)	111.37(9)

N(1)-C(7)-H(7A)	109.4
C(6)-C(7)-H(7A)	109.4
N(1)-C(7)-H(7B)	109.4
C(6)-C(7)-H(7B)	109.4
H(7A)-C(7)-H(7B)	108.0
N(1)-C(8)-C(9)	109.04(9)
N(1)-C(8)-H(8A)	109.9
C(9)-C(8)-H(8A)	109.9
N(1)-C(8)-H(8B)	109.9
C(9)-C(8)-H(8B)	109.9
H(8A)-C(8)-H(8B)	108.3
C(1)-C(9)-C(8)	110.99(9)
C(1)-C(9)-H(9A)	109.4
C(8)-C(9)-H(9A)	109.4
C(1)-C(9)-H(9B)	109.4
C(8)-C(9)-H(9B)	109.4
H(9A)-C(9)-H(9B)	108.0
N(2)-C(10)-N(1)	121.15(10)
N(2)-C(10)-O(3)	125.14(10)
N(1)-C(10)-O(3)	113.67(9)
N(3)-C(11)-N(2)	171.44(12)
C(17)-C(12)-C(13)	121.74(10)
C(17)-C(12)-O(3)	121.46(10)
C(13)-C(12)-O(3)	116.65(10)
C(12)-C(13)-C(14)	119.02(11)
C(12)-C(13)-H(13)	120.5
C(14)-C(13)-H(13)	120.5
C(15)-C(14)-C(13)	120.00(11)
C(15)-C(14)-H(14)	120.0
C(13)-C(14)-H(14)	120.0
C(16)-C(15)-C(14)	120.24(11)
C(16)-C(15)-H(15)	119.9
C(14)-C(15)-H(15)	119.9
C(15)-C(16)-C(17)	120.46(12)
C(15)-C(16)-H(16)	119.8
C(17)-C(16)-H(16)	119.8
C(12)-C(17)-C(16)	118.54(11)

C(12)-C(17)-H(17)	120.7
C(16)-C(17)-H(17)	120.7
O(1)-C(18)-H(18A)	109.5
O(1)-C(18)-H(18B)	109.5
H(18A)-C(18)-H(18B)	109.5
O(1)-C(18)-H(18C)	109.5
H(18A)-C(18)-H(18C)	109.5
H(18B)-C(18)-H(18C)	109.5
O(2)-C(19)-H(19A)	109.5
O(2)-C(19)-H(19B)	109.5
H(19A)-C(19)-H(19B)	109.5
O(2)-C(19)-H(19C)	109.5
H(19A)-C(19)-H(19C)	109.5
H(19B)-C(19)-H(19C)	109.5

Symmetry transformations used to generate equivalent atoms:

Table 4. Anisotropic displacement parameters ($\text{\AA}^2 \times 10^3$) for suck0809. The anisotropic displacement factor exponent takes the form: $-2 \sum_{i,j} h_i a_i^* b_j^* U^{ij} + \dots + 2 \sum_i h_i a_i^* b_i^* U^{ii}$

	U11	U22	U33	U23	U13	U12
O(1)	22(1)	44(1)	27(1)	-3(1)	-11(1)	-3(1)
O(2)	20(1)	32(1)	30(1)	-9(1)	-10(1)	-4(1)
O(3)	34(1)	25(1)	26(1)	-3(1)	-16(1)	-8(1)
N(1)	24(1)	31(1)	20(1)	-6(1)	-7(1)	-8(1)
N(2)	32(1)	28(1)	20(1)	-6(1)	-9(1)	-6(1)
N(3)	52(1)	37(1)	23(1)	-9(1)	-3(1)	-13(1)
C(1)	18(1)	24(1)	22(1)	-10(1)	-4(1)	1(1)
C(2)	20(1)	26(1)	23(1)	-5(1)	-4(1)	-1(1)
C(3)	20(1)	30(1)	26(1)	-10(1)	-10(1)	4(1)
C(4)	17(1)	26(1)	27(1)	-14(1)	-6(1)	1(1)
C(5)	22(1)	23(1)	22(1)	-8(1)	-6(1)	-1(1)
C(6)	21(1)	26(1)	21(1)	-10(1)	-6(1)	-1(1)
C(7)	29(1)	31(1)	26(1)	-6(1)	-12(1)	-9(1)
C(8)	20(1)	34(1)	21(1)	-10(1)	-3(1)	-6(1)

C(9)	22(1)	28(1)	24(1)	-7(1)	-7(1)	-5(1)
C(10)	25(1)	23(1)	23(1)	-6(1)	-11(1)	-1(1)
C(11)	32(1)	23(1)	25(1)	-4(1)	-6(1)	-6(1)
C(12)	22(1)	25(1)	18(1)	-6(1)	-7(1)	-3(1)
C(13)	24(1)	22(1)	28(1)	-10(1)	-6(1)	1(1)
C(14)	27(1)	36(1)	31(1)	-19(1)	-6(1)	-6(1)
C(15)	29(1)	46(1)	34(1)	-13(1)	-16(1)	-2(1)
C(16)	37(1)	31(1)	52(1)	-11(1)	-22(1)	7(1)
C(17)	35(1)	26(1)	40(1)	-16(1)	-13(1)	3(1)
C(18)	29(1)	48(1)	27(1)	-3(1)	-14(1)	1(1)
C(19)	25(1)	32(1)	30(1)	-11(1)	-5(1)	-7(1)

Table 5. Hydrogen coordinates ($\times 10^4$) and isotropic displacement parameters ($\text{\AA}^2 \times 10^3$) for suck0809.

	x	y	z	U(eq)
H(2)	10558	9099	-1416	29
H(5)	8591	4744	2010	27
H(7A)	10648	5634	2911	35
H(7B)	12020	5003	2026	35
H(8A)	14408	7102	311	31
H(8B)	14855	8496	649	31
H(9A)	12381	9588	241	31
H(9B)	13368	9166	-901	31
H(13)	15190	10439	3278	30
H(14)	17284	10380	4298	36
H(15)	18724	8245	4885	42
H(16)	18115	6182	4439	47
H(17)	16041	6231	3403	38
H(18A)	8669	9739	-2481	55
H(18B)	7777	8841	-3086	55
H(18C)	9667	8488	-2908	55
H(19A)	6773	3260	1694	45
H(19B)	4841	3533	1575	45
H(19C)	5628	4298	2315	45

Table 6. Torsion angles [°] for suck0809.

C(6)-C(1)-C(2)-C(3)	0.60(16)
C(9)-C(1)-C(2)-C(3)	179.36(10)
C(18)-O(1)-C(3)-C(2)	13.41(16)
C(18)-O(1)-C(3)-C(4)	-166.22(10)
C(1)-C(2)-C(3)-O(1)	-178.85(10)
C(1)-C(2)-C(3)-C(4)	0.77(16)
C(19)-O(2)-C(4)-C(5)	4.56(15)
C(19)-O(2)-C(4)-C(3)	-176.23(9)
O(1)-C(3)-C(4)-O(2)	-0.81(14)
C(2)-C(3)-C(4)-O(2)	179.54(10)
O(1)-C(3)-C(4)-C(5)	178.45(10)
C(2)-C(3)-C(4)-C(5)	-1.20(16)
O(2)-C(4)-C(5)-C(6)	179.46(9)
C(3)-C(4)-C(5)-C(6)	0.27(16)
C(2)-C(1)-C(6)-C(5)	-1.54(15)
C(9)-C(1)-C(6)-C(5)	179.71(10)
C(2)-C(1)-C(6)-C(7)	176.30(10)
C(9)-C(1)-C(6)-C(7)	-2.45(16)
C(4)-C(5)-C(6)-C(1)	1.11(16)
C(4)-C(5)-C(6)-C(7)	-176.83(10)
C(10)-N(1)-C(7)-C(6)	135.49(11)
C(8)-N(1)-C(7)-C(6)	-43.66(13)
C(1)-C(6)-C(7)-N(1)	11.92(15)
C(5)-C(6)-C(7)-N(1)	-170.18(9)
C(10)-N(1)-C(8)-C(9)	-114.03(11)
C(7)-N(1)-C(8)-C(9)	65.07(12)
C(6)-C(1)-C(9)-C(8)	22.22(14)
C(2)-C(1)-C(9)-C(8)	-156.51(10)
N(1)-C(8)-C(9)-C(1)	-51.09(12)
C(11)-N(2)-C(10)-N(1)	-169.96(11)
C(11)-N(2)-C(10)-O(3)	7.38(18)
C(8)-N(1)-C(10)-N(2)	-176.74(11)
C(7)-N(1)-C(10)-N(2)	4.21(16)

C(8)-N(1)-C(10)-O(3)	5.63(15)
C(7)-N(1)-C(10)-O(3)	-173.42(10)
C(12)-O(3)-C(10)-N(2)	44.54(16)
C(12)-O(3)-C(10)-N(1)	-137.95(10)
C(10)-N(2)-C(11)-N(3)	174.0(9)
C(10)-O(3)-C(12)-C(17)	44.48(15)
C(10)-O(3)-C(12)-C(13)	-139.83(10)
C(17)-C(12)-C(13)-C(14)	-0.40(17)
O(3)-C(12)-C(13)-C(14)	-176.07(10)
C(12)-C(13)-C(14)-C(15)	-0.19(17)
C(13)-C(14)-C(15)-C(16)	0.47(19)
C(14)-C(15)-C(16)-C(17)	-0.2(2)
C(13)-C(12)-C(17)-C(16)	0.70(18)
O(3)-C(12)-C(17)-C(16)	176.16(11)
C(15)-C(16)-C(17)-C(12)	-0.4(2)

Symmetry transformations used to generate equivalent atoms:

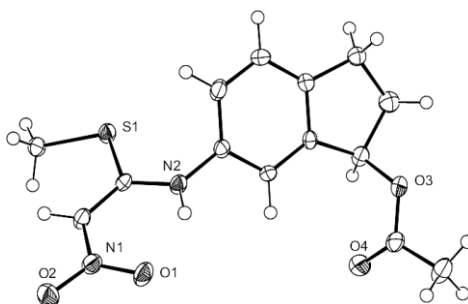


Table 1. Crystal data and structure refinement for try2.

Identification code	try2	
Empirical formula	C ₁₄ H ₁₆ N ₂ O ₄ S	
Formula weight	308.35	
Temperature	123(2) K	
Wavelength	0.71073 Å	
Crystal system	Monoclinic	
Space group	P2 ₁ /n	
Unit cell dimensions	a = 12.3537(5) Å	α = 90°.
	b = 7.4476(4) Å	β = 91.537(4)°.
	c = 15.1359(5) Å	γ = 90°.

Volume	1392.08(10) Å ³
Z	4
Density (calculated)	1.471 Mg/m ³
Absorption coefficient	0.251 mm ⁻¹
F(000)	648
Crystal size	0.20 x 0.06 x 0.02 mm ³
Theta range for data collection	3.05 to 28.51°.
Index ranges	-16<=h<=11, -9<=k<=8, -19<=l<=19
Reflections collected	6145
Independent reflections	3122 [R(int) = 0.0348]
Completeness to theta = 26.00°	99.9 %
Absorption correction	Semi-empirical from equivalents
Max. and min. transmission	1.00000 and 0.98631
Refinement method	Full-matrix least-squares on F ²
Data / restraints / parameters	3122 / 0 / 193
Goodness-of-fit on F ²	0.818
Final R indices [I>2sigma(I)]	R1 = 0.0382, wR2 = 0.0695
R indices (all data)	R1 = 0.0858, wR2 = 0.0751
Largest diff. peak and hole	0.344 and -0.261 e.Å ⁻³

Table 2. Atomic coordinates ($\times 10^4$) and equivalent isotropic displacement parameters (Å² $\times 10^3$) for try2. $U(\text{eq})$ is defined as one third of the trace of the orthogonalized U^{ij} tensor.

	x	y	z	U(eq)
S(1)	6435(1)	562(1)	3855(1)	22(1)
O(1)	6116(1)	-1520(2)	1034(1)	27(1)
O(2)	4374(1)	-1080(2)	1105(1)	31(1)
O(3)	11649(1)	-227(2)	1764(1)	24(1)
O(4)	10734(1)	1815(2)	948(1)	37(1)
N(1)	5301(1)	-1032(2)	1449(1)	23(1)
N(2)	7324(1)	-856(2)	2450(1)	21(1)
C(1)	5404(2)	-416(3)	2313(1)	21(1)
C(2)	6379(2)	-333(3)	2780(1)	17(1)
C(3)	5064(2)	1254(3)	4020(1)	23(1)
C(4)	8354(2)	-872(3)	2887(1)	18(1)

C(5)	9215(2)	-54(3)	2483(1)	19(1)
C(6)	10240(2)	-150(3)	2884(1)	17(1)
C(7)	10393(2)	-1019(3)	3693(1)	24(1)
C(8)	9526(2)	-1825(3)	4093(1)	30(1)
C(9)	8517(2)	-1765(3)	3688(1)	25(1)
C(10)	11287(2)	623(3)	2579(1)	23(1)
C(13)	11341(2)	553(3)	997(1)	25(1)
C(14)	11843(2)	-344(3)	227(1)	33(1)
C(11)	12127(6)	-23(10)	3286(5)	28(2)
C(12)	11543(4)	-1233(7)	3929(3)	22(1)
C(11A)	12097(6)	364(10)	3334(5)	25(2)
C(12A)	11567(5)	-646(8)	4042(3)	28(2)

Table 3. Bond lengths [\AA] and angles [$^\circ$] for try2.

S(1)-C(2)	1.7583(19)
S(1)-C(3)	1.7930(19)
O(1)-N(1)	1.255(2)
O(2)-N(1)	1.2458(19)
O(3)-C(13)	1.344(2)
O(3)-C(10)	1.468(2)
O(4)-C(13)	1.204(2)
N(1)-C(1)	1.388(2)
N(2)-C(2)	1.340(2)
N(2)-C(4)	1.419(2)
N(2)-H(1N)	0.884(19)
C(1)-C(2)	1.381(3)
C(1)-H(1)	0.9500
C(3)-H(3A)	0.9800
C(3)-H(3B)	0.9800
C(3)-H(3C)	0.9800
C(4)-C(5)	1.383(3)
C(4)-C(9)	1.392(3)
C(5)-C(6)	1.391(3)
C(5)-H(5)	0.9500
C(6)-C(7)	1.393(3)
C(6)-C(10)	1.500(3)
C(7)-C(8)	1.381(3)

C(7)-C(12)	1.464(5)
C(7)-C(12A)	1.555(6)
C(8)-C(9)	1.376(3)
C(8)-H(8)	0.9500
C(9)-H(9)	0.9500
C(10)-C(11A)	1.512(7)
C(10)-C(11)	1.548(8)
C(10)-H(10)	1.0000
C(13)-C(14)	1.492(3)
C(14)-H(14A)	0.9800
C(14)-H(14B)	0.9800
C(14)-H(14C)	0.9800
C(14)-H(14D)	0.9800
C(14)-H(14E)	0.9800
C(14)-H(14F)	0.9800
C(11)-C(12)	1.522(9)
C(11)-H(11C)	0.9900
C(11)-H(11D)	0.9900
C(12)-H(12A)	0.9900
C(12)-H(12B)	0.9900
C(11A)-C(12A)	1.476(9)
C(11A)-H(11A)	0.9900
C(11A)-H(11B)	0.9900
C(12A)-H(12C)	0.9900
C(12A)-H(12D)	0.9900
C(2)-S(1)-C(3)	102.91(9)
C(13)-O(3)-C(10)	117.00(16)
O(2)-N(1)-O(1)	121.54(16)
O(2)-N(1)-C(1)	117.58(17)
O(1)-N(1)-C(1)	120.89(16)
C(2)-N(2)-C(4)	127.43(16)
C(2)-N(2)-H(1N)	110.2(14)
C(4)-N(2)-H(1N)	122.4(14)
C(2)-C(1)-N(1)	123.63(18)
C(2)-C(1)-H(1)	118.2
N(1)-C(1)-H(1)	118.2
N(2)-C(2)-C(1)	123.49(17)

N(2)-C(2)-S(1)	116.26(14)
C(1)-C(2)-S(1)	120.22(15)
S(1)-C(3)-H(3A)	109.5
S(1)-C(3)-H(3B)	109.5
H(3A)-C(3)-H(3B)	109.5
S(1)-C(3)-H(3C)	109.5
H(3A)-C(3)-H(3C)	109.5
H(3B)-C(3)-H(3C)	109.5
C(5)-C(4)-C(9)	120.04(18)
C(5)-C(4)-N(2)	118.74(16)
C(9)-C(4)-N(2)	121.14(18)
C(4)-C(5)-C(6)	119.08(17)
C(4)-C(5)-H(5)	120.5
C(6)-C(5)-H(5)	120.5
C(5)-C(6)-C(7)	120.54(18)
C(5)-C(6)-C(10)	128.90(17)
C(7)-C(6)-C(10)	110.54(17)
C(8)-C(7)-C(6)	119.88(18)
C(8)-C(7)-C(12)	127.1(3)
C(6)-C(7)-C(12)	111.9(2)
C(8)-C(7)-C(12A)	131.0(2)
C(6)-C(7)-C(12A)	108.6(2)
C(12)-C(7)-C(12A)	17.6(3)
C(9)-C(8)-C(7)	119.67(18)
C(9)-C(8)-H(8)	120.2
C(7)-C(8)-H(8)	120.2
C(8)-C(9)-C(4)	120.8(2)
C(8)-C(9)-H(9)	119.6
C(4)-C(9)-H(9)	119.6
O(3)-C(10)-C(6)	112.19(16)
O(3)-C(10)-C(11A)	111.7(3)
C(6)-C(10)-C(11A)	106.1(3)
O(3)-C(10)-C(11)	103.5(3)
C(6)-C(10)-C(11)	103.6(3)
C(11A)-C(10)-C(11)	11.2(5)
O(3)-C(10)-H(10)	112.3
C(6)-C(10)-H(10)	112.3

C(11A)-C(10)-H(10)	101.6
C(11)-C(10)-H(10)	112.3
O(4)-C(13)-O(3)	123.56(19)
O(4)-C(13)-C(14)	124.9(2)
O(3)-C(13)-C(14)	111.5(2)
C(13)-C(14)-H(14A)	109.5
C(13)-C(14)-H(14B)	109.5
H(14A)-C(14)-H(14B)	109.5
C(13)-C(14)-H(14C)	109.5
H(14A)-C(14)-H(14C)	109.5
H(14B)-C(14)-H(14C)	109.5
C(13)-C(14)-H(14D)	109.5
H(14A)-C(14)-H(14D)	141.1
H(14B)-C(14)-H(14D)	56.3
H(14C)-C(14)-H(14D)	56.3
C(13)-C(14)-H(14E)	109.5
H(14A)-C(14)-H(14E)	56.3
H(14B)-C(14)-H(14E)	141.1
H(14C)-C(14)-H(14E)	56.3
H(14D)-C(14)-H(14E)	109.5
C(13)-C(14)-H(14F)	109.5
H(14A)-C(14)-H(14F)	56.3
H(14B)-C(14)-H(14F)	56.3
H(14C)-C(14)-H(14F)	141.1
H(14D)-C(14)-H(14F)	109.5
H(14E)-C(14)-H(14F)	109.5
C(12)-C(11)-C(10)	107.8(5)
C(12)-C(11)-H(11C)	110.1
C(10)-C(11)-H(11C)	110.1
C(12)-C(11)-H(11D)	110.1
C(10)-C(11)-H(11D)	110.1
H(11C)-C(11)-H(11D)	108.5
C(7)-C(12)-C(11)	104.6(4)
C(7)-C(12)-H(12A)	110.8
C(11)-C(12)-H(12A)	110.8
C(7)-C(12)-H(12B)	110.8
C(11)-C(12)-H(12B)	110.8

H(12A)-C(12)-H(12B)	108.9
C(12A)-C(11A)-C(10)	108.4(5)
C(12A)-C(11A)-H(11A)	110.0
C(10)-C(11A)-H(11A)	110.0
C(12A)-C(11A)-H(11B)	110.0
C(10)-C(11A)-H(11B)	110.0
H(11A)-C(11A)-H(11B)	108.4
C(11A)-C(12A)-C(7)	105.8(4)
C(11A)-C(12A)-H(12C)	110.6
C(7)-C(12A)-H(12C)	110.6
C(11A)-C(12A)-H(12D)	110.6
C(7)-C(12A)-H(12D)	110.6
H(12C)-C(12A)-H(12D)	108.7

Symmetry transformations used to generate equivalent atoms:

Table 4. Anisotropic displacement parameters ($\text{\AA}^2 \times 10^3$) for try2. The anisotropic displacement factor exponent takes the form: $-2 \sum h^2 a^{*2} U^{11} + \dots + 2 h k a^* b^* U^{12}$

	U11	U22	U33	U23	U13	U12
S(1)	19(1)	31(1)	18(1)	-5(1)	2(1)	1(1)
O(1)	24(1)	36(1)	21(1)	-6(1)	8(1)	0(1)
O(2)	22(1)	45(1)	26(1)	-5(1)	-4(1)	-2(1)
O(3)	20(1)	28(1)	23(1)	-1(1)	6(1)	3(1)
O(4)	37(1)	44(1)	30(1)	5(1)	4(1)	13(1)
N(1)	22(1)	29(1)	18(1)	-1(1)	2(1)	-5(1)
N(2)	19(1)	28(1)	15(1)	-5(1)	2(1)	0(1)
C(1)	18(1)	27(1)	17(1)	-4(1)	4(1)	-4(1)
C(2)	17(1)	17(1)	17(1)	2(1)	4(1)	-4(1)
C(3)	21(1)	29(1)	20(1)	-2(1)	4(1)	6(1)
C(4)	17(1)	21(1)	16(1)	-4(1)	2(1)	2(1)
C(5)	19(1)	23(1)	14(1)	1(1)	1(1)	2(1)
C(6)	15(1)	17(1)	19(1)	-4(1)	2(1)	2(1)
C(7)	20(1)	32(2)	21(1)	3(1)	2(1)	7(1)
C(8)	29(1)	40(2)	22(1)	13(1)	5(1)	11(1)

C(9)	21(1)	26(1)	29(1)	5(1)	9(1)	1(1)
C(10)	21(1)	25(1)	22(1)	-2(1)	3(1)	-2(1)
C(13)	18(1)	32(1)	24(1)	4(1)	3(1)	-7(1)
C(14)	29(1)	43(2)	28(1)	-5(1)	10(1)	-5(1)

Table 5. Hydrogen coordinates ($\times 10^4$) and isotropic displacement parameters ($\text{\AA}^2 \times 10^3$) for try2.

	x	y	z	U(eq)
H(1)	4769	-31	2598	25
H(3A)	4839	2092	3551	35
H(3B)	5016	1847	4595	35
H(3C)	4589	200	4003	35
H(5)	9109	564	1938	22
H(8)	9627	-2418	4645	36
H(9)	7924	-2340	3958	30
H(10)	11261	1962	2532	27
H(14A)	12302	-1337	438	49
H(14B)	12283	526	-89	49
H(14C)	11272	-812	-172	49
H(14D)	11602	255	-320	49
H(14E)	11622	-1608	207	49
H(14F)	12633	-267	290	49
H(11C)	12716	-695	3003	34
H(11D)	12448	1018	3604	34
H(12A)	11771	-2498	3861	26
H(12B)	11692	-853	4548	26
H(11A)	12734	-310	3128	30
H(11B)	12348	1544	3560	30
H(12C)	11558	71	4592	34
H(12D)	11954	-1787	4164	34
H(1N)	7226(16)	-1220(30)	1898(13)	30(6)

Table 6. Torsion angles [°] for try2.

O(2)-N(1)-C(1)-C(2)	178.5(2)
O(1)-N(1)-C(1)-C(2)	-1.6(3)
C(4)-N(2)-C(2)-C(1)	-177.9(2)
C(4)-N(2)-C(2)-S(1)	4.1(3)
N(1)-C(1)-C(2)-N(2)	-0.7(3)
N(1)-C(1)-C(2)-S(1)	177.17(15)
C(3)-S(1)-C(2)-N(2)	175.58(16)
C(3)-S(1)-C(2)-C(1)	-2.5(2)
C(2)-N(2)-C(4)-C(5)	-128.4(2)
C(2)-N(2)-C(4)-C(9)	54.7(3)
C(9)-C(4)-C(5)-C(6)	0.4(3)
N(2)-C(4)-C(5)-C(6)	-176.47(17)
C(4)-C(5)-C(6)-C(7)	-1.6(3)
C(4)-C(5)-C(6)-C(10)	-179.8(2)
C(5)-C(6)-C(7)-C(8)	1.3(3)
C(10)-C(6)-C(7)-C(8)	179.9(2)
C(5)-C(6)-C(7)-C(12)	170.5(3)
C(10)-C(6)-C(7)-C(12)	-10.9(3)
C(5)-C(6)-C(7)-C(12A)	-171.1(3)
C(10)-C(6)-C(7)-C(12A)	7.5(3)
C(6)-C(7)-C(8)-C(9)	0.1(3)
C(12)-C(7)-C(8)-C(9)	-167.3(3)
C(12A)-C(7)-C(8)-C(9)	170.5(3)
C(7)-C(8)-C(9)-C(4)	-1.2(3)
C(5)-C(4)-C(9)-C(8)	1.0(3)
N(2)-C(4)-C(9)-C(8)	177.8(2)
C(13)-O(3)-C(10)-C(6)	92.4(2)
C(13)-O(3)-C(10)-C(11A)	-148.7(3)
C(13)-O(3)-C(10)-C(11)	-156.6(3)
C(5)-C(6)-C(10)-O(3)	-66.5(3)
C(7)-C(6)-C(10)-O(3)	115.15(19)
C(5)-C(6)-C(10)-C(11A)	171.3(3)
C(7)-C(6)-C(10)-C(11A)	-7.1(4)
C(5)-C(6)-C(10)-C(11)	-177.4(3)
C(7)-C(6)-C(10)-C(11)	4.2(4)

C(10)-O(3)-C(13)-O(4)	-5.2(3)
C(10)-O(3)-C(13)-C(14)	174.89(17)
O(3)-C(10)-C(11)-C(12)	-113.6(4)
C(6)-C(10)-C(11)-C(12)	3.6(5)
C(11A)-C(10)-C(11)-C(12)	108(3)
C(8)-C(7)-C(12)-C(11)	-179.1(4)
C(6)-C(7)-C(12)-C(11)	12.7(5)
C(12A)-C(7)-C(12)-C(11)	-69.7(11)
C(10)-C(11)-C(12)-C(7)	-9.6(6)
O(3)-C(10)-C(11A)-C(12A)	-118.8(5)
C(6)-C(10)-C(11A)-C(12A)	3.8(6)
C(11)-C(10)-C(11A)-C(12A)	-75(3)
C(10)-C(11A)-C(12A)-C(7)	0.5(6)
C(8)-C(7)-C(12A)-C(11A)	-176.2(4)
C(6)-C(7)-C(12A)-C(11A)	-4.9(5)
C(12)-C(7)-C(12A)-C(11A)	99.2(12)

Symmetry transformations used to generate equivalent atoms:

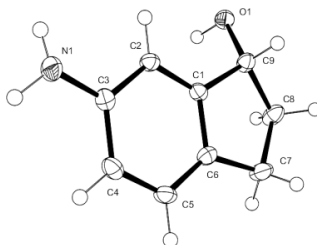


Table 1. Crystal data and structure refinement for donna79.

Identification code	donna79	
Empirical formula	C ₉ H ₁₁ N O	
Formula weight	149.19	
Temperature	123(2) K	
Wavelength	0.71073 Å	
Crystal system	Monoclinic	
Space group	P21	
Unit cell dimensions	a = 4.8474(2) Å	$\alpha = 90^\circ$.
	b = 6.5783(3) Å	$\beta = 93.045(4)^\circ$.

	$c = 12.1138(4) \text{ \AA}$	$\gamma = 90^\circ$.
Volume	$385.74(3) \text{ \AA}^3$	
Z	2	
Density (calculated)	1.284 Mg/m^3	
Absorption coefficient	0.084 mm^{-1}	
F(000)	160	
Crystal size	$0.42 \times 0.22 \times 0.10 \text{ mm}^3$	
Theta range for data collection	$3.37 \text{ to } 29.75^\circ$.	
Index ranges	$-6 \leq h \leq 6, -9 \leq k \leq 8, -15 \leq l \leq 16$	
Reflections collected	3827	
Independent reflections	1942 [R(int) = 0.0212]	
Completeness to theta = 27.00°	99.8 %	
Absorption correction	None	
Refinement method	Full-matrix least-squares on F^2	
Data / restraints / parameters	1942 / 1 / 112	
Goodness-of-fit on F^2	1.046	
Final R indices [$I > 2\sigma(I)$]	$R1 = 0.0418, wR2 = 0.0928$	
R indices (all data)	$R1 = 0.0494, wR2 = 0.0973$	
Absolute structure parameter	0.2(15)	
Largest diff. peak and hole	$0.276 \text{ and } -0.177 \text{ e.\AA}^{-3}$	

Table 2. Atomic coordinates ($\times 10^4$) and equivalent isotropic displacement parameters ($\text{\AA}^2 \times 10^3$) for donna79. $U(\text{eq})$ is defined as one third of the trace of the orthogonalized U^{ij} tensor.

	x	y	z	U(eq)
O(1)	-1362(3)	6522(2)	3665(1)	22(1)
N(1)	3536(3)	13892(2)	4214(1)	24(1)
C(1)	521(3)	9488(2)	2696(1)	17(1)
C(2)	1160(3)	10826(2)	3559(1)	18(1)
C(3)	3040(3)	12389(2)	3401(1)	19(1)
C(4)	4297(4)	12544(3)	2387(1)	22(1)
C(5)	3598(3)	11212(3)	1528(1)	22(1)
C(6)	1688(3)	9688(2)	1676(1)	19(1)
C(7)	530(4)	8117(3)	873(1)	26(1)
C(8)	-904(4)	6589(3)	1613(1)	25(1)

C(9)	-1508(3)	7743(2)	2687(1)	20(1)
------	----------	---------	---------	-------

Table 3. Bond lengths [Å] and angles [°] for donna79.

O(1)-C(9)	1.4299(18)
O(1)-H(1H)	0.94(3)
N(1)-C(3)	1.408(2)
N(1)-H(2N)	0.91(2)
N(1)-H(1N)	0.86(2)
C(1)-C(2)	1.388(2)
C(1)-C(6)	1.393(2)
C(1)-C(9)	1.511(2)
C(2)-C(3)	1.394(2)
C(2)-H(2)	0.9500
C(3)-C(4)	1.403(2)
C(4)-C(5)	1.389(2)
C(4)-H(4)	0.9500
C(5)-C(6)	1.383(2)
C(5)-H(5)	0.9500
C(6)-C(7)	1.507(2)
C(7)-C(8)	1.538(2)
C(7)-H(7A)	0.9900
C(7)-H(7B)	0.9900
C(8)-C(9)	1.548(2)
C(8)-H(8A)	0.9900
C(8)-H(8B)	0.9900
C(9)-H(9)	1.0000
C(9)-O(1)-H(1H)	107.7(15)
C(3)-N(1)-H(2N)	113.7(12)
C(3)-N(1)-H(1N)	115.7(14)
H(2N)-N(1)-H(1N)	112.7(17)
C(2)-C(1)-C(6)	121.57(15)
C(2)-C(1)-C(9)	127.30(14)
C(6)-C(1)-C(9)	111.09(13)
C(1)-C(2)-C(3)	119.04(15)
C(1)-C(2)-H(2)	120.5

C(3)-C(2)-H(2)	120.5
C(2)-C(3)-C(4)	119.42(15)
C(2)-C(3)-N(1)	120.71(15)
C(4)-C(3)-N(1)	119.71(15)
C(5)-C(4)-C(3)	120.66(16)
C(5)-C(4)-H(4)	119.7
C(3)-C(4)-H(4)	119.7
C(6)-C(5)-C(4)	119.91(15)
C(6)-C(5)-H(5)	120.0
C(4)-C(5)-H(5)	120.0
C(5)-C(6)-C(1)	119.32(15)
C(5)-C(6)-C(7)	129.95(15)
C(1)-C(6)-C(7)	110.72(14)
C(6)-C(7)-C(8)	103.66(13)
C(6)-C(7)-H(7A)	111.0
C(8)-C(7)-H(7A)	111.0
C(6)-C(7)-H(7B)	111.0
C(8)-C(7)-H(7B)	111.0
H(7A)-C(7)-H(7B)	109.0
C(7)-C(8)-C(9)	106.32(14)
C(7)-C(8)-H(8A)	110.5
C(9)-C(8)-H(8A)	110.5
C(7)-C(8)-H(8B)	110.5
C(9)-C(8)-H(8B)	110.5
H(8A)-C(8)-H(8B)	108.7
O(1)-C(9)-C(1)	114.67(12)
O(1)-C(9)-C(8)	114.69(14)
C(1)-C(9)-C(8)	103.11(13)
O(1)-C(9)-H(9)	108.0
C(1)-C(9)-H(9)	108.0
C(8)-C(9)-H(9)	108.0

Symmetry transformations used to generate equivalent atoms:

Table 4. Anisotropic displacement parameters ($\text{\AA}^2 \times 10^3$) for donna79. The anisotropic displacement factor exponent takes the form: $-2p^2 [h^2 a^* 2U^{11} + \dots + 2 h k a^* b^* U^{12}]$

	U11	U22	U33	U23	U13	U12
O(1)	24(1)	23(1)	19(1)	5(1)	1(1)	-4(1)
N(1)	28(1)	21(1)	23(1)	-2(1)	1(1)	-8(1)
C(1)	16(1)	17(1)	17(1)	5(1)	1(1)	0(1)
C(2)	20(1)	18(1)	15(1)	2(1)	2(1)	-2(1)
C(3)	18(1)	16(1)	21(1)	3(1)	-2(1)	-1(1)
C(4)	20(1)	19(1)	26(1)	4(1)	2(1)	-4(1)
C(5)	22(1)	25(1)	19(1)	6(1)	6(1)	-2(1)
C(6)	21(1)	20(1)	15(1)	1(1)	1(1)	2(1)
C(7)	37(1)	27(1)	16(1)	-1(1)	6(1)	-8(1)
C(8)	38(1)	19(1)	18(1)	1(1)	0(1)	-5(1)
C(9)	24(1)	18(1)	16(1)	3(1)	-1(1)	-4(1)

Table 5. Hydrogen coordinates ($\times 10^4$) and isotropic displacement parameters ($\text{\AA}^2 \times 10^3$) for donna79.

	x	y	z	U(eq)
H(2)	328	10677	4247	21
H(4)	5640	13571	2288	26
H(5)	4432	11347	839	26
H(7A)	2021	7454	476	32
H(7B)	-808	8736	325	32
H(8A)	313	5408	1780	30
H(8B)	-2644	6095	1240	30
H(9)	-3414	8321	2597	24
H(2N)	5170(50)	14560(30)	4156(15)	30(6)
H(1H)	450(60)	6030(40)	3764(18)	51(7)
H(1N)	3260(40)	13530(30)	4881(18)	37(6)

Table 6. Torsion angles [$^\circ$] for donna79.

C(6)-C(1)-C(2)-C(3)	-0.7(2)
---------------------	---------

C(9)-C(1)-C(2)-C(3)	-178.12(15)
C(1)-C(2)-C(3)-C(4)	-1.7(2)
C(1)-C(2)-C(3)-N(1)	173.71(15)
C(2)-C(3)-C(4)-C(5)	2.8(2)
N(1)-C(3)-C(4)-C(5)	-172.69(16)
C(3)-C(4)-C(5)-C(6)	-1.4(2)
C(4)-C(5)-C(6)-C(1)	-1.1(2)
C(4)-C(5)-C(6)-C(7)	177.78(16)
C(2)-C(1)-C(6)-C(5)	2.2(2)
C(9)-C(1)-C(6)-C(5)	179.94(15)
C(2)-C(1)-C(6)-C(7)	-176.91(15)
C(9)-C(1)-C(6)-C(7)	0.87(18)
C(5)-C(6)-C(7)-C(8)	166.60(17)
C(1)-C(6)-C(7)-C(8)	-14.44(19)
C(6)-C(7)-C(8)-C(9)	21.96(19)
C(2)-C(1)-C(9)-O(1)	-44.0(2)
C(6)-C(1)-C(9)-O(1)	138.34(15)
C(2)-C(1)-C(9)-C(8)	-169.41(15)
C(6)-C(1)-C(9)-C(8)	12.97(17)
C(7)-C(8)-C(9)-O(1)	-146.73(14)
C(7)-C(8)-C(9)-C(1)	-21.38(17)

Symmetry transformations used to generate equivalent atoms:

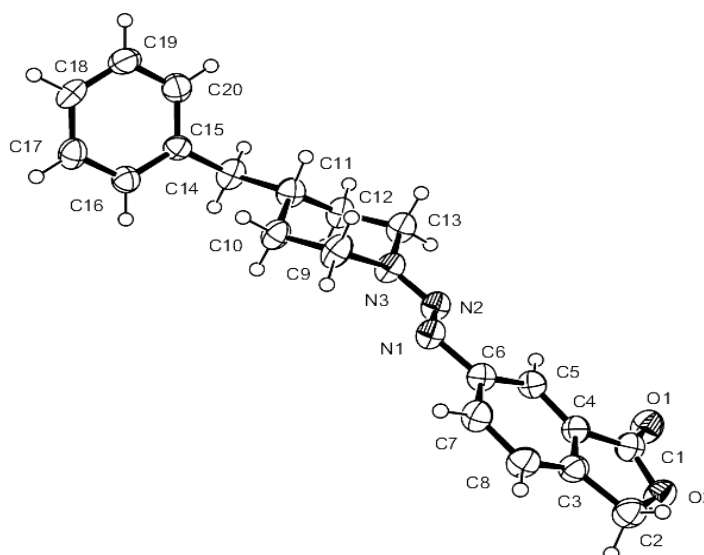


Table 1. Crystal data and structure refinement for donnamc1.

Identification code	donnamc1	
Empirical formula	C ₂₀ H ₂₁ N ₃ O ₂	
Formula weight	335.40	
Temperature	123(2) K	
Wavelength	1.54180 Å	
Crystal system	Monoclinic	
Space group	P2 ₁ /n	
Unit cell dimensions	a = 5.9760(3) Å	α = 90°.
	b = 17.3545(8) Å	β = 93.623(4)°.
	c = 16.6243(7) Å	γ = 90°.
Volume	1720.67(14) Å ³	
Z	4	
Density (calculated)	1.295 Mg/m ³	
Absorption coefficient	0.683 mm ⁻¹	
F(000)	712	
Crystal size	0.3 x 0.08 x 0.06 mm ³	
Theta range for data collection	5.10 to 73.18°.	
Index ranges	-5 ≤ h ≤ 7, -21 ≤ k ≤ 21, -15 ≤ l ≤ 20	
Reflections collected	8659	
Independent reflections	3379 [R(int) = 0.0210]	
Completeness to theta = 70.00°	99.7 %	
Absorption correction	Semi-empirical from equivalents	
Max. and min. transmission	1.00000 and 0.89116	

Refinement method	Full-matrix least-squares on F ²
Data / restraints / parameters	3379 / 2 / 266
Goodness-of-fit on F ²	1.034
Final R indices [I>2sigma(I)]	R1 = 0.0451, wR2 = 0.1093
R indices (all data)	R1 = 0.0618, wR2 = 0.1229
Largest diff. peak and hole	0.139 and -0.209 e.Å ⁻³

Table 2. Atomic coordinates ($\times 10^4$) and equivalent isotropic displacement parameters ($\text{\AA}^2 \times 10^3$) for donnamc1. U(eq) is defined as one third of the trace of the orthogonalized U^{ij} tensor.

	x	y	z	U(eq)
O(1)	1648(2)	4242(1)	8614(1)	53(1)
O(2)	5052(2)	4517(1)	9183(1)	48(1)
N(1)	3119(2)	1120(1)	9242(1)	39(1)
N(2)	1234(2)	1121(1)	8837(1)	40(1)
N(3)	331(2)	431(1)	8704(1)	42(1)
C(1)	3366(3)	4019(1)	8958(1)	42(1)
C(2)	6929(3)	4108(1)	9583(1)	48(1)
C(3)	6212(3)	3280(1)	9566(1)	39(1)
C(4)	4080(3)	3237(1)	9194(1)	37(1)
C(5)	2923(3)	2553(1)	9073(1)	36(1)
C(6)	4007(3)	1877(1)	9334(1)	37(1)
C(7)	6171(3)	1921(1)	9709(1)	42(1)
C(8)	7290(3)	2614(1)	9836(1)	44(1)
C(11)	-1683(3)	-1013(1)	8209(1)	42(1)
C(9)	1307(16)	-309(5)	9058(3)	47(1)
C(10)	796(5)	-979(2)	8492(2)	42(1)
C(12)	-2479(8)	-290(3)	7849(2)	41(1)
C(13)	-2028(5)	397(2)	8415(2)	44(1)
C(14)	-2230(5)	-1724(1)	7675(2)	43(1)
C(15)	-1629(7)	-2502(3)	8026(3)	35(1)
C(16)	380(7)	-2860(2)	7886(2)	40(1)
C(17)	885(6)	-3593(2)	8189(2)	43(1)
C(18)	-648(7)	-3979(2)	8639(2)	41(1)
C(19)	-2663(7)	-3628(4)	8798(4)	49(1)

C(20)	-3184(11)	-2902(4)	8488(3)	46(1)
C(18A)	28(17)	-3857(5)	8422(5)	41(1)
C(10A)	5(10)	-913(3)	8865(4)	42(1)
C(13A)	-1368(10)	480(3)	8013(4)	44(1)
C(19A)	-1875(18)	-3705(9)	8802(9)	49(1)
C(14A)	-3211(9)	-1647(3)	8161(3)	43(1)
C(17A)	843(14)	-3304(5)	7945(5)	43(1)
C(12A)	-2918(17)	-189(6)	8089(5)	41(1)
C(16A)	-222(16)	-2605(5)	7861(5)	40(1)
C(9A)	1550(30)	-225(10)	8841(8)	47(1)
C(20A)	-2850(20)	-2983(10)	8720(7)	46(1)
C(15A)	-2137(19)	-2442(7)	8241(6)	35(1)

Table 3. Bond lengths [\AA] and angles [$^\circ$] for donnamc1.

O(1)-C(1)	1.2062(19)
O(2)-C(1)	1.361(2)
O(2)-C(2)	1.453(2)
N(1)-N(2)	1.2755(17)
N(1)-C(6)	1.4216(19)
N(2)-N(3)	1.3257(18)
N(3)-C(9A)	1.361(19)
N(3)-C(13)	1.461(3)
N(3)-C(13A)	1.487(5)
N(3)-C(9)	1.513(8)
C(1)-C(4)	1.469(2)
C(2)-C(3)	1.498(2)
C(2)-H(2A)	0.9900
C(2)-H(2B)	0.9900
C(3)-C(4)	1.383(2)
C(3)-C(8)	1.385(2)
C(4)-C(5)	1.382(2)
C(5)-C(6)	1.396(2)
C(5)-H(5)	0.9500
C(6)-C(7)	1.402(2)
C(7)-C(8)	1.385(2)

C(7)-H(7)	0.9500
C(8)-H(8)	0.9500
C(11)-C(14A)	1.429(5)
C(11)-C(10A)	1.449(6)
C(11)-C(12)	1.458(5)
C(11)-C(10)	1.527(3)
C(11)-C(14)	1.542(3)
C(11)-C(12A)	1.616(10)
C(11)-H(11A)	1.011(10)
C(11)-H(11B)	1.001(10)
C(9)-C(10)	1.516(9)
C(9)-H(9A)	0.9900
C(9)-H(9B)	0.9900
C(10)-H(10A)	0.9900
C(10)-H(10B)	0.9900
C(12)-C(13)	1.532(5)
C(12)-H(12A)	0.9900
C(12)-H(12B)	0.9900
C(13)-H(13A)	0.9900
C(13)-H(13B)	0.9900
C(14)-C(15)	1.505(6)
C(14)-H(14A)	0.9900
C(14)-H(14B)	0.9900
C(15)-C(16)	1.385(5)
C(15)-C(20)	1.423(9)
C(16)-C(17)	1.395(4)
C(16)-H(16)	0.9500
C(17)-C(18)	1.391(4)
C(17)-H(17)	0.9500
C(18)-C(19)	1.390(5)
C(18)-H(18)	0.9500
C(19)-C(20)	1.389(9)
C(19)-H(19)	0.9500
C(20)-H(20)	0.9500
C(18A)-C(17A)	1.355(9)
C(18A)-C(19A)	1.361(13)
C(18A)-H(18A)	0.9500

C(10A)-C(9A)	1.510(19)
C(10A)-H(10C)	0.9900
C(10A)-H(10D)	0.9900
C(13A)-C(12A)	1.496(13)
C(13A)-H(13C)	0.9900
C(13A)-H(13D)	0.9900
C(19A)-C(20A)	1.38(2)
C(19A)-H(19A)	0.9500
C(14A)-C(15A)	1.523(13)
C(14A)-H(14C)	0.9900
C(14A)-H(14D)	0.9900
C(17A)-C(16A)	1.373(8)
C(17A)-H(17A)	0.9500
C(12A)-H(12C)	0.9900
C(12A)-H(12D)	0.9900
C(16A)-C(15A)	1.372(9)
C(16A)-H(16A)	0.9500
C(9A)-H(9A1)	0.9900
C(9A)-H(9A2)	0.9900
C(20A)-C(15A)	1.319(19)
C(20A)-H(20A)	0.9500
C(1)-O(2)-C(2)	110.62(13)
N(2)-N(1)-C(6)	111.53(12)
N(1)-N(2)-N(3)	115.04(12)
N(2)-N(3)-C(9A)	121.3(8)
N(2)-N(3)-C(13)	117.70(15)
C(9A)-N(3)-C(13)	121.0(8)
N(2)-N(3)-C(13A)	109.1(2)
C(9A)-N(3)-C(13A)	120.6(8)
C(13)-N(3)-C(13A)	31.9(2)
N(2)-N(3)-C(9)	124.0(4)
C(9A)-N(3)-C(9)	15.8(8)
C(13)-N(3)-C(9)	115.7(4)
C(13A)-N(3)-C(9)	125.2(4)
O(1)-C(1)-O(2)	121.35(15)
O(1)-C(1)-C(4)	130.26(16)
O(2)-C(1)-C(4)	108.38(13)

O(2)-C(2)-C(3)	104.39(13)
O(2)-C(2)-H(2A)	110.9
C(3)-C(2)-H(2A)	110.9
O(2)-C(2)-H(2B)	110.9
C(3)-C(2)-H(2B)	110.9
H(2A)-C(2)-H(2B)	108.9
C(4)-C(3)-C(8)	119.75(14)
C(4)-C(3)-C(2)	108.33(14)
C(8)-C(3)-C(2)	131.91(15)
C(5)-C(4)-C(3)	123.35(14)
C(5)-C(4)-C(1)	128.38(14)
C(3)-C(4)-C(1)	108.26(14)
C(4)-C(5)-C(6)	117.32(14)
C(4)-C(5)-H(5)	121.3
C(6)-C(5)-H(5)	121.3
C(5)-C(6)-C(7)	119.25(14)
C(5)-C(6)-N(1)	125.49(14)
C(7)-C(6)-N(1)	115.25(13)
C(8)-C(7)-C(6)	122.58(15)
C(8)-C(7)-H(7)	118.7
C(6)-C(7)-H(7)	118.7
C(3)-C(8)-C(7)	117.74(15)
C(3)-C(8)-H(8)	121.1
C(7)-C(8)-H(8)	121.1
C(14A)-C(11)-C(10A)	123.1(3)
C(14A)-C(11)-C(12)	116.7(3)
C(10A)-C(11)-C(12)	113.6(3)
C(14A)-C(11)-C(10)	130.6(2)
C(10A)-C(11)-C(10)	31.5(2)
C(12)-C(11)-C(10)	112.3(2)
C(14A)-C(11)-C(14)	40.6(2)
C(10A)-C(11)-C(14)	129.9(3)
C(12)-C(11)-C(14)	113.6(2)
C(10)-C(11)-C(14)	111.96(18)
C(14A)-C(11)-C(12A)	112.9(5)
C(10A)-C(11)-C(12A)	106.2(4)
C(12)-C(11)-C(12A)	18.6(3)

C(10)-C(11)-C(12A)	115.5(4)
C(14)-C(11)-C(12A)	123.9(4)
C(14A)-C(11)-H(11A)	64.9(15)
C(10A)-C(11)-H(11A)	74.9(15)
C(12)-C(11)-H(11A)	109.5(15)
C(10)-C(11)-H(11A)	104.7(15)
C(14)-C(11)-H(11A)	104.1(16)
C(12A)-C(11)-H(11A)	91.2(16)
C(14A)-C(11)-H(11B)	104(3)
C(10A)-C(11)-H(11B)	109(3)
C(12)-C(11)-H(11B)	80(3)
C(10)-C(11)-H(11B)	78(3)
C(14)-C(11)-H(11B)	64(3)
C(12A)-C(11)-H(11B)	99(3)
H(11A)-C(11)-H(11B)	167(3)
N(3)-C(9)-C(10)	110.6(4)
N(3)-C(9)-H(9A)	109.5
C(10)-C(9)-H(9A)	109.5
N(3)-C(9)-H(9B)	109.5
C(10)-C(9)-H(9B)	109.5
H(9A)-C(9)-H(9B)	108.1
C(9)-C(10)-C(11)	112.0(4)
C(9)-C(10)-H(10A)	109.2
C(11)-C(10)-H(10A)	109.2
C(9)-C(10)-H(10B)	109.2
C(11)-C(10)-H(10B)	109.2
H(10A)-C(10)-H(10B)	107.9
C(11)-C(12)-C(13)	112.2(3)
C(11)-C(12)-H(12A)	109.2
C(13)-C(12)-H(12A)	109.2
C(11)-C(12)-H(12B)	109.2
C(13)-C(12)-H(12B)	109.2
H(12A)-C(12)-H(12B)	107.9
N(3)-C(13)-C(12)	111.2(3)
N(3)-C(13)-H(13A)	109.4
C(12)-C(13)-H(13A)	109.4
N(3)-C(13)-H(13B)	109.4

C(12)-C(13)-H(13B)	109.4
H(13A)-C(13)-H(13B)	108.0
C(15)-C(14)-C(11)	117.3(2)
C(15)-C(14)-H(14A)	108.0
C(11)-C(14)-H(14A)	108.0
H(11B)-C(14)-H(14A)	121.7
C(15)-C(14)-H(14B)	108.0
C(11)-C(14)-H(14B)	108.0
H(11B)-C(14)-H(14B)	68.8
H(14A)-C(14)-H(14B)	107.2
C(16)-C(15)-C(20)	118.3(5)
C(16)-C(15)-C(14)	121.7(4)
C(20)-C(15)-C(14)	119.9(4)
C(15)-C(16)-C(17)	121.3(4)
C(15)-C(16)-H(16)	119.4
C(17)-C(16)-H(16)	119.4
C(18)-C(17)-C(16)	119.9(3)
C(18)-C(17)-H(17)	120.0
C(16)-C(17)-H(17)	120.0
C(19)-C(18)-C(17)	120.0(4)
C(19)-C(18)-H(18)	120.0
C(17)-C(18)-H(18)	120.0
C(20)-C(19)-C(18)	120.2(5)
C(20)-C(19)-H(19)	119.9
C(18)-C(19)-H(19)	119.9
C(19)-C(20)-C(15)	120.3(6)
C(19)-C(20)-H(20)	119.9
C(15)-C(20)-H(20)	119.9
C(17A)-C(18A)-C(19A)	118.4(9)
C(17A)-C(18A)-H(18A)	120.8
C(19A)-C(18A)-H(18A)	120.8
C(11)-C(10A)-C(9A)	118.2(7)
C(11)-C(10A)-H(10C)	107.8
C(9A)-C(10A)-H(10C)	107.8
H(11A)-C(10A)-H(10C)	111.3
C(11)-C(10A)-H(10D)	107.8
C(9A)-C(10A)-H(10D)	107.8

H(11A)-C(10A)-H(10D)	69.3
H(10C)-C(10A)-H(10D)	107.1
N(3)-C(13A)-C(12A)	106.6(5)
N(3)-C(13A)-H(13C)	110.4
C(12A)-C(13A)-H(13C)	110.4
N(3)-C(13A)-H(13D)	110.4
C(12A)-C(13A)-H(13D)	110.4
H(13C)-C(13A)-H(13D)	108.6
C(18A)-C(19A)-C(20A)	119.2(13)
C(18A)-C(19A)-H(19A)	120.4
C(20A)-C(19A)-H(19A)	120.4
C(11)-C(14A)-C(15A)	115.4(6)
C(11)-C(14A)-H(14C)	108.4
C(15A)-C(14A)-H(14C)	108.4
H(11A)-C(14A)-H(14C)	134.1
C(11)-C(14A)-H(14D)	108.4
C(15A)-C(14A)-H(14D)	108.4
H(11A)-C(14A)-H(14D)	68.3
H(14C)-C(14A)-H(14D)	107.5
C(18A)-C(17A)-C(16A)	120.3(10)
C(18A)-C(17A)-H(17A)	119.8
C(16A)-C(17A)-H(17A)	119.8
C(13A)-C(12A)-C(11)	114.7(7)
C(13A)-C(12A)-H(12C)	108.6
C(11)-C(12A)-H(12C)	108.6
C(13A)-C(12A)-H(12D)	108.6
C(11)-C(12A)-H(12D)	108.6
H(12C)-C(12A)-H(12D)	107.6
C(15A)-C(16A)-C(17A)	122.0(11)
C(15A)-C(16A)-H(16A)	119.0
C(17A)-C(16A)-H(16A)	119.0
N(3)-C(9A)-C(10A)	110.2(13)
N(3)-C(9A)-H(9A1)	109.6
C(10A)-C(9A)-H(9A1)	109.6
N(3)-C(9A)-H(9A2)	109.6
C(10A)-C(9A)-H(9A2)	109.6
H(9A1)-C(9A)-H(9A2)	108.1

C(15A)-C(20A)-C(19A) 123.8(14)
 C(15A)-C(20A)-H(20A) 118.1
 C(19A)-C(20A)-H(20A) 118.1
 C(20A)-C(15A)-C(16A) 116.2(12)
 C(20A)-C(15A)-C(14A) 123.3(10)
 C(16A)-C(15A)-C(14A) 120.4(9)

Symmetry transformations used to generate equivalent atoms:

Table 4. Anisotropic displacement parameters ($\text{\AA}^2 \times 10^3$) for donnamc1. The anisotropic displacement factor exponent takes the form: $-2 \sum_{i,j} h_i a_i^* b_j^* U^{ij}$

	U ¹¹	U ²²	U ³³	U ²³	U ¹³	U ¹²
O(1)	53(1)	42(1)	62(1)	4(1)	-10(1)	9(1)
O(2)	50(1)	38(1)	55(1)	2(1)	-4(1)	-1(1)
N(1)	40(1)	36(1)	40(1)	-2(1)	-8(1)	2(1)
N(2)	40(1)	38(1)	39(1)	-2(1)	-7(1)	1(1)
N(3)	42(1)	34(1)	47(1)	1(1)	-12(1)	0(1)
C(1)	45(1)	39(1)	42(1)	-1(1)	0(1)	2(1)
C(2)	42(1)	44(1)	57(1)	1(1)	-4(1)	-1(1)
C(3)	39(1)	38(1)	41(1)	-1(1)	1(1)	-1(1)
C(4)	39(1)	36(1)	35(1)	0(1)	0(1)	4(1)
C(5)	35(1)	38(1)	35(1)	0(1)	-2(1)	4(1)
C(6)	38(1)	37(1)	34(1)	-1(1)	-2(1)	1(1)
C(7)	41(1)	39(1)	46(1)	0(1)	-8(1)	6(1)
C(8)	37(1)	44(1)	51(1)	0(1)	-9(1)	0(1)
C(11)	41(1)	41(1)	43(1)	-5(1)	-7(1)	1(1)
C(9)	49(3)	32(2)	55(4)	5(2)	-20(3)	3(2)
C(10)	43(2)	33(1)	50(2)	4(1)	-8(1)	3(1)
C(12)	44(2)	36(2)	40(2)	-4(2)	-12(2)	4(1)
C(13)	41(2)	38(1)	52(2)	-2(1)	-12(1)	3(1)
C(14)	48(1)	38(1)	41(1)	-2(1)	-11(1)	1(1)
C(15)	30(3)	36(1)	39(3)	0(2)	-2(2)	-2(2)
C(16)	37(2)	38(3)	44(1)	0(2)	2(1)	2(2)
C(17)	41(1)	36(2)	52(2)	-2(1)	-7(2)	5(2)

C(18)	55(3)	27(2)	42(2)	3(1)	-5(2)	-7(1)
C(19)	59(3)	41(2)	49(1)	-4(1)	14(3)	-13(3)
C(20)	36(2)	43(2)	59(3)	-11(3)	0(2)	-2(2)
C(18A)	55(3)	27(2)	42(2)	3(1)	-5(2)	-7(1)
C(10A)	43(2)	33(1)	50(2)	4(1)	-8(1)	3(1)
C(13A)	41(2)	38(1)	52(2)	-2(1)	-12(1)	3(1)
C(19A)	59(3)	41(2)	49(1)	-4(1)	14(3)	-13(3)
C(14A)	48(1)	38(1)	41(1)	-2(1)	-11(1)	1(1)
C(17A)	41(1)	36(2)	52(2)	-2(1)	-7(2)	5(2)
C(12A)	44(2)	36(2)	40(2)	-4(2)	-12(2)	4(1)
C(16A)	37(2)	38(3)	44(1)	0(2)	2(1)	2(2)
C(9A)	49(3)	32(2)	55(4)	5(2)	-20(3)	3(2)
C(20A)	36(2)	43(2)	59(3)	-11(3)	0(2)	-2(2)
C(15A)	30(3)	36(1)	39(3)	0(2)	-2(2)	-2(2)

Table 5. Hydrogen coordinates ($\times 10^4$) and isotropic displacement parameters ($\text{\AA}^2 \times 10^3$) for donnamc1.

	x	y	z	U(eq)
H(2A)	7213	4290	10144	57
H(2B)	8306	4179	9291	57
H(5)	1450	2543	8823	44
H(7)	6898	1458	9883	51
H(8)	8748	2631	10098	53
H(11A)	-2490(40)	-1115(15)	8715(10)	50
H(11B)	-940(80)	-1040(30)	7687(16)	50
H(9A)	666	-412	9582	56
H(9B)	2951	-253	9154	56
H(10A)	1225	-1467	8770	51
H(10B)	1707	-930	8017	51
H(12A)	-4111	-328	7710	49
H(12B)	-1726	-201	7344	49
H(13A)	-2442	880	8127	53
H(13B)	-2972	351	8881	53

H(14A)	-3860	-1720	7526	51
H(14B)	-1449	-1664	7171	51
H(16)	1434	-2601	7577	47
H(17)	2276	-3828	8089	52
H(18)	-319	-4482	8837	50
H(19)	-3687	-3885	9121	59
H(20)	-4583	-2671	8585	56
H(18A)	767	-4339	8489	50
H(10C)	949	-1382	8893	51
H(10D)	-773	-887	9372	51
H(13C)	-632	454	7496	53
H(13D)	-2207	971	8031	53
H(19A)	-2529	-4090	9119	59
H(14C)	-4094	-1621	7638	51
H(14D)	-4272	-1588	8591	51
H(17A)	2158	-3400	7669	52
H(12C)	-3946	-214	7598	49
H(12D)	-3841	-97	8553	49
H(16A)	385	-2222	7528	47
H(9A1)	2443	-181	9361	56
H(9A2)	2592	-295	8408	56
H(20A)	-4094	-2871	9027	56

Table 6. Torsion angles [°] for donnamc1.

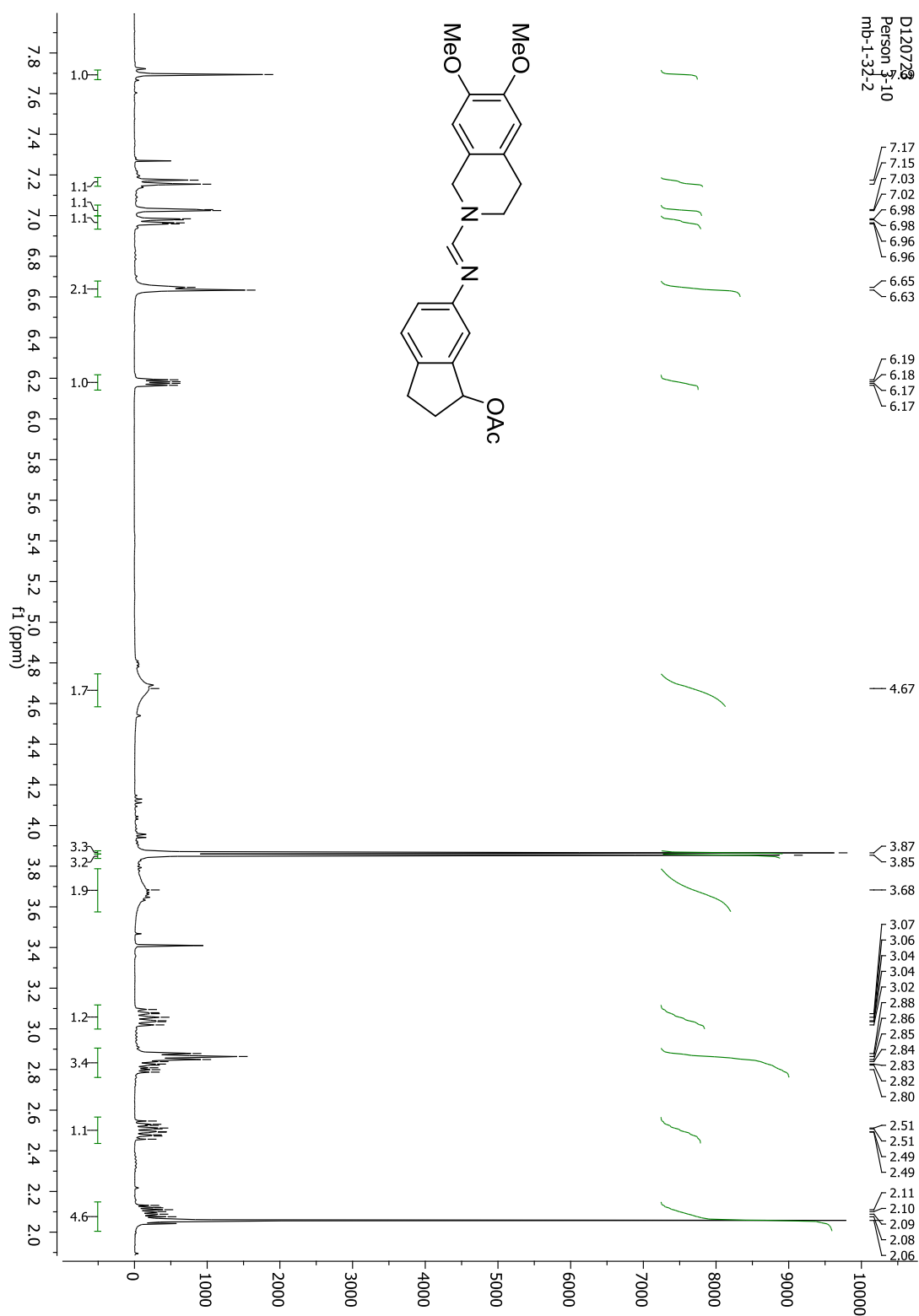
C(6)-N(1)-N(2)-N(3)	178.05(12)
N(1)-N(2)-N(3)-C(9A)	-13.2(7)
N(1)-N(2)-N(3)-C(13)	165.95(18)
N(1)-N(2)-N(3)-C(13A)	-160.4(3)
N(1)-N(2)-N(3)-C(9)	5.2(4)
C(2)-O(2)-C(1)-O(1)	-179.91(16)
C(2)-O(2)-C(1)-C(4)	-0.80(17)
C(1)-O(2)-C(2)-C(3)	0.97(18)
O(2)-C(2)-C(3)-C(4)	-0.78(18)
O(2)-C(2)-C(3)-C(8)	178.29(17)

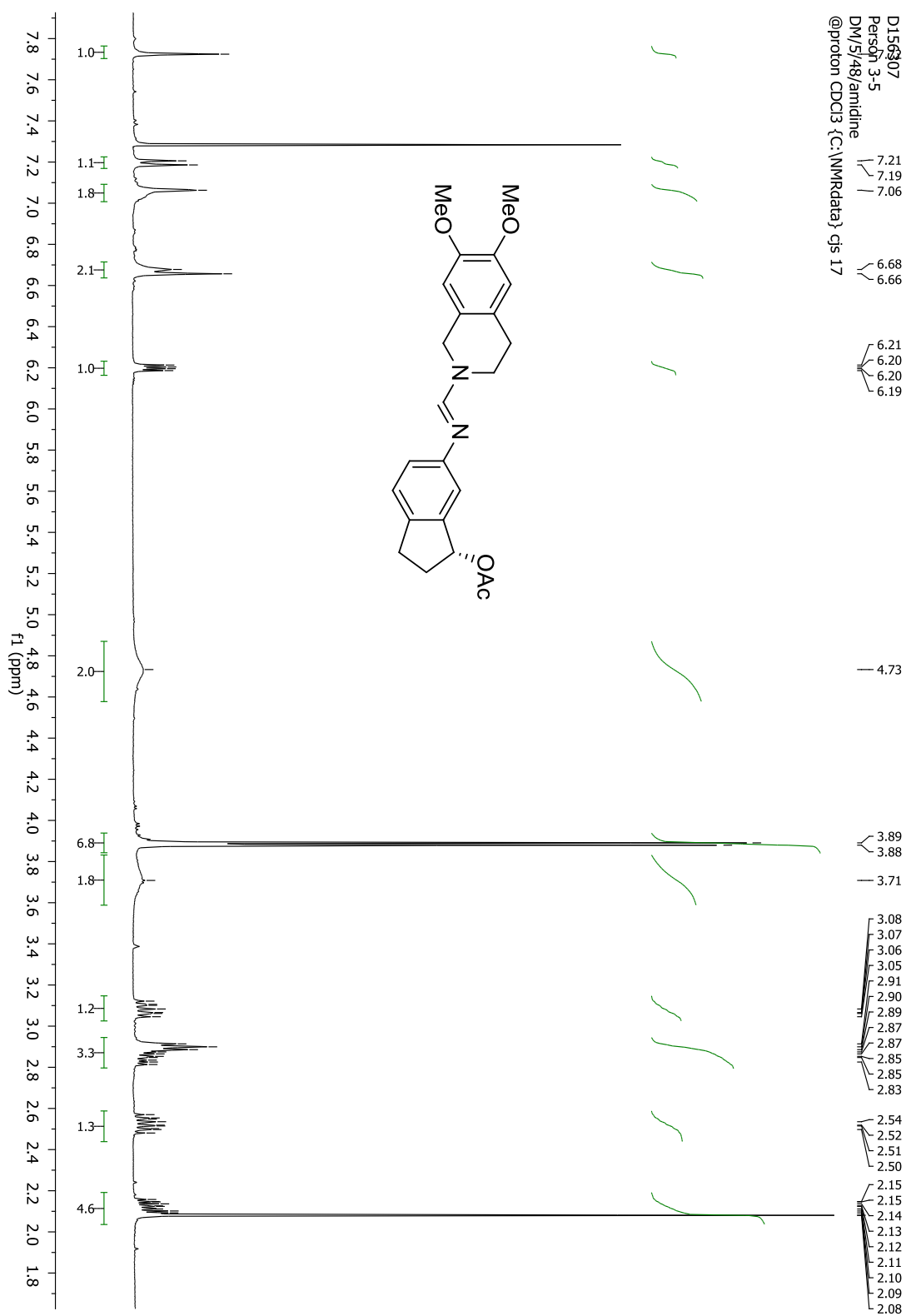
C(8)-C(3)-C(4)-C(5)	0.2(2)
C(2)-C(3)-C(4)-C(5)	179.44(14)
C(8)-C(3)-C(4)-C(1)	-178.87(14)
C(2)-C(3)-C(4)-C(1)	0.34(18)
O(1)-C(1)-C(4)-C(5)	0.2(3)
O(2)-C(1)-C(4)-C(5)	-178.77(15)
O(1)-C(1)-C(4)-C(3)	179.28(18)
O(2)-C(1)-C(4)-C(3)	0.27(18)
C(3)-C(4)-C(5)-C(6)	-1.0(2)
C(1)-C(4)-C(5)-C(6)	177.95(15)
C(4)-C(5)-C(6)-C(7)	0.7(2)
C(4)-C(5)-C(6)-N(1)	-178.09(14)
N(2)-N(1)-C(6)-C(5)	4.4(2)
N(2)-N(1)-C(6)-C(7)	-174.47(13)
C(5)-C(6)-C(7)-C(8)	0.2(2)
N(1)-C(6)-C(7)-C(8)	179.12(15)
C(4)-C(3)-C(8)-C(7)	0.7(2)
C(2)-C(3)-C(8)-C(7)	-178.29(17)
C(6)-C(7)-C(8)-C(3)	-0.9(3)
N(2)-N(3)-C(9)-C(10)	-148.7(4)
C(9A)-N(3)-C(9)-C(10)	-63(4)
C(13)-N(3)-C(9)-C(10)	50.2(6)
C(13A)-N(3)-C(9)-C(10)	14.6(7)
N(3)-C(9)-C(10)-C(11)	-49.7(5)
C(14A)-C(11)-C(10)-C(9)	-133.6(4)
C(10A)-C(11)-C(10)-C(9)	-44.8(5)
C(12)-C(11)-C(10)-C(9)	54.3(3)
C(14)-C(11)-C(10)-C(9)	-176.5(3)
C(12A)-C(11)-C(10)-C(9)	34.3(5)
C(14A)-C(11)-C(12)-C(13)	131.7(4)
C(10A)-C(11)-C(12)-C(13)	-20.7(5)
C(10)-C(11)-C(12)-C(13)	-55.0(4)
C(14)-C(11)-C(12)-C(13)	176.7(3)
C(12A)-C(11)-C(12)-C(13)	49.2(16)
N(2)-N(3)-C(13)-C(12)	146.7(2)
C(9A)-N(3)-C(13)-C(12)	-34.1(8)
C(13A)-N(3)-C(13)-C(12)	65.0(5)

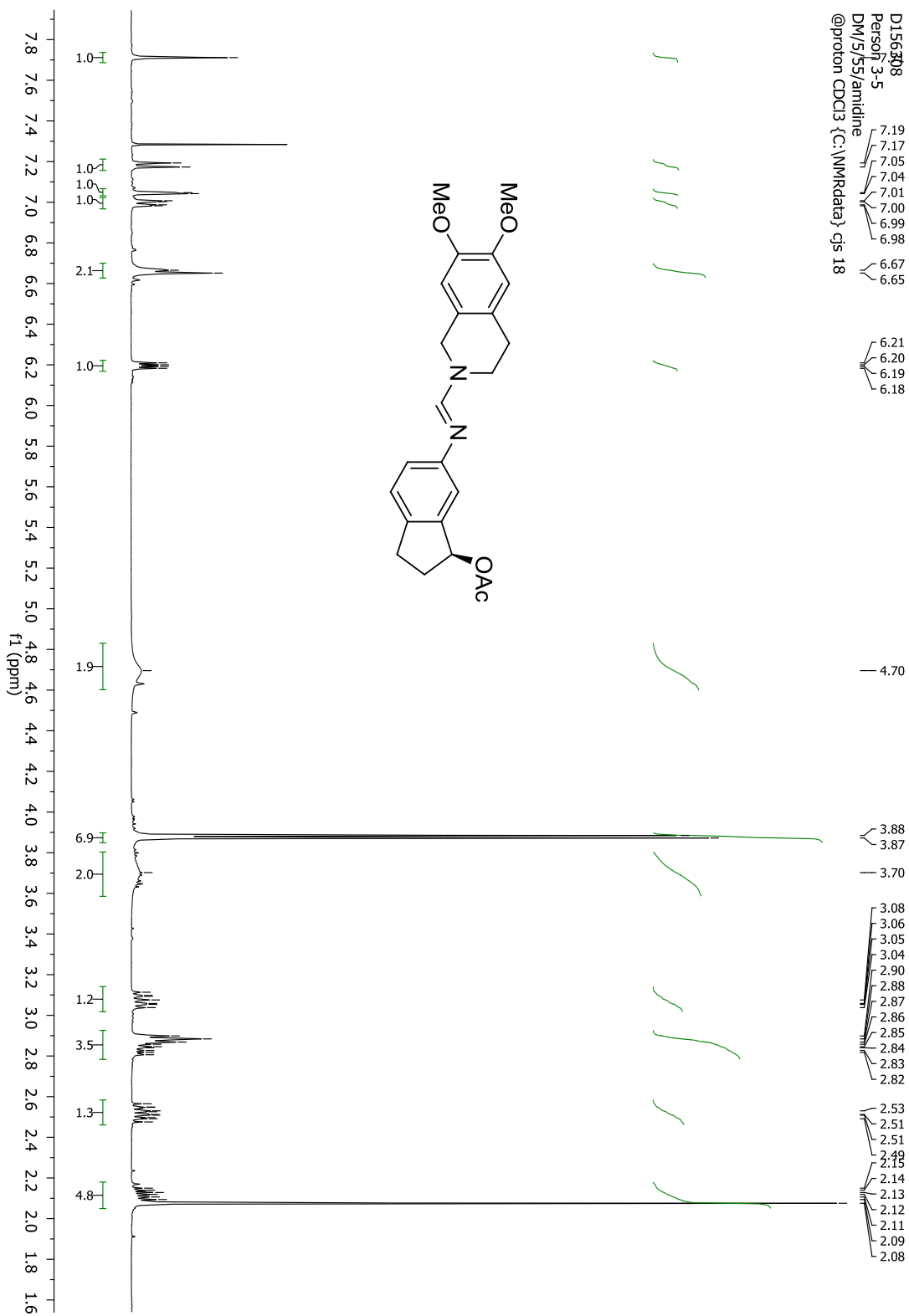
C(9)-N(3)-C(13)-C(12)	-51.0(4)
C(11)-C(12)-C(13)-N(3)	53.0(4)
C(14A)-C(11)-C(14)-C(15)	-71.3(4)
C(10A)-C(11)-C(14)-C(15)	25.6(5)
C(12)-C(11)-C(14)-C(15)	-175.4(3)
C(10)-C(11)-C(14)-C(15)	56.2(3)
C(12A)-C(11)-C(14)-C(15)	-157.6(5)
C(11)-C(14)-C(15)-C(16)	-94.6(4)
C(11)-C(14)-C(15)-C(20)	88.0(5)
C(20)-C(15)-C(16)-C(17)	-0.2(6)
C(14)-C(15)-C(16)-C(17)	-177.7(3)
C(15)-C(16)-C(17)-C(18)	0.3(6)
C(16)-C(17)-C(18)-C(19)	-1.3(6)
C(17)-C(18)-C(19)-C(20)	2.1(8)
C(18)-C(19)-C(20)-C(15)	-1.9(9)
C(16)-C(15)-C(20)-C(19)	1.0(8)
C(14)-C(15)-C(20)-C(19)	178.5(5)
C(14A)-C(11)-C(10A)-C(9A)	179.1(9)
C(12)-C(11)-C(10A)-C(9A)	-30.4(10)
C(10)-C(11)-C(10A)-C(9A)	64.1(10)
C(14)-C(11)-C(10A)-C(9A)	128.6(9)
C(12A)-C(11)-C(10A)-C(9A)	-48.6(10)
N(2)-N(3)-C(13A)-C(12A)	-158.3(4)
C(9A)-N(3)-C(13A)-C(12A)	54.2(9)
C(13)-N(3)-C(13A)-C(12A)	-46.3(5)
C(9)-N(3)-C(13A)-C(12A)	36.3(7)
C(17A)-C(18A)-C(19A)-C(20A)	-3.1(18)
C(10A)-C(11)-C(14A)-C(15A)	-52.5(6)
C(12)-C(11)-C(14A)-C(15A)	157.9(4)
C(10)-C(11)-C(14A)-C(15A)	-13.9(7)
C(14)-C(11)-C(14A)-C(15A)	62.0(5)
C(12A)-C(11)-C(14A)-C(15A)	178.0(5)
C(19A)-C(18A)-C(17A)-C(16A)	0.9(15)
N(3)-C(13A)-C(12A)-C(11)	-50.8(7)
C(14A)-C(11)-C(12A)-C(13A)	-171.4(5)
C(10A)-C(11)-C(12A)-C(13A)	50.9(7)
C(12)-C(11)-C(12A)-C(13A)	-65.5(16)

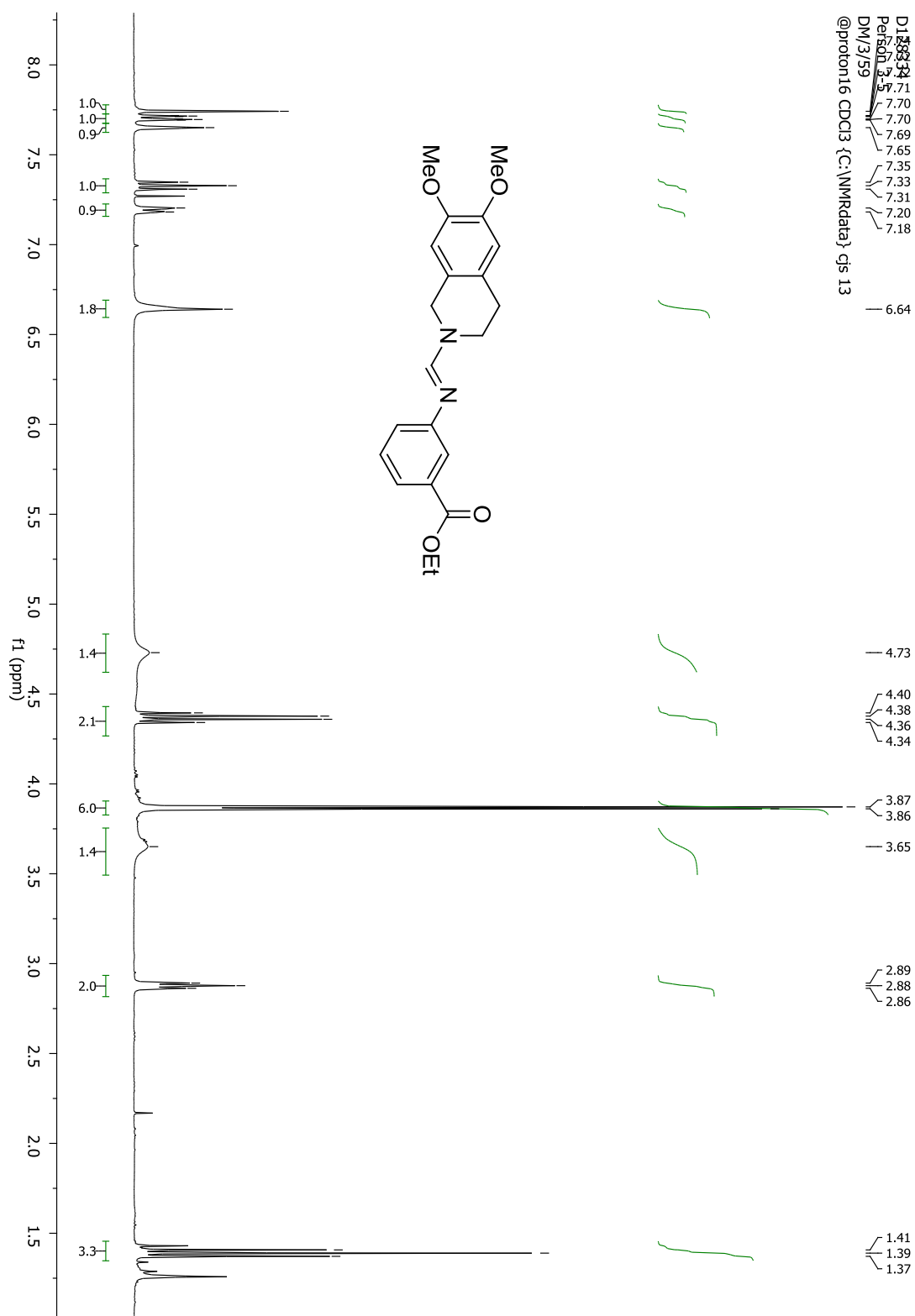
C(10)-C(11)-C(12A)-C(13A)	18.6(7)
C(14)-C(11)-C(12A)-C(13A)	-126.6(6)
C(18A)-C(17A)-C(16A)-C(15A)	-0.7(14)
N(2)-N(3)-C(9A)-C(10A)	164.5(6)
C(13)-N(3)-C(9A)-C(10A)	-14.6(12)
C(13A)-N(3)-C(9A)-C(10A)	-52.0(11)
C(9)-N(3)-C(9A)-C(10A)	60(4)
C(11)-C(10A)-C(9A)-N(3)	50.3(13)
C(18A)-C(19A)-C(20A)-C(15A)	6(2)
C(19A)-C(20A)-C(15A)-C(16A)	-5.2(18)
C(19A)-C(20A)-C(15A)-C(14A)	-179.6(11)
C(17A)-C(16A)-C(15A)-C(20A)	2.7(16)
C(17A)-C(16A)-C(15A)-C(14A)	177.3(8)
C(11)-C(14A)-C(15A)-C(20A)	132.3(10)
C(11)-C(14A)-C(15A)-C(16A)	-41.8(11)

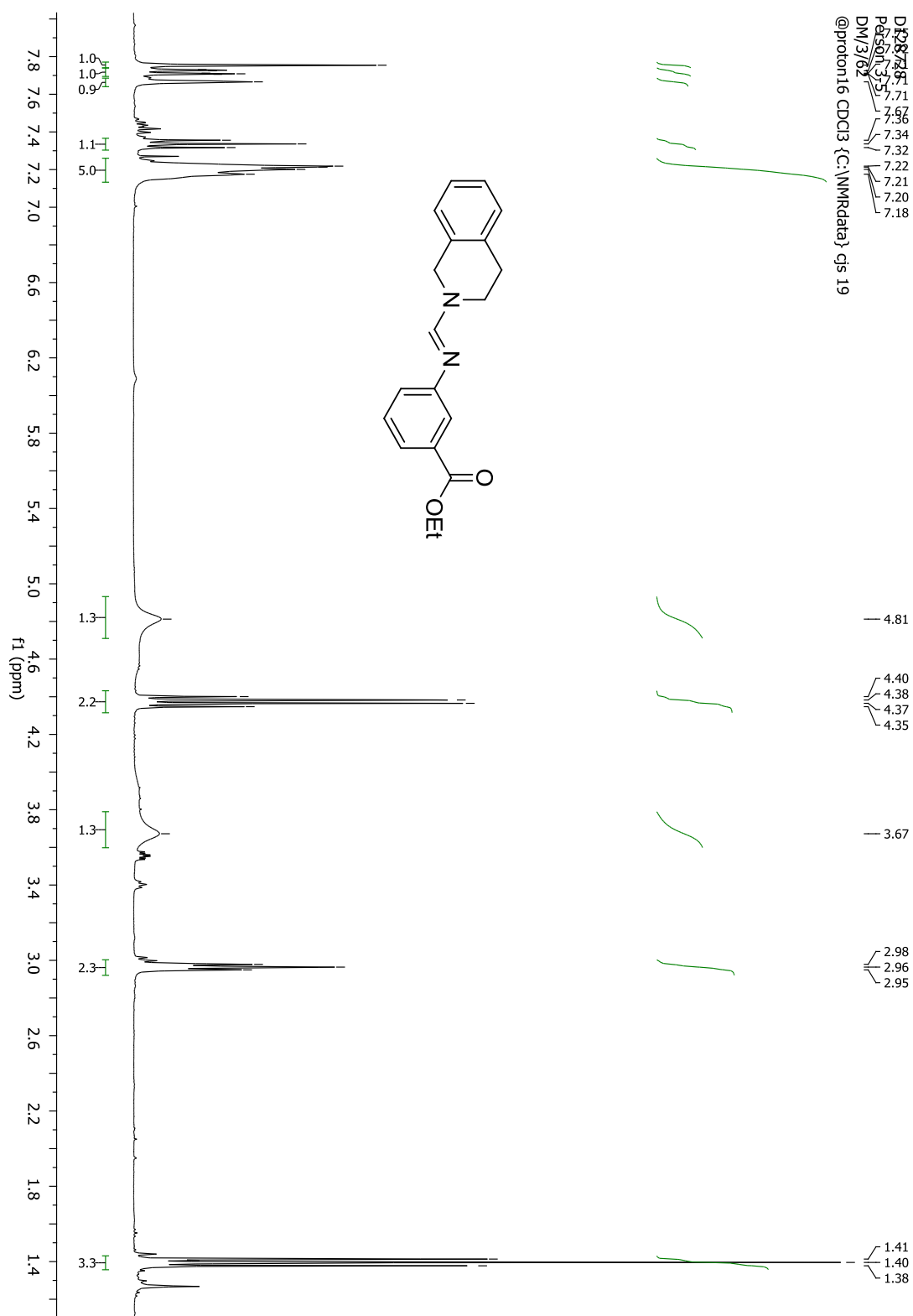
Symmetry transformations used to generate equivalent atoms:

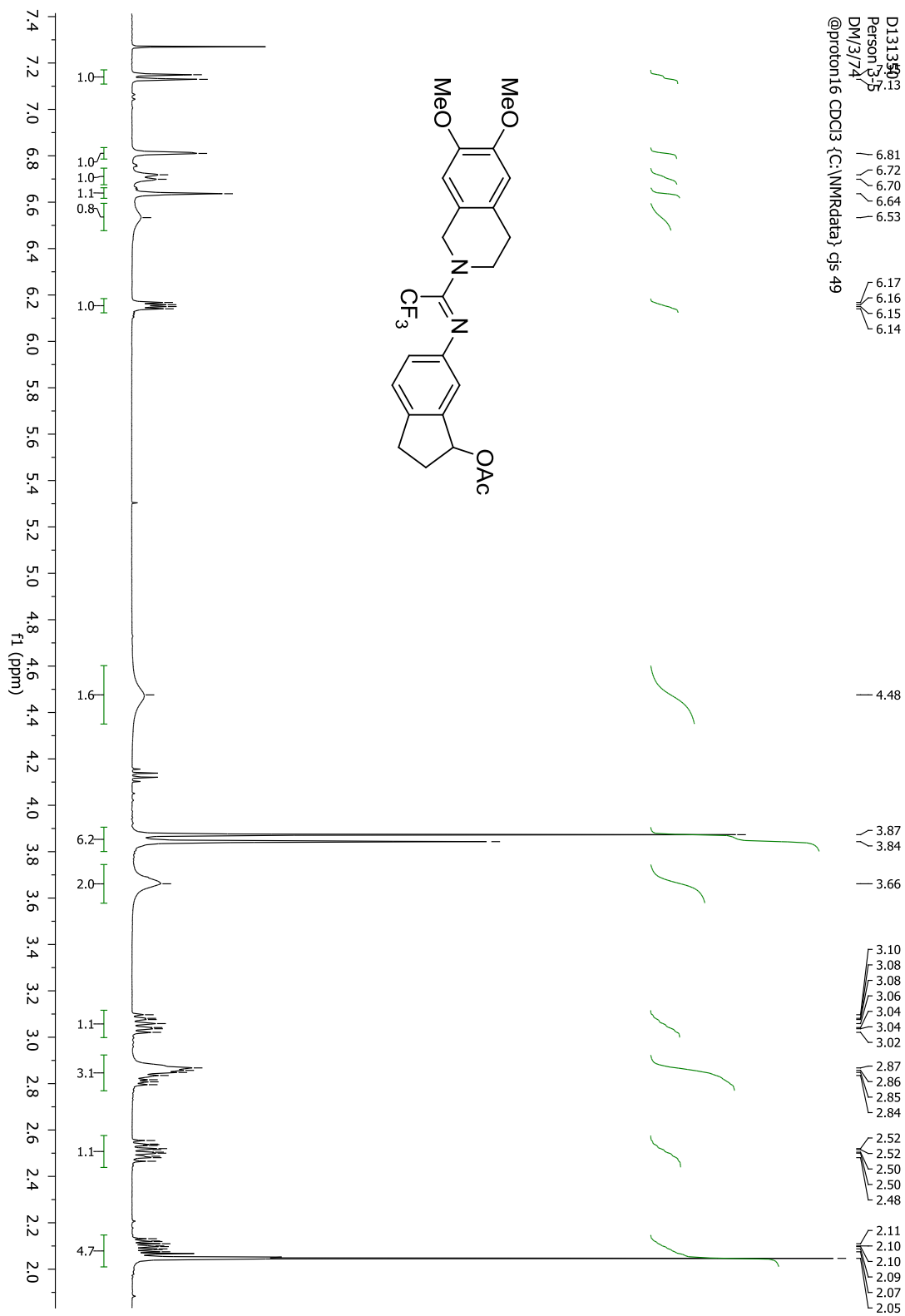
8.2 ^1H NMR spectra

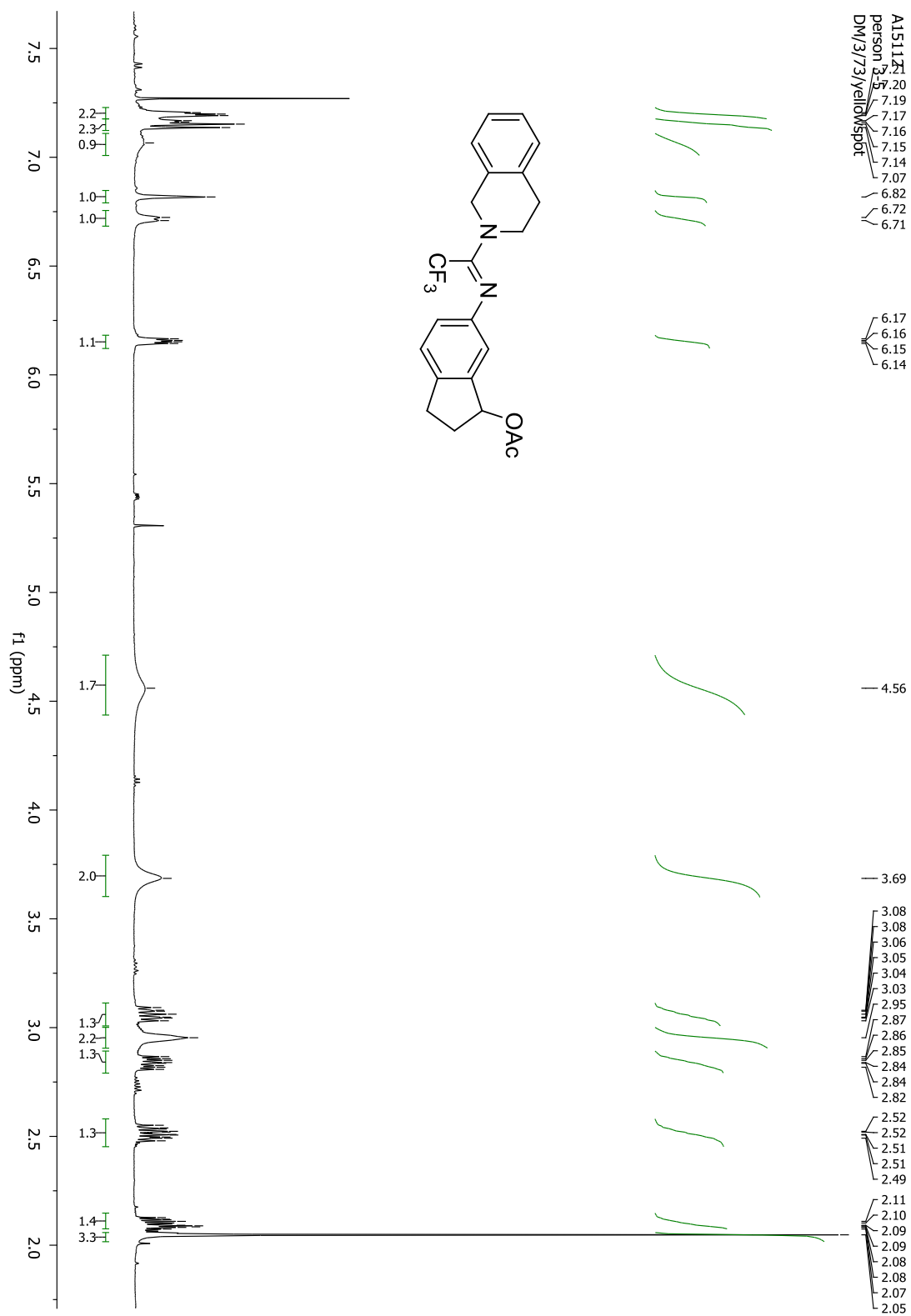


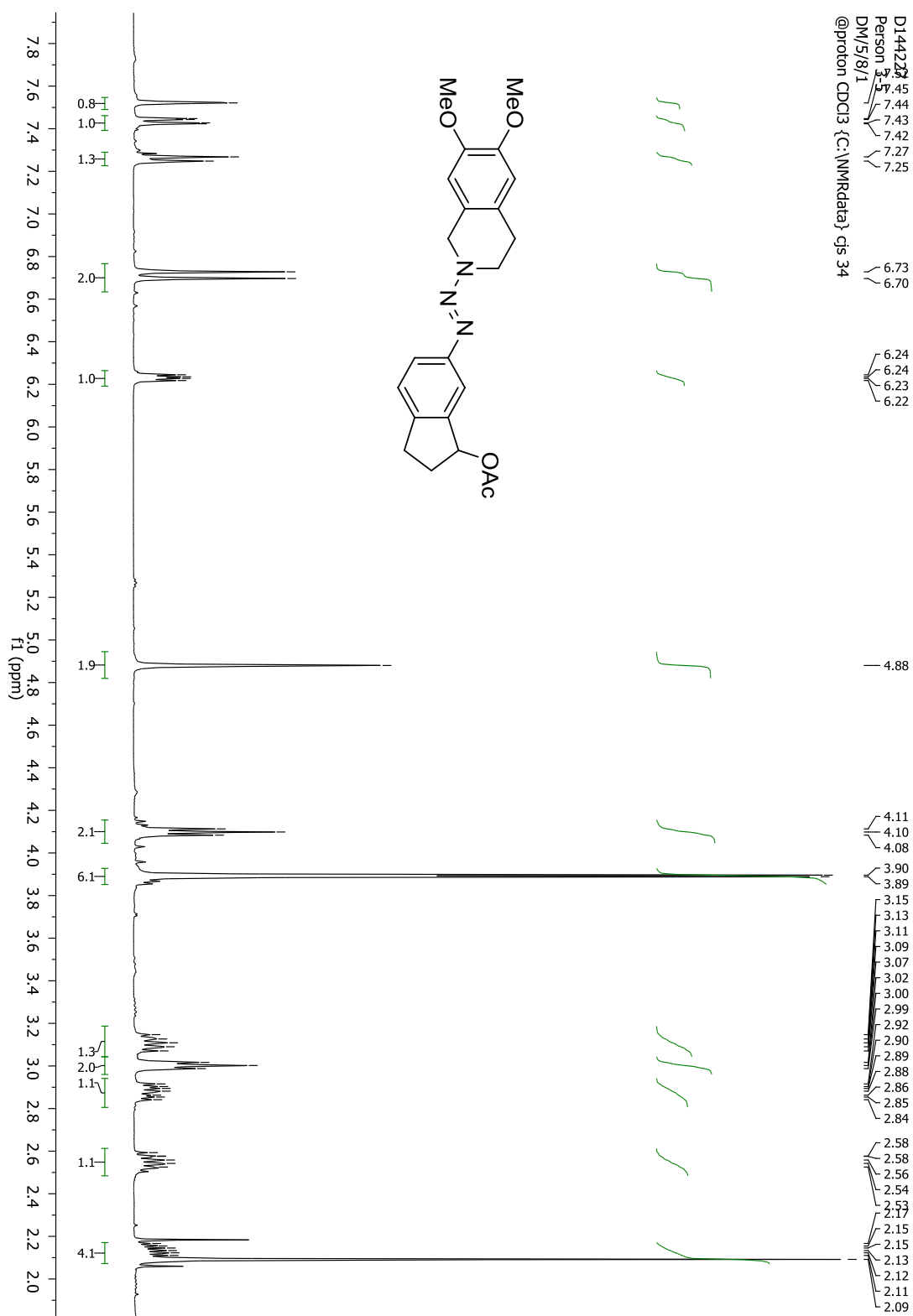


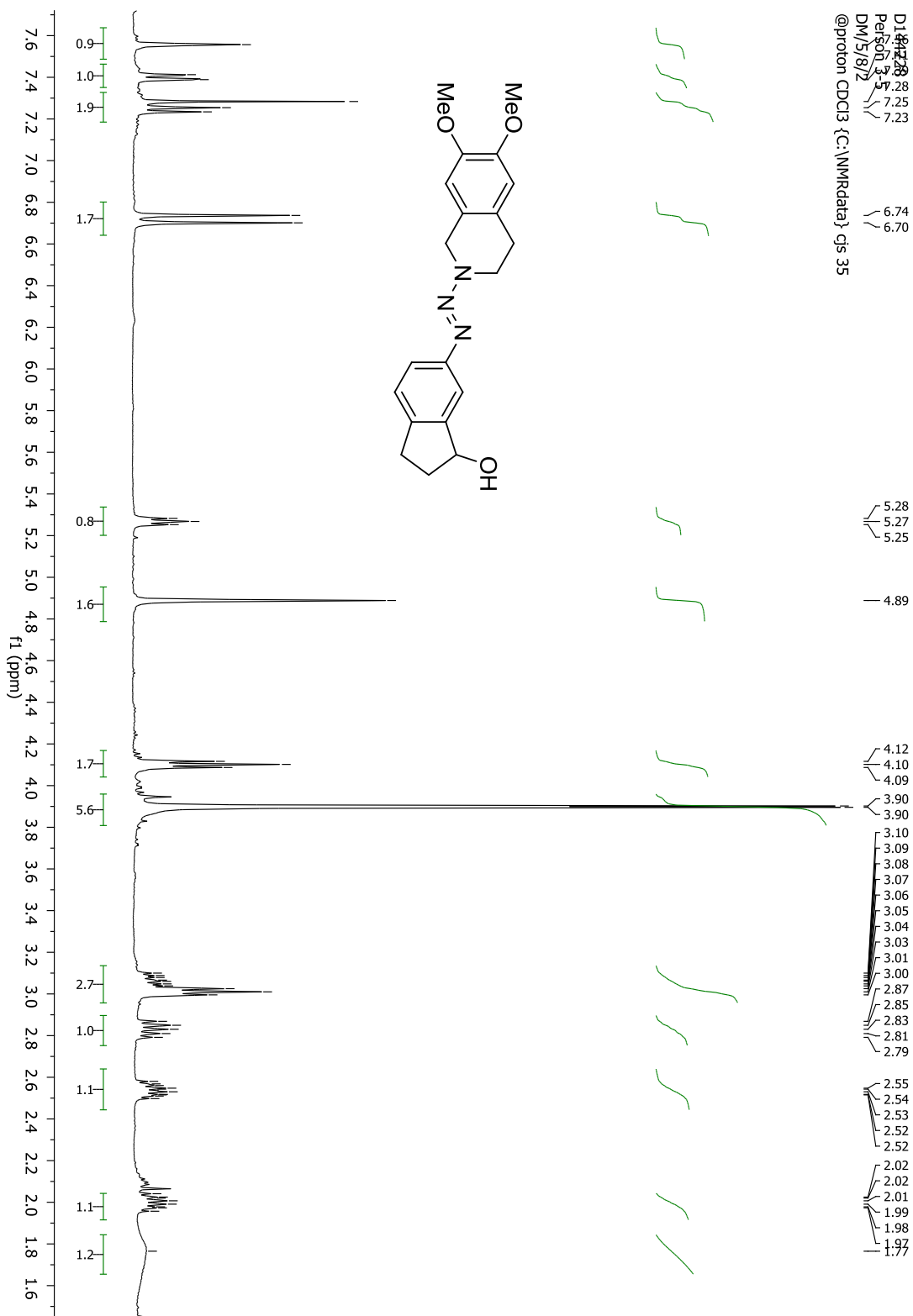


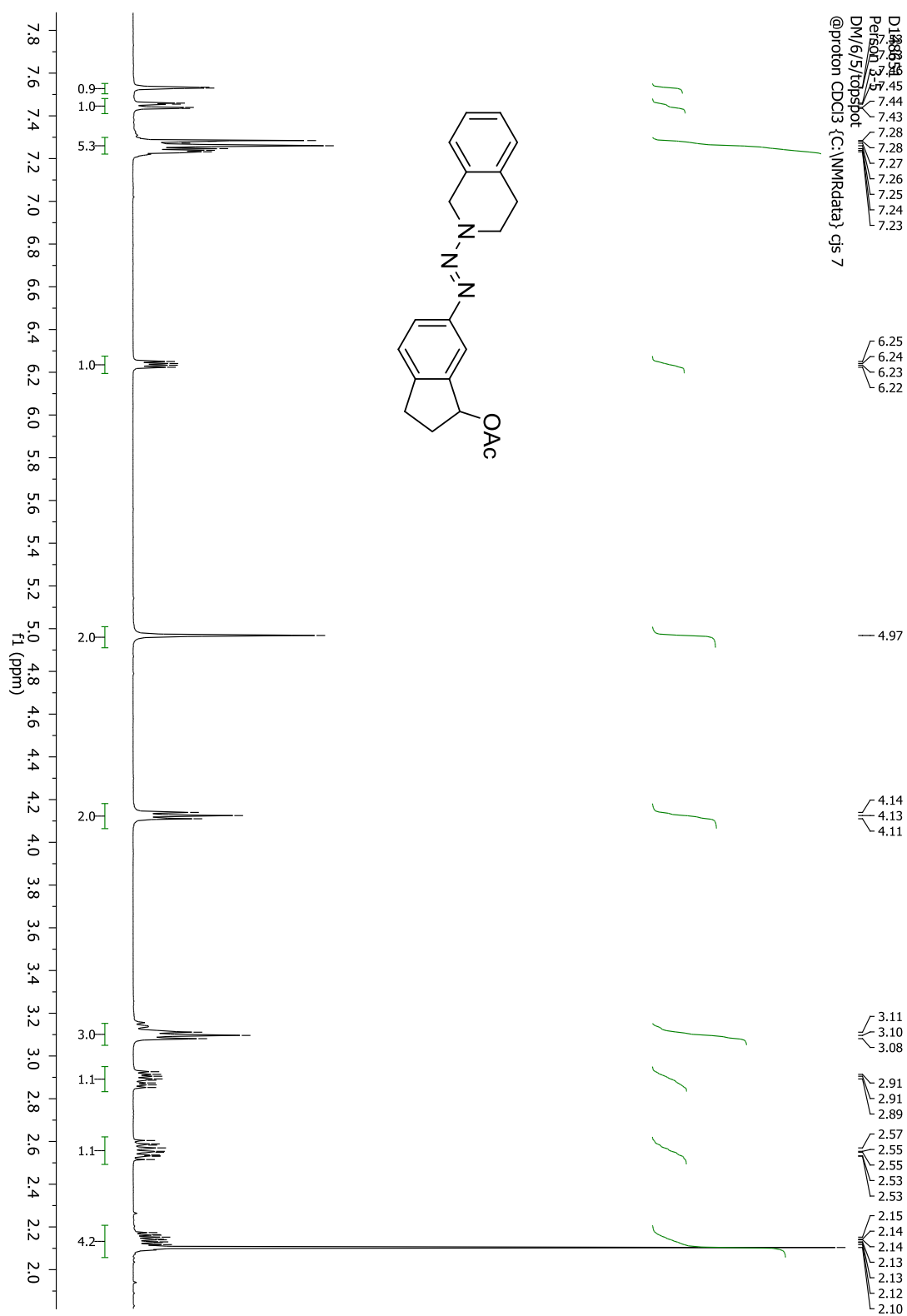


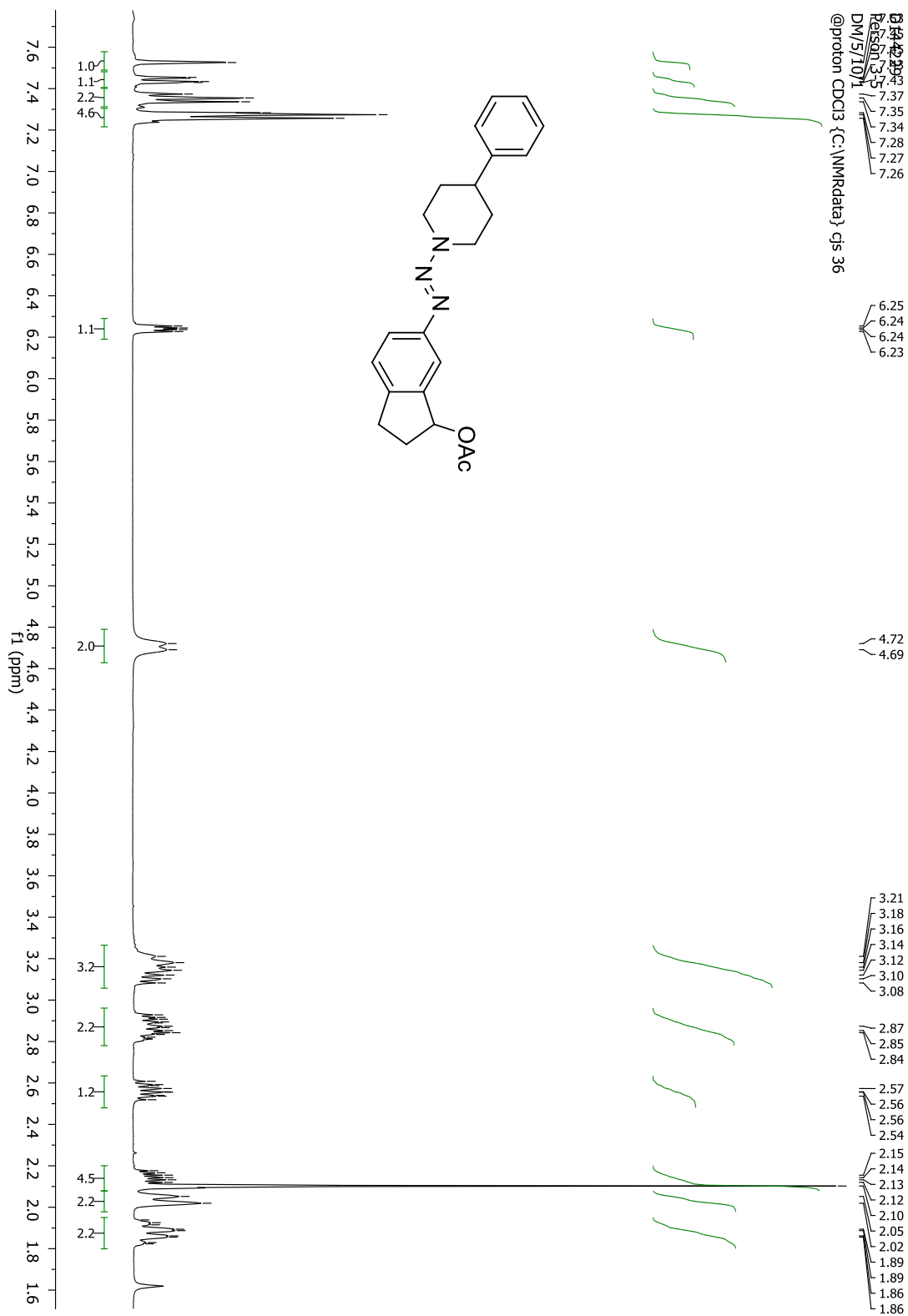


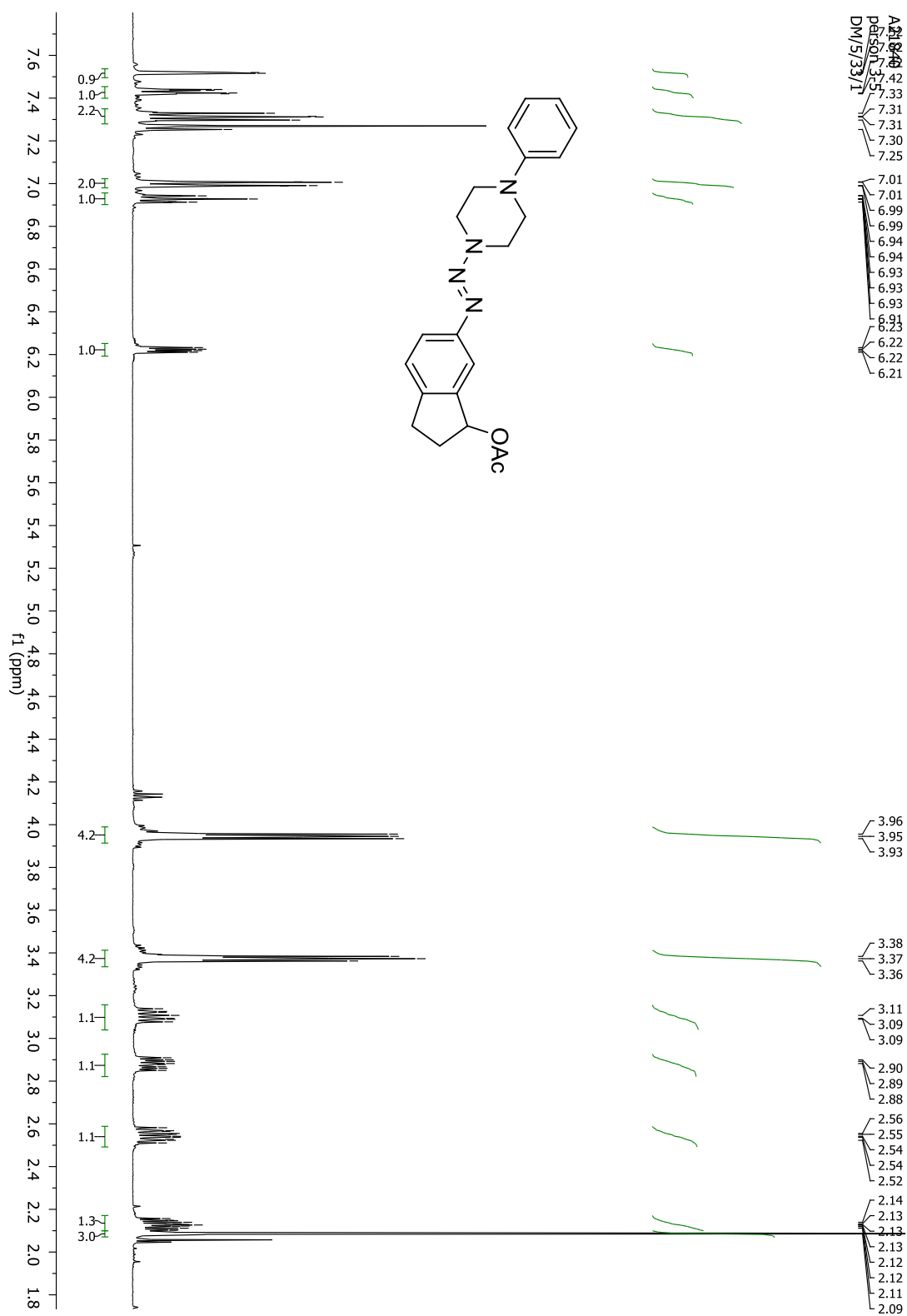


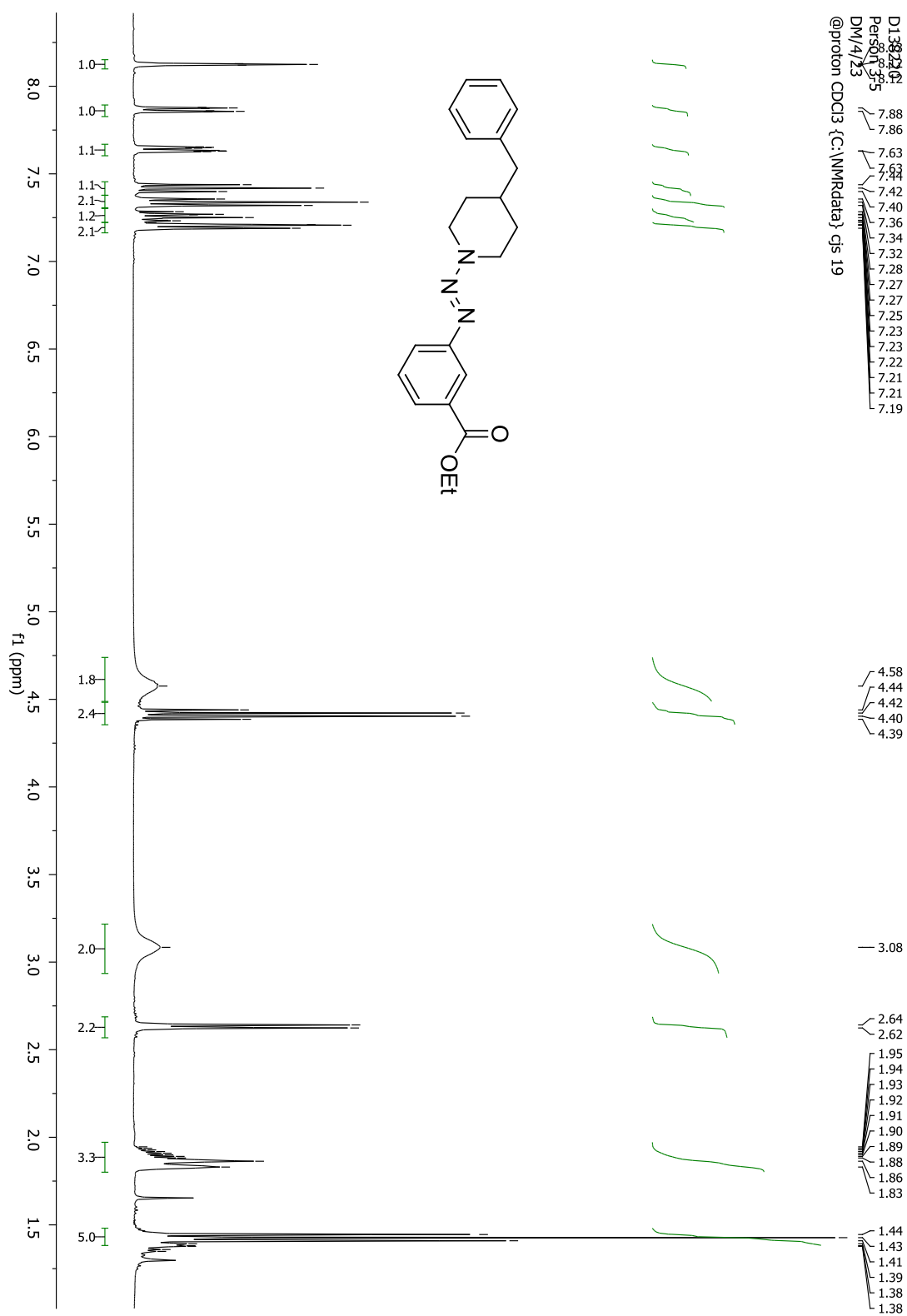


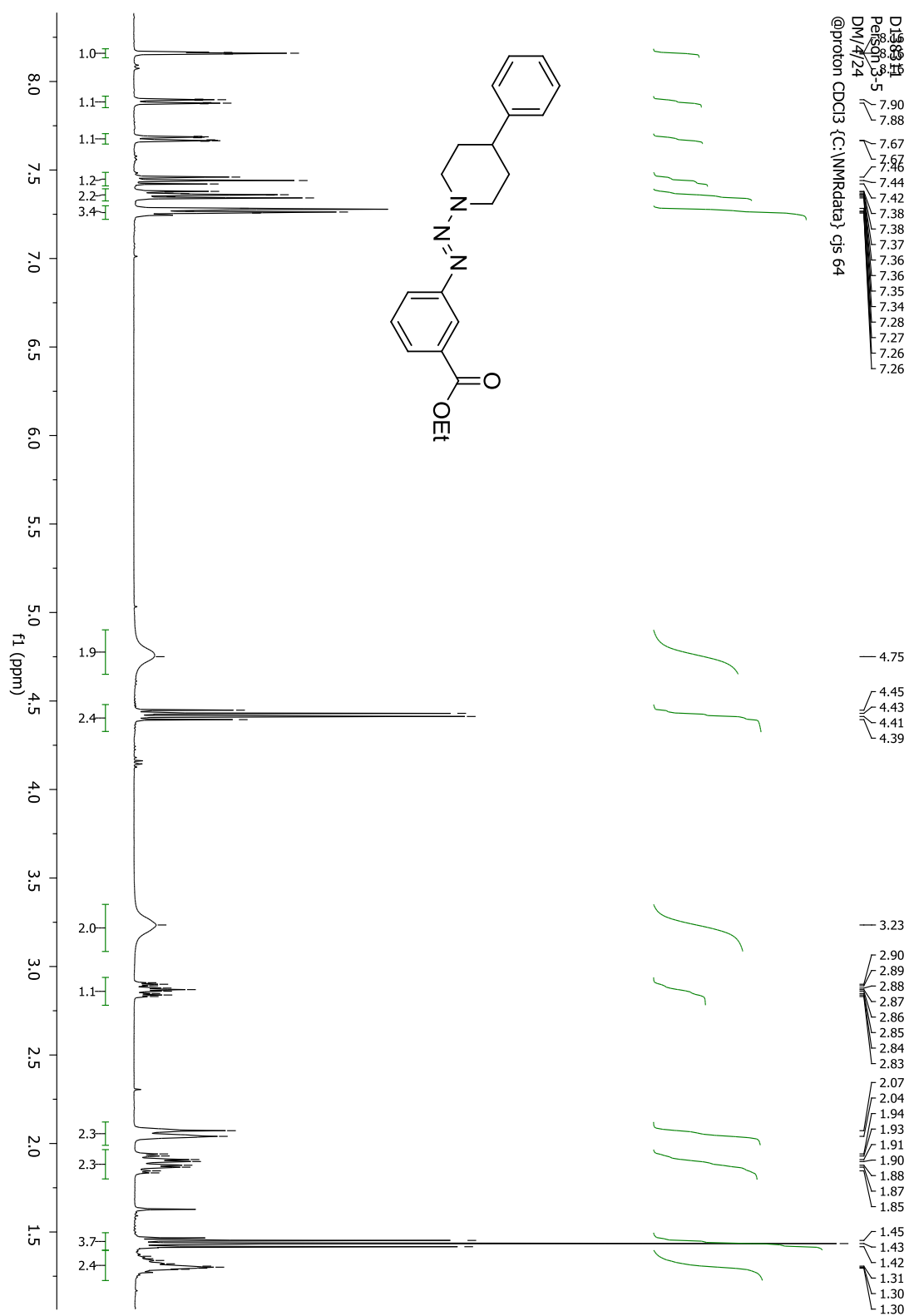


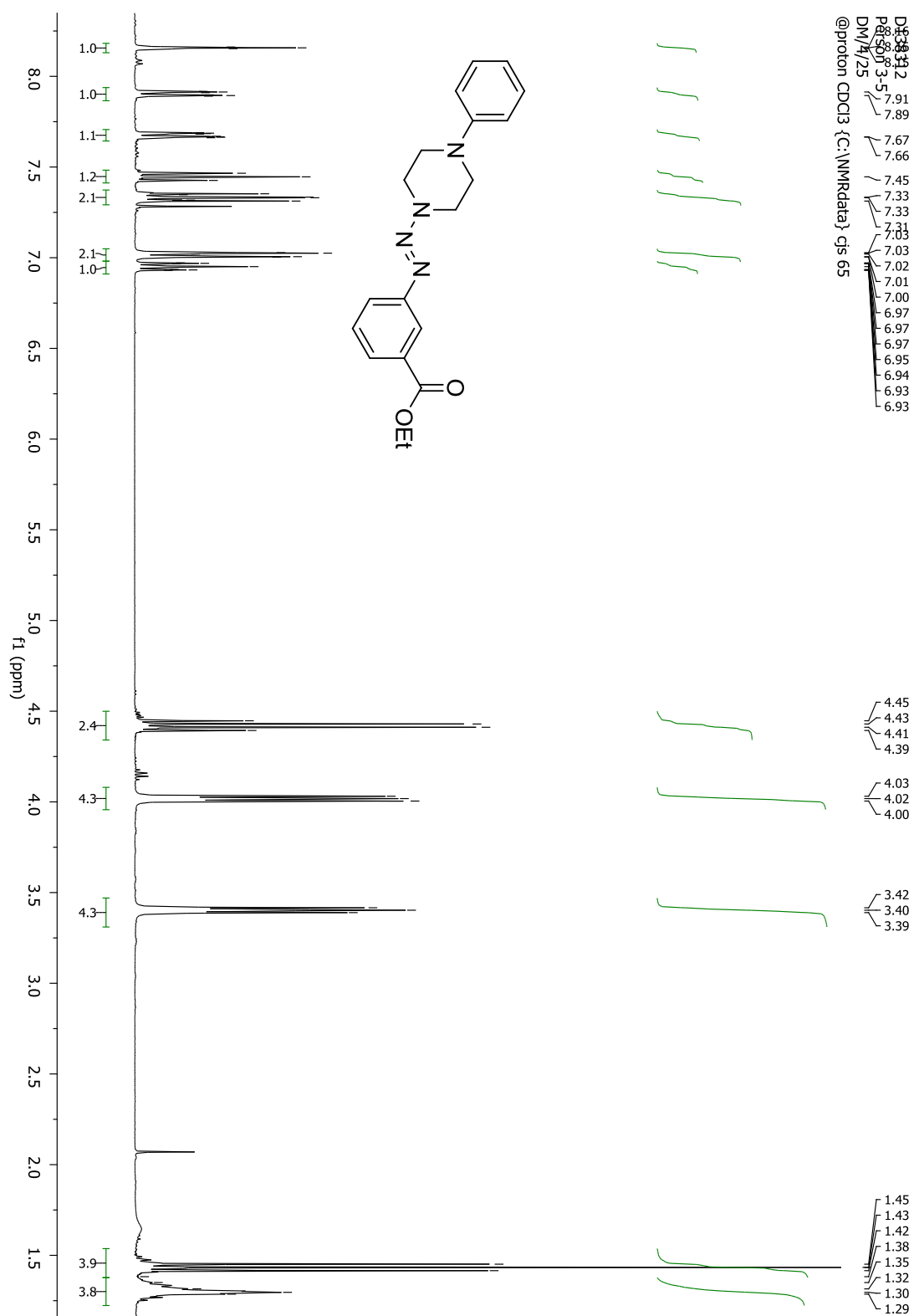




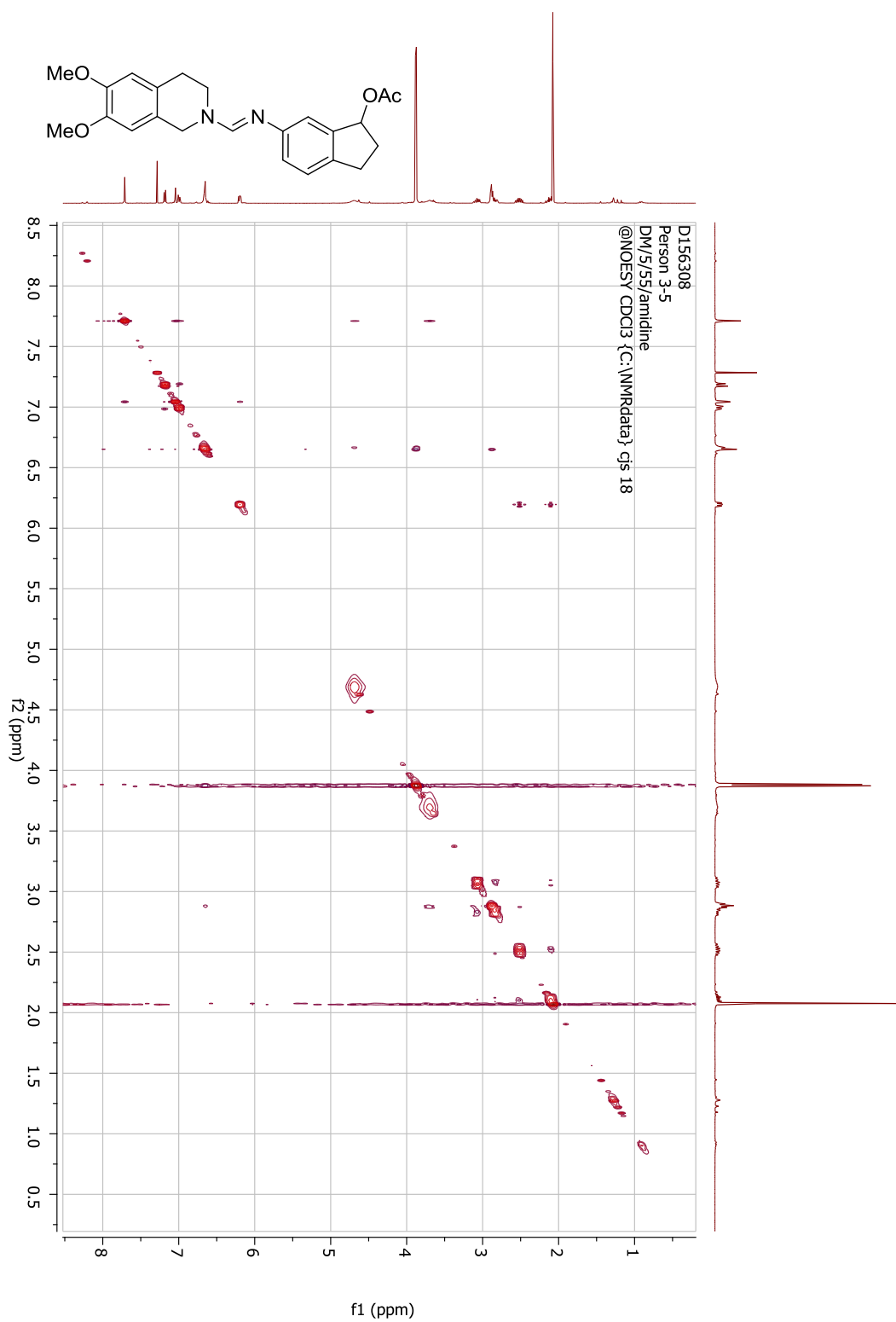


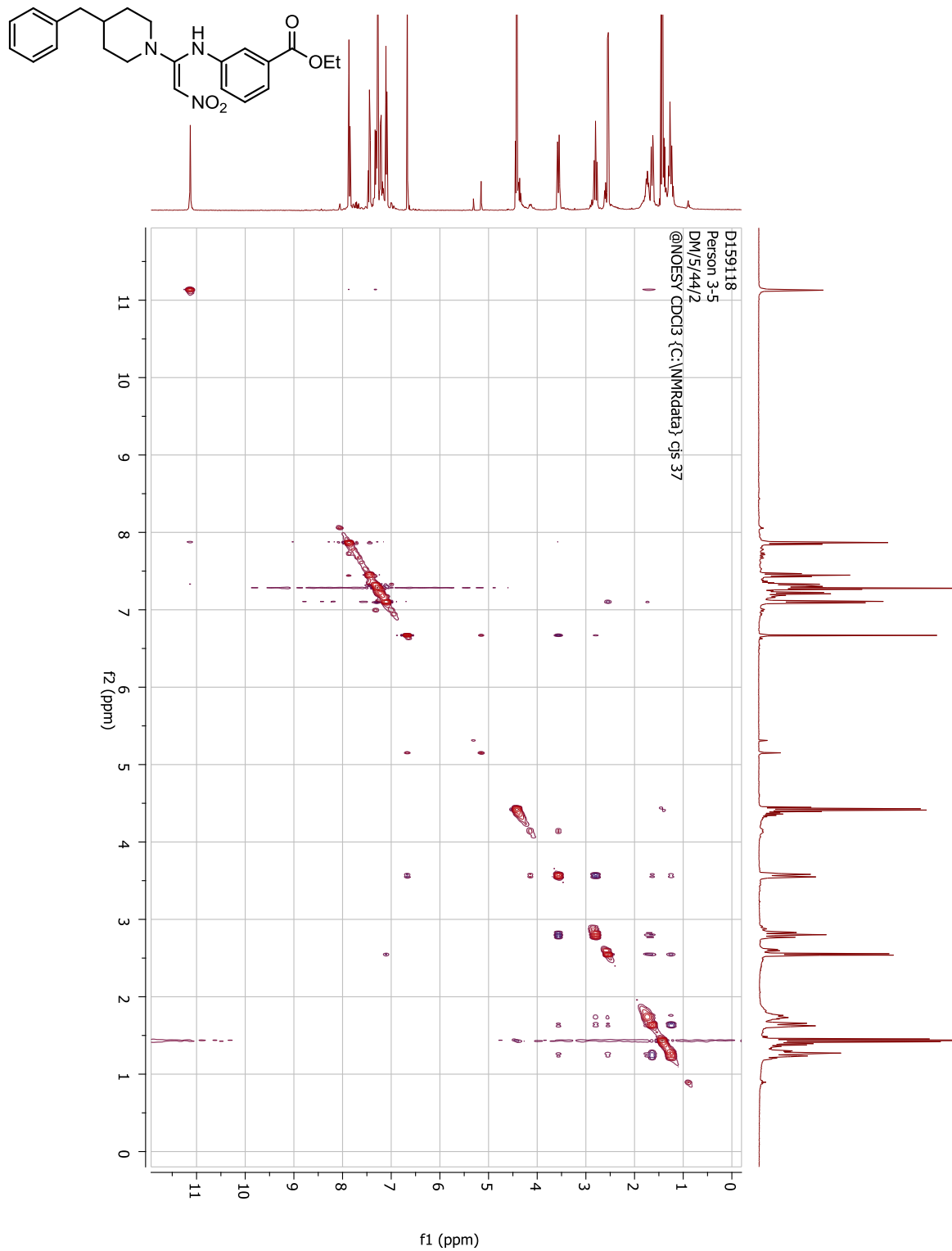


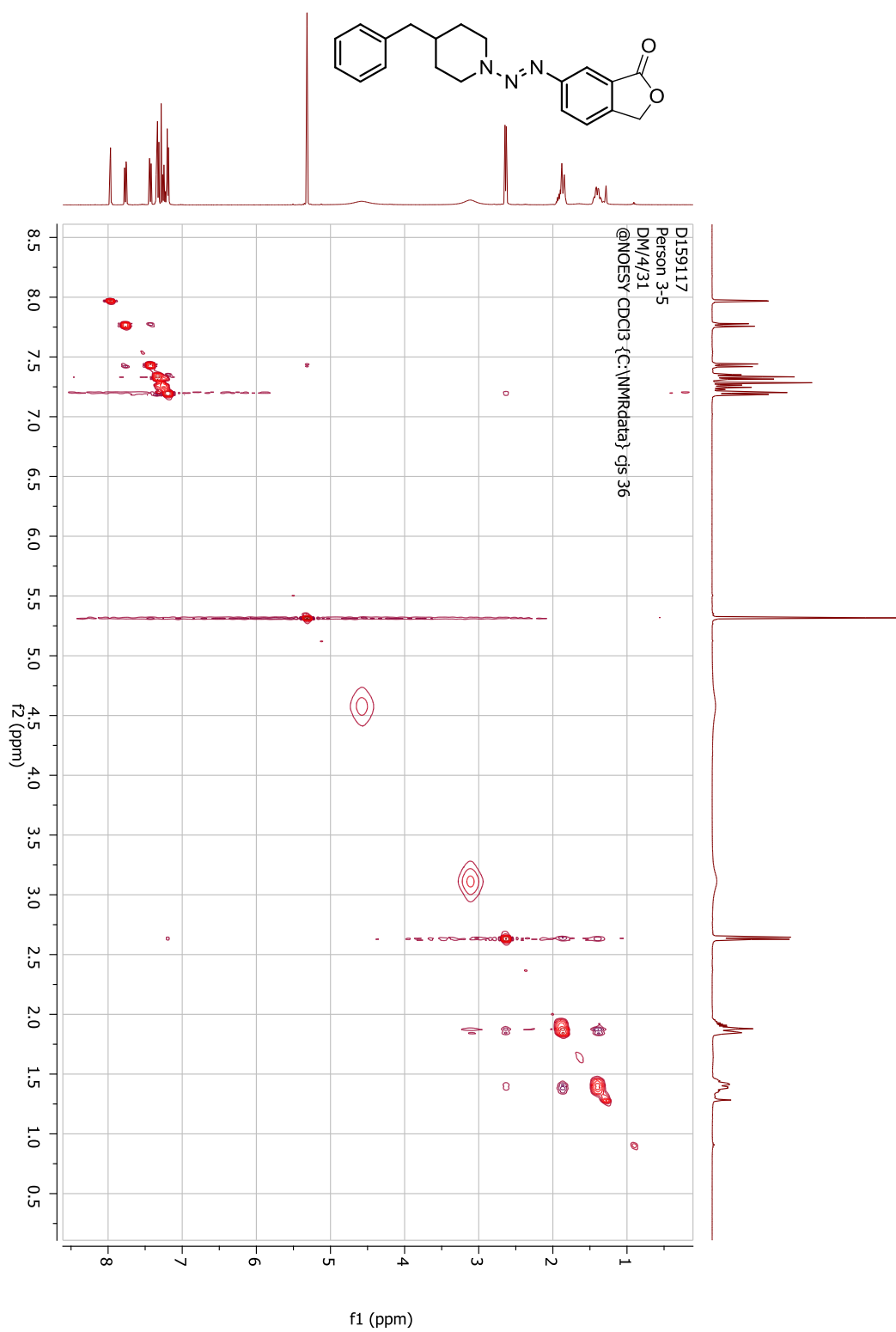




8.3 NOESY spectra







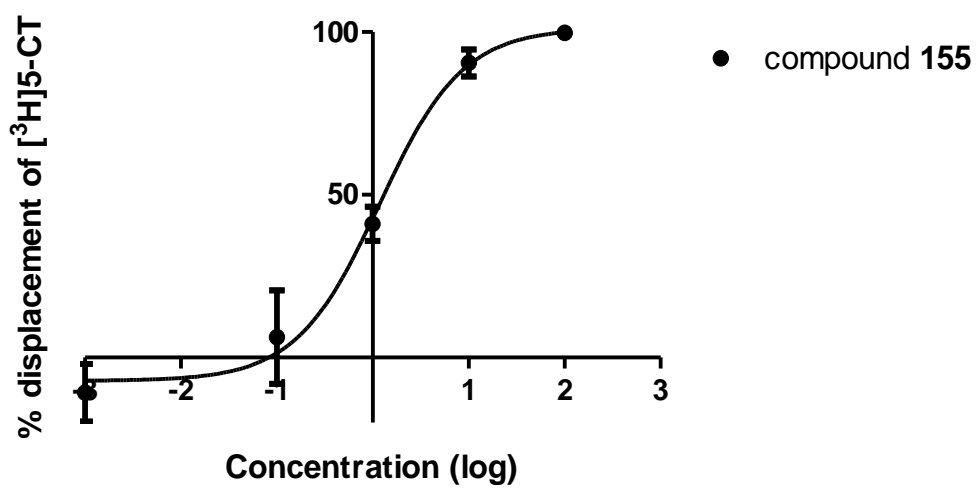
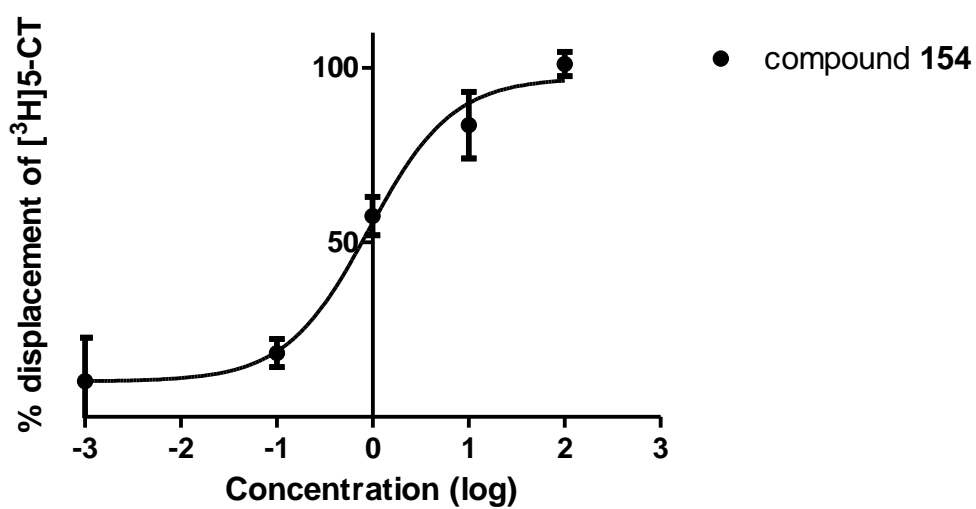
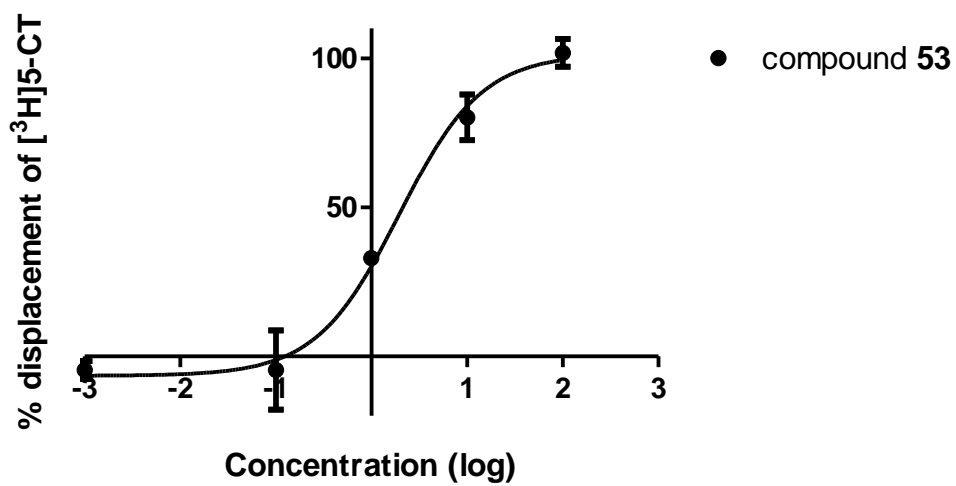
8.4 IC₅₀ example graphs

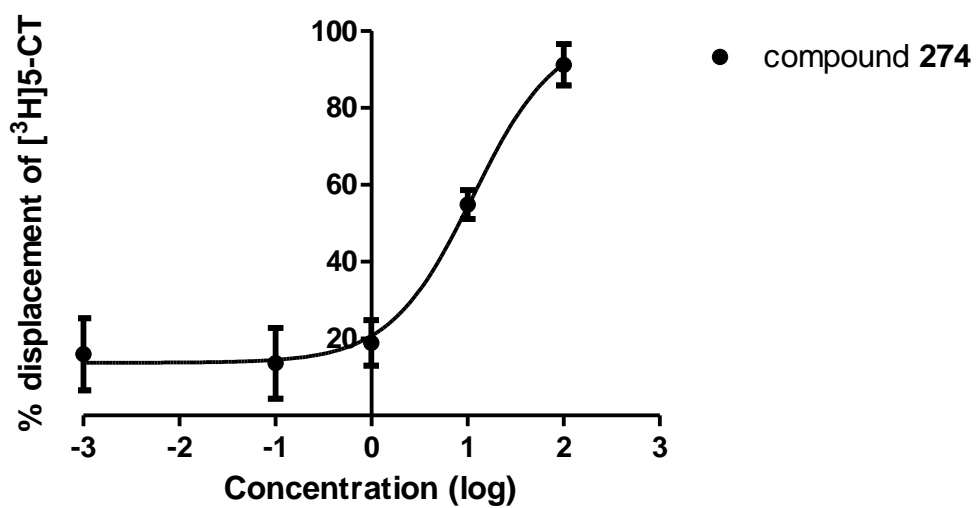
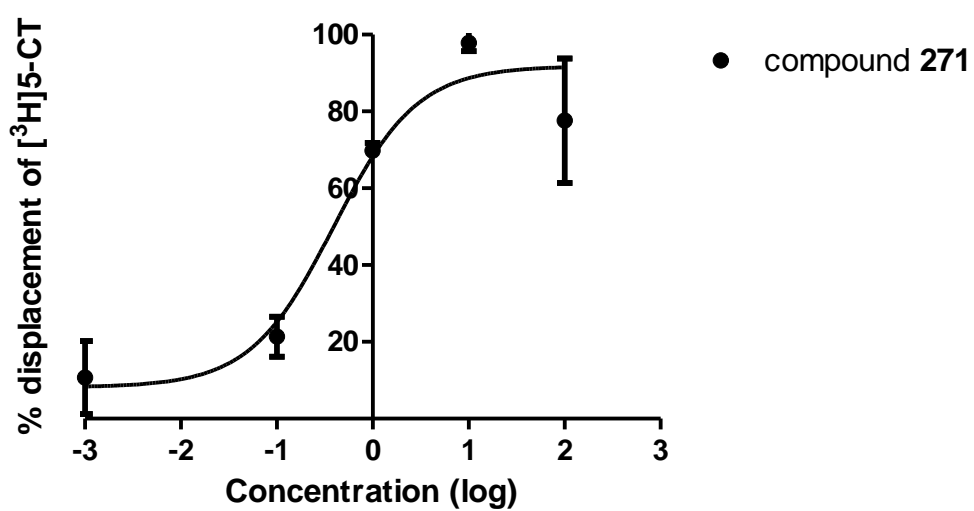
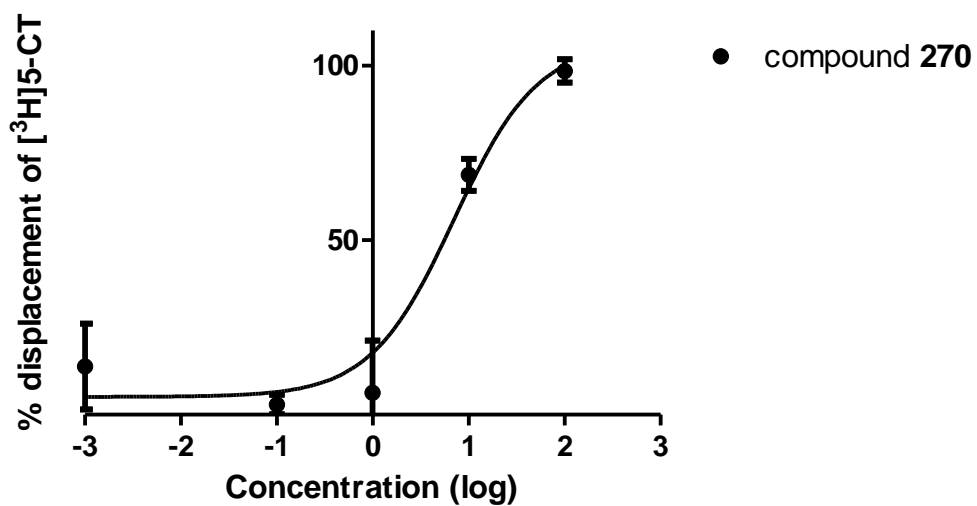
IC₅₀ graphs were generated using GraphPad Prism5 from competition binding assays where the concentration of test compound was varied (100, 10, 1, 0.1 μM). The assays were carried out in triplicate and n = 3. IC₅₀ values generated were averaged and converted to *K_i* using the Cheng–Prusoff equation.²¹⁸

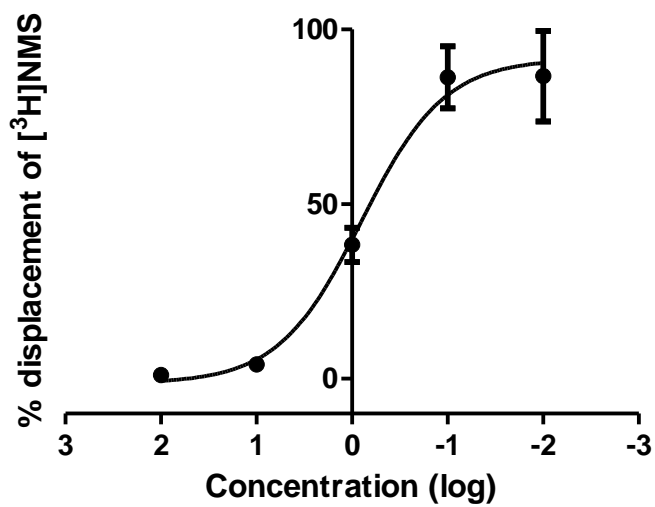
$$K_i = \frac{IC_{50}}{1 + \frac{[S]}{K_m}}$$

where *K_i* is the binding affinity of the selected test compound, IC₅₀ is the inhibition constant of the test compound, [S] is substrate (radioligand) concentration and *K_m* is the concentration of substrate (radioligand) at which binding activity is at half maximal.

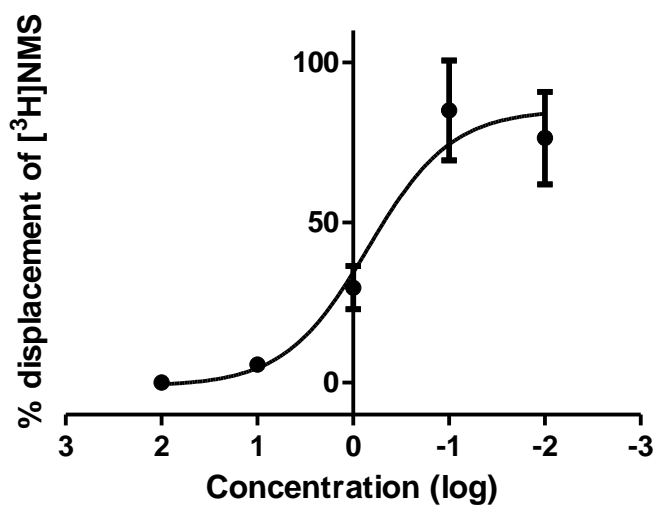
8.4.1 5-HT₇ IC₅₀ example graphs



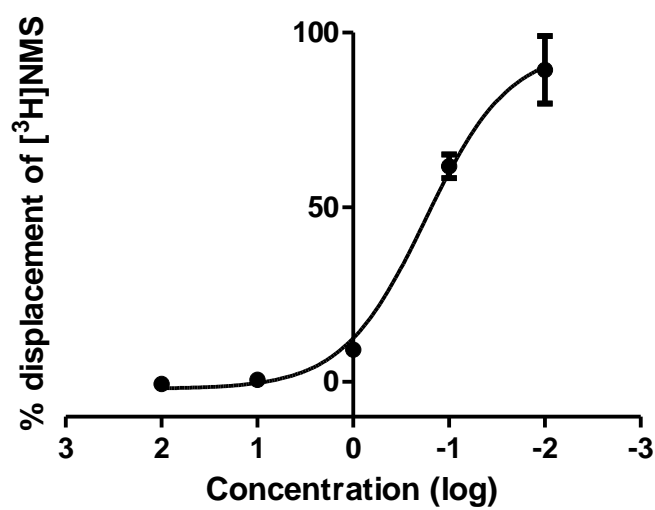


8.4.2 M_4 IC_{50} example graphs

● compound 53



● compound 154



● compound 155

